SYNTHESIS, ANTIMICROBIAL AND ANTIOXIDANT STUDIES OF NEW BENZOTHIAZOLE DERIVATIVES

Thesis Submitted for the Award of the Degree of

DOCTOR OF PHILOSOPHY

In

Chemistry

By

Tanzeela Qadir

Registration Number
(11919669)

Supervised by

Dr. Praveen Kumar Sharma (14155)
Department of Chemistry,
School of Chemical Engineering and Physical Sciences,
Lovely Professional University, Punjab

LOVELY PROFESSIONAL UNIVERSITY, PUNJAB

2024

DEDICATION

This thesis is dedicated to my parents

Ghulam Qadir

And

Hameeda Begum

Who have given me invaluable educational opportunities.

DECLARATION

I, hereby declared that the presented work in the thesis entitled "Synthesis, Antimicrobial and Antioxidant Studies of new Benzothiazole Derivatives" in fulfillment of degree of **Doctor of Philosophy (Ph.D.)** is the outcome of research work carried out by me under the supervision of Dr. Praveen Kumar Sharma, working as Professor, in the Department of Chemistry, School of Chemical Engineering and Physical Sciences, Lovely Professional University, Punjab, India. In keeping with the general practice of reporting scientific observations, due acknowledgements have been made whenever the work described here has been based on the findings of other investigator. This work has not been submitted in part or full to any other University or Institute for the award of any degree.

(Signature of Scholar)

Tanzeela Qadir
Registration No.:11919669
Department of Chemistry,
School of Chemical Engineering and Physical Sciences,
Lovely Professional University, Punjab, India

CERTIFICATE

This is to certify that the work reported in the Ph. D. thesis entitled "Synthesis, Antimicrobial and Antioxidant Studies of new Benzothiazole Derivatives" submitted in fulfillment of the requirement for the reward of degree of **Doctor of Philosophy (Ph.D.)** in the Department of Chemistry, School of Chemical Engineering and Physical Sciences, Lovely Professional University, is a research work carried out by Tanzeela Qadir, 11919669, is bonafide record of her original work carried out under my supervision and that no part of thesis has been submitted for any other degree, diploma or equivalent course.

(Signature of Supervisor)

Dr. Praveen Kumar Sharma

Professor

Department of Chemistry,

School of Chemical Engineering and Physical Sciences,

Lovely Professional University, Punjab India

ABSTRACT

This work illustrates the synthesis of 2-azidobenzothiazoles from substituted 2-aminobenzothiazoles using sodium nitrite and sodium azide under mild conditions. A comprehensive *in vitro* investigation was conducted with the primary objective of assessing the antibacterial effectiveness of 2-azidobenzothiazoles and the antibiofilm potential of the most potent compound, 2-azido-6-nitrobenzothiazole, referred to as 2d. Overall eight compounds were examined for their antibacterial activity against Gram (+) bacteria, *Staphylococcus aureus* (ATCC 25923), *Enterococcus faecalis* (ATCC 51299), *Bacillus cereus* (ATCC 10876) and Gram (-) bacteria, *Escherichia coli* (ATCC 10536), *Pseudomonas aeruginosa* (ATCC 10145), *Klebsiella pneumoniae* (ATCC BAA-2146) and Clinical isolates of Gram (+) Methicillin Resistant *Staphylococcus aureus* (MRSA) and Gram (-) Multi-Drug Resistant *Escherichia coli* (MDRE). The MIC values by broth dilution method showed that compound 2d exhibited significant antibacterial potential against *Enterococcus faecalis* and *Staphylococcus aureus* with MIC of 8 µg/mL, while other synthesized compounds had only moderate effects against all the tested bacteria. Notably, all the compounds were found to be active against the resistant strains MRSA and MDRE at MIC 128 µg/mL. The MBC of compound 2d was equivalent to 16 µg/mL for both *Enterococcus faecalis* and *Staphylococcus aureus.* The kill kinetics analysis demonstrated efficient concentration and time-dependent bactericidal activity of compound 2d against *Staphylococcus aureus* and *Enterococcus faecalis*. Additionally, post-antibiotic effect studies revealed a prolonged suppression of bacterial growth for 5.33 hours with *Staphylococcus aureus* and 5.66 hours with *Enterococcus faecalis* irrespective of the concentration, even after the removal of the compound. In the context of antibiofilm activity, compound 2d exhibited remarkable biofilm inhibition potential against the tested Gram (+) bacteria, *Staphylococcus aureus, and Enterococcus faecalis*, and significant inhibitory effects were observed at the MIC for other tested bacteria. The biofilm inhibition percentage ranged from 30.82% to 70.04% from the lowest to highest concentration of compound 2d, for *Staphylococcus aureus* and 44.54% to 73.04% for *Enterococcus faecalis*. Furthermore, biofilm eradication assays demonstrated up to 70% eradication of mature biofilms (formed at 24, 48, and 72 hours) of *Staphylococcus aureus* and *Enterococcus faecalis*, highlighting the potential of compound 2d to disrupt and eliminate established biofilms. The selective cytotoxicity of compound 2d towards bacterial cells was

evidenced by extended exposure of the HEK-293 cell line to higher concentrations of the compound. It was demonstrated by the significant proportion of viable HEK-293 cells, indicating a favorable safety profile for the compound 2d. After the comprehensive examination of the synthesized compounds for their antibacterial efficacy, their potential as antioxidants was further explored through the application of the DPPH method. The results of this assessment revealed a noteworthy and robust antioxidant activity, underscoring the ability of synthesized compounds to effectively scavenge free radicals and thus offering the potential for applications in oxidative stress mitigation and related areas of study.

In addition to this, a novel class of antimycobacterial chemical structures, based on the benzothiazole amide derivatives, has been synthesized. A total of twelve benzothiazole amide derivatives with distinct structural variations were successfully synthesized and subsequently assessed for *in vitro* testing against the *Mycobacterium tuberculosis* (MTB) H37Rv strain (ATCC 27294) to evaluate their potential as anti-tubercular agents. All the synthesized compounds were examined with the aid of FTIR, NMR, and mass spectral analysis. Notably, the structures of selected compounds, namely 5a, 5g, and 5l, were further verified through single-crystal X-ray diffraction. This high-precision technique provided definitive evidence of their molecular structures. All synthesized compounds displayed potential anti-mycobacterial activity with MICs in the low range (1.6-25 μg/mL). The synthesized compounds were also subjected to evaluation of toxicity profiles, binding interactions with target protein, and molecular dynamics simulation. The compounds 5a, 5f, 5g, 5h, and 5l have shown significant docking scores *i.e.*, -8.0, -8.9, -9.1, -8.9, -8.8 kcal/mol respectively to interact with tuberculosis protein followed by other compounds with the related targets of DprE1, Polyketide synthase, and Protein kinase B. This implies that these compounds could serve as valuable scaffolds for the development of lead compounds in the ongoing effort to combat tuberculosis infections. Their effectiveness against *Mycobacterium tuberculosis*, combined with their low toxicity and strong binding interactions with relevant proteins, make them promising candidates for further drug development. Moreover, all the synthesized compounds were subjected to antioxidant activity assessment utilizing the DPPH method, revealing that all compounds exhibited varying degrees of moderate to substantial antioxidant activity.

Furthermore, a series of benzothiazole-based Schiff base ligands have been synthesized. The significance of schiff bases in organic chemistry is crucial due to their antitumor, antiviral,

antifungal, and antibacterial properties. Conventionally, Schiff base synthesis involves an organic base catalyst like piperidine. However, the emergence of base-free organic compound synthesis with heterogeneous catalysts has gained attention for its simplicity, high yield, and catalyst reusability. This study reports a comparative investigation into the synthesis of novel Schiff bases featuring indole components, utilizing piperidine as the organic base catalyst. Both methods yielded products with high efficiency, comprehensively characterized through diverse spectroscopic analyses. All the synthesized benzothiazole-indole based Schiff bases were assessed for their antioxidant activity along with the antimycobacterial activity. Notably, all the compounds exhibited robust antioxidant activity, emphasizing their potential as antioxidant agents capable of combating oxidative stress. Compound 3b showed remarkable antimycobacterial efficacy with MIC 1.6 µg/mL against the *Mycobacterium Tuberculosis* H37Rv strain (ATCC 27294). This finding not only underscores the diverse biological activities of these compounds but also positions compound 3b as a promising candidate for novel antimycobacterial treatments, holding significant implications for pharmaceutical research.

ACKNOWLEDGEMENTS

Though words are seldom sufficient to express gratitude and feelings, it gives me an opportunity to acknowledge those who helped me during the course of my studies.

First, I bow in reverence to ***Almighty*** *the cherisher and sustainer to benediction giving me the required zeal for completion of my research work. The successful completion of any research work is a matter of great endeavourance but, the personal and practical support of numerous people makes the job entirely enjoyable and simple. It is a pleasant aspect that I have now the opportunity to express my gratitude to them.*

I wish to express my deepest gratitude and indebtedness to my revered supervisor ***Dr. Praveen Kumar Sharma, Professor, Department of Chemistry, School of Chemical Engineering and Physical Sciences, Lovely Professional University, Punjab****, for his constant support, kind encouragement, immensely valuable ideas, suggestions and for having an unwavering attention. I have been amazingly fortunate to have a supervisor who gave me the freedom to explore on my own and at the same time the guidance to recover when my steps faltered. I shall remain indebted to him for his confidence in my work and most importantly for his kind affection during my Doctoral research. Simply his contribution is beyond the preview of acknowledgments and I feel very much honored. It has been a real privilege for me to get an opportunity to work under him, a teacher par excellence.*

I feel privileged to my sincere regards and gratitude to ***Dr. Syed Wajahat Amin Shah****,* ***Professor****,* ***Department of Chemistry****,* ***University of Kashmir****, for his valuable guidance and constant encouragement throughout my research work. I am also thankful to all the faculty members of the University for their Generous Support, encouragement, and valuable suggestions to improve the present work.*

I render my sincere thanks to ***Dr. Kailash Chandra Juglaan****,* ***HOS, School of Chemical Engineering and Physical Sciences, Lovely Professional University, Punjab*** *for giving me an opportunity to become a scholar of this esteemed department and for providing necessary amenities required for my research work.*

I would like to express my heartfelt appreciation to ***Dr. Gurpinder Singh*** *and* ***Dr. Harpreet Kaur*** *for their invaluable guidance and support throughout the course of my research work. Their expertise, keen insights, and thoughtful suggestions have played a pivotal role in shaping*

the direction and quality of my research. Their dedication to fostering intellectual growth and their willingness to share their knowledge have been instrumental in my academic journey. I feel incredibly fortunate to have had the privilege of working alongside such esteemed mentors who have not only enriched my research but also inspired me to aim for excellence. Their mentorship has been a cornerstone of my success, and I am truly grateful for their contributions to my research endeavors.

My heartfelt thanks to all my teachers right from school until now and all my well-wishers for their constant encouragement and wishes for my career. I also extend my thanks to all those, who have been directly or indirectly related to my project work.

My parents have been a strong pillar of support for me and my research would not have seen the day's light without their constant motivation. I owe them a lot. Thanks to ***my mother*** *for being my rock and helping me in touch with reality throughout my life. Special thanks to* ***my father*** *for letting me do it 'my way' and for encouraging and inspiring me to reach my dreams.*

I must record my sincere thanks to my esteemed siblings for their steady encouragement, timely support, unconditional love, and moral support, without whom I would never have enjoyed so many opportunities.

I particularly thank my colleagues for those sleepless nights, we were working together before deadlines and for all the fun we had during this research work. Without their precious support, it would not have been possible to conduct this research. I would like to express my gratitude towards their moral and emotional support that helped me in the completion of this thesis and inspired me to work tirelessly to accomplish this task. I also express my gratitude to all who knowingly and unknowingly contributed to the completion of this thesis.

Date: 06-05-2024 ***(Tanzeela Qadir)***

Place: Lovely Professional University, Punjab

TABLE OF CONTENTS

LIST OF TABLES

LIST OF FIGURES

LIST OF SCHEMES

LIST OF ABBREVIATIONS

ABBREVIATIONS	DESCRIPTION
AMP	Ampicillin
AMR	Antimicrobial Resistance
AMK	Amikacin
ATCC	American Type Culture Collection
ATP	Adenosine triphosphate
AchE	Acetylcholinesterase
BchE	Butyrylcholinesterase
BSA	Bovine Serum Albumin
BSC	Biosafety Cabinet
BTC6T	(2-(*n*-hexylamino)-4-(3`-*N*, *N*-dimethylamino-propyl) amino-6-(benzothiazol-2-yl) thio-1, 3, 5-s-triazine)
BTC8T	(2-(*n*-octylamino)-4-(3`-*N*, *N*-dimethylamino-propyl) amino-6-(benzothiazol-2-yl) thio-1, 3, 5-s-triazine)
CFU	Colony Forming Units
CF	Cystic Fibrosis
CIP	Ciprofloxacin
CV	Crystal Violet
CLSI	Clinical and Laboratory Standards Institute
CHIKV	Chikungunya virus
CAN	Cerium Ammonium Nitrate
DBN	1, 5-Diazabicyclo [4.3.0] non-5-ene
DBU	1, 8-diazabicyclo [5.4.0] undec-7-ene
DMP	Dess-Martin Periodinane
DMF	*N*, *N*-dimethylformamide
DCM	Dichloromethane
DMSO	Dimethyl sulfoxide
DABCO	1, 4-diazabicyclo [2.2.2] octane
DNA	Deoxyribonucleic Acid
DAPI	4', 6-Diamdino-2-Phenylindole
DMSO	Dimethyl Sulfoxide

DMF	Dimethylformamide
DNA	Deoxyribonucleic acid
DPPH	2, 2-diphenyl-1-picrylhydrazyl
ECACC	European Collection of Authenticated Cell Cultures
EDTA	Ethylenediamine tetra acetic Acid
EDG	Electron Donating Group
EWG	Electron Withdrawing Group
EIS	Electrochemical Impedance spectroscopy
ESKAPE	Enterococcus faecium, Staphylococcus aureus, Klebsiella pneumoniae, Acinetobacter baumannii, Pseudomonas aeruginosa, and Enterobacter species
FBS	Foetal Bovine Serum
FRAP	Ferric Reducing Antioxidant Power
FTIR	Fourier Transform Infrared Spectroscopy
GC	Growth Control
HCl	Hydrogen Chloride
HEK-293	Human Embryonic Kidney Cell Lines
hERG	ether-a-go-go-related gene
HCMV	Human Cytomegalovirus
ICLAC	International Cell Line Authentication Committee
ISO	International Organization for Standardization
LD50	Lethal Dose
MCF	Michigan Cancer Foundation
MABA	Microplate Alamar Blue assay
MDA	Malondialdehyde
MIC	Minimum Inhibitory Concentration
MBC	Minimum Bactericidal Concentration
MTT	(3-(4,5-Dimethylthiazol-2-yl)-2,5-Diphenyltetrazolium Bromide)
MRSA	Methicillin Resistant Staphylococcus Aureus
MDRE	Multi-Drug Resistant Escherichia Coli
MDR	Multidrug Resistance
MDR-TB	Multi-Drug Resistant Tuberculosis

MHB	Mueller Hinton Broth
MTB	Mycobacterium Tuberculosis
MC	Media Control
MDS	Molecular Dynamic Simulation
ns	Nanoseconds
nm	Nanometer
NSS	Normal Saline Solution
NMP	1-Methyl-2-pyrrolidinone
NA	Nutrient Agar
NCCS	National Centre for Cell Sciences
NaCl	Sodium Chloride
NSAIDs	Non-steroidal Anti-inflammatory Drugs
NMR	Nuclear magnetic resonance
OD	Optical Density
OECD	Economic Cooperation and Development
ORTEP	Oak Ridge Thermal-Ellipsoid Plot Program
OLEDs	Organic light-emitting diodes
PAE	Post Antibiotic Effect
PI	Propidium Iodide
PBS	Phosphate Buffer Saline
PIFA	Phenyliodine (III) Bis (trifluoroacetate)
PDAIS	Poly [4-diacetoxyiodo] styrene
PET	Positron emission tomography
RFTA	Riboflavin-2', 3', 4', 5'-tetraacetate
RNA	Ribonucleic acid
RMSF	Root Mean Square Fluctuations
RMSD	Root Mean Squarer Deviation
RNA	Ribonucleic Acid
RGy	Radius of Gyration
STR	Streptomycin
SAR	Structure-activity relationship
TBAI	Tetra-*n*-butylammonium iodide
THF	Tetrahydrofuran
TBAB	Tetra-*n*-butylammonium bromide

TEMPO	(2, 2, 6, 6-Tetramethylpiperidin-1-yl) oxyl
TEA	Triethylamine
TB	Tuberculosis
TDR-TB	Totally Drug Resistant Tuberculosis
TLC	Thin Layer Chromatography
XDR-TB	Extensively Drug-Resistant Tuberculosis

CHAPTER-1

INTRODUCTION

1.1. Heterocyclic Compounds

Heterocyclic compounds, commonly referred to as heterocycles, are organic chemical compounds characterized by a ring-like structure that incorporates one or more heteroatoms. These heteroatoms include elements like nitrogen, oxygen, sulfur, and others. The general structure of heterocycles resembles that of cyclic organic compounds comprised solely of carbon atoms, the replacement of one or more carbon atoms with heteroatoms imparts unique physicochemical properties to heterocycles, setting them apart from their all-carbon ring counterparts. This distinctiveness makes heterocyclic compounds invaluable in various fields of chemistry and industry. Heterocycles constitute a captivating and indispensable category of organic compounds with profound implications across a wide spectrum of scientific disciplines. The structural diversity and the unique properties conferred by heteroatoms make heterocycles a versatile and intriguing field of study in chemistry. The significance of heterocycles extends to the very foundation of life itself. In the realm of biochemistry, heterocycles are fundamental components of the genetic code. The nitrogenous bases adenine and guanine, integral to DNA, and uracil and cytosine, crucial in RNA, are heterocyclic compounds. These bases play an irreplaceable role in the storage and transmission of genetic information, underlining the indispensable nature of heterocycles in the continuity of life. Heterocycles are equally prominent in the world of pharmacology and medicine. A substantial portion of drugs and pharmaceuticals on the market contain heterocyclic motifs within their structures. The antimalarial drug quinine and antibiotics like penicillin also feature heterocyclic components. Such drugs owe their therapeutic efficacy to the specific properties conferred by heterocycles, emphasizing their pivotal role in improving human health. Beyond biology and medicine, heterocyclic chemistry extends its reach into materials science and technology. Researchers harness the versatility of heterocyclic compounds in the design and development of innovative materials. These include conducting polymers, which have applications in electronics and optoelectronics, and various dyes and pigments with applications in textiles, paints, and inks. Heterocyclic compounds also have a vital function in the synthesis of OLEDs, organic photovoltaics, and other cutting-edge technologies. Heterocyclic chemistry is also the cornerstone of synthetic organic chemistry. Researchers have developed a rich arsenal of synthetic methodologies for constructing a wide array of heterocyclic structures. These methodologies have proven indispensable in the creation of new pharmaceuticals, agrochemicals, and advanced materials [1-10].

In summary, heterocycles occupy a central and multifaceted role in the realm of organic chemistry and extend their influence into biology, medicine, materials science, and technology. Their unique structures, reactivity, and ubiquity in nature make them a captivating subject of study, with profound implications for addressing some of the most pressing challenges in science and innovation. Understanding the intricacies of heterocyclic compounds is not only a cornerstone of organic chemistry but also a gateway to innovation across a broad spectrum of scientific and technological disciplines.

1.2. Applications of Heterocyclic Compounds

Heterocycles play a pivotal role in numerous domains of science and technology because of the variety of chemical properties and applications that they possess. In the realm of pharmaceuticals, heterocyclic compounds are the backbone of countless drugs, from antibiotics like penicillin to anti-cancer agents such as paclitaxel. Additionally, they are vital components in agrochemicals, contributing to the development of pesticides and herbicides that safeguard crops. Heterocycles also find utility in the realm of materials science, where they serve as building blocks for polymers and conductive materials. Furthermore, in the field of organic electronics, they are used to fabricate OLEDs and organic photovoltaic cells. In summary, the applications of heterocycles are far-reaching, spanning pharmaceuticals, agriculture, materials science, and electronics, and they continue to drive innovation across various industries.

1.2.1. Anticancer Activity

Heterocycles have emerged as promising anticancer agents. These compounds exhibit diverse chemical structures and can target various molecular pathways involved in cancer progression. Heterocyclic compounds, through their ability to interact with specific cellular components, disrupt vital processes like DNA replication, protein synthesis, and cell signaling, ultimately inhibiting cancer cell growth and proliferation. Researchers continue to explore and design novel heterocyclic compounds with enhanced anticancer properties, offering hope for the development of more effective and targeted cancer treatments in the future.

Liu *et al.* described the synthesis of phenanthroindolizidine **1** and phenanthroquinolizidine alkaloids **2** as possible candidates for anticancer drugs. They demonstrated remarkable IC_{50} values, with phenanthroindolizidine **1** at 166 nM and phenanthroquinolizidine **2** at 2.1 nM. Most of the synthesized compounds displayed strong anti-proliferative effects against BEL-7402 and A549 cells. Notably, compound **2** exhibited the highest activity during the initial screening. A

detailed analysis of the mechanisms involved demonstrated that compound **2** efficiently inhibited cell growth and the formation of cell colonies by causing a slowdown in the progression of the S phase, achieved by blocking the synthesis of DNA [11].

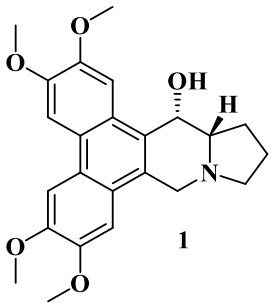

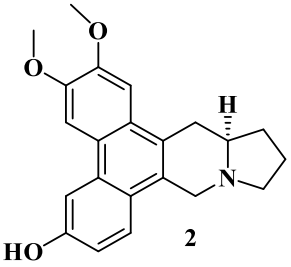

Thiazolyl derivatives **3** were examined for their antitumor activity against the hepatocarcinoma cell line. Most of these were quite effective against tumor cells and few displayed exceptional potencies. Analysis of aminothiazole derivatives after being screened for anticancer activity revealed that the carboxylate derivative of aminothiazole **4** manifested remarkable activity. Various alkylthiazole and alkylamine indazole derivatives **5** have been synthesized employing regioselective cyclization of indazolyldithio carbamates and thioureidoindazoles [12].

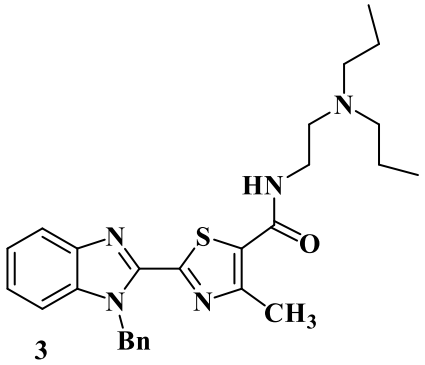

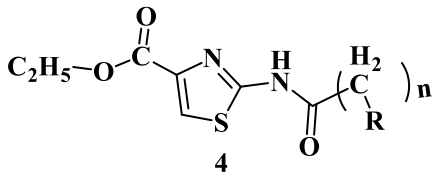

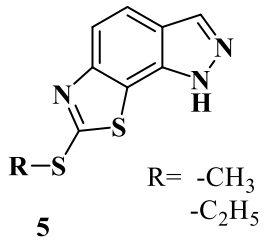

Wang *et al.* synthesized C-11 labeled fluorinated 2-arylbenzothiazoles **6** (GI_{50}< 0.1 nM for MCF-7 and MDA 468 breast cancer cell lines), which are employed in PET imaging of tyrosine kinase in cancer. Fluorinated 2-arylbenzothiazoles are novel prospective anticancer medicines that inhibit breast, lung, and colon cancer cell lines effectively and selectively [13].

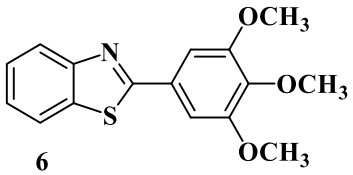

6

Scattolin *et al*. portrayed the synthesis and effectiveness of sulfenylated 2-phenylimidazo [1, 2-a] pyridines **7-9** as promising candidates for cancer treatment. All compounds demonstrate good/excellent activity against different human cancer cell lines *i.e.*, HepG2 (liver), MDA MB 231 (breast), A549 (lung), SKMEL-28 (skin melanoma), Hela (cervical), U87MG (glioblastoma), and DU-145 (prostate) by employing MTT assay [14].

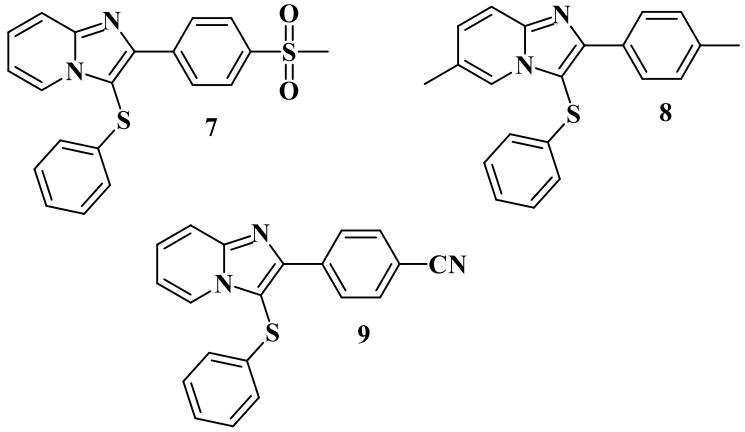

Fu *et al.* described the synthesis of 2-(4-hydroxy-3-methoxyphenyl)-benzothiazole. These compounds effectively hinder the proliferation and invasiveness of breast cancer cells. Additionally, compound **10** diminishes the ability to form cell clusters and it enhances the levels of the carboxyl terminus of the Hsp70-interacting protein, leading to the inhibition of cancer-promoting pathways. This ultimately lowers the ability of breast cancer cells to form tumors and metastasize [15].

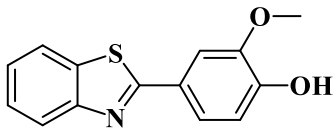

10

1.2.2. Anti-inflammatory Activity

Heterocycles have demonstrated their potential as effective anti-inflammatory agents. These compounds can modulate various inflammatory pathways in the body, offering a promising approach to combat inflammatory conditions such as arthritis, asthma, and autoimmune disorders. Heterocyclic compounds can inhibit key enzymes and signaling molecules involved in the inflammatory response, thus reducing the production of inflammatory mediators. Their diverse chemical structures provide a basis for designing drugs with specific anti-inflammatory properties and minimal side effects. As researchers continue to explore the therapeutic potential of heterocycles, they hold significant promise for the development of novel anti-inflammatory treatments that can improve the quality of life for individuals suffering from chronic inflammatory diseases.

Sondhi *et al.* synthesized 2-thiopyrimidine derivatives **11** and assessed for biological activity. The compounds showed good analgesic (50%), anti-inflammatory (37.4%), and kinase (CDK-1; IC_{50}: 0 μM, CDK-5; IC_{50}: >10 μM and GSK-3; IC_{50}: >10 μM) inhibitory activity [16].

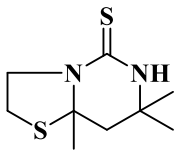

11

Balkan *et al.* described the synthesis of some thiazolo [4, 5-*d*] pyrimidine-7 (6*H*)-one derivative and investigated them for different biological activities. Compound **12 (**ED_{50}: 129 mg/kg) demonstrated anti-inflammatory and analgesic properties similar to acetyl-salicylic acid while compound **13** showed high anti-inflammatory activity (35%).

A series of formazylindoles were synthesized and evaluated for their effectiveness in reducing inflammation induced by carrageenan in albino rats. The results demonstrated a notable reduction in edema with a lower likelihood of causing ulcers, indicating their promising anti-inflammatory properties. Friedel Crafts' acylation between benzoxazine derivatives and substituted thiazoles afforded certain compounds that could act as possible cyclooxygenase-2 inhibitors. The inhibition activity was elucidated through chromogenic assay and one compound of the series **12** showed potent inhibitory activity. A substituted thiazole ring attached to quinazolines was synthesized by treating different isothiocyanates with amidines and screened for anti-inflammation activity for acute inflammation. Two compounds of the series showed

prominent inhibition activity. Numerous polysubstituted thiazoles after being tested for their anti-inflammatory activity demonstrated that compound **13** showed anti-inflammatory as well as analgesic activity with a fast mode of action [17].

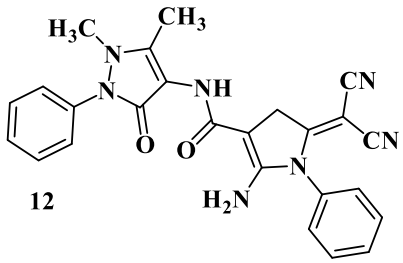

12

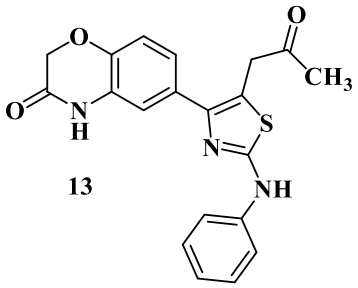

13

Mochona *et al.* accomplished the synthesis of tetrahydro pyridine derivatives **14** & **15** with substantial anti-inflammatory activity. The impact of substituents on pharmacological activity was tested in male Sprague-Dawley rats using the carrageenan-induced paw edema experiment. Analogs containing electron-donating substituents at positions 4 and 2 of the benzene moiety displayed strong anti-inflammatory effects, similar to Indomethacin [18].

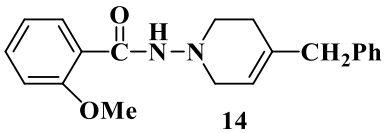

14

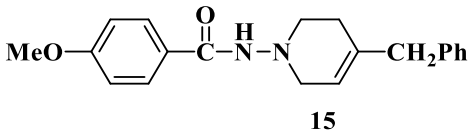

15

Amir *et al.* synthesized 2-substituted aryl 1, 3, 4-oxadiazoles **16** and tested for anti-inflammatory action (22.34% to 72.34%). Several synthesized compounds have anti-inflammatory properties similar to the standard drug ibuprofen. Moreover, in comparison to the standard antibiotic ofloxacin, all these compounds exhibit significant antibacterial effectiveness against *S. aureus* and *E. coli* [19].

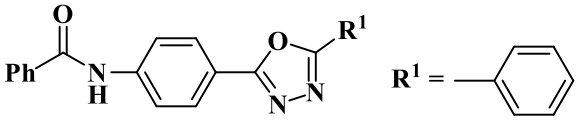

16

Kumar *et al.* synthesized indole-functionalized oxadiazoles **17** as potent anti-inflammatory agents. These derivatives were assessed to determine their anti-inflammatory and analgesic effects, demonstrating properties similar to those of the reference drugs [20].

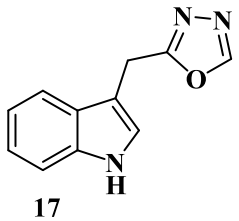

17

1.2.3. Antiviral Activity

Heterocycles have gained significant attention as potential antiviral agents. Their diverse chemical structures enable them to target various phases of the viral life cycle. Heterocyclic compounds have demonstrated the ability to inhibit key viral enzymes, disrupt viral protein interactions, and interfere with viral genome replication. This versatility makes them valuable candidates for the emergence of antiviral drugs against various types of viruses, including influenza, HIV, hepatitis, and emerging viral threats. Ongoing research into heterocyclic compounds holds promise for the creation of effective antiviral treatments and contributes to the global effort to combat viral infections.

Schwarz *et al.* reported the synthesis of Kaempferol and Kaempferol glycosides as possible candidates for 3a channel proteins of coronaviruses. The Kaempferol compound **18** with an IC_{50} value of 20 μM could be used to produce novel antiviral agents with increased bioavailability. In particular, the glycosides of Kaempferol **19** & **20** with IC_{50} values of 2.3 and 10 μM respectively appear to be important candidates for exploration as anti-coronaviral drugs. The significance of multi-target medicines is highlighted by the fact that they block the 3a channel, inhibiting virus replication and obstructing other viral life cycle stages [21].

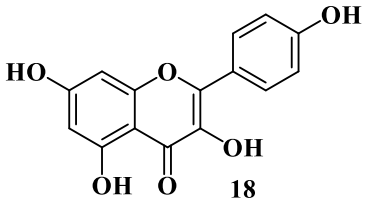

18

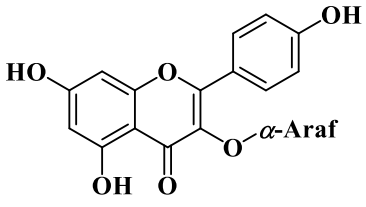

19

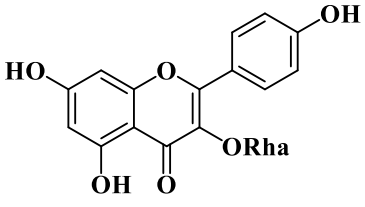

20

Araf: arabinofuranose
Rha: rhamnose

Hwa *et al.* explored some coumarin-based heterocyclic compounds **21** (CC_{50}: 178, 117, and 144 μM respectively; EC_{50}: 19.1, 10.2, and 17.2 μM respectively) & **22** (CC_{50}: 126 and 107 μM; EC_{50}: 58 and 19.0 μM) as the most potent inhibitors against the Chikungunya virus (CHIKV) [22].

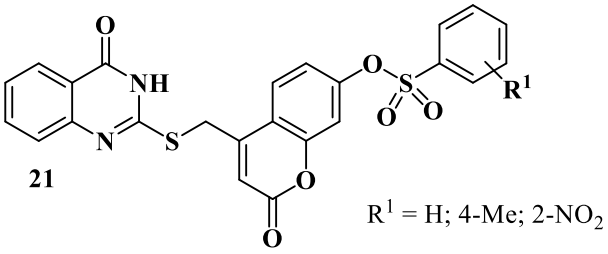

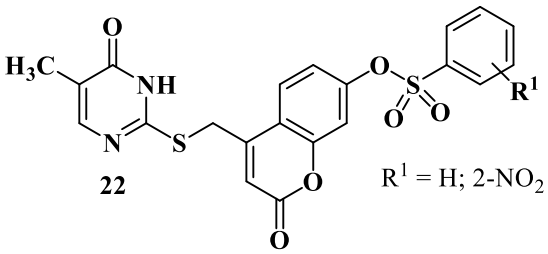

Kaur *et al.* synthesized and tested quinoline derivatives **23** for antiviral activity. The synthesized quinoline derivatives displayed remarkable antiviral activity [23].

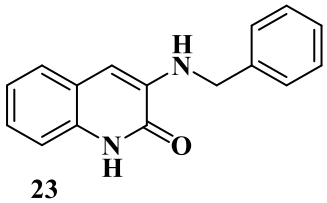

Kovaleva *et al*. synthesized *N*-heterocyclic hydrazine derivatives of camphor. Compound **24** showed the highest activity against the H1N1 influenza virus [24].

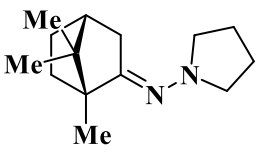

1.2.4. Antibacterial Activity

Heterocycles garnered significant interest as potential antibacterial agents. Their diverse chemical structures offer a wide range of possibilities for designing molecules that can target

bacterial pathogens. Heterocyclic compounds have demonstrated effectiveness in inhibiting bacterial growth and disrupting essential cellular processes in various ways, including interfering with DNA replication, inhibiting protein synthesis, and disrupting cell membrane integrity. As antibiotic resistance becomes an increasingly pressing global health concern, the exploration of heterocycles as antibacterial agents presents a promising avenue for the development of new and innovative treatments to combat bacterial infections and address the evolving challenges of antibiotic resistance.

El-Hashash *et al.* synthesized heterocyclic chalcone derivatives **25**, **27**, **28,** and spiro heterocycles **26** and evaluated them for antibacterial activity. Most of the synthesized compounds show the strongest antibacterial efficacy against all the microorganisms tested with the diameter of the zones equal to 1.1-1.2 cm (moderate activity; 55-65%) and 1.8-2.0 cm (high activity; 85-100%) respectively [25].

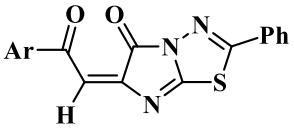

25

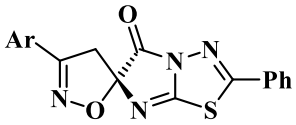

26

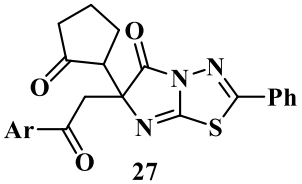

27

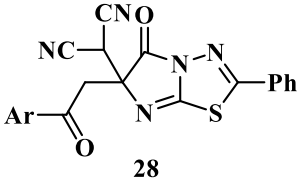

28

Ar = C_6H_4(4-$NHCOCH_3$)

Bouzian *et al.* synthesized new quinoline compounds **29** and **30** and investigated their antibacterial efficacy against *E. coli*, *S. aureus*, *E. faecalis*, and *P. aeruginosa*. These compounds exhibited outstanding antibacterial effectiveness specifically against *E. coli* and *S. aureus*, with a MIC of 6.25 μg/mL [26].

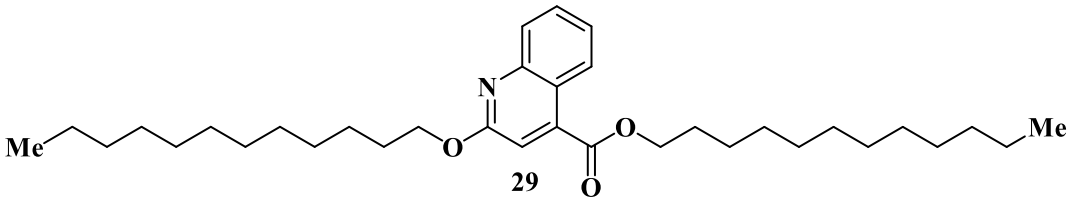

29

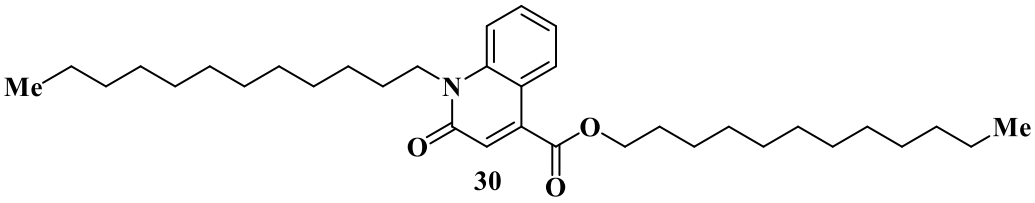

30

Santosh *et al.* synthesized novel triazole-linked chalcone derivatives **31** & **32** and screened them for antibacterial efficacy against *B. subtilis*, *P. aeruginosa*, *S. aureus*, and *E. coli* with MIC values ranging between 44-79 and 63-82 mM respectively [27].

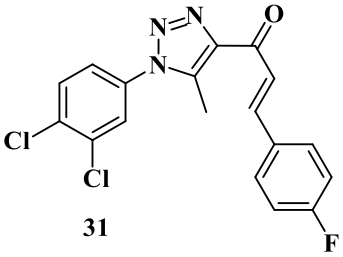

31

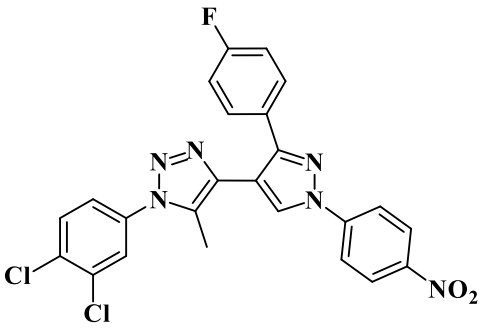

32

Kritchenkov *et al.* synthesized novel chitosan derivatives **33** and tested them for antibacterial activity. When compared to commercial antibiotics ampicillin and gentamicin, the synthesized compound has a strong antibacterial activity [28].

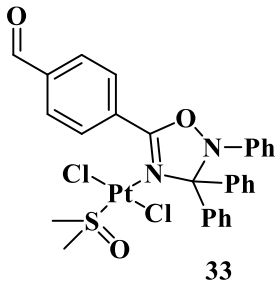

33

Burmeister *et al*. synthesized Ruthenium (II) *N*-heterocyclic carbene complexes as antibacterial agents and bacterial thioredoxin reductase inhibitors. Compound **34** was the most potent against *S. aureus*, having a MIC value of 19.5 μM [29].

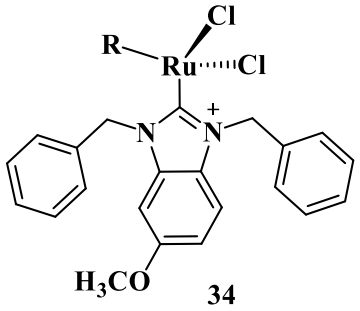

34

1.2.5. Anti-Alzheimer Activity

Heterocycles have shown promise in the realm of Alzheimer's disease research. These compounds possess the potential to modulate various biochemical processes implicated in the onset and progression of Alzheimer's. Heterocyclic compounds can interact with specific targets in the brain, such as amyloid plaques and neurofibrillary tangles, which are hallmark features of the disease. Through their ability to mitigate these pathological factors and possibly enhance cognitive function, heterocycles represent a compelling avenue for the development of innovative anti-Alzheimer's therapies, providing a ray of hope in the quest to combat this devastating neurodegenerative disorder.

Abdalla *et al.* synthesized some pyrimidine and thiopyrimidine hybrids **35 & 36** with IC_{50} values of 4.10, 3.41, 3.28, and 9.51 nM respectively fused with steroidal structure and tested them against Alzheimer's disease. Most of these compounds have shown remarkable activity against Alzheimer's disease [30].

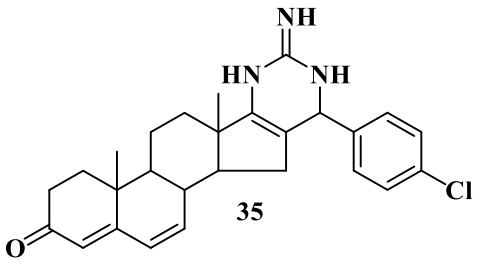

35

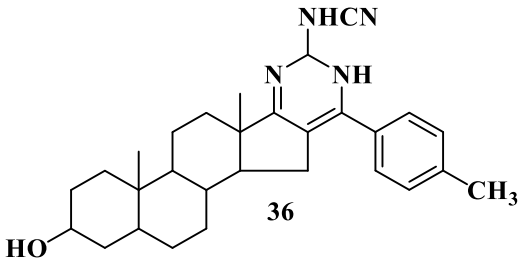

36

Attaby *et al.* synthesized bipyridine derivatives **37** and assessed them for anti-Alzheimer activity. Their relative efficacy as anti-Alzheimer drugs in comparison to Flurbiprofen is high enough,

however, their relative potency reduced following their reactions to afford the equivalent bipyridine-5-carbonitriles [31].

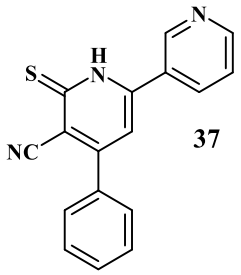

37

Gulcin *et al.* synthesized tris (2-pyridyl) phosphine (selenide) sulfide **39**, 4-benzyl-6-(thiophene-2- yl) pyrimidin-2-amine **40,** and sulphur-containing pyrroles **38** as potent substances to block or impede the progression of Alzheimer's disease. All the compounds showed IC_{50} values in the range of 13.51-26.55 nM against α-glycosidase, 0.54-31.22 nM against BchE, and 13.13-22.21 nM against AchE. As a result, nitrogen, phosphorus, selenium, and sulphur-containing heterocyclic compounds exhibited significant inhibitory profiles against the identified metabolic enzymes [32].

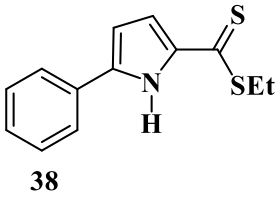

38

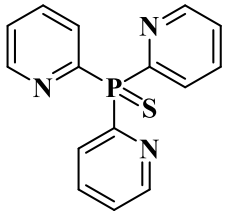

39

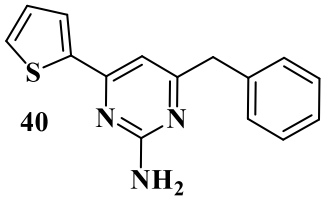

40

Rastegari *et al.* synthesized derivatives of 1, 2, 3-triazole chromenone carboxamide, specifically compound **41**, which displayed robust inhibitory activity against acetylcholinesterase, boasting an IC50 value of 1.80 μM. Moreover, this compound displayed effective neuroprotective qualities by mitigating H_2O_2-induced cell mortality in PC12 neurons. Additionally, it demonstrated the ability to chelate metal ions, specifically Fe^{2+}, Cu^{2+}, and Zn^{2+} [33].

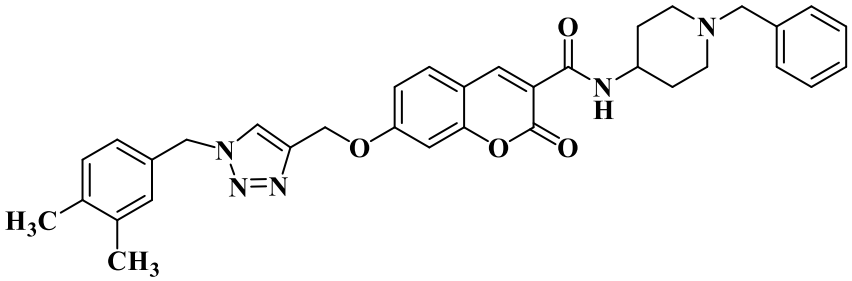

41

Attaby *et al.* synthesized 2-substituted thienopyridines and tested them against Alzheimer's disease. In general, the compounds with phenyl moiety **42** have shown high activity against Alzheimer's disease as compared to the compounds with phenyl-*p*-methoxy moiety **43**. Also, the potency of synthesized compounds as anti-Alzheimer agents relative to Flurbiprofen is high enough [34].

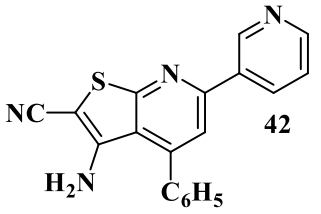

42

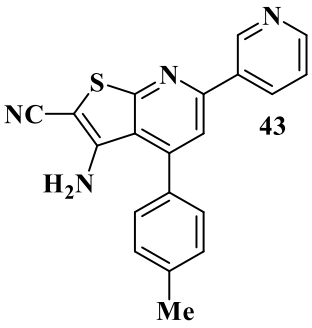

43

Latif *et al.* synthesized heterocyclic compounds derived from benzimidazole-2-thiol and investigated their *in vitro* anticholinesterase potential. They conducted assessments on AchE and BchE enzymes across various concentrations, spanning from 62.5 to 1000 μg/mL. Remarkably, two of the synthesized compounds, specifically compound **44** and compound **45**, displayed substantial efficacy against the enzymes under examination. Compound **44**, in particular, exhibited dual inhibitory effects, with IC_{50} values of 121.2 μM for AchE and 38.3 μM for BchE, respectively [35].

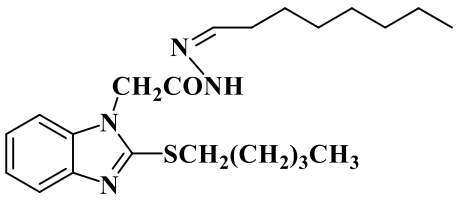

44

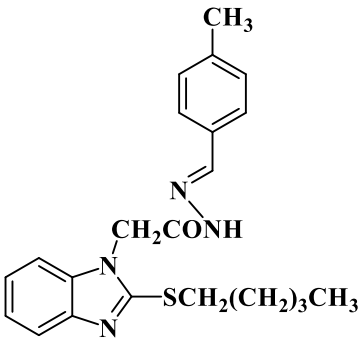

45

1.2.6. Antidiabetic Activity

Heterocycles have surfaced as potential contenders for the creation of medications to combat diabetes. These compounds display a broad spectrum of pharmacological effects that can be harnessed to address diabetes and its complications. Heterocyclic compounds have been shown to influence insulin signaling, improve glucose metabolism, and reduce insulin resistance. Additionally, some heterocyclic compounds possess antioxidant properties, which can mitigate oxidative stress often associated with diabetes. As researchers delve deeper into the potential of heterocycles, they offer hope for innovative and more effective treatments to manage diabetes and its associated complications, providing better options for individuals affected by this prevalent metabolic disorder.

Prabhat *et al.* developed the synthesis of benzothiazoles and explored their antidiabetic activity. In diabetic rats, the synthesized compound **46** caused a greater drop in blood glucose than the other compounds. The estimated LD50 values for the compounds that were synthesized fell within the range of 100 to 1000 mg/kg [36].

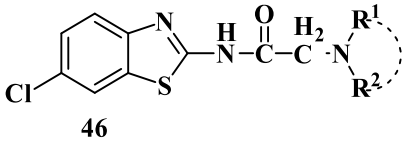

46

-NR^1R^2 = diethanolamino; morpholino; piperidino; 4-sulfanilido

Nabil *et al.* synthesized curcumin-based heterocyclic compounds **47** & **48** with IC_{50} values of 200.2 and 95.5 μM respectively as potent antidiabetic agents. The authors revealed that pyranone and pyrimidinone derivatives of curcumin exhibit high potential against diabetics [37].

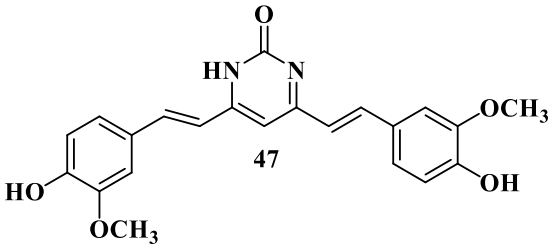

47

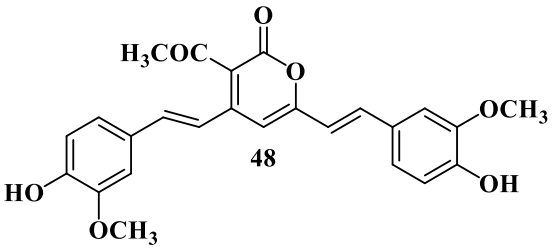

48

Dalavai *et al.* synthesized quinolinyl amino nitriles and evaluated them for different biological properties. Compounds **49 & 50** demonstrated promising antidiabetic activity with an IC_{50} value of 100 μg/mL [38].

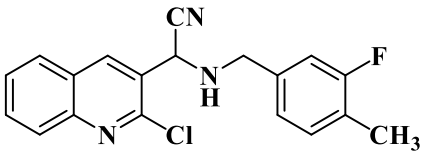

49

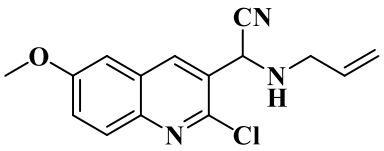

50

Toumi *et al.* synthesized rhodanine-fused spirooxindole pyrrolidine hybrids **51** with IC_{50} values of 1.49±0.10, 1.50±0.07, and 1.57±0.10 μM±SD respectively & **52** with IC_{50} value of 1.59±0.08 μM±SD as new *α*-amylase inhibitors. The majority of the synthesized compounds demonstrated high *α*-amylase inhibition [39].

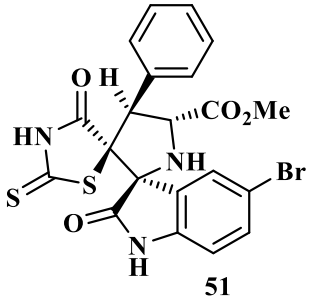

51

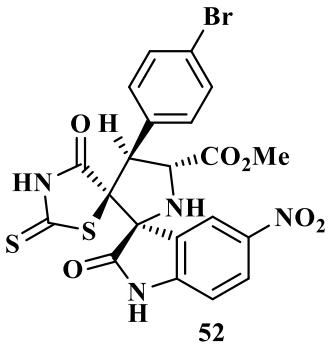

52

1.2.7. Antifungal Activity

Heterocycles have proven to be valuable candidates as anti-fungal agents. Fungal infections pose a significant health threat, and the rise of antifungal resistance has underscored the need for novel treatment options. Heterocyclic compounds exhibit a wide spectrum of antifungal activities, with mechanisms that target crucial fungal cellular processes. These compounds can disrupt fungal cell membranes, inhibit key enzymes involved in fungal growth, and interfere with nucleic acid synthesis, ultimately preventing fungal proliferation and survival. As researchers continue to explore the vast chemical diversity of heterocycles, they hold great promise for the development of more effective and targeted antifungal therapies to combat a broad range of fungal infections, from common skin conditions to life-threatening systemic diseases. As the number of fungus infections rises, so does the need for the anti-fungal medicine Ampho B **53**, which is often used to treat fungal infections [40].

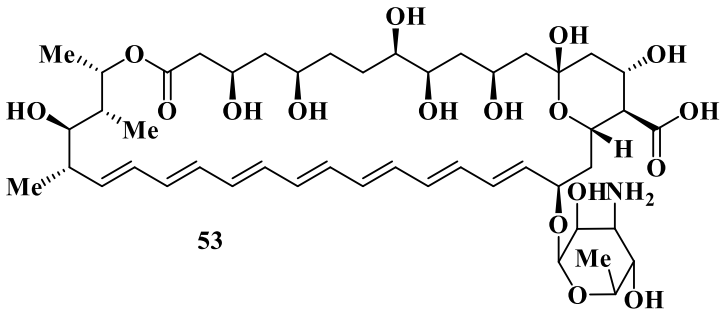

53

Tighadouini *et al.* synthesized *β*-keto-enol pyridine and furan hybrids and examined their antifungal activity against *B. subtilis*, *M. luteus,* and *F. oxysporum*. Compound **54** with an IC_{50} value of 12.83 μg/mL manifested excellent antifungal efficacy against the tested fungal strains [41].

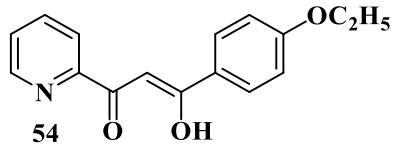

54

Morcoss *et al.* pioneered the synthesis of benzimidazole derivatives **55** as potent antifungal agents targeting *C. neoformans var. grubii* and *C. albicans*, demonstrating MIC values spanning from 4 to 16 μg/mL [42].

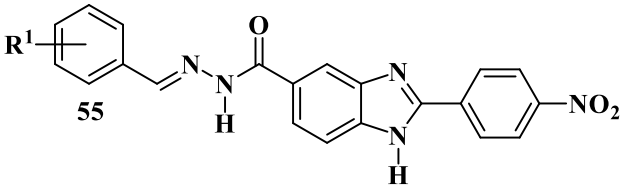

55

R^1 = H; 4-Cl; 2,4-Cl

Zhao *et al.* synthesized heterocyclic derivatives **56** and **57**, investigating their antifungal potential against *C. neoformans*, and *C. albicans A. fumigatus*, revealing MIC values of 0.5, 0.0625, and 4 μg/mL, respectively [43].

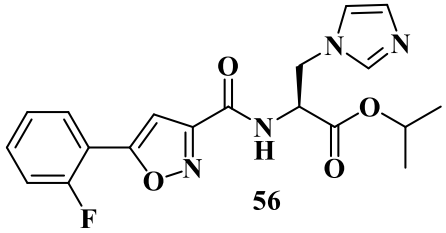

56

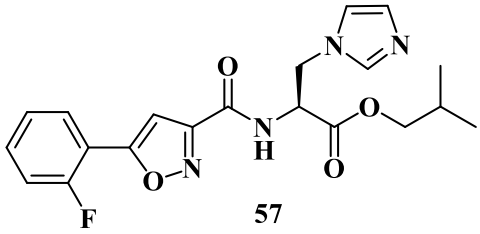

57

Mi *et al.* developed the synthesis of chitosan derivatives **58** that incorporate heterocyclic components, exhibiting notable antifungal potency. They evaluated their *in vitro* antifungal

effectiveness against pathogenic fungi from two plant species, *Colletotrichum lagenarium* and *Phomopsis asparagi*, utilizing the plate growth rate method [44].

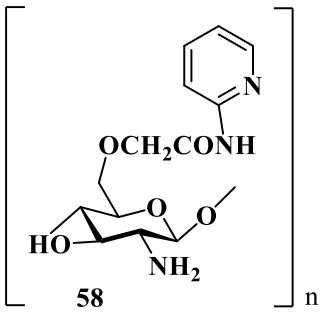

58

1.2.8. Heterocycles as Agrochemicals

Heterocycles have arisen as one of the prominent agents for crop protection. Cutting-edge development in the synthesis and design of agrochemicals has formed the backbone of the agrochemical industry. More than 70% of the already introduced agrochemicals possess heterocyclic scaffolds primarily containing one or more nitrogen atoms. State-of-the-art organic chemistry used to manufacture advanced crop protection chemicals includes the production of three commercially available fungicides, boscalid, fludioxonil, and benomyl. Crop protection chemistry has occupied an important domain in organic chemistry as structure-based designs are needed to achieve the required targets. Pinoxaden is a new herbicide used to reduce the growth of grass weeds in cereals. Similarly, the nitrogen-containing fungicide Bixafen shows significant activity against a broad spectrum of cereal diseases. Another commonly used insecticide is a nitrogen heterocycle called Indoxacarb **59**, which is effective against Lepidoptera in fruits, vegetables, and cotton. a) Pinoxaden b) Bixafen c) Indoxacarb.

The structure-based design has been an emerging discipline within crop protection research. The likelihood of finding better analogs has increased by incorporating virtual screening methods. Nitrogen heterocycles form prominent scaffolds in this regard. A potential library of such herbicides can be generated, keeping the core structure the same and altering the attached linkers. Structural optimization of certain basic nitrogen heterocycles has led to the discovery of various novel heterocycles. For example, using heterocyclic herbicides like flupropacil and imadapyracil as a template led to the discovery of triazoylpyridines possessing fungicidal activity from the former, and phenylpyridadinones were selected as leads from the latter. Better analogs were

synthesized after replacing the 1, 3, 5-triazine nucleus with a pyrimidine nucleus, considering the structural similarity and the characteristics of known bleaching herbicides. A distinct class of fungicides has arisen due to speculative chemistry that attempted to introduce the carboxylic group into the pyridine nucleus. *N*-butylated pyridines have also shown dominant fungicidal properties. This compound became a lead in synthesizing many potent fungicides that have shown better results and a broad fungicidal spectrum. This led to the discovery of the fact that the 2, 6-disubstituted pyridine ring is one of the major structures that possess fungicidal activity. Dramatically enhanced fungicidal activity has been reported in derivatives comprising a 1, 2, 4-triazole ring attached to the pyridine ring. SAR studies reveal that a striking change in the activity can be observed by replacing the pyrimidine ring with a pyridine ring. Finally, pyridinyl pyrimidine derivatives were selected as promising candidates for pre-commercialization. Moreover, introducing certain groups like the trifluoromethyl group at position 6 of the pyrimidindione ring significantly added to its herbicidal activity. Upon structural optimization of flupropacil, the herbicidal activity was noticed while changing the heterocyclic ring, the phenyl ring, or the substituents, and it was revealed that the 2, 4, 5-trisubstituted phenyl ring would lead to optimum activity. Nitrogen heterocycles have also proved beneficial in controlling undesired vegetation, unchecked growth of weeds, a significant reduction in productivity, *etc*. The invention of certain heteroaryl azoles and their *N*-oxides is noteworthy. Certain heterocyclic compounds like azines or azoles bearing trifluoromethoxy group show remarkable biological activity and are used as proinsecticides, growth regulators, and herbicides. In this context, 2-amino-5-trifluromethoxy benzothiazole and thiazolo-5- carboxylic acid are known for their fungicidal property. 2-thiohydantoins are also being utilized in the synthesis of various fungicides and herbicides. The incorporation of the trifluoromethoxy group further enhances its activity in the structure. The group also showed a similar effect on being linked to pyrimidines and quinolines. Certain azoles are also responsible for enhancing the resistance of plants toward various abiotic factors. The fungicidal action of various azoles like prothioconazole and tebuconazole is very well known and is based on sterol biosynthesis inhibition. These stress-tolerating effects are expected to give a linear correlation of stunting or growth regulatory action. In oilseed, it has been observed that a combination of certain azoles with abscisic acid increases the plant resistance against certain abiotic factors that result in abnormal stunting of plants. It has been revealed that fertilizers that usually counteract abiotic stress conditions like osmotic stress,

water-logging, drought, cold temperature, heat exposure, salinity, increased exposure to minerals, *etc*., are mostly nitrogen-bearing heterocycles. In this regard, mention should be made of NPK fertilizers that are highly commercialized. Insecticidal compounds of general formula **60**; Where A represents a 6/5 membered heteroaryl group comprising one or more heteroatoms selected from N, O, or S. Y represents a three-membered straight chain with at least one of the three members being CH_2-, O, S or N-R′ where R′ represents the group **61**; Where R represents hydrogen or halogen atom, X represents CH or N, R represents a methyl group or hydrogen atom, and Y represents nitro or cyano group. The bioefficacy of sulfanyl derivatives of thiadiazoles was evaluated against two phytopathogenic fungi, *Rhizoctonia solani,* and *Rhizoctonia bataticola*. The most effective compounds among these were nano-sized to further enhance their fungicidal activity. The nano-forms of 1, 3, 4-thiadiazole derivatives were characterized via electron microscopy and a particle size analyzer. The nano-forms showed 2-3 times higher fungicidal activity than the corresponding conventional-sized 1, 3, 4-thiadiazole derivatives. Nano sizing of potent thiadiazoles thus enhanced the bioactivity of those heterocycles more than the generally used compounds. Certain novel heterocycles have shown predominant insecticidal activity. Aryl alkyl imidazole **62** shows prominent insecticidal activity against cotton aphids [45].

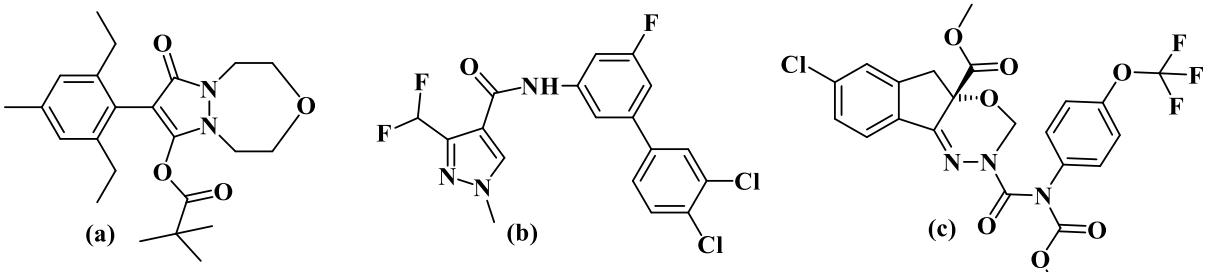

59

(a) Pinoxaden (b) Bixafen (c) Indoxacarb

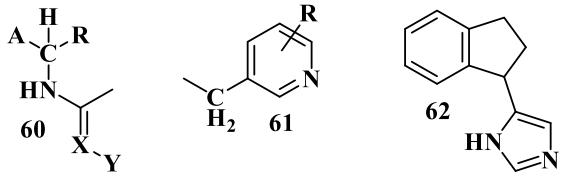

1.2.9. Heterocycles as Dyes

Heterocycles Heterocyclic compounds have found widespread use in the field of dyes and pigments due to their diverse chemical structures, vibrant colors, and tunable properties. These

compounds serve as the building blocks for a vast array of dyes used in textiles, paints, inks, and other applications. One common example is the class of azo dyes, which often contain heterocyclic rings as key components. Azo dyes are known for their bright and intense colors, making them popular choices for coloring textiles and other materials. Pyrazolones and pyridones, both heterocyclic compounds, are frequently used as intermediates in the synthesis of azo dyes. Another group of heterocyclic dyes includes the anthraquinone dyes, which are characterized by their deep and stable colors. Anthraquinone itself contains a heterocyclic ring and serves as a precursor for various blue, red, and violet dyes used in the textile and printing industries. Heterocyclic compounds also contribute to the development of organic pigments with excellent light fastness and colorfastness properties. Examples include phthalocyanine pigments, which are used in a diverse array of uses, including inkjet inks, paints, and plastics. In addition to this, other heterocycles like Imidazole-containing hetero-system, six-membered heterocyclic rings containing nitrogen, and pyrazine ring (a convenient moiety for functionally diverse chromophores) are also known for their significant dye-inducing ability. Thermal isomerization kinetics has been reported in neutral azo dyes like those in benzothiazoles. These green light-activable molecules have become promising building blocks for molecular switches [46].

Overall, the versatility of heterocyclic compounds allows for the creation of a broad spectrum of dyes and pigments with diverse colors and performance characteristics, making them indispensable in the world of coloration and visual aesthetics **63-65**.

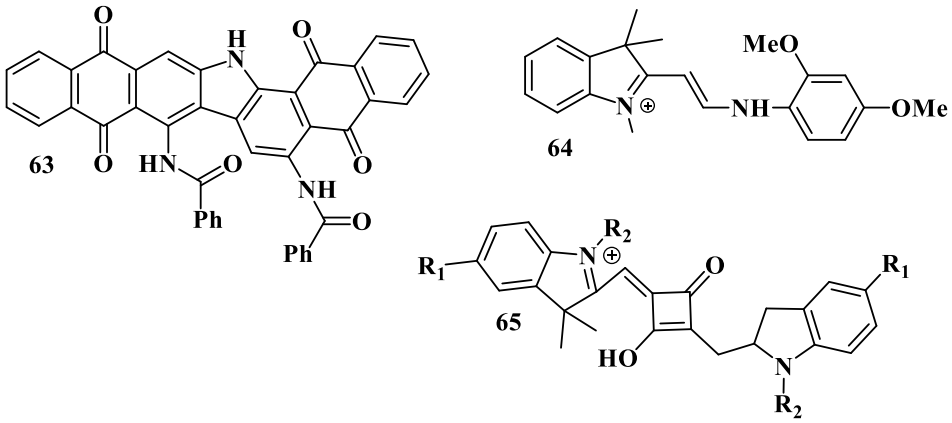

1.2.10. Heterocycles as Corrosion Inhibitors

Heterocycles also find significant applications as corrosion inhibitors in the realm of materials protection and corrosion control. Heterocyclic compounds, particularly those containing nitrogen, sulfur, or oxygen atoms within their ring structures, exhibit remarkable corrosion

inhibition properties. These heterocyclic compounds function as protective shields on the metal surface, creating a thin layer that hinders the electrochemical processes responsible for corrosion. Examples of heterocyclic corrosion inhibitors include imidazoles, triazoles, thiazoles, and pyridines, among others. These compounds are often added to coatings, paints, or corrosion-resistant fluids to enhance the longevity and performance of metal structures and components. The versatility of heterocyclic corrosion inhibitors lies in their ability to tailor their chemical structure to specific corrosion environments and metal types, making them valuable tools in mitigating the economic and safety challenges posed by corrosion in various industrial settings. Their application extends to pipelines, storage tanks, aircraft, and numerous other critical infrastructure components, ensuring the protection and durability of materials in diverse and corrosive conditions.

Iron and its alloys are essential and are being used extensively in industries. As such, it becomes mandatory to identify materials for their corrosion inhibition. Corrosion inhibitors ensure that there is no/less metal dissolution. In this context, it has been noticed that heterocyclic compounds containing electronegative functional groups and conjugated π-electron systems display strong inhibitory properties. There is also a peculiar interaction between the metal surface and functional groups that contain heteroatoms like nitrogen, oxygen, and sulphur. Nitrogen heterocycles, particularly pyrazine and quinoxaline derivatives, are common corrosion inhibitors mainly due to the presence of two or more nitrogen atoms that facilitate electrophilic attack. Many quinoxalines derivatives are currently being explored for their significant corrosion inhibition activity against copper and steel in an acidic medium. Similarly, pyrazines are a component of certain polycyclic compounds of industrial and biomedical importance. All its compounds can act as bridging ligands and have a characteristic low-lying unoccupied π-molecular orbital. Due to this, pyrazines have been preferably investigated as corrosion inhibitors in different acidic mediums. Pyrazines and their derivatives have different inhibition activities depending on the nature of metal-heteroatom interactions of any specific metal in an acidic solution. Recently, molecular simulation studies have revealed the mechanism of corrosion inhibition via the interaction of molecules with the surface atoms of the metal. Electrochemical Impedance spectroscopy gives a detailed analysis of the kinetics of surface properties and electrode processes. Augmentin, also a nitrogen heterocycle showed maximum inhibition efficiency of 93.6% at 300 ppm and acted as a mixed-type inhibitor. Lansoprazole and

Esomeprazole showed prominent corrosion inhibition properties for copper in 1M HNO_3 revealed by using Tafel polarization, electrochemical impedance spectroscopy, scanning electron microscopy, and weight loss techniques. Amlodipine Besylate exhibits corrosion inhibition activity that increases with an increase in concentration. Benzothiazole shows corrosion inhibition efficiency on stainless steel in 3M H_2SO_4 after being analyzed via various techniques like potentiodynamic polarization, optical microscopy, IR spectroscopy, *etc*. Results revealed effective corrosion inhibition and significant chemisorption. Cephapirin serves as a corrosion inhibitor for carbon steel in HCl and demonstrates effective mixed-type inhibition behavior. Another Nitrogen heterocycle employed for corrosion inhibition is Clopidogrel, and the efficiency reached 80-90% **66-74** [47-50].

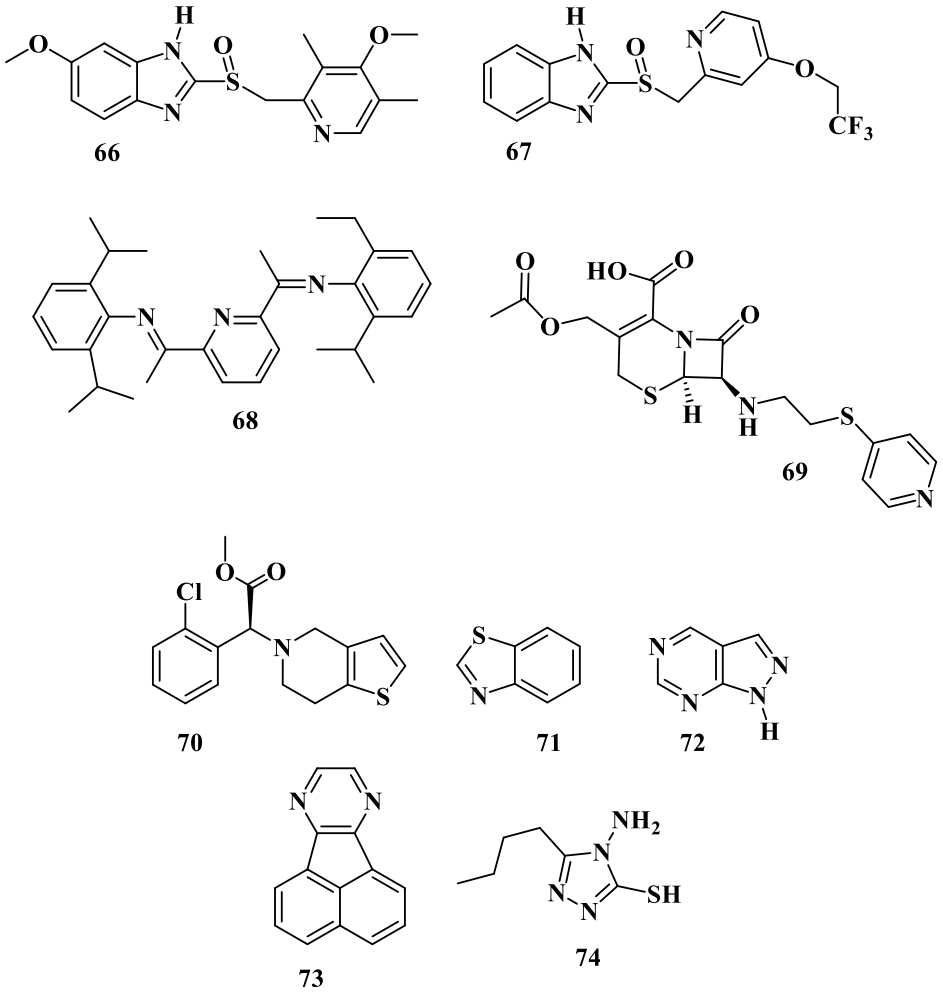

1.2.11. Heterocycles as Antioxidants

Heterocycles play a crucial role in the realm of antioxidants, where their unique chemical structures and properties contribute to their effectiveness in combating oxidative stress. These compounds, characterized by the presence of at least one non-carbon atom within a ring structure, exhibit diverse antioxidant activities. For instance, certain heterocyclic compounds like flavonoids, which contain oxygen heteroatoms in their ring structures, are known for their ability to scavenge free radicals and prevent cellular damage caused by oxidative stress. Similarly, nitrogen-containing heterocycles such as quinolines and pyridines possess redox-active properties, making them potent antioxidants that can intercept harmful reactive oxygen species (ROS) and inhibit lipid peroxidation. The versatile nature of heterocycles, combined with their capacity to modulate redox processes, underscores their significance in the development of novel antioxidants with potential applications in various fields, including pharmaceuticals and food science.

Thiazole and thiophene derivative **75** obtained from acetyl coumarin and thiazolines via cyclization of various thiosemicarbazones **76** were assessed for their antioxidant activity. All those compounds exhibited remarkable radical scavenging activity. Thiazolidinone derivatives of 1,3-thiazole and 1,3,4-thiadiazole **77** via *in vitro* tests, like DPPH and TBARS, demonstrated good results, constituting a potential class of candidates for drug development [51].

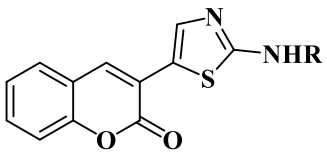

75

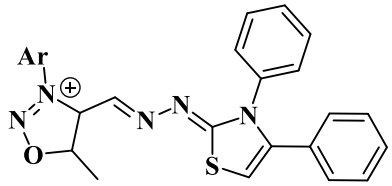

76

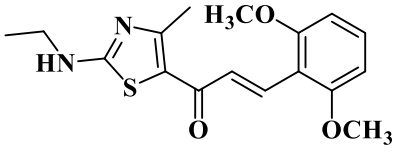

77

R = -$COCH_2CN$, -N

Ar = C_6H_6, 4-$CH_3OC_6H_4$, 4-$C_2H_5OC_6H_4$

A series of sulfanyl derivatives of thiazoles were designed and studied for their antioxidant properties by determining their effect on the formation of superoxide anion. Studies revealed

chlorobenzyl derivative **78** as the most potent superoxide ion scavenger. A novel series of urea, selenourea, and thiourea derivatives with thiazole moiety **79** were characterized and screened for their antioxidant activity using various radical scavenging methods. A preliminary examination of the structure-activity relationship showed that these compounds exhibited potent anti-oxidizing ability, making this class of compounds worthy of further investigation [52].

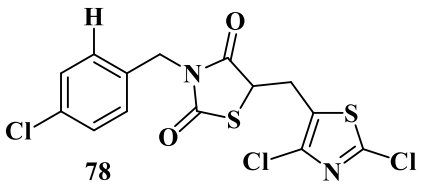

78

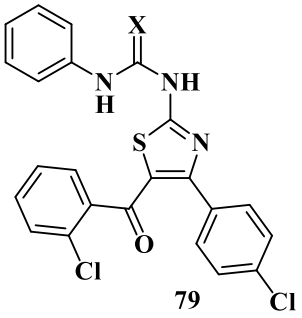

79

Various spiro and oxo-hydrazone derivatives of imidazole **80** and **81** have been synthesized and evaluated for antioxidant activity. All the compounds have a similar scaffold and were evaluated by different methods, like FRAP, Anti-LPO, ABTS radical scavenging, *etc*. A structure-activity relationship analysis was performed, and a relationship between the biological, physicochemical, and medicinal properties of the derived compounds was analyzed. In addition to this, the pharmacokinetics of these compounds suggest that their nature complies with the drugs already used as antioxidants. The findings explained that the oxohydrazone and spirothiazolidine derivatives of thiazole could be promising candidates for further structural modifications to obtain more potent antioxidant agents [53].

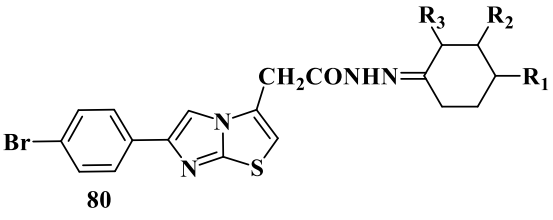

80

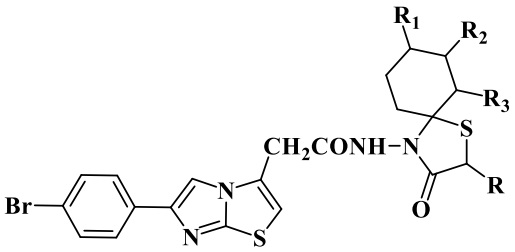

81

1.3. Conclusion

Heterocyclic compounds represent a crucial category of organic molecules in the field of medicinal chemistry, serving as medications for diverse diseases. The remarkable achievements underscore the broad spectrum of therapeutic applications associated with these compounds. Their significance lies in being versatile targets for synthesis and pivotal structural elements in both organic synthesis and medicinal chemistry due to their compelling biological activities. The pharmaceutical community has shown significant interest in the multifaceted applications of heterocycles, including their potential as anticancer, anti-inflammatory, antifungal, antibacterial, anti-Alzheimer, antiviral, antidiabetic agents, and more. Notably, an increasing array of heterocycles is being recognized as potential drug candidates in ongoing drug development endeavors.

References

1. Khan, A., Jasinski, J.P., Smolenski, V.A., Hotchkiss, E.P., Kelley, P.T., Shalit, Z.A., Kaur, M., Paul, K. and Sharma, R., 2018. Enhancement in anti-tubercular activity of indole based thiosemicarbazones on complexation with copper (I) and silver (I) halides: structure elucidation, evaluation and molecular modelling. *Bioorganic Chemistry*, *80*, pp.303-318.
2. Qadir, T., Altaf, S., Aasif, M., Fadul, A.N., Yatoo, G.N., Jangid, K., Mir, M.A., Shah, W.A. and Sharma, P.K., 2023. Design, synthesis, and unraveling the antibacterial and antibiofilm potential of 2-azidobenzothiazoles: Insights from a comprehensive in vitro study. *Frontiers in Chemistry*, *11*, p.1264747.
3. Qadir, T., Amin, A., Sharma, P.K., Jeelani, I. and Abe, H., 2022. A review on medicinally important heterocyclic compounds. *The Open Medicinal Chemistry Journal*, *16*(1).
4. Mahmood, R.M.U. and Aljamali, N.M., 2020. Synthesis, Spectral Investigation and Microbial Studying of Pyridine-Heterocyclic Compounds. *European Journal of Molecular and Clinical Medicine*, *7*(11), pp.4444-4453.
5. Midya, S.P., Landge, V.G., Sahoo, M.K., Rana, J. and Balaraman, E., 2018. Cobalt-catalyzed acceptorless dehydrogenative coupling of aminoalcohols with alcohols: direct access to pyrrole, pyridine and pyrazine derivatives. *Chemical Communications*, *54*(1), pp.90-93.
6. Chaucer, P. and Sharma, P.K., 2020. Study of thiazines as potential anticancer agents. *Plant Archives*, *20*(2), pp.3199-3202.
7. Zhang, H. and Liu, C., 2017. Synthesis and properties of furan/thiophene substituted difluoroboron β-diketonate derivatives bearing a triphenylamine moiety. *Dyes and Pigments*, *143*, pp.143-150.
8. Amin, A., Qadir, T., Sharma, P.K., Jeelani, I. and Abe, H., 2022. A Review on the Medicinal and Industrial Applications of N-Containing Heterocycles. *The Open Medicinal Chemistry Journal*, *16*(1).
9. Hossain, M. and Nanda, A.K., 2018. A review on heterocyclic: synthesis and their application in medicinal chemistry of imidazole moiety. *Science*, *6*(5), pp.83-94.
10. Jampilek, J., 2019. Heterocycles in medicinal chemistry. *Molecules*, *24*(21), p.3839.
11. Liu, Y., Qing, L., Meng, C., Shi, J., Yang, Y., Wang, Z., Han, G., Wang, Y., Ding, J., Meng, L.H. and Wang, Q., 2017. 6-OH-phenanthroquinolizidine alkaloid and its derivatives exert

potent anticancer activity by delaying S phase progression. *Journal of medicinal chemistry*, *60*(7), pp.2764-2779.

12. Thigulla, Y., Kumar, T.U., Trivedi, P., Ghosh, B. and Bhattacharya, A., 2017. One-Step Synthesis of Fused Chromeno [4, 3-b] pyrrolo [3, 2-h] quinolin-7 (1H)-One Compounds and their Anticancer Activity Evaluation. *Chemistry Select*, *2*(9), pp.2718-2721.
13. Wang, M., Gao, M., Mock, B.H., Miller, K.D., Sledge, G.W., Hutchins, G.D. and Zheng, Q.H., 2006. Synthesis of carbon-11 labeled fluorinated 2-arylbenzothiazoles as novel potential PET cancer imaging agents. *Bioorganic & medicinal chemistry*, *14*(24), pp.8599-8607.
14. Scattolin, T., Bortolamiol, E., Rizzolio, F., Demitri, N. and Visentin, F., 2020. Allyl palladium complexes bearing carbohydrate-based N-heterocyclic carbenes: Anticancer agents for selective and potent in vitro cytotoxicity. *Applied Organometallic Chemistry*, *34*(10), p.e5876.
15. Fu, D.J., Zhang, Y.F., Chang, A.Q. and Li, J., 2020. β-Lactams as promising anticancer agents: Molecular hybrids, structure activity relationships and potential targets. *European Journal of Medicinal Chemistry*, *201*, p.112510.
16. Sondhi, S.M., Goyal, R.N., Lahoti, A.M., Singh, N., Shukla, R. and Raghubir, R., 2005. Synthesis and biological evaluation of 2-thiopyrimidine derivatives. *Bioorganic & medicinal chemistry*, *13*(9), pp.3185-3195.
17. Balkan, A., Gören, Z., Urgun, H., Çalış, Ü., Çakar, A.N., Atilla, P. and Uzbay, T., 2002. Evaluation of the analgesic and anti-inflammatory activities of some thiazolo [4, 5-d] pyrimidines. *Arzneimittelforschung*, *52*(06), pp.462-467.
18. Mochona, B., Wilson, T. and Redda, K., 2003. Synthesis and anti-inflammatory activities of N-benzoylamino-1, 2, 3, 6-tetrahydropyridine analogs. *Drugs under experimental and clinical research*, *29*(4), pp.131-140.
19. Amir, M., Khan, M.S.Y. and Zaman, M.S., 2004. Synthesis, characterization and biological activities of substituted oxadiazole, triazole, thiadiazole and 4-thiazolidinone derivatives.
20. Kumar, D., Kumar, R.R., Pathania, S., Singh, P.K., Kalra, S. and Kumar, B., 2021. Investigation of indole functionalized pyrazoles and oxadiazoles as anti-inflammatory agents: Synthesis, in-vivo, in-vitro and in-silico analysis. *Bioorganic Chemistry*, *114*, p.105068.

21. Schwarz, S., Sauter, D., Wang, K., Zhang, R., Sun, B., Karioti, A., Bilia, A.R., Efferth, T. and Schwarz, W., 2014. Kaempferol derivatives as antiviral drugs against the 3a channel protein of coronavirus. *Planta medica*, *80*(02/03), pp.177-182.
22. Hwu, J.R., Kapoor, M., Tsay, S.C., Lin, C.C., Hwang, K.C., Horng, J.C., Chen, I.C., Shieh, F.K., Leyssen, P. and Neyts, J., 2015. Benzouracil–coumarin–arene conjugates as inhibiting agents for chikungunya virus. *Antiviral research*, *118*, pp.103-109.
23. Kaur, R. and Kumar, K., 2021. Synthetic and medicinal perspective of quinolines as antiviral agents. *European Journal of Medicinal Chemistry*, *215*, p.113220.
24. Kovaleva, K.S., Yarovaya, O.I., Gatilov, Y.V., Slita, A.V., Esaulkova, Y.L., Zarubaev, V.V., Rudometova, N.B., Shcherbakova, N.S., Shcherbakov, D.N. and Salakhutdinov, N.F., 2021. Synthesis and antiviral activity of N-heterocyclic hydrazine derivatives of camphor and fenchone. *Chemistry of Heterocyclic Compounds*, *57*, pp.455-461.
25. El-Hashash, M.A., Rizk, S.A. and Atta-Allah, S.R., 2015. Synthesis and regioselective reaction of some unsymmetrical heterocyclic chalcone derivatives and spiro heterocyclic compounds as antibacterial agents. *Molecules*, *20*(12), pp.22069-22083.
26. Bouzian, Y., Karrouchi, K., Sert, Y., Lai, C.H., Mahi, L., Ahabchane, N.H., Talbaoui, A., Mague, J.T. and Essassi, E.M., 2020. Synthesis, spectroscopic characterization, crystal structure, DFT, molecular docking and in vitro antibacterial potential of novel quinoline derivatives. *Journal of Molecular Structure*, *1209*, p.127940.
27. Santosh, R., Selvam, M.K., Kanekar, S.U. and Nagaraja, G.K., 2018. Synthesis, characterization, antibacterial and antioxidant studies of some heterocyclic compounds from triazole-linked chalcone derivatives. *Chemistry Select*, *3*(23), pp.6338-6343.
28. Kritchenkov, A.S., Egorov, A.R., Artemjev, A.A., Kritchenkov, I.S., Volkova, O.V., Kiprushkina, E.I., Zabodalova, L.A., Suchkova, E.P., Yagafarov, N.Z., Tskhovrebov, A.G. and Kurliuk, A.V., 2020. Novel heterocyclic chitosan derivatives and their derived nanoparticles: Catalytic and antibacterial properties. *International journal of biological macromolecules*, *149*, pp.682-692.
29. Burmeister, H., Dietze, P., Preu, L., Bandow, J.E. and Ott, I., 2021. Evaluation of ruthenium (II) N-heterocyclic carbene complexes as antibacterial agents and inhibitors of bacterial thioredoxin reductase. *Molecules*, *26*(14), p.4282.

30. Abdalla, M.M., Al-Omar, M.A., Al-Salahi, R.A., Amr, A.G.E. and Sabrye, N.M., 2012. A new investigation for some steroidal derivatives as anti-Alzheimer agents. *International Journal of Biological Macromolecules*, *51*(1-2), pp.56-63.
31. M Abdel-Fattah, A., A Attaby, F., AA Elneairy, M. and NM Gouda, M., 2012. Synthesis, Characterization and Antimicrobial Activity of Pyridine-3-Carbonitrile Derivatives. *Current Bioactive Compounds*, *8*(2), pp.176-187.
32. Gülçin, İ., Trofimov, B., Kaya, R., Taslimi, P., Sobenina, L., Schmidt, E., Petrova, O., Malysheva, S., Gusarova, N., Farzaliyev, V. and Sujayev, A., 2020. Synthesis of nitrogen, phosphorus, selenium and sulfur-containing heterocyclic compounds–determination of their carbonic anhydrase, acetylcholinesterase, butyrylcholinesterase and α-glycosidase inhibition properties. *Bioorganic Chemistry*, *103*, p.104171.
33. Rastegari, A., Nadri, H., Mahdavi, M., Moradi, A., Mirfazli, S.S., Edraki, N., Moghadam, F.H., Larijani, B., Akbarzadeh, T. and Saeedi, M., 2019. Design, synthesis and anti-Alzheimer's activity of novel 1, 2, 3-triazole-chromenone carboxamide derivatives. *Bioorganic chemistry*, *83*, pp.391-401.
34. Attaby, F., El-Ghandour, A.H., Sayed, A.R., El Bassuony, A.A. and El-Reedy, A.A., 2013. Synthesis, Reactions and Biological Evaluation of 3-Amino-6-(subs.) thieno [2, 3-b] pyridine-2-carbohydrazides. *Current Bioactive Compounds*, *9*(2), pp.167-181.
35. Latif, A., Bibi, S., Ali, S., Ammara, A., Ahmad, M., Khan, A., Al-Harrasi, A., Ullah, F. and Ali, M., 2021. New multitarget directed benzimidazole-2-thiol-based heterocycles as prospective anti-radical and anti-Alzheimer's agents. *Drug Development Research*, *82*(2), pp.207-216.
36. Mariappan, G., Prabhat, P., Sutharson, L., Banerjee, J., Patangia, U. and Nath, S., 2012. Synthesis and antidiabetic evaluation of benzothiazole derivatives. *Journal of the Korean Chemical Society*, *56*(2), pp.251-256.
37. Nabil, S., Abd El-Rahman, S.N., Al-Jameel, S.S. and Elsharif, A.M., 2018. Conversion of curcumin into heterocyclic compounds as potent anti-diabetic and anti-histamine agents. *Biological and pharmaceutical Bulletin*, *41*(7), pp.1071-1077.
38. Dalavai, R., Gomathi, K., Naresh, K. and Nawaz Khan, F.R., 2022. One-Pot Synthesis of Quinolinyl Amino Nitriles and Their Antidiabetic, Anti-inflammatory, Antioxidant, and Molecular Docking Studies. *Polycyclic Aromatic Compounds*, *42*(4), pp.1581-1595.

39. Toumi, A., Boudriga, S., Hamden, K., Sobeh, M., Cheurfa, M., Askri, M., Knorr, M., Strohmann, C. and Brieger, L., 2021. Synthesis, antidiabetic activity and molecular docking study of rhodanine-substituted spirooxindole pyrrolidine derivatives as novel α-amylase inhibitors. *Bioorganic Chemistry*, *106*, p.104507.
40. Gallis, H.A., Drew, R.H. and Pickard, W.W., 1990. Amphotericin B: 30 years of clinical experience. *Reviews of infectious diseases*, *12*(2), pp.308-329.
41. Tighadouini, S., Radi, S., Benabbes, R., Youssoufi, M.H., Shityakov, S., El Massaoudi, M. and Garcia, Y., 2020. Synthesis, biochemical characterization, and theoretical studies of novel β-keto-enol pyridine and furan derivatives as potent antifungal agents. *ACS omega*, *5*(28), pp.17743-17752.
42. Morcoss, M.M., El Shimaa, M.N., Ibrahem, R.A., Abdel-Rahman, H.M., Abdel-Aziz, M. and Abou El-Ella, D.A., 2020. Design, synthesis, mechanistic studies and in silico ADME predictions of benzimidazole derivatives as novel antifungal agents. *Bioorganic chemistry*, *101*, p.103956.
43. Zhao, S., Zhang, X., Wei, P., Su, X., Zhao, L., Wu, M., Hao, C., Liu, C., Zhao, D. and Cheng, M., 2017. Design, synthesis and evaluation of aromatic heterocyclic derivatives as potent antifungal agents. *European Journal of Medicinal Chemistry*, *137*, pp.96-107.
44. Mi, Y., Zhang, J., Chen, Y., Sun, X., Tan, W., Li, Q. and Guo, Z., 2020. New synthetic chitosan derivatives bearing benzenoid/heterocyclic moieties with enhanced antioxidant and antifungal activities. *Carbohydrate polymers*, *249*, p.116847.
45. Sanemitsu, Y. and Kawamura, S., 2008. Studies on the synthetic development for the discovery of novel heterocyclic agrochemicals. *Journal of pesticide science*, *33*(2), pp.175-177.
46. Cai, S., Hu, X., Han, J., Zhang, Z., Li, X., Wang, C. and Su, J., 2013. Efficient organic dyes containing dibenzo heterocycles as conjugated linker part for dye-sensitized solar cells. *Tetrahedron*, *69*(8), pp.1970-1977.
47. Chami, R., Boudalia, M., Echihi, S., El Fal, M., Bellaouchou, A., Guenbour, A., Tabyaoui, M., Essassi, E.M., Zarrouk, A. and Ramli, Y., 2017. Thermodynamic study and electrochemical Investigation of 4-chloro-1H-pyrazolo [3, 4-d] pyrimidine as a corrosion Inhibitor for mild steel in hydrochloric acid Solution. *Journal of Materials and Environmental Science*, *8*(11), pp.4182-4192.

48. Karthik, G. and Sundaravadivelu, M., 2017. Experimental and theoretical studies of anti-ulcer drugs with benzimidazole rings as corrosion inhibitor for copper in 1 M nitric acid medium. *Journal of adhesion science and Technology*, *31*(5), pp.530-551.
49. Abdallah, M., Ahmed, S.A., Altass, H.M., Zaafarany, I.A., Salem, M., Aly, A.I. and Hussein, E.M., 2019. Competent inhibitor for the corrosion of zinc in hydrochloric acid based on 2, 6-bis-[1-(2-phenylhydrazono) ethyl] pyridine. *Chemical Engineering Communications*, *206*(2), pp.137-148.
50. Saranya, J., Sounthari, P., Parameswari, K. and Chitra, S., 2016. Acenaphtho [1, 2-b] quinoxaline and acenaphtho [1, 2-b] pyrazine as corrosion inhibitors for mild steel in acid medium. *Measurement*, *77*, pp.175-186.
51. Harnett, J.J., Roubert, V., Dolo, C., Charnet, C., Spinnewyn, B., Cornet, S., Rolland, A., Marin, J.G., Bigg, D. and Chabrier, P.E., 2004. Phenolic thiazoles as novel orally-active neuroprotective agents. *Bioorganic & medicinal chemistry letters*, *14*(1), pp.157-160.
52. Shih, M.H. and Ke, F.Y., 2004. Syntheses and evaluation of antioxidant activity of sydnonyl substituted thiazolidinone and thiazoline derivatives. *Bioorganic & medicinal chemistry*, *12*(17), pp.4633-4643.
53. De, S., Adhikari, S., Tilak-Jain, J., Menon, V.P. and Devasagayam, T.P.A., 2008. Antioxidant activity of an aminothiazole compound: possible mechanisms. *Chemico-Biological Interactions*, *173*(3), pp.215-223.

CHAPTER-2

REVIEW OF LITERATURE

2.1. Introduction

Benzothiazoles constitute a group of heterocyclic compounds that have garnered significant attention in the fields of chemistry, pharmaceuticals, and materials science due to their diverse chemical properties and versatile applications. The unique structural arrangement of the benzothiazole compound imparts distinctive chemical reactivity and a range of beneficial properties to benzothiazoles. Benzothiazoles have a significant role in the synthesis of a diverse array of biologically active compounds, drugs, and agricultural chemicals. They are a key component in several drug classes, including antibiotics, anti-cancer agents, anti-inflammatory drugs, and antioxidants owing to their ability to modulate biological processes. Additionally, benzothiazole derivatives have shown promise in treating neurological disorders, making them crucial in the realm of neuropharmacology. In materials science, benzothiazoles are utilized as additives in rubber manufacturing to enhance the durability and resilience of tires. They also serve as fluorescent dyes, contributing to the development of optoelectronic devices like OLEDs. Furthermore, benzothiazoles have applications in analytical chemistry as indicators for metal ion detection and quantification. Their versatile chemistry allows for the creation of tailored molecules with specific properties, making them indispensable in various scientific and industrial endeavors. In essence, benzothiazoles represent a fascinating class of compounds with multifaceted roles and continue to play a pivotal part in advancing our understanding and application of organic chemistry. A variety of synthetic pathways have been accomplished for the formation of benzothiazole derivatives. The primary method extensively employed for producing benzothiazole compounds consists of combining 2-aminobenzenethiol with cyano or carbonyl compounds through condensation. Riadi *et al.* discovered that the condensation reaction of 2-aminobenzenethiol with aromatic aldehydes in toluene under reflux conditions may be employed to synthesize benzothiazoles. A copper-catalyzed method has been reported to achieve 2-substituted benzothiazoles through condensation of benzo-thiols and nitriles. In addition, several researchers have discovered that the preparation of benzothiazoles can also be achieved from aniline when it reacts with compounds like carbon disulfide, piperidine, and isothiocyanate. However, there are various disadvantages associated with these traditional methods like low yield, weak selectivity, extreme response conditions, or toxic reagents. On the contrary, green chemistry advocates using techniques that limit or avoid the usage and processing of raw

materials or by-products that can harm ecological balance. Primarily, in the past decade, numerous eco-friendly methods have been designed to afford benzothiazoles [1-10].

2.2. Synthetic Routes to Benzothiazoles

2.2.1. Cyclization Methods

Liu *et al.* developed a process catalyzed by DBN for synthesizing benzothiazoles through a cyclization reaction involving 2-aminothiophenols **1** and CO_2 **2**, in the presence of diethylsilane **3**. Many benzothiazole derivatives **4** were afforded excellent yields (**Scheme-2.1**). This study showcases the essential contribution of hydrosilane in the synthesis of benzothiazoles, effectively preventing the formation of unwanted by-products like benzothiazolones. This method gives an eco-friendly path for synthesizing benzothiazoles and their derivatives [11]. Furthermore, Gao *et al*. produced a series of benzothiazoles using a high-yield catalyst like an ionic liquid based on acetate to cyclized 2-aminobenzenethiol molecules **6** with CO_2 **7** in the presence of hydrosilane **8** (**Scheme-2.2**). Regarding the different catalysts, reaction pressure, and temperature, the authors also examined this reaction under various conditions. The excellent results were achieved by conducting the reaction with [Bmim] [OAc] at 60 °C. In addition, [Bmim] [OAc] was found to be eco-friendly and the yield of benzothiazole remained nearly constant after the ionic liquid was used for five consecutive iterations. This may potentially mark the inaugural approach for producing benzothiazoles without the need for metals, under mild conditions, utilizing CO_2 as a starting material [12]. Chun *et al*. developed the reaction of 2-aminobenzenethiols **11** with CO_2 **12** and phenylsilane **13** in the presence of DBU to synthesize benzothiazoles **14** in excellent yields (**Scheme-2.3**). There was a comprehensive substrate spectrum and functional group resistance for this reaction. Additionally, the initial catalyst salt could be recovered and employed repeatedly without experiencing any decrease in its effectiveness [13]. Folgueiras *et al.* discovered that a flow electrochemical reactor can be utilized for the synthesis of benzothiazoles **17** without the need for supporting electrolytes or catalysts, resulting in moderate to good yields and high current performance using arylthioamides **16** (**Scheme-2.4**). The simple scale-up of the reaction significantly enhanced the recorded methodologies for the production of benzothiazoles in this process [14]. Bouchet *et al*. efficiently synthesized benzothiazoles **19** with moderate to good yields from thiobenzanilides **18** by utilizing potassium peroxydisulfate as an oxidizing agent and riboflavin as a photosensitizer, the reaction was catalyzed under visible-light

exposure through a cyclization process (**Scheme-2.5**). Riboflavin is a cheap natural reagent as a photocatalyst that demonstrates substantial facilities over transition-metal catalysis. Moreover, many functional groups were approved by the present technique, and the desired productions were made [15]. Rey *et al*. stated that the preparation of 2-substituted benzothiazoles **21** was done effectively via cyclization of thioformanilides **20** in the presence of toluene and 1, 2-dichloroethane at 83.5 °C induced by chloranil under irradiation (**Scheme-2.6**). The main step in the mechanism was the abstraction of hydrogen from thiobenzamide by triplet chloranil. The procedure is simple and provides readily isolated products from low to high yield [16]. Bose *et al*. have established a sustainable, effective, and expeditious methodology for the development of benzothiazoles **23** from sulfamide substrates **22** via cyclization reaction. The reaction took place under ambient temperature conditions, employing DMP as the catalyst and DCM as a solvent (**Scheme-2.7**). The mechanism discloses that the reaction attains significant yields by following a path involving thiyl radicals to generate the novel oxybis benzothiazole compound. This process is also adaptable for generating diverse sets of heterocycles through solid-phase synthesis. This approach offers the advantage of brief reaction time, high activity, high yield, mild reaction conditions, and so on [17]. Downer *et al*. introduced a general method for transforming thiobenzamides **24** into benzothiazoles **25** through the formation of active intermediates like aryl radical cations (**Scheme-2.8**). The use of CAN in aqueous acetonitrile or PIFA in trifluoroethanol was utilized in this process to facilitate cyclization at ambient temperature within 30 minutes in moderate yields [18]. Xu *et al.* accomplished a simple methodology for synthesizing benzothiazole derivatives **27** with good yields through the intramolecular C-S bond formation of aromatic substrates. This reaction was accomplished by initiating the cyclization of thioamide derivatives **26** using visible light and TEMPO (**Scheme-2.9**). Notably, this photochemical cyclization requires no additional photosensitizer, base, or metal catalyst [19]. Cheng *et al.* documented a method that utilizes visible light in the presence of oxygen to prepare benzothiazoles **29** from thioanilides **28**, either through the formation of C-S or C-H bonds (**Scheme-2.10**). The functional group affinity of the present technique was tested and the outcome revealed that several functional groups could be tolerated by this process. This method is complementary to the current procedures for synthesizing benzothiazoles by providing outstanding selectivity, excellent efficiency, and an environmentally friendly character.

Furthermore, the process employs cheap, easily accessible molecular oxygen as the terminal oxidant [20].

Feng *et al*. examined the metal-free, base-promoted preparation of 2-substituted (N, C, O) benzothiazoles **31** from substituted thioamides/carbamothioates/thioureas **30** via intramolecular cyclization involving the coupling of C-S bond in the presence of dioxane (**Scheme-2.11**). Under these conditions, a wide range of functional groups was allowed, and desired products were achieved in high yields. This approach has some benefits of transition metal-free, moderate reaction conditions, shorter reaction time, and broad scope of applications [21]. Wang *et al*. studied an effective and transition metal-catalyzed preparation of benzothiazole derivatives using $Na_2S_2O_3$ as the oxidant in DMSO with the addition of pyridine at 80 °C and $FeCl_3$ as the catalyst (**Scheme-2.12**). Preliminary mechanistic experiments demonstrated that the desired products were highly selective and achieved high yields. The proposed reaction mechanism showed that the thioyl radical formation was done when Fe (III) oxidized the *N*-phenyl benzothioamide, while Fe (III) was reduced to Fe (II).Compounds **33**, **35**, and **37** were obtained by first forming a thioyl radical intermediate through cyclization, which was then oxidized using $Na_2S_2O_8$ [22]. Luo *et al.* described a method wherein 2-chloromethyl benzothiazole **40** was synthesized via a condensation reaction under microwave irradiation. In this process, 2-aminothiophenol **38** and chloroacetyl chloride **39** were employed with the addition of acetic acid (**Scheme-2.13**). Notably, the microwave-assisted technique demonstrated effectiveness, environmental friendliness, and superior efficiency in terms of both yield and reaction time compared to conventional methods [23]. Racane *et al.* suggested that nitro-substituted 2-aminothiophenol **41** could undergo condensation with 4-nitrobenzoylchloride **42** in the presence of acetic acid for about 4 hours under reflux conditions to effectively synthesize nitro-amidino benzothiazoles **43** (**Scheme-2.14**). The desired products were prepared by pinner reaction with the use of target compounds as the starting materials [24]. Dar *et al*. explored the one-pot synthesis of S-aryl/alkyl benzothiazole-2-carbothioate derivatives **47** from the reaction between oxalyl chloride **45**, thiols **46**, and 2-aminothiophenol **44** accompanied by TBAI (**Scheme-2.15**). The existing methodology advocates the preparation of benzothiazoles in excellent yield with an extensive variety of substrates through the formation of C-S and C-N bonds simultaneously. This method provides benefits such as mild reaction conditions and high efficacy [25]. Nadaf *et al*. reported an appropriate reaction media and promoters, $[Hbim]BF_4$ and $[bbim]BF_4$ ionic liquids to synthesize

2-aryl benzothiazoles **50** via condensation of aromatic acid chloride compounds **49** with 2-aminobenzenethiol **48** under moderate reaction conditions **48** (**Scheme-2.16**). In the study, a variety of recently produced ionic liquids were synthesized and assessed for their suitability in these reactions. The ambient reaction conditions, recyclability of non-volatile ionic liquids, and the absence of catalysts make an eco-friendly methodology susceptible to scale-up [26]. Kumar *et al*. reported a solvent-free and efficient methodology to synthesize a library of benzothiazole derivatives **53** through condensation of *ortho*-aminothiophenol **51** with acyl chlorides **52** accompanied by a catalytic amount of silica-supported $NaHSO_4$ (**Scheme-2.17**). The preparation of catalyst $NaHSO_4$-SiO_2 could be done easily from silica gel and $NaHSO_4$, these are non-toxic and inexpensive. In addition, simple filtration could easily remove the catalyst due to the heterogeneous nature of the reaction. Some of the benefits of the present protocol are a quick work process, easy availability, high yield, reusability, and the use of environmentally benign catalysts [27]. Wu *et al*. described the preparation of novel benzothiazoles (**Scheme-2.18**). In this study, zinc salt of 4-amino-3-mercaptobenzoic acid **54** was deferred at 80 °C for 2 hours in pyridine with *p*-nitro benzoyl chloride **55** and upon treatment with thionyl chloride ($SOCl_2$), 2-(4′-nitrophenyl)-benzothiazole-6-carbonyl chloride **56** was achieved successfully. Meanwhile, dibenzothiazole-containing compounds **59** were afforded by the addition of 5-substituted aminothiophenol **58** and heating to reflux for about 3 hours [28]. Loukrakpam *et al*. explored a one-pot synthesis of benzothiazoles under metal-free conditions. The reaction proceeded with the treatment of aryl methyl ketones **60** with 2-aminothiophenol **61** (**Scheme-2.19**). Preliminary mechanistic studies revealed that aromatic ketones initially react with $TsNBr_2$ in DMSO. Moreover, the condensation of 2-aminothiophenol with the crude reaction mixture, followed by Michael addition and oxidative dehydrogenation sequence gives 2-acylbenzothiazoles **62** [29]. Liao *et al*. presented an effective synthesis of 2-arylbenzothiazoles **65** under conditions that were free of both I_2 and metal catalysts. This synthesis involved combining 2-aminobenzenethiols **63** with aryl ketones **64**, utilizing molecular oxygen as the oxidizing agent (**Scheme-2.20**). Various solvents were employed to conduct a comparative examination. However, in terms of yield, DMSO/chlorobenzene has been proven as the most suitable solvent mixture. In addition, this strategy of benzothiazoles under I_2 and metal-free conditions and also benzothiazoles had very good functional group universality which demonstrated that raw materials substituted for methyl,

nitro, chlorine, methoxy, bromine, and fluorine can be favorably transformed into a product of the analogous substituent [30].

Mayo *et al*. achieved the high-yield preparation of a library of 2-substituted benzothiazoles **68** without the need for metals, radiation, or oxidants. The reaction was accomplished by combining 2-aminobenzenethiols **66** and *β*-diketones **67** with toluenesulfonic acid as the catalyst (**Scheme-2.21**). The authors attempted various acids, for instance, trifluoroacetic acid (CF_3COOH), acetic acid, and benzoic acid (PhCOOH) to test the optimal catalytic system (CH_3COOH). However, in terms of yield, $TsOH{\cdot}H_2O$ was selected as the best catalyst. The mechanism elucidated that the reaction between 2-aminothiophenol and *β*-diketones, catalyzed by the Bronsted acid ($TsOH{\bullet}H_2O$), would take place, resulting in the formation of a ketimine intermediate through a condensation process. The intramolecular nucleophilic addition reaction would eventually take place, subsequently, a C-C bond cleavage occurs to yield the intended product. The benefits of this method include simple experimental steps, moderate reaction conditions, raw materials that are simple and readily available, strong universality of the substratum, and so on, and a good prospect of use [31]. Elderfield *et al*. synthesized 2, 2-disubstituted benzothiazolines **71** via condensation of 2-aminobenzenethiols **69** with ketones **70** (**Scheme-2.22**). Notably, pyrolysis of benzothiazoline leads to the formation of 2-substituted benzothiazole, and when exposed to reflux conditions, it releases hydrocarbons [32].

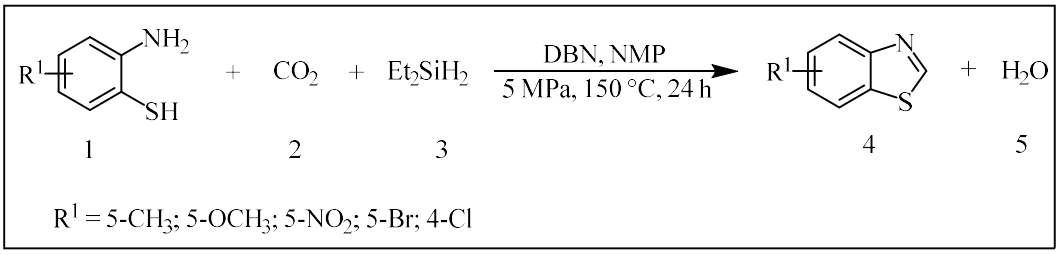

Scheme-2.1: DBN catalyzed preparation of benzothiazoles from 2-aminothiophenols.

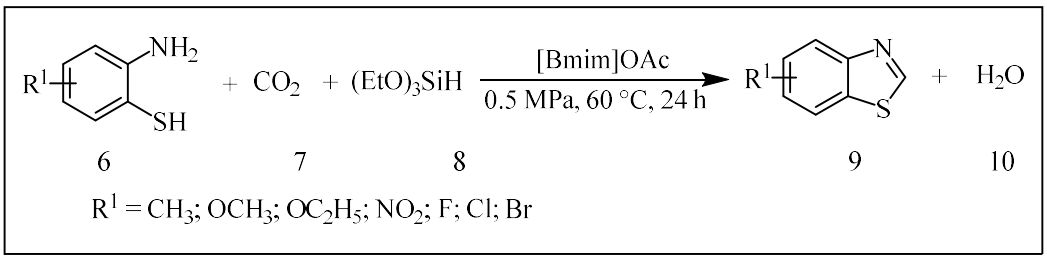

Scheme-2.2: Preparation of benzothiazoles from 2-aminothiophenol in the presence of hydrosilane.

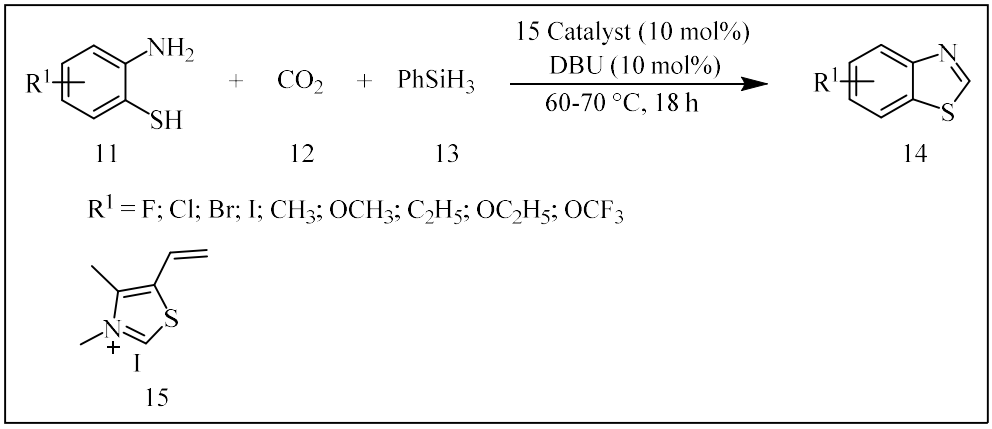

Scheme-2.3: Conversion of 2-aminobenzenethiols to benzothiazoles in the presence of DBU.

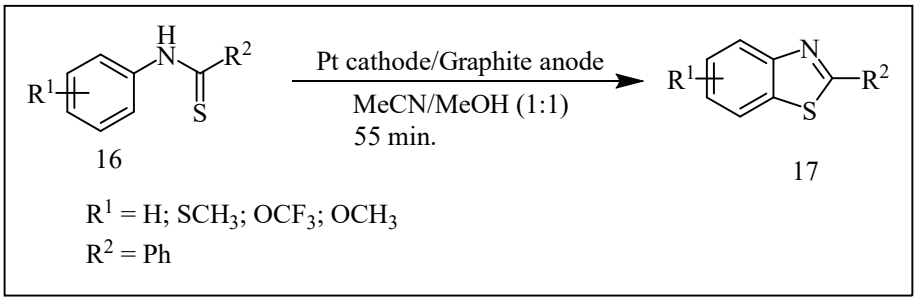

Scheme-2.4: Catalyst-free synthesis of benzothiazoles.

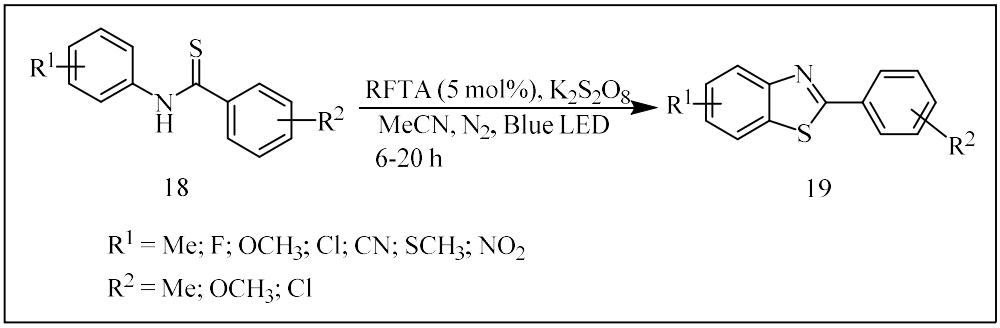

Scheme-2.5: Preparation of benzothiazoles from thiobenzanilides under visible light.

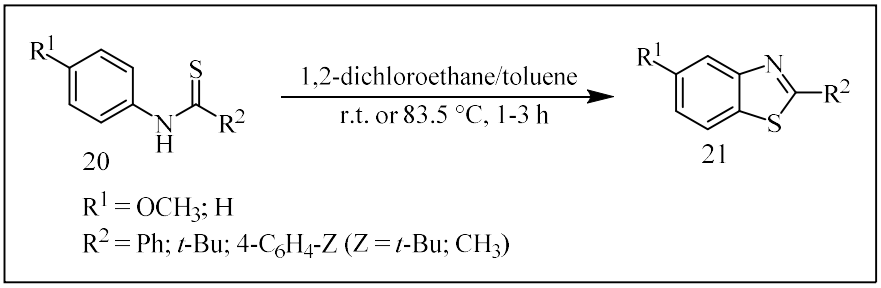

Scheme-2.6: Radical cyclization of thioformanilides.

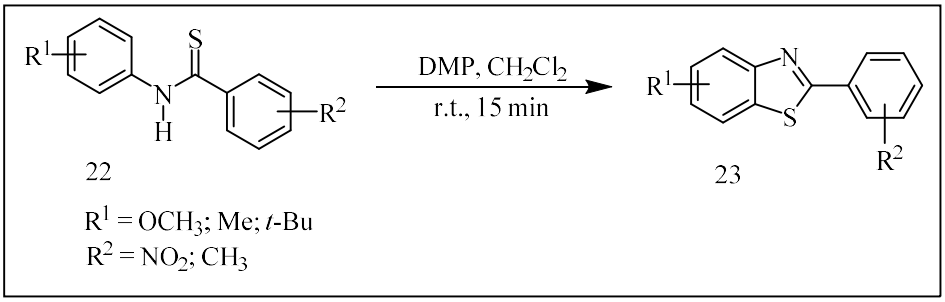

Scheme-2.7: Synthesis of benzothiazoles from sulfamide substrates.

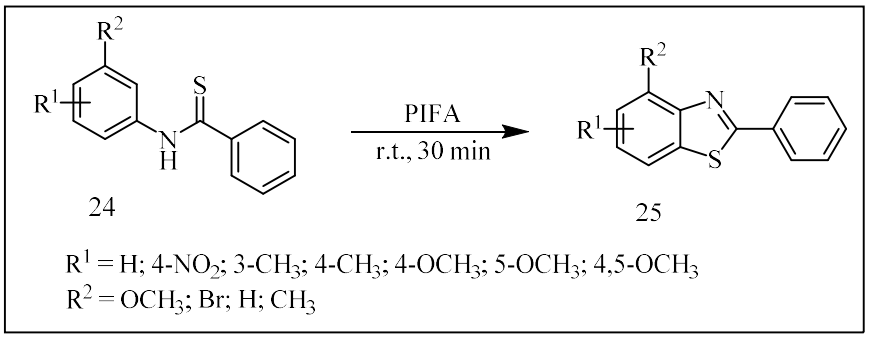

Scheme-2.8: Conversion of thiobenzamides to benzothiazoles at room temperature.

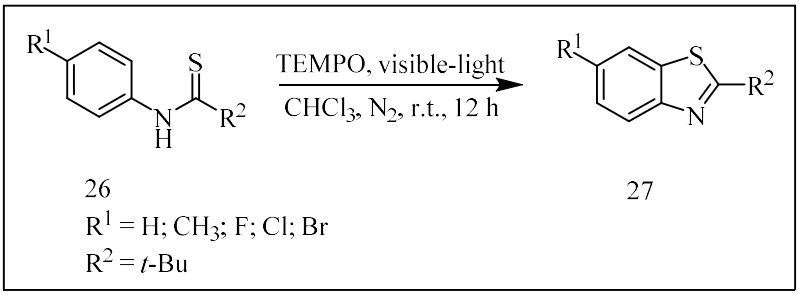

Scheme-2.9: Conversion of thioamide derivatives to benzothiazoles.

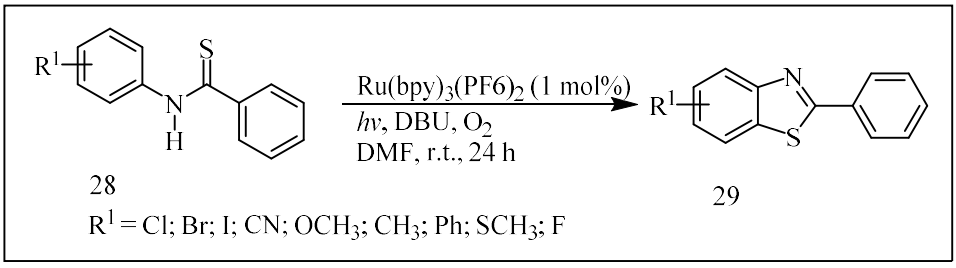

Scheme-2.10: Conversion of thioanilides to benzothiazoles.

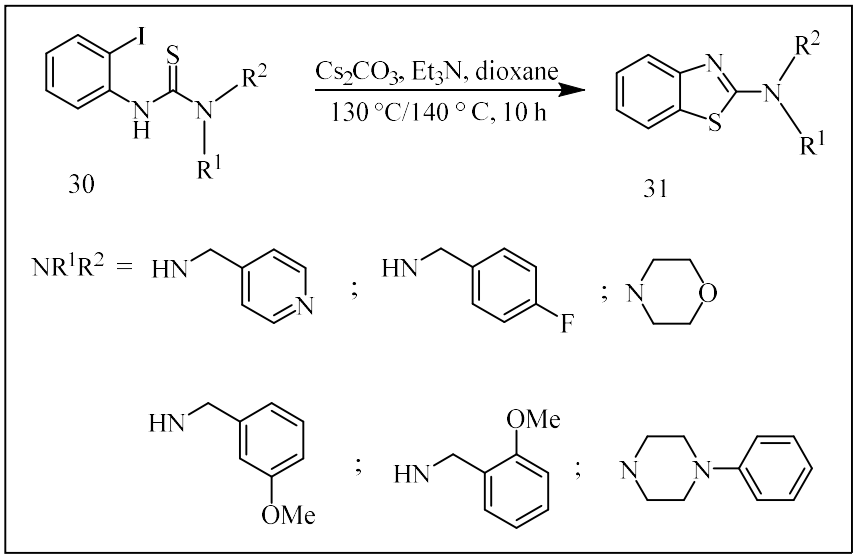

Scheme-2.11: Synthesis of 2-substituted benzothiazoles.

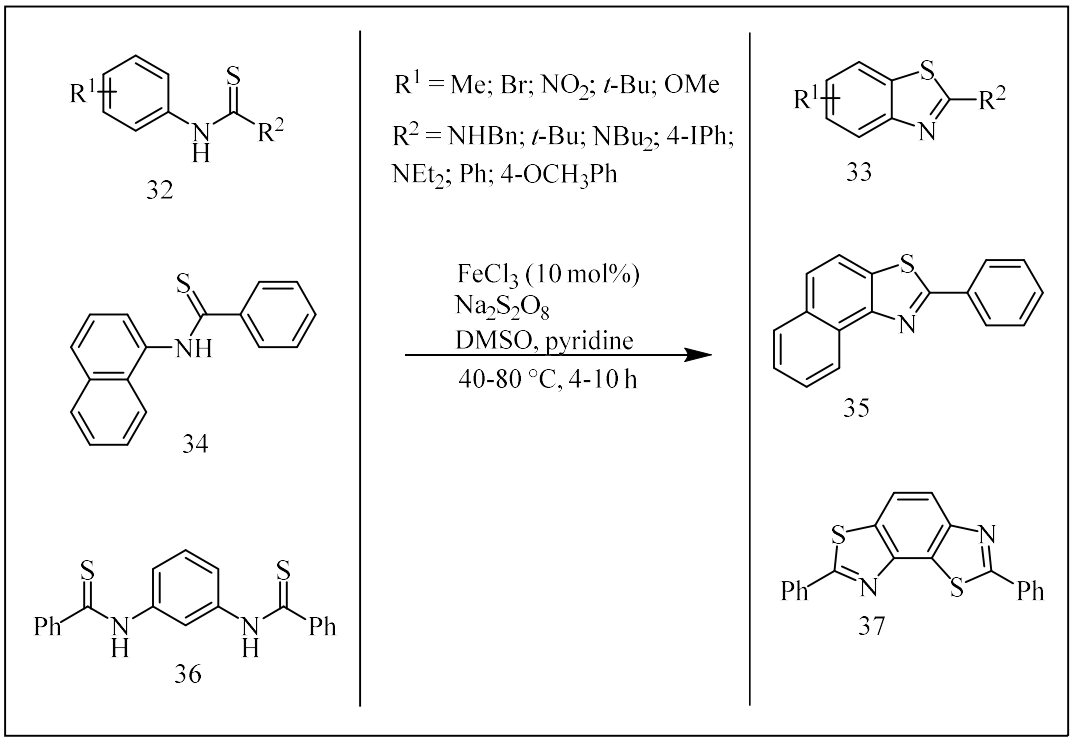

Scheme-2.12: Synthesis of benzothiazoles employing transition-metal catalysts.

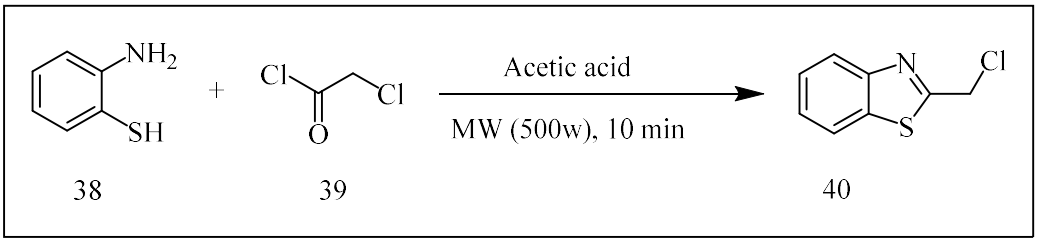

Scheme-2.13: Synthesis of benzothiazoles under microwave conditions.

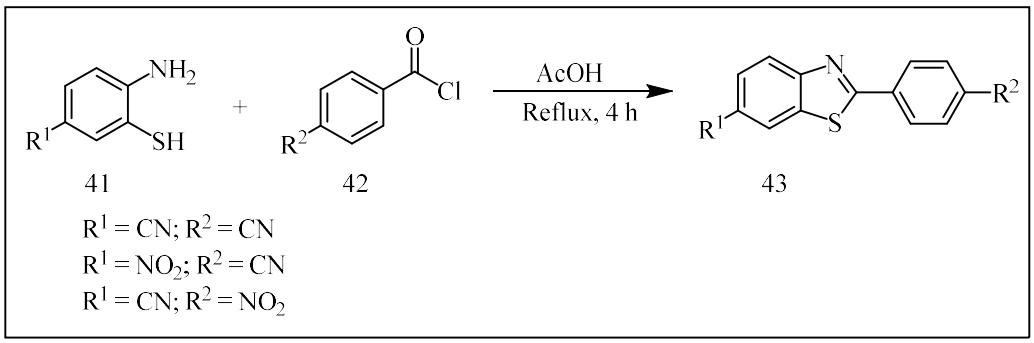

Scheme-2.14: Conversion of nitro-substituted 2-aminothiophenol to benzothiazoles.

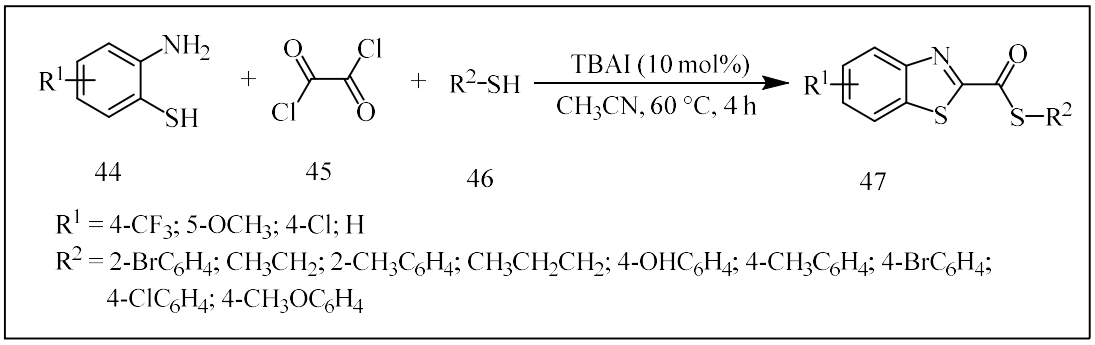

Scheme-2.15: Reaction of 2-aminothiophenol, thiols, and oxalyl chloride.

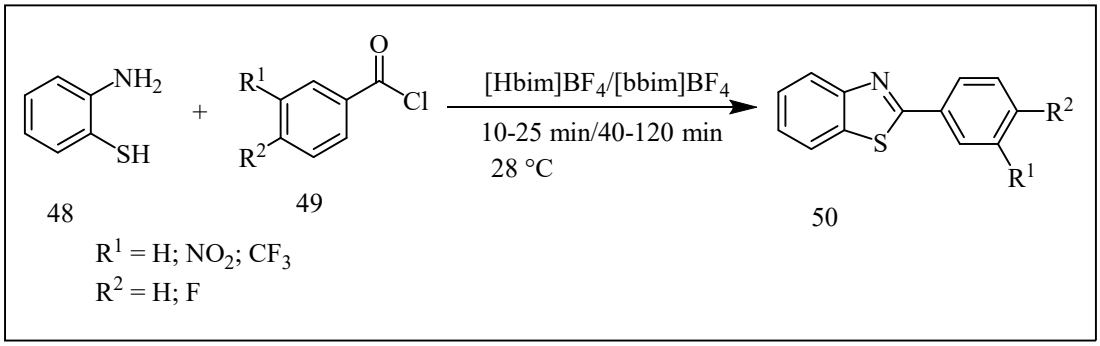

Scheme-2.16: Conversion of 2-aminobenzenethiol to 2-aryl benzothiazoles.

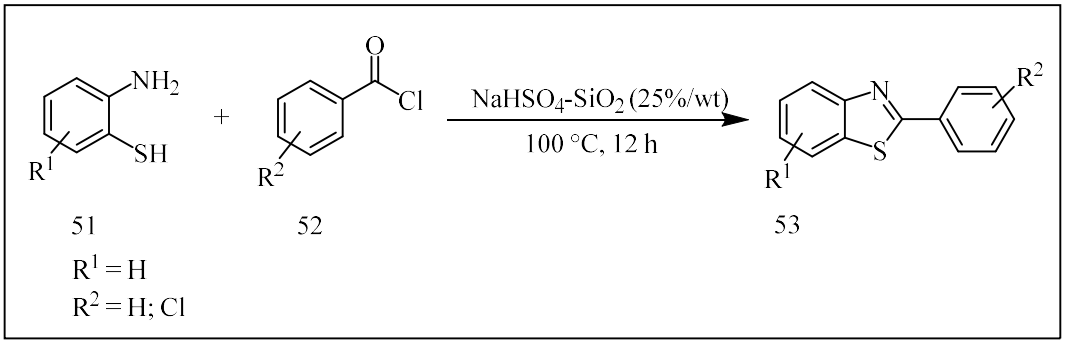

Scheme-2.17: Solvent-free synthesis of benzothiazoles.

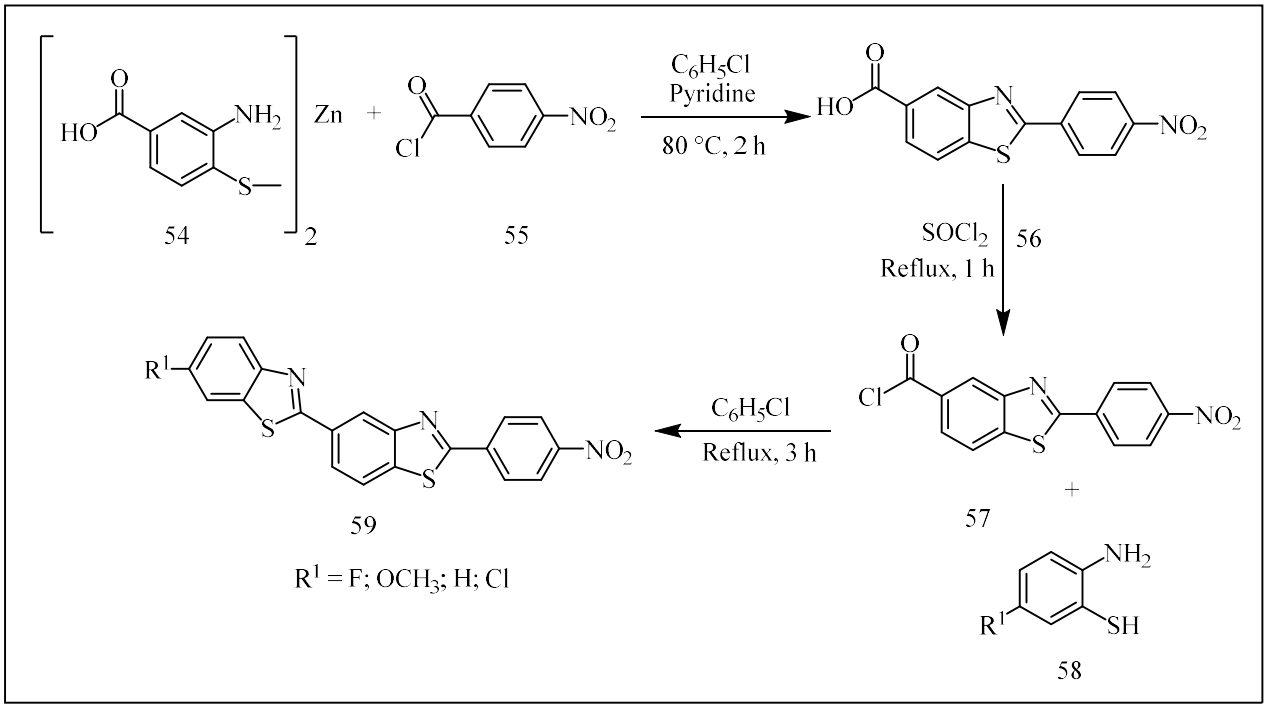

Scheme-2.18: Synthesis of 2-(4′-nitrophenyl)-benzothiazole-6-carbonyl chloride.

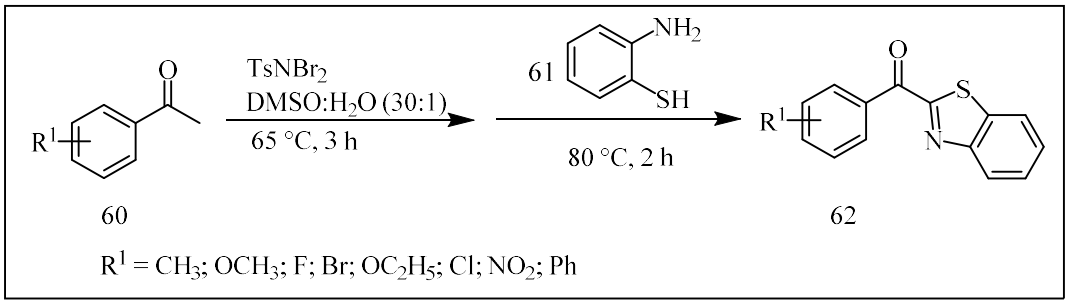

Scheme-2.19: Preparation of benzothiazole derivatives under metal-free conditions.

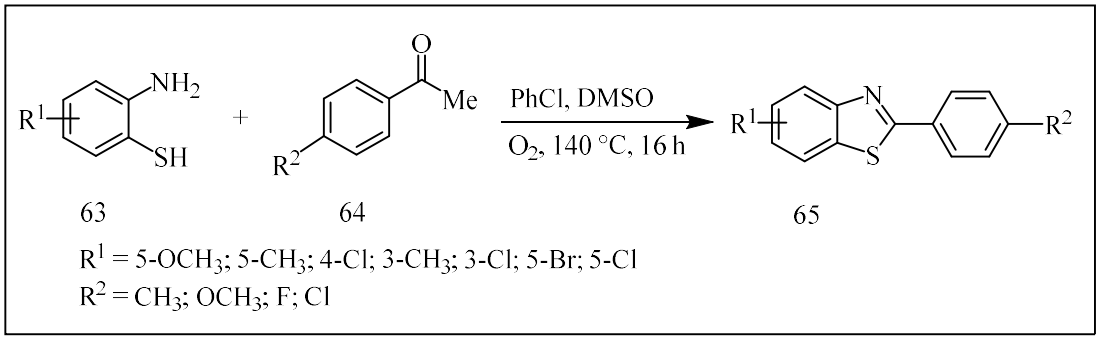

Scheme-2.20: Metal-free synthesis of 2-arylbenzothiazoles.

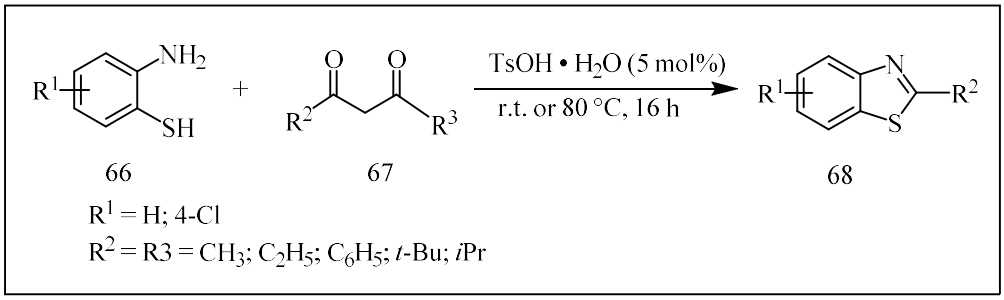

Scheme-2.21: Acid-catalyzed preparation of benzothiazoles from 2-aminobenzenethiols.

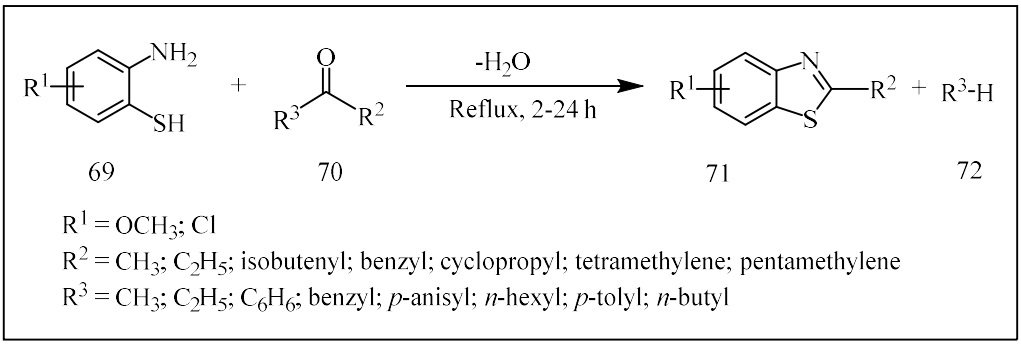

Scheme-2.22: Conversion of 2-aminobenzenethiol to 2, 2-disubstituted benzothiazolines.

2.2.2. Condensation Methods

Bhat *et al.* investigated the microwave-irradiated rapid synthesis of 2-aryl-benzothiazoles **75** from a variety of aryl aldehydes **74** and 2-aminothiophenol **73** utilizing acacia concinna as a biocatalyst (**Scheme-2.23**). Compared to the traditional approach, the present protocol possesses distinguishing characteristics such as an environmentally friendly nature, less reaction time, solvent-free, and excellent yields of the desired products [33]. Ye *et al*. accomplished a visible-light supported preparation of benzothiazoles **78** from 2-aminothiophenol **76** and various aldehydes **77** via condensation reaction (**Scheme-2.24**). The reaction system under atmospheric

air was irradiated for 6 hours with a 12W blue LED. The universality of this reaction condition has been explored by examining a range of aldehydes. The results have indicated that aliphatic, aromatic, and aldehydes containing heteroatoms can all undergo this transformation successfully. The findings provided a systematic, non-transitional metal catalyst, an additional additive, and an appropriate synthetic route to benzothiazoles [34]. Maleki *et al.* discovered that benzothiazoles **81** can be obtained in high yields by catalyzing the condensation reaction of 2-aminothiophenol **79** with aromatic aldehydes **80** at ambient temperature using NH_4Cl as a catalyst (**Scheme-2.25**). Furthermore, NH_4Cl has shown hydrogen bonding activation of carbonyl compounds to enhance the reaction by nucleophilic attack of amines to provide the desired product. Evidently, because of the less reaction time, recyclable catalyst, metal-free, acid-free, and excellent yield, this approach is a green chemistry reaction route for the formation of benzothiazole and its derivatives [35]. Bista *et al*. developed the reaction of *ortho*-aminobenzenethiol **82** with various substituted bisthiophene derivatives **83** under reflux conditions for approximately 1 hour, in the presence of DMSO to achieve 2-bisthiophene substituted benzothiazoles **84** (**Scheme-2.26**). The assessment was carried out on the fluorescence properties of products. In the 450-600 nm range, they have shown strong fluorescence as well as major stokes shifts and high quantum yields. The above-mentioned compounds could be utilized as fluorescent indicators because of their strong fluorescence [36]. Merroun *et al*. successfully achieved a systematic, straightforward, and environmentally friendly approach to produce benzothiazole derivatives **87**. This was accomplished by condensing ortho-aminothiophenol **85** with different aromatic aldehydes **86**, using SnP_2O_7 as an innovative heterogeneous catalyst (**Scheme-2.27**). The excellent yields and reduced reaction times achieved for different benzothiazole derivatives synthesis demonstrate that a novel catalyst is extremely intriguing due to its strong catalytic activity and reusability without any degradation of its activity [37]. Praveen *et al*. explained that microwave-assisted conditions are effective in promoting the synthesis of benzothiazoles **90**. This synthesis involves condensing 2-aminobenzenethiol **88** with benzaldehyde derivatives **89** using PIFA as an oxidizing reagent (**Scheme-2.28**). The present protocol has several appealing characteristics including reduced reaction time, satisfactory yield, and broad substrate scope. In contrast to the conventional heating method, the utilization of microwave technology has the potential to reduce reaction time, enhance reaction yields, and expand the applicability of the substrates [38]. Guo *et al*. proposed an efficient methodology to synthesize a series of benzothiazoles **93** via

condensation of *ortho*-aminothiophenol **91** with different derivatives of aldehydes **92** under ambient conditions, for approximately 1 hour, in ethanol with the H_2O_2/HCl system present (**Scheme-2.29**). The optimal ratio for the coupling was determined to be 1:1:6:3 of *ortho*-aminothiophenol/aldehydes/H_2O_2/HCl. The key benefits of this method involve high yields, reduced reaction time, and facile and quick separation of the required products [39]. Kumar *et al*. synthesized benzothiazole derivatives **96** via condensation of 2-aminobenzenethiol **94** with benzaldehyde derivatives **95** in dichloromethane using PDAIS (**Scheme-2.30**). The significant advantage of this technique involves the conversion of PDAIS to polymer-supported iodobenzene, which is collected by filtering and reused [40]. A simple and effective methodology to synthesize 2-arylbenzothiazoles **99** has been established by Maphupha *et al*. by reacting ortho-aminothiophenol **97** with an aromatic aldehyde through condensation **98**. The cost-effective commercial laccase served as a catalyst, resulting in the formation of the desired compounds with yields ranging from moderate to outstanding [41] (**Scheme-2.31**).

Coelho *et al.* developed a simple and effective method for synthesizing benzothiazoles **102**. This method involves the condensation of disulfides of 2-aminothiophenol **100** with carboxylic acids **101**, and it is facilitated at room temperature in the presence of tributylphosphine [42]. By making use of different carboxylic acids and 2-aminothiophenol disulfides with donor/withdrawing substituents, the universality of this technique was examined; this led to the synthesis of benzothiazoles with high yields. The benefits of this methodology involve the addition of non-toxic reagents and moderate reaction conditions (**Scheme-2.32**). Gupta *et al*. described that molecular iodine was utilized to achieve a cost-effective and excellent yield of benzothiazole derivatives **105** in a one-pot, solvent-free, and solid-phase condensation involving ortho-aminothiophenol **103** with derivatives of benzoic acid **104** for 10 minutes (**Scheme-2.33**). The novel approach significantly reduces cost by 17-fold when compared to polyphosphoric acid and [pmim]-Br catalyzed microwave synthesis because the reaction does not necessitate any extra chemicals or solvents. The benefits of using iodine are that it is nonselective, low-priced, requires a shorter reaction time, and can be conducted without the use of any solvents [43]. Sharghi *et al.* have presented an uncomplicated and highly productive approach for producing a range of 2-substituted aliphatic and aromatic benzothiazoles **108**. This approach involves the condensation of 2-aminothiophenol **106** with various types of aromatic or aliphatic carboxylic acids **107** (**Scheme-2.34**). Methanesulfonic acid was proven to be a successful combination for

accelerating this condensation process, facilitating the swift production of benzothiazoles with favorable yields. Furthermore, without reducing yield, silica gel could be reused several times. The benefits of this method include the utilization of readily accessible carboxylic acids and standard reaction conditions [44]. Reuf *et al*. reported that 2-substituted benzothiazoles **111** were synthesized under microwave irradiation for 3-4 minutes by conducting a condensation reaction between ortho-aminothiophenol **109** and a range of fatty acids **110** (**Scheme-2.35**). The reaction was completed by using P_4S_{10} as a catalyst with a high production yield. This is an inexpensive, rapid, and solvent-free protocol [45]. Mokhir *et al*. synthesized 2-cyanomethyl benzothiazole **114** by utilizing glacial acetic acid as a catalyst; ortho-aminothiophenol **112** was subjected to a condensation reaction with malonodinitrile **113** (**Scheme-2.36**). In the subsequent step, conc. HCl was slowly introduced to a mixture of 2-cyanomethyl benzothiazole in a solution of isopropanol and water to synthesize 2-benzothiazolylcyanoxime, a potent multidentate ligand suitable for chemical coordination [46]. Zandt *et al*. accomplished the 24-hour synthesis of benzothiazole derivative **117** via condensation of 2-amino-4, 5, 7-trifluorothiophenol hydrochloride **115** with *N*-cyanomethyl-4-fluoro-2-hydroxy-benzamide **116** in ethanol reflux [47] (**Scheme-2.37**). Sun *et al*. developed the copper-catalyzed production of 2-substituted benzothiazoles **120** using ortho-aminobenzenethiols **118** and nitriles **119** containing diverse functional groups (**Scheme-2.38**). Upon optimizing the reaction parameters, it was found that the most favorable catalytic conditions, involving $Cu(OAc)_2$ and Et_3N, yielded the best outcomes. Preliminary mechanistic studies revealed that the formation of sulfilimine, followed by intramolecular cyclization produces benzothiazoles in excellent yield [48]. Khalil *et al*. studied that the synthesis of benzothiazoles **123** could be done from *ortho*-aminothiophenol **121** and amino ester **122** by utilizing polyphosphoric acid as a catalyst. Subsequently, neutralized using an aqueous ammonia solution, the desired products were successfully obtained with satisfactory yields [49] (**Scheme-2.39**). Manfroni *et al*. synthesized benzothiazole derivatives **126** via condensation of different substituted *ortho*-aminothiophenol **124** with ethyl cyanoacetate **125**, which furnishes corresponding products in moderate to good yields [50] (**Scheme-2.40**). Reddy *et al*. developed the exclusive formation of trifluoroacetonyl benzothiazole **129** under microwave irradiation conditions upon treatment of *ortho*-aminothiophenol **127** with trifluoroacetyl ketene diethyl acetal **128** in the presence of toluene for 8 minutes [51] (**Scheme-2.41**). The preparation of some novel benzothiazole derivatives **134** from benzothiazolyl carboxyhydrazide **133** and aryl

acids in the presence of phosphoryl chloride was examined by Rajeeva *et al*. [52] (**Scheme-2.42**). Bastug *et al*. established the simple, versatile, and systematic synthesis of different benzothiazole derivatives **137** by conducting a reaction involving functionalized orthoesters **136** and substituted anilines **135** through condensation under ambient conditions (**Scheme-2.43**). The versatility of this protocol enables the creation of new libraries of heterocyclic compounds containing multifunctional sites. A broad array of substituted orthoesters has been synthesized using a modified Pinner sequence [53]. Karlsson *et al.* produced (2, 6'-dibenzothiazole)-2'-thiol **140** by reacting 4-(benzothiazole-2-yl)-2-bromoaniline **138** with ortho-ethyl potassium dithiocarbonate **139** in the presence of DMF at a temperature of 140 °C for 4 hours. Similarly, Yang *et al*. presented a systematic method for the highly efficient synthesis of polyfluorinated 2-benzylthiobenzothiazoles **143** using various substituted anilines **138** and ortho-ethyl potassium dithiocarbonate **139**. The current procedure reduces the required reaction time and enables the attainment of yields ranging from good to excellent [54] (**Scheme-2.44**). Murru *et al.* investigated the copper-catalyzed direct synthesis of substituted benzothiazoles **146** using ortho-haloaryl isothiocyanates **144** and various aromatic nucleophiles **145** that include O or S heteroatoms. This intramolecular C-S bond formation (**Scheme-2.45**) offers an efficient method for producing both O- and S-substituted 1, 3-benzothiazoles. Contrarily, thiols and alcohols were less reactive in this method [55].

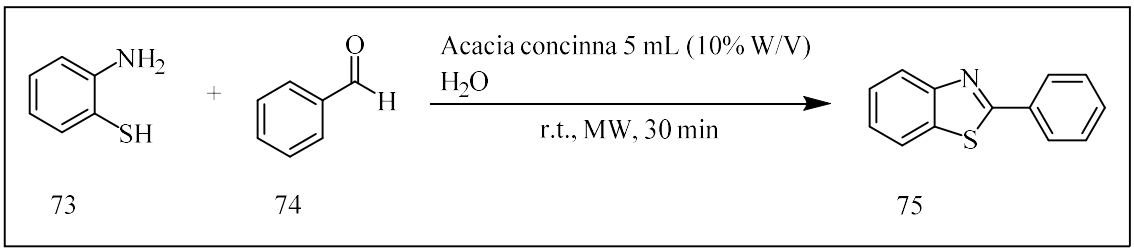

Scheme-2.23: Microwave-assisted synthesis of 2-aryl-benzothiazoles.

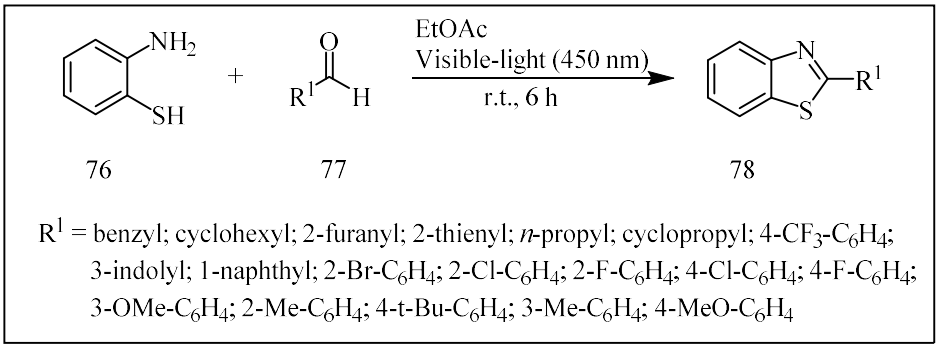

Scheme-2.24: Synthesis of benzothiazoles from 2-aminothiophenol under visible-light.

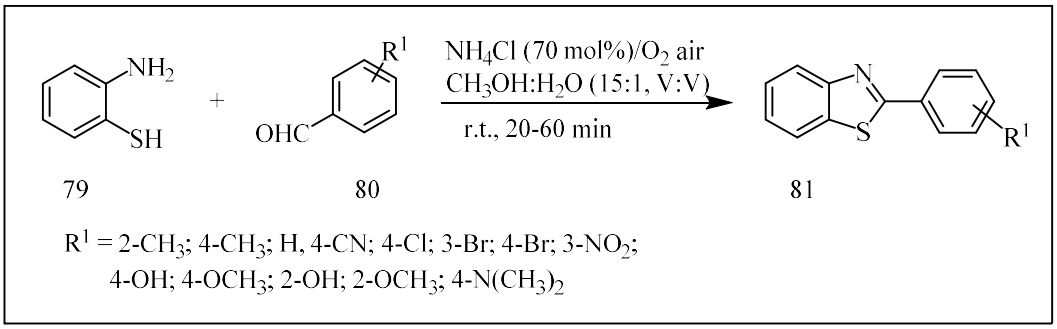

Scheme-2.25: NH_4Cl catalyzed preparation of benzothiazoles.

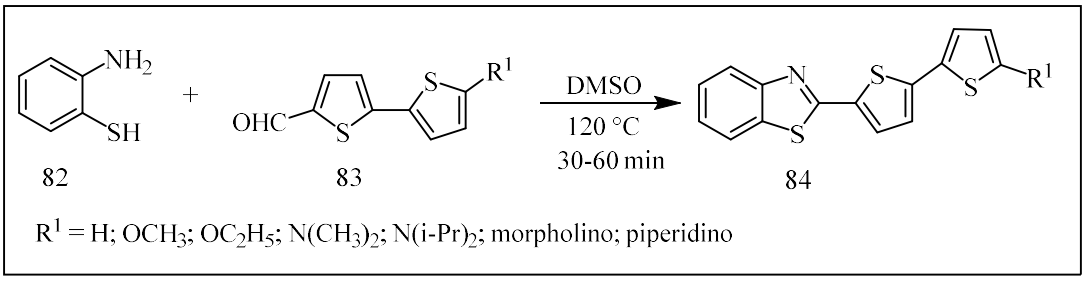

Scheme-2.26: Preparation of 2-bisthiophene substituted benzothiazole.

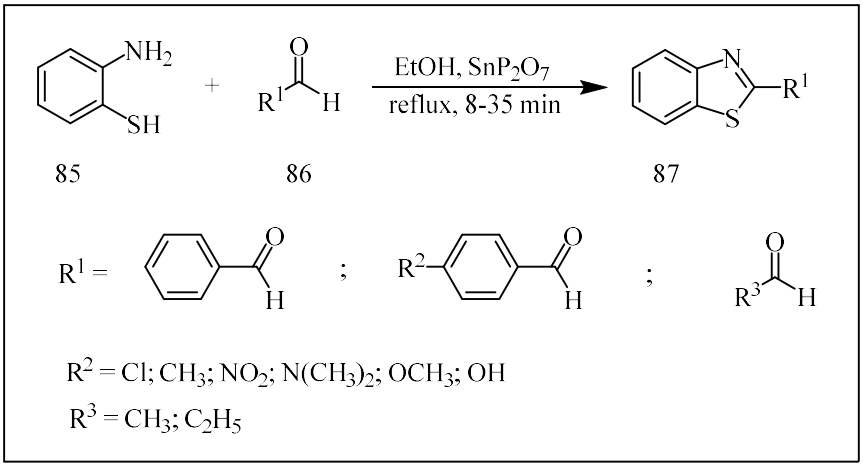

Scheme-2.27: Green synthesis of benzothiazoles from *ortho*-aminothiophenol.

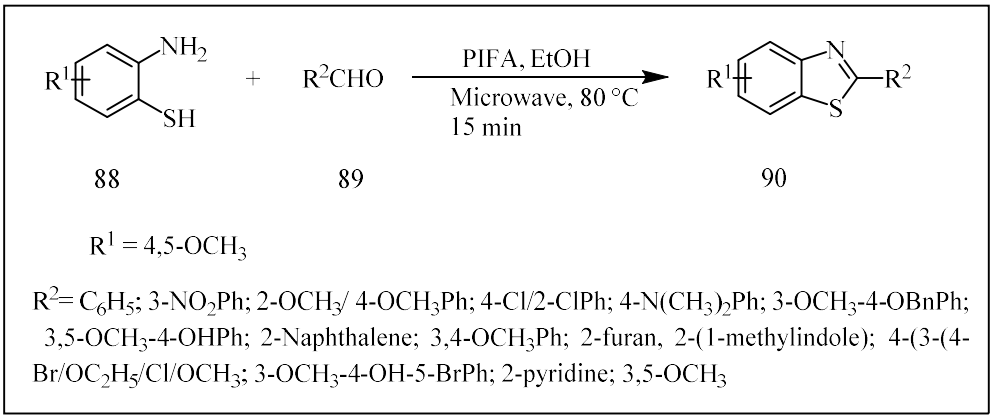

Scheme-2.28: Reaction of 2-aminobenzenethiol with benzaldehydes.

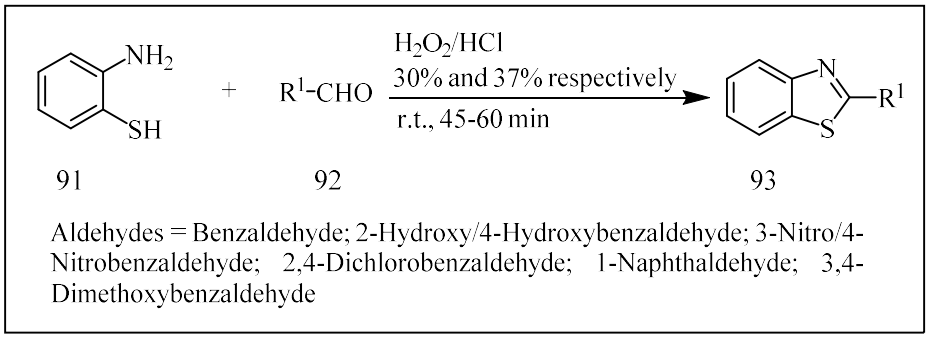

Scheme-2.29: Synthesis of a series of benzothiazole derivatives.

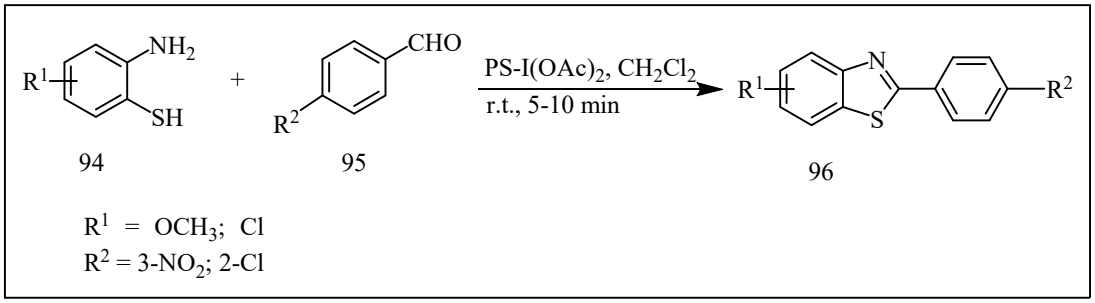

Scheme-2.30: Reaction of 2-aminobenzenethiol with benzaldehyde derivatives.

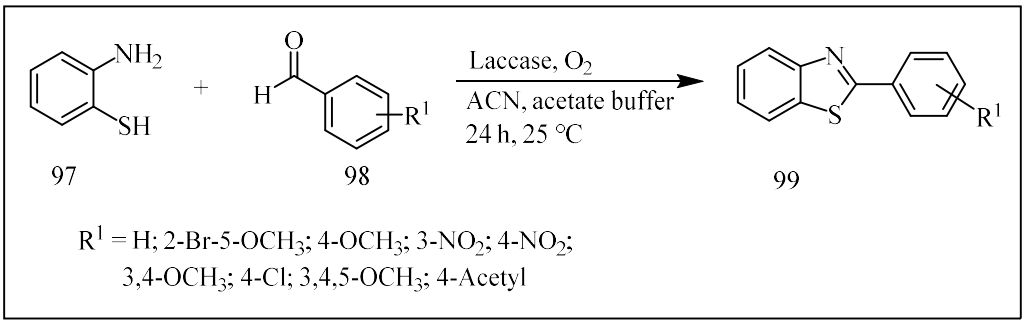

Scheme-2.31: Preparation of 2-arylbenzothiazole.

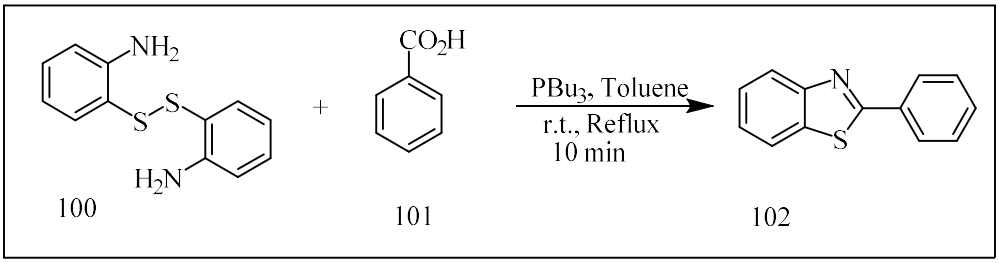

Scheme-2.32: Preparation of benzothiazoles from 2-aminothiophenol disulfides and carboxylic acids.

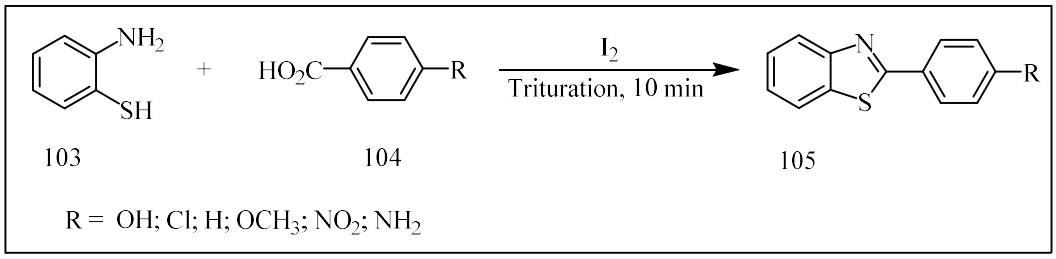

Scheme-2.33: Solvent-free synthesis of benzothiazole derivatives.

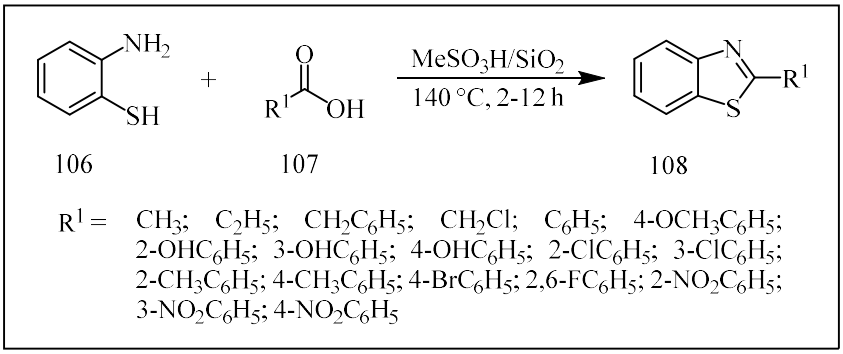

Scheme-2.34: Synthesis of 2-substituted aliphatic and aromatic benzothiazoles.

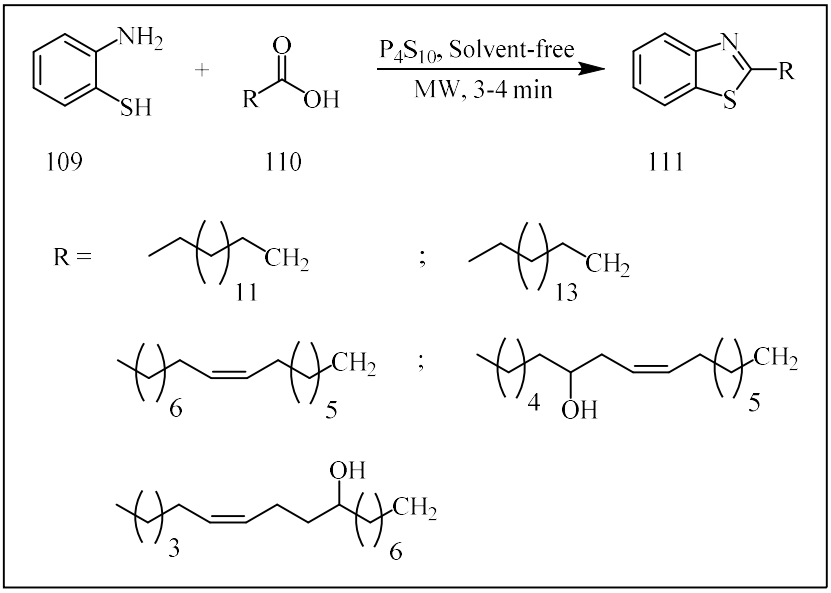

Scheme-2.35: Reaction of *ortho*-aminothiophenol and fatty acids.

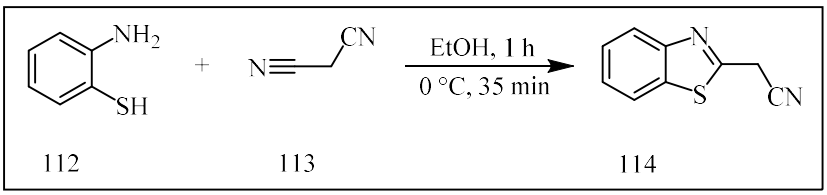

Scheme-2.36: Condensation of 2-aminothiophenol with malonodinitrile.

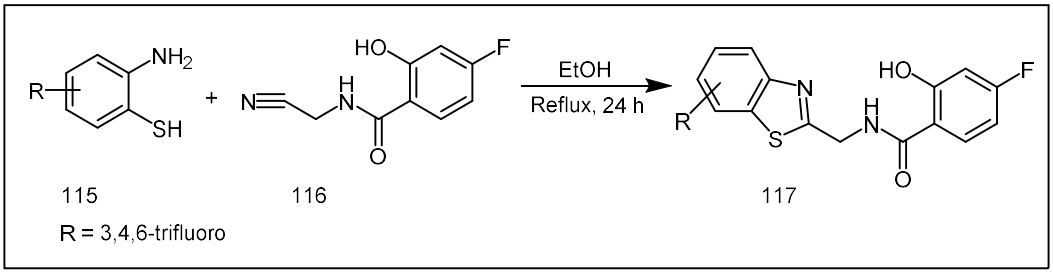

Scheme-2.37: Preparation of 4-fluoro-2-hydroxy-*N* (4, 5, 7-trifluorobenzothiazol-2-ylmethyl)-benzamide.

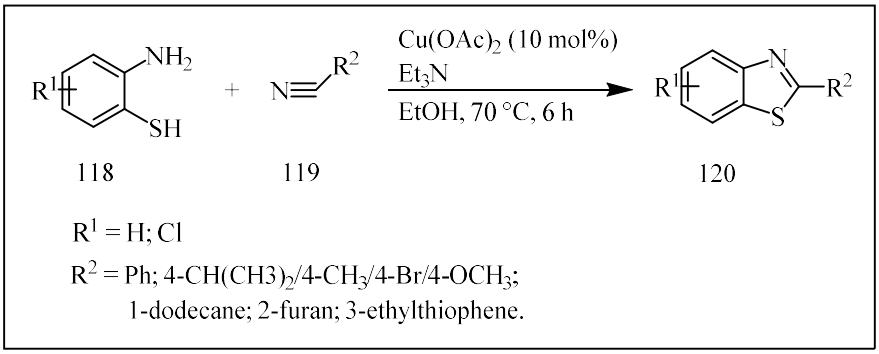

Scheme-2.38: Copper-catalyzed synthesis of benzothiazole derivatives.

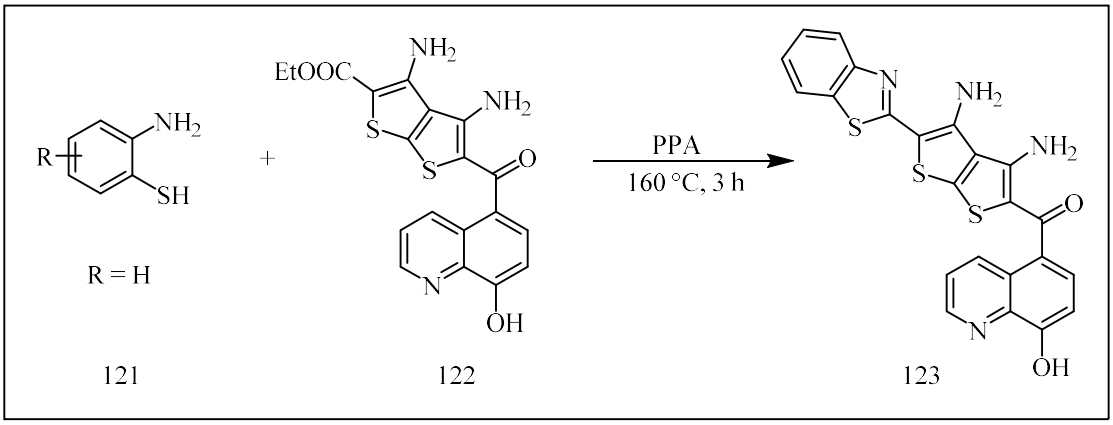

Scheme-2.39: Condensation of *ortho*-aminothiophenol with amino ester.

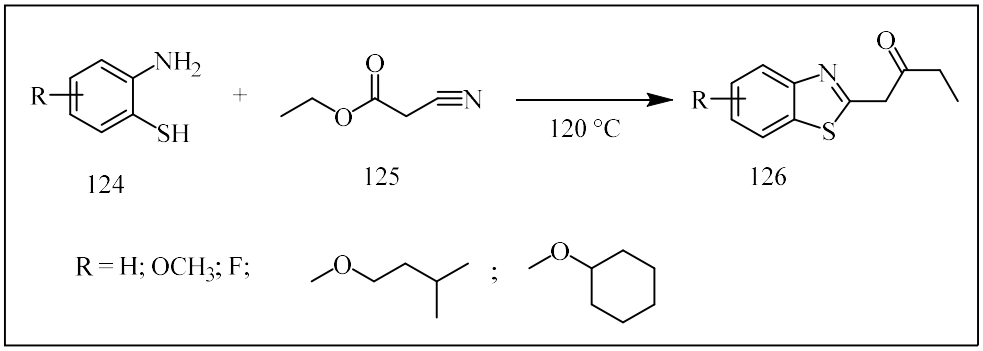

Scheme-2.40: Condensation of *ortho*-aminothiophenol with ethyl cyanoacetate.

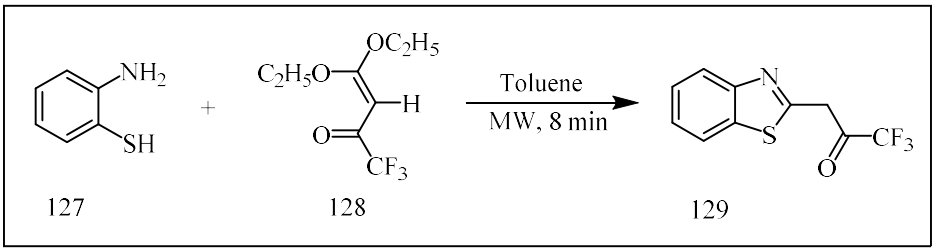

Scheme-2.41: Synthesis of trifluoroacetonyl benzothiazole under microwave irradiation.

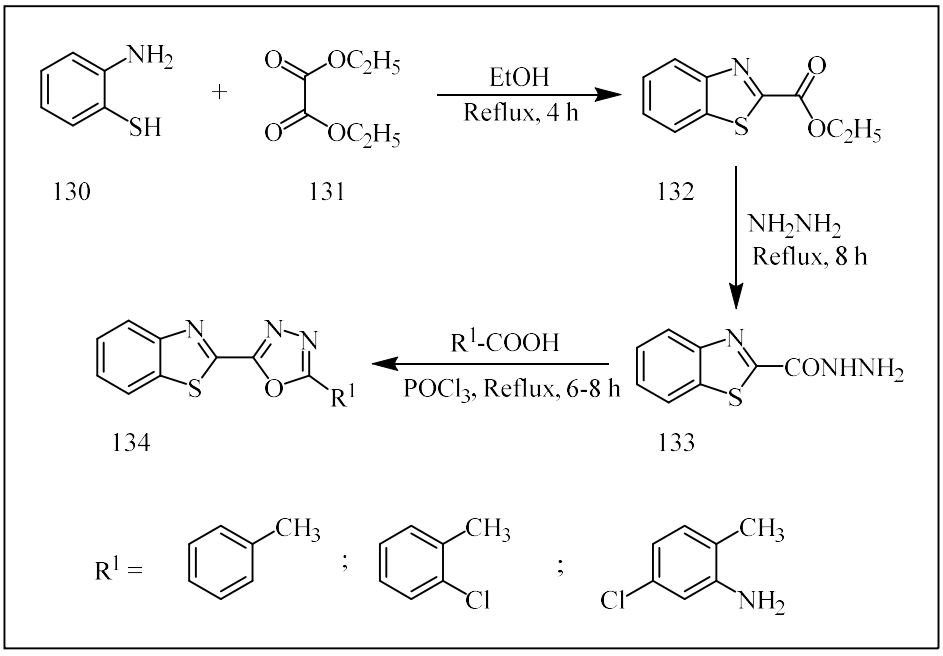

Scheme-2.42: Condensation of benzothiazolyl carboxyhydrazide with aryl acids.

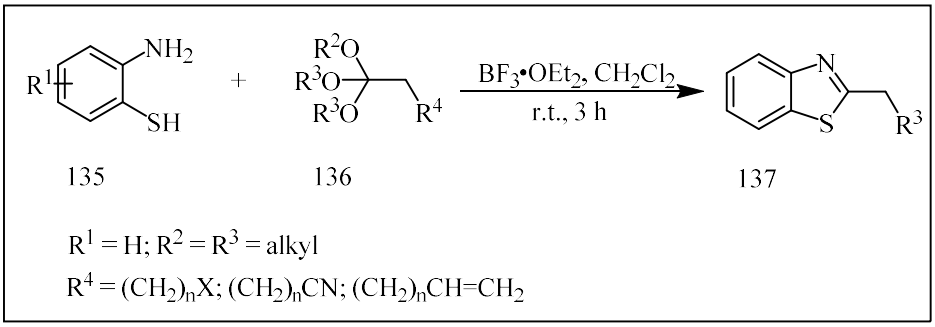

Scheme-2.43: Preparation of benzothiazole derivatives from substituted anilines and orthoesters.

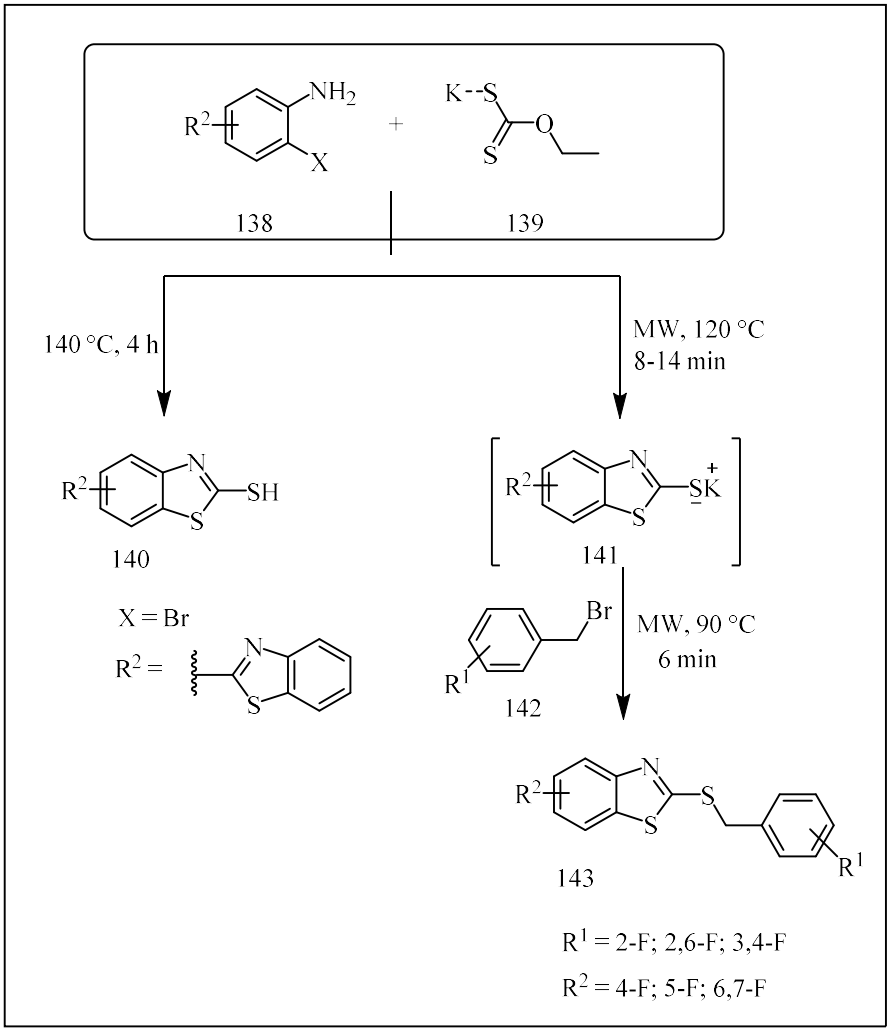

Scheme-2.44: Synthesis of (2, 6'-dibenzothiazole)-2'-thiol.

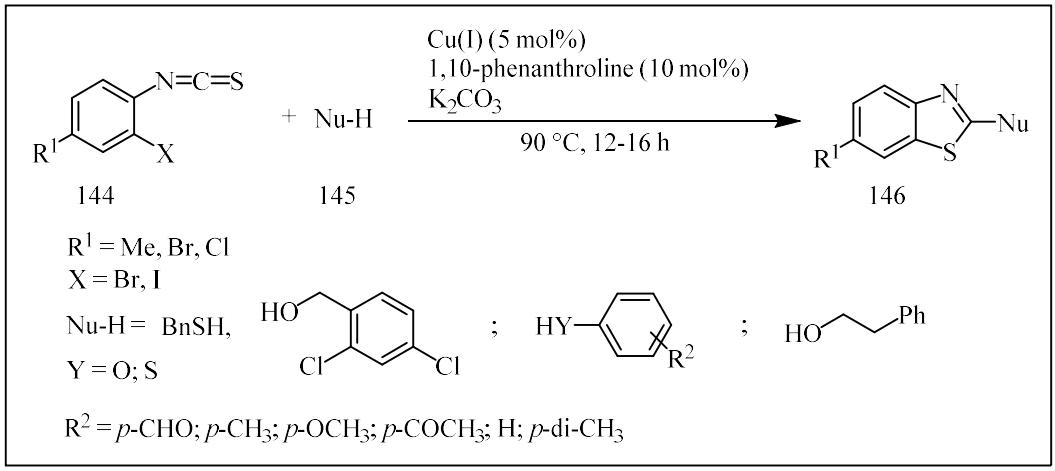

Scheme-2.45: Synthesis of 2-substituted-1, 3-benzothiazoles.

2.3. Applications of Benzothiazoles

Benzothiazole, a class of thiazole featuring a benzene-fused ring, has emerged as a valuable moiety in medicinal, synthetic, and pharmaceutical chemistry because of its remarkable biological activities. Researchers began studying various 2-aminobenzothiazoles as central muscle depressants in the 1950s, subsequently shifting their focus towards synthesizing these derivatives. Considering their notable biological activities, the synthesis of benzothiazoles and their derivatives has become a prominent research and discussion topic. Numerous derivatives have been synthesized and assessed for their multifaceted effects, including antifungal, anti-proliferative, and antioxidant properties. Notably, a substantial number of benzothiazole derivatives exhibit potent anticancer activities, and a comprehensive understanding of the SAR has been achieved for various cancer cell lines. Furthermore, benzothiazole acts as a robust antimicrobial agent, further underscoring its versatility. In light of these factors, derivatives of benzothiazole and its analogs continue to hold substantial importance in the research domain, as evidenced by the numerous patents related to this compound. Moreover, a multitude of benzothiazole derivatives are currently progressing through various stages of clinical trials. Benzothiazoles have also gained recognition for their antioxidant properties. Their structural features, such as the presence of sulfur, allow them to effectively scavenge free radicals and reactive oxygen species (ROS), thereby acting as antioxidants. Benzothiazoles have been explored for their potential to protect cells and tissues from oxidative damage, which is associated with various diseases.

2-Aminobenzothiazoles are considered the building blocks of many pharmaceuticals and agrochemicals. As a result, different derivatives of benzothiazole have been synthesized using morpholine, piperazine, and their derivatives because these compounds obtain strong significance because of their multiple pharmacological domains. For example, the synthesis of benzothiazole by using secondary amines as substrates: thiomorpholine, 1, 4-dioxa-8-azaspiro [4.5] decane and 1-phenylpiperazine also exhibit very good reactivity in the production of 2-aminobenzothiazoles. The reaction of isothiocyanate with morpholine produces 2-aminobenzothiazoles in excellent yield. Benzothiazole-piperazine compounds were prepared and evaluated for their cytotoxic impacts on various cancer cell lines, including hepatocellular (HepG-2), prostate (DU-145), breast (MCF-7), and colorectal (HCT-116) cancer cells. To illustrate, *N*-(6-methylbenzothiazol-2-yl)-2-(4-substitutedpiperazinyl) acetamides were created by treating 2-chloro-N-(6-methylbenzothiazol-2-yl) acetamides with piperazine and anhydrous K_2CO_3. Both piperazine-based and morpholine-based benzothiazole derivatives demonstrated significant activity against cancer cell lines, along with human liver cancer, prostate cancer, acute B-lymphoblastic leukemia, lung fibroblast cells, breast adenocarcinoma, lung cancer, and skin melanoma. The latter compound was particularly effective against BeI7402. Hela cells, MCF-7, and HepG2, and cancer cell lines, highlighting their potential as anticancer agents. Additionally, two benzothiazole derivatives, BTC6T and BTC8T, were synthesized and assessed for their corrosion inhibition properties against steel. These inhibitors exhibited superior efficacy and stability compared to previously studied benzothiazole-based inhibitors, as determined through potentiodynamic polarization, weight loss methods, and EIS. Furthermore, thiazole pyrimidine compounds were investigated for their ability to hinder the proliferation of various microorganisms, encompassing various strains of Mucor species. Notably, methoxy benzothiazole derivatives displayed excellent antimicrobial properties, suggesting the potential use of thiazoles in addressing conditions such as Mucormycosis (Black Fungus), a subject of growing research interest.

The concept of utilizing structure-activity relationships has evolved significantly over the past decade and has proven to be a successful strategy for discovering new drugs. It is a rapidly advancing theme within medicinal chemistry. Benzothiazoles are particularly valuable in this regard, as they serve as both core structures and capping fragments for designing and synthesizing targeted molecules efficiently. Their inherent affinity for various biological

receptors makes them a versatile resource for medicinal chemists. The molecules with the structures mentioned represent a class of compounds highly adept at binding to multiple receptors. Utilizing these molecules empowers medicinal chemists to rapidly identify bioactive compounds across a broad spectrum of therapeutic fields over an extended timeframe. Heterocyclic compounds containing nitrogen and sulfur are of significant importance not only in the life sciences but also in various industrial sectors, including specialty and fine chemistry. Among these, benzothiazoles stand out as a noteworthy category of medicinal compounds with diverse biological effects. They are rarely encountered in natural substances from marine or terrestrial sources, yet they possess advantageous biological properties. Moreover, benzothiazoles are acknowledged for their occurrence as fragrance constituents in tea leaves and cranberries, or as flavor compounds produced by fungi like *Aspergillus clavatus* and *Polyporus frondosus*. Recent research has explored benzothiazole derivatives as potential histamine H2 receptor antagonists, inhibitors of stearoyl coenzyme A d-9 desaturase, inhibitors of selective fatty acid amide hydrolase, antagonists of the LTD4 receptor, and antagonists of the orexin receptor. Furthermore, they find applications as agents for plant protection, intermediates in dye production, appetite suppressants, imaging agents for β-amyloid plaques, and sensitizers in photography [56-61].

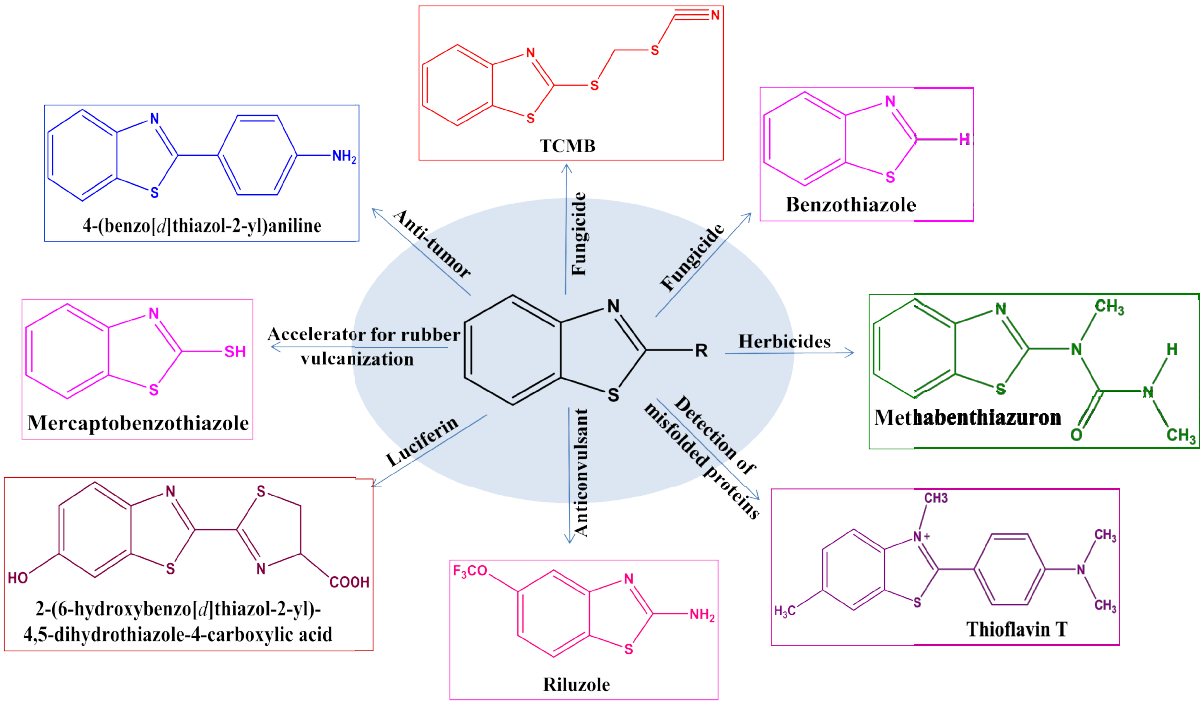

Fig.-2.1: Popular benzothiazole molecules.

2.4. Antibiotic Resistance

Antibiotic resistance refers to the capacity of bacteria to withstand the actions of antibiotics that were previously effective in treating the infections they are responsible for, stands out as a critical concern in the realm of AMR, compared to other forms of resistance such as antiviral or antifungal resistance, due to several reasons [62]. Firstly, antibiotics are widely used for treating a range of bacterial infections, including life-threatening conditions such as sepsis and pneumonia. In contrast, antifungal and antiviral are used for treating fungal and viral infections, respectively, which generally have a lower incidence and severity as compared to bacterial infections [63]. Secondly, the development of new antibiotics has stagnated in recent decades, resulting in a reduction in the efficacy of current antibiotics in combating bacterial infections. In contrast, several new antiviral and antifungal have been developed in recent years, including those for HIV, hepatitis C, and invasive fungal infections [64]. Thirdly, the economic burden of antibiotic resistance is estimated to be higher than that of antifungal and antiviral resistance, due to the higher incidence and severity of bacterial infections. Research conducted in the United States estimated that the annual economic cost is over $55 billion, primarily due to increased healthcare costs and productivity losses [65]. In response to the escalating problem of antibiotic resistance, the WHO issued a list of the most “critical pathogens” in February 2017, termed **“ESKAPE”**, these biofilm-associated superbugs pose an imminent threat to human health, thereby necessitating utmost priority in their management [66]. The acronym "ESKAPE" was first introduced by a team of researchers led by Louis B. Rice, MD, at Case Western Reserve University in Cleveland, Ohio, who noted the growing concern of antibiotic resistance in these specific pathogens [67]. These microorganisms have been recognized as a significant source of infections acquired in healthcare settings. They are responsible for various infections, such as pneumonia, bloodstream infections, urinary tract infections, and surgical site infections. Their remarkable capacity to resist the effects of antibacterial agents is notable, and they are frequently linked to high rates of illness and death [68].

2.5. Antibiotic Discovery & Development: Combating Bacterial Resistance in Bacterial cells & Biofilm communities

Drug discovery is one approach that can potentially be used to combat both biofilms and AMR. Developing new drugs that are effective against biofilms and resistant bacteria is critical for

improving the treatment of bacterial infections [69]. The burgeoning challenge of antibiotic resistance further complicated by biofilm formation among ESKAPE pathogens is significantly aggravated by the slow progress in the exploration and creation of novel antibiotics, demanding an urgent and concerted effort to revitalize this pipeline which is rapidly drying up. Research and development to discover and develop new antibiotics aiming at disruption of biofilm, through screening of natural products, modifying existing antibiotics, and developing novel drug targets has been identified as the most crucial [70]. The development and application of antibiotics have made significant contributions to medical technology and life expectancy, but the emergence of AMR calls for continued research and development of new antimicrobials. Between 1949 and 1980, the most significant developments concerning the different classes of antibiotics occurred. However, since 1987, there has been a lack of major discoveries in new classes of antibiotics, leading to an "antibiotic discovery void".

The widespread proliferation of drug-resistant pathogens is making antibiotics increasingly ineffective. The COVID-19 pandemic has exacerbated an already significant issue of secondary infections associated with MDR bacteria, which primarily affects immunocompromised patients, particularly those receiving care in healthcare settings. The substantial incidence of secondary infections during COVID-19 in hospitalized patients, coupled with the rampant misuse of antibiotics, has created a perfect storm that threatens to unleash dire consequences on healthcare, the economy, and society at large. Critical medical procedures such as cancer chemotherapy, organ transplantation, and surgical interventions will increasingly become perilous due to resistance strains. Thus, the pressing need for novel antibiotic development becomes more pronounced antibiotics [71].

2.6. Conclusion

Benzothiazoles exhibit a wide range of applications in both the pharmaceutical and industrial sectors. With the progression of eco-friendly protocols and sustainable chemical processes that emphasize operational simplicity, enhanced selectivity, cost efficiency, and high product yields, various methodologies have been periodically introduced for the synthesis of benzothiazole and its derivatives. Notably, considerable focus has been directed towards producing benzothiazole derivatives through the condensation of *ortho*-aminothiophenol with diverse nitriles, esters, aldehydes, ketones, and acids. It is noteworthy that the efficient synthesis of 2-

aminobenzothiazoles has been achieved using bromine, involving the reaction of various aromatic amines with sodium thiocyanate, potassium thiocyanate, or ammonium thiocyanate.

References

1. Zhilitskaya, L.V., Shainyan, B.A. and Yarosh, N.O., 2021. Modern approaches to the synthesis and transformations of practically valuable benzothiazole derivatives. *Molecules*, *26*(8), p.2190.
2. Qadir, T., Amin, A., Salhotra, A., Sharma, P.K., Jeelani, I. and Abe, H., 2022. Recent advances in the synthesis of benzothiazole and its derivatives. *Current Organic Chemistry*, *26*(2), pp.189-214.
3. Du, H., Sun, Y., Yang, R., Zhang, W., Wan, C., Chen, J., Kahramanoğlu, İ. and Zhu, L., 2021. Benzothiazole (BTH) induced resistance of navel orange fruit and maintained fruit quality during storage. *Journal of Food Quality*, *2021*, pp.1-8.
4. Jiang, P., Liu, L., Tan, J. and Du, H., 2021. Visible-light-promoted photocatalyst-free alkylation and acylation of benzothiazoles. *Organic & Biomolecular Chemistry*, *19*(20), pp.4487-4491.
5. Dhawale, K.D., Ingale, A.P., Shinde, S.V., Thorat, N.M. and Patil, L.R., 2021. ZnO-NPs catalyzed condensation of 2-aminothiophenol and aryl/alkyl nitriles: Efficient green synthesis of 2-substituted benzothiazoles. *Synthetic Communications*, *51*(10), pp.1588-1601.
6. Amin, A., Qadir, T., Salhotra, A., Sharma, P.K., Jeelani, I. and Abe, H., 2022. Pharmacological Significance of Synthetic Bioactive Thiazole Derivatives. *Current Bioactive Compounds*, *18*(9), pp.77-89.
7. Ma, H., Zhuang, C., Xu, X., Li, J., Wang, J., Min, X., Zhang, W., Zhang, H. and Miao, Z., 2017. Discovery of benzothiazole derivatives as novel non-sulfamide NEDD8 activating enzyme inhibitors by target-based virtual screening. *European journal of medicinal chemistry*, *133*, pp.174-183.
8. Kim, J. and Oh, K., 2020. Copper-Catalyzed Aerobic Oxidation of Amines to Benzothiazoles via Cross Coupling of Amines and Arene Thiolation Sequence. *Advanced Synthesis & Catalysis*, *362*(17), pp.3576-3582.
9. Qi, Y., Chen, Y., Xiu, F.R. and Hou, J., 2020. An aptamer-based colorimetric sensing of acetamiprid in environmental samples: Convenience, sensitivity and practicability. *Sensors and Actuators B: Chemical*, *304*, p.127359.

10. Chun, S., Yang, S. and Chung, Y.K., 2017. Synthesis of benzothiazoles from 2-aminobenzenethiols in the presence of a reusable polythiazolium precatalyst under atmospheric pressure of carbon dioxide. *Tetrahedron*, *73*(25), pp.3438-3442.
11. Gao, X., Yu, B., Zhao, Y., Hao, L. and Liu, Z., 2014. Hydrosilane-promoted cyclization of 2-aminothiophenols by CO 2 to benzothiazoles. *RSC Advances*, *4*(100), pp.56957-56960.
12. Gao, X., Yu, B., Yang, Z., Zhao, Y., Zhang, H., Hao, L., Han, B. and Liu, Z., 2015. Ionic liquid-catalyzed C–S bond construction using CO2 as a C1 building block under mild conditions: A metal-free route to synthesis of benzothiazoles. *ACS Catalysis*, *5*(11), pp.6648-6652.
13. Chun, S., Yang, S. and Chung, Y.K., 2017. Synthesis of benzothiazoles from 2-aminobenzenethiols in the presence of a reusable polythiazolium precatalyst under atmospheric pressure of carbon dioxide. *Tetrahedron*, *73*(25), pp.3438-3442.
14. Folgueiras-Amador, A.A., Qian, X.Y., Xu, H.C. and Wirth, T., 2018. Catalyst-and supporting-electrolyte-free electrosynthesis of benzothiazoles and thiazolopyridines in continuous flow. *Chemistry–A European Journal*, *24*(2), pp.487-491.
15. Bouchet, L.M., Heredia, A.A., Arguello, J.E. and Schmidt, L.C., 2019. Riboflavin as photoredox catalyst in the cyclization of thiobenzanilides: synthesis of 2-substituted benzothiazoles. *Organic letters*, *22*(2), pp.610-614.
16. Rey, V., Soria-Castro, S.M., Argüello, J.E. and Peñéñory, A.B., 2009. Photochemical cyclization of thioformanilides by chloranil: An approach to 2-substituted benzothiazoles. *Tetrahedron Letters*, *50*(33), pp.4720-4723.
17. Bose, D.S. and Idrees, M., 2006. Hypervalent iodine mediated intramolecular cyclization of thioformanilides: expeditious approach to 2-substituted benzothiazoles. *The Journal of Organic Chemistry*, *71*(21), pp.8261-8263.
18. Downer-Riley, N.K. and Jackson, Y.A., 2008. Conversion of thiobenzamides to benzothiazoles via intramolecular cyclization of the aryl radical cation. *Tetrahedron*, *64*(33), pp.7741-7744.
19. Xu, Z.M., Li, H.X., Young, D.J., Zhu, D.L., Li, H.Y. and Lang, J.P., 2018. Exogenous photosensitizer-, metal-, and base-free visible-light-promoted C–H thiolation via reverse hydrogen atom transfer. *Organic letters*, *21*(1), pp.237-241.

20. Cheng, Y., Yang, J., Qu, Y. and Li, P., 2012. Aerobic visible-light photoredox radical C–H functionalization: Catalytic synthesis of 2-substituted benzothiazoles. *Organic Letters*, *14*(1), pp.98-101.
21. Feng, E., Huang, H., Zhou, Y., Ye, D., Jiang, H. and Liu, H., 2010. Metal-free synthesis of 2-substituted (N, O, C) benzothiazoles via an intramolecular C− S bond formation. *Journal of Combinatorial Chemistry*, *12*(4), pp.422-429.
22. Wang, H., Wang, L., Shang, J., Li, X., Wang, H., Gui, J. and Lei, A., 2012. Fe-catalyzed oxidative C–H functionalization/C–S bond formation. *Chemical Communications*, *48*(1), pp.76-78.
23. Luo, B., Li, D., Zhang, A.L. and Gao, J.M., 2018. Synthesis, antifungal activities and molecular docking studies of benzoxazole and benzothiazole derivatives. *Molecules*, *23*(10), p.2457.
24. Racané, L., Kralj, M., Šuman, L., Stojković, R., Tralić-Kulenović, V. and Karminski-Zamola, G., 2010. Novel amidino substituted 2-phenylbenzothiazoles: Synthesis, antitumor evaluation in vitro and acute toxicity testing in vivo. *Bioorganic & medicinal chemistry*, *18*(3), pp.1038-1044.
25. Dar, A.A., Shadab, M., Khan, S., Ali, N. and Khan, A.T., 2016. One-pot synthesis and evaluation of antileishmanial activities of functionalized S-alkyl/aryl benzothiazole-2-carbothioate scaffold. *The Journal of Organic Chemistry*, *81*(8), pp.3149-3160.
26. Nadaf, R.N., Siddiqui, S.A., Daniel, T., Lahoti, R.J. and Srinivasan, K.V., 2004. Room temperature ionic liquid promoted regioselective synthesis of 2-aryl benzimidazoles, benzoxazoles and benzthiazoles under ambient conditions. *Journal of Molecular Catalysis A: Chemical*, *214*(1), pp.155-160.
27. Kumar, K.R., Satyanarayana, P.V.V. and Srinivasa Reddy, B., --Promoted Solvent-Free Synthesis of Benzoxazoles, Benzimidazoles, and Benzothiazole Derivatives. *Journal of Chemistry*, *2013*.
28. Wu, C., Wei, J., Gao, K. and Wang, Y., 2007. Dibenzothiazoles as novel amyloid-imaging agents. *Bioorganic & medicinal chemistry*, *15*(7), pp.2789-2796.
29. Loukrakpam, D.C. and Phukan, P., 2019. TsNBr2 Mediated Synthesis of 2-Acylbenzothiazoles and Quinoxalines from Aryl Methyl Ketones under Metal Free Condition. *Chemistry Select*, *4*(11), pp.3180-3184.

30. Liao, Y., Qi, H., Chen, S., Jiang, P., Zhou, W. and Deng, G.J., 2012. Efficient 2-aryl benzothiazole formation from aryl ketones and 2-aminobenzenethiols under metal-free conditions. *Organic letters*, *14*(23), pp.6004-6007.
31. Mayo, M.S., Yu, X., Zhou, X., Feng, X., Yamamoto, Y. and Bao, M., 2014. Convenient synthesis of benzothiazoles and benzimidazoles through Brønsted acid catalyzed cyclization of 2-amino thiophenols/anilines with β-diketones. *Organic letters*, *16*(3), pp.764-767.
32. Elderfield, R.C. and McClenachan, E.C., 1960. Pyrolysis of the Products of the Reaction of o-Aminobenzenethiols with Ketones1. *Journal of the American Chemical Society*, *82*(8), pp.1982-1988.
33. Bhat, R., Karhale, S., Arde, S. and Helavi, V., 2019. Acacia concinna pod catalyzed synthesis of 2-arylbenzothia/(oxa) zole derivatives. *Iranian Journal of Catalysis*, *9*(2), pp.173-179.
34. Ye, L.M., Chen, J., Mao, P., Mao, Z.F., Zhang, X.J. and Yan, M., 2017. Visible-light-promoted synthesis of benzothiazoles from 2-aminothiophenols and aldehydes. *Tetrahedron Letters*, *58*(9), pp.874-876.
35. Maleki, B. and Salehabadi, H., 2010. Ammonium chloride; as a mild and efficient catalyst for the synthesis of some 2-arylbenzothiazoles and bisbenzothiazole derivatives. *European Journal of Chemistry*, *1*(4), pp.377-380.
36. Batista, R.M., Costa, S.P. and Raposo, M.M.M., 2004. Synthesis of new fluorescent 2-(2′, 2 ″-bithienyl)-1, 3-benzothiazoles. *Tetrahedron letters*, *45*(13), pp.2825-2828.
37. Merroun, Y., Chehab, S., Ghailane, T., Akhazzane, M., Souizi, A. and Ghailane, R., 2019. Preparation of tin-modified mono-ammonium phosphate fertilizer and its application as heterogeneous catalyst in the benzimidazoles and benzothiazoles synthesis. *Reaction Kinetics, Mechanisms and Catalysis*, *126*(1), pp.249-264.
38. Praveen, C., Nandakumar, A., Dheenkumar, P., Muralidharan, D. and Perumal, P.T., 2012. Microwave-assisted one-pot synthesis of benzothiazole and benzoxazole libraries as analgesic agents. *Journal of Chemical Sciences*, *124*, pp.609-624.
39. Guo, H.Y., Li, J.C. and Le Shang, Y., 2009. A simple and efficient synthesis of 2-substituted benzothiazoles catalyzed by H2O2/HCl. *Chinese Chemical Letters*, *20*(12), pp.1408-1410.
40. Kumar, A., Maurya, R.A. and Ahmad, P., 2009. Diversity oriented synthesis of benzimidazole and benzoxa/(thia) zole libraries through polymer-supported hypervalent iodine reagent. *Journal of Combinatorial Chemistry*, *11*(2), pp.198-201.

41. Maphupha, M., Juma, W.P., de Koning, C.B. and Brady, D., 2018. A modern and practical laccase-catalyzed route suitable for the synthesis of 2-arylbenzimidazoles and 2-arylbenzothiazoles. *RSC advances*, *8*(69), pp.39496-39510.
42. Coelho, F.L. and Campo, L.F., 2017. Synthesis of 2-arylbenzothiazoles via direct condensation between in situ generated 2-aminothiophenol from disulfide cleavage and carboxylic acids. *Tetrahedron Letters*, *58*(24), pp.2330-2333.
43. Pal, S., Patra, G. and Bhunia, S., 2009. Microwave-assisted syntheses of 2-phenylbenzothiazoles. *Synthetic Communications®*, *39*(7), pp.1196-1203.
44. Sharghi, H. and Asemani, O., 2009. Methanesulfonic acid/SiO2 as an efficient combination for the synthesis of 2-substituted aromatic and aliphatic benzothiazoles from carboxylic acids. *Synthetic Communications®*, *39*(5), pp.860-867.
45. Rauf, A., Gangal, S. and Sharma, S., 2008. Solvent-free synthesis of 2-alkyl and 2-alkenylbenzothiazoles from fatty acids under microwave irradiation.
46. Mokhir, A.A., Domasevich, K.V., Dalley, N.K., Kou, X., Gerasimchuk, N.N. and Gerasimchuk, O.A., 1999. Syntheses, crystal structures and coordination compounds of some 2-hetarylcyanoximes. *Inorganica chimica acta*, *284*(1), pp.85-98.
47. Van Zandt, M.C., Sibley, E.O., McCann, E.E., Combs, K.J., Flam, B., Sawicki, D.R., Sabetta, A., Carrington, A., Sredy, J., Howard, E. and Mitschler, A., 2004. Design and synthesis of highly potent and selective (2-arylcarbamoyl-phenoxy)-acetic acid inhibitors of aldose reductase for treatment of chronic diabetic complications. *Bioorganic & medicinal chemistry*, *12*(21), pp.5661-5675.
48. Sun, Y., Jiang, H., Wu, W., Zeng, W. and Wu, X., 2013. Copper-catalyzed synthesis of substituted benzothiazoles via condensation of 2-aminobenzenethiols with nitriles. *Organic letters*, *15*(7), pp.1598-1601.
49. Khalil, Z.H., Yanni, A.S., Gaber, A.M. and Abdel-Mohsen, S.A., 2000. Synthesis and reactions of some new 5-carbonyl (4-amino-3-cyano-2-substituted thiophene-5-yl)-8-hydroxyquinoline (part ii). Synthesis of thiazole; isoxazole; pyrazole, pyrimidine and pyridazine derivatives as possible antimicrobial agents. *Phosphorus, Sulfur, and Silicon and the Related Elements*, *166*(1), pp.57-69.
50. Manfroni, G., Meschini, F., Barreca, M.L., Leyssen, P., Samuele, A., Iraci, N., Sabatini, S., Massari, S., Maga, G., Neyts, J. and Cecchetti, V., 2012. Pyridobenzothiazole derivatives as

new chemotype targeting the HCV NS5B polymerase. *Bioorganic & medicinal chemistry*, *20*(2), pp.866-876.

51. Reddy, A.C.S., Rao, P.S. and Venkataratnam, R.V., 1997. Fluoro organics: Facile syntheses of novel 2-or 4-trifluoromethyl-1H-arylo-1, 5-diazepines, oxazepines, thiazepines, 2-(1, 1, 1-trifluoroacetonyl) imidazoles, oxazoles and thiazoles. *Tetrahedron*, *53*(16), pp.5847-5854.
52. Rajeeva, B., Srinivasulu, N. and Shantakumar, S.M., 2009. Synthesis and Antimicrobial Activity of some New 2-Substituted Benzothiazole Derivatives. *Journal of chemistry*, *6*, pp.775-779.
53. Bastug, G., Eviolitte, C. and Marko, I.E., 2012. Functionalized orthoesters as powerful building blocks for the efficient preparation of heteroaromatic bicycles. *Organic letters*, *14*(13), pp.3502-3505.
54. Karlsson, H.J., Bergqvist, M.H., Lincoln, P. and Westman, G., 2004. Syntheses and DNA-binding studies of a series of unsymmetrical cyanine dyes: structural influence on the degree of minor groove binding to natural DNA. *Bioorganic & medicinal chemistry*, *12*(9), pp.2369-2384.
55. Murru, S., Mondal, P., Yella, R. and Patel, B.K., 2009. Copper (I)-Catalyzed Cascade Synthesis of 2-Substituted 1, 3-Benzothiazoles: Direct Access to Benzothiazolones.
56. Tariq, S., Kamboj, P. and Amir, M., 2019. Therapeutic advancement of benzothiazole derivatives in the last decennial period. *Archiv der Pharmazie*, *352*(1), p.1800170.
57. Banerjee, S., Payra, S. and Saha, A., 2017. A review on synthesis of benzothiazole derivatives. *Current Organocatalysis*, *4*(3), pp.164-181.
58. Song, Y., Hu, L., Cheng, Q., Chen, Z., Su, H., Liu, H., Liu, R., Zhu, S. and Zhu, H., 2022. Benzothiazole derivatives with varied π-conjugation: synthesis, tunable solid-state emission, and application in single-component LEDs. *Journal of Materials Chemistry C*, *10*(16), pp.6392-6401.
59. Kamal, A., Syed, M.A.H. and Mohammed, S.M., 2015. Therapeutic potential of benzothiazoles: A patent review (2010–2014). *Expert opinion on therapeutic patents*, *25*(3), pp.335-349.
60. Henary, M., Paranjpe, S. and Owens, E.A., 2013. Synthesis and applications of benzothiazole containing cyanine dyes. *Heterocyclic Communications*, *19*(1), pp.1-11.

61. Agarwal, S., Gandhi, D. and Kalal, P., 2017. Benzothiazole: A versatile and multitargeted pharmacophore in the field of medicinal chemistry. *Letters in Organic Chemistry*, *14*(10), pp.729-742.
62. Aslam, B., Wang, W., Arshad, M.I., Khurshid, M., Muzammil, S., Rasool, M.H., Nisar, M.A., Alvi, R.F., Aslam, M.A., Qamar, M.U. and Salamat, M.K.F., 2018. Antibiotic resistance: a rundown of a global crisis. *Infection and drug resistance*, pp.1645-1658.
63. Ventola, C.L., 2015. The antibiotic resistance crisis: part 1: causes and threats. *Pharmacy and therapeutics*, *40*(4), p.277.
64. Hughes, D. and Karlén, A., 2014. Discovery and preclinical development of new antibiotics. *Upsala journal of medical sciences*, *119*(2), pp.162-169.
65. Dadgostar, P., 2019. Antimicrobial resistance: implications and costs. *Infection and drug resistance*, pp.3903-3910.
66. Mancuso, G., Midiri, A., Gerace, E. and Biondo, C., 2021. Bacterial antibiotic resistance: The most critical pathogens. *Pathogens*, *10*(10), p.1310.
67. Rice, L.B., 2008. Federal funding for the study of antimicrobial resistance in nosocomial pathogens: no ESKAPE. *The Journal of infectious diseases*, *197*(8), pp.1079-1081.
68. Boucher, H.W., Talbot, G.H., Bradley, J.S., Edwards, J.E., Gilbert, D., Rice, L.B., Scheld, M., Spellberg, B. and Bartlett, J., 2009. Bad bugs, no drugs: no ESKAPE! An update from the Infectious Diseases Society of America. *Clinical infectious diseases*, *48*(1), pp.1-12.
69. Sauer, K., Stoodley, P., Goeres, D.M., Hall-Stoodley, L., Burmølle, M., Stewart, P.S. and Bjarnsholt, T., 2022. The biofilm life cycle: Expanding the conceptual model of biofilm formation. *Nature Reviews Microbiology*, *20*(10), pp.608-620.
70. Vaughn, V.M., Gandhi, T.N., Petty, L.A., Patel, P.K., Prescott, H.C., Malani, A.N., Ratz, D., McLaughlin, E., Chopra, V. and Flanders, S.A., 2021. Empiric antibacterial therapy and community-onset bacterial coinfection in patients hospitalized with coronavirus disease 2019 (COVID-19): a multi-hospital cohort study. *Clinical Infectious Diseases*, *72*(10), pp.e533-e541.
71. Hein, C.D., Liu, X.M. and Wang, D., 2008. Click chemistry, a powerful tool for pharmaceutical sciences. *Pharmaceutical research*, *25*, pp.2216-2230.

CHAPTER-3

MATERIALS AND METHODS

This chapter provides a succinct overview of the materials used and methodologies implemented in this study. The details are systematically delineated into distinct sections to facilitate a thorough comprehension.

3.1. Chemistry

The chemicals and solvents utilized in this study were procured from E. Merck (India) and Sigma Aldrich chemicals, and they were used as received without any further purification. Thin-layer chromatography (TLC) was conducted on pre-coated aluminum sheets (Silica gel 60 F254, Merck Germany). The visualization of the synthesized compounds on TLC was achieved using ultraviolet (UV) light at a wavelength of 254 nm. The melting points of all compounds were determined using a Veego instrument with model specifications REC-22038 A2 and these values are reported without correction. Single crystal X-ray diffraction (SCXRD) was performed using a *Bruker* D8-Venture single crystal X-ray diffractometer equipped with a digital camera. ^{1}H NMR and ^{13}C NMR spectra were recorded on a Bruker Avance DX spectrometer operating at 400 and 100 MHz, respectively from IIT Delhi, India. The chemical shifts are reported relative to the residual deuterated solvent peaks, with chemical shifts denoted in ppm. Splitting patterns are indicated as s (singlet), d (doublet), t (triplet), q (quartet), dd (doublet of doublet), or m (multiplet), while coupling constants (J) are expressed in hertz. Mass spectra were obtained using Electrospray Ionization Mass Spectrometry (ESI-MS) on an AB-Sciex 2000 (Applied Biosystem) instrument and a GCMS-QP 5000 (Shimadzu) mass spectrometer. Infrared spectra were recorded neat on a Perkin Elmer FT-IR spectrometer using the ATR technique. Solvent evaporation was carried out under reduced pressure using a rotary evaporator (IKA).

3.2. *In Vitro* Antibacterial Activity

(Note: The antibacterial experiments were carried out at the Centre of Research for Development and P.G Programme in Microbiology, within the School of Biological Sciences at the University of Kashmir, Srinagar, Jammu and Kashmir, India).

3.2.1. Chemicals and Reagents

MHB, NA, Gram Staining Kit, and Crystal Violet (cell culture tested) used in the study were supplied by HiMedia. DMSO, Methanol, Glycerol, [Aqueous] Acetic Acid, NaCl, Isopropanol, Absolute Ethanol, Resazurin, and MTT were purchased from Merck (India). DAPI Stain and PI counter stain were purchased from Thermo Fischer Scientific. FBS, BSA, DMEM, Trypsin, and

PBS were obtained from Gibco (Thermo Fischer Scientific). All chemicals used were of analytical research grade.

3.2.2. Plasticware and Glassware

Flat bottomed 96-well microtiter plates with lids, 12 well cell culture plates, 15 and 50 mL Falcon tubes, Micro centrifuge Eppendorf tubes (1.5 mL and 2mL), Micropipettes and tips, Multichannel pipette, 500 mL Erlenmeyer flasks, Autoclaved disposable Petri plates (90 mm), 500 mL Reagent bottles, Cell Culture flasks (T25 & T75), Cuvettes, Cryopreservation boxes, Microscopic Glass Slides, Autoclavable biohazard bags, Gloves, Plastic filters, Parafilm, Filter paper. All the materials were supplied by Tarsons.

3.2.3. Instruments

Biosafety Cabinet-II Laminar Air Flow (ESCO, SENITAL GOLD), Spectrophotometer (SPECTRO-STAR NANO, BMG Labtech), Analytical Balance, Vortex mixer, Shaker Incubator, CO2 incubator, Shaker Incubator (Labtech), Fluorescent Bright field Microscope (Magnus MU2A), 96 well Microplate Reader (MULTISKAN GO, Thermo Scientific).

3.2.4. Software

Graph Pad Prism version 9, Pyrex, Biorender- Image Software, GROMACS 2021.2, and Microsoft Excel, Chemdraw.

3.2.5. Bacterial Strains

Gram (+) bacteria; *Staphylococcus aureus* (ATCC 25923), *Enterococcus faecalis* (ATCC 51299), *Bacillus cereus* (MTCC 121) and Gram (-) bacteria; *Escherichia coli* (ATCC 10536), *Pseudomonas aeruginosa* (ATCC 10145), *Klebsiella pneumoniae* (NCTC 13440) were frozen as glycerol stocks and stored at –80 °C. For each experiment, the frozen bacterial stock was thawed and grown in MHB to the mid-logarithmic phase of growth under proper incubated conditions and then used.

3.2.6. Media Preparation

3.2.6.1. Preparation of Liquid Media: Mueller Hinton Broth

A quantity of 10.25 grams of MHB powder was suspended in 500 mL of distilled water (for each experiment). The mixture was filtered using filter paper. After filtration, the dissolved mixture was autoclaved at 121 ºC at 15 psi pressure, and allowed to cool below 40 ºC after which it was

incubated overnight before use to check for any contamination. This media was preferred for the study as it is a non-selective and non-differential media, free of inhibitors that can interfere with the growth of bacteria.

3.2.6.2. Preparation of Nutrient Agar

14 grams of NA powder was dissolved in 500 mL of distilled water. The mixture was autoclaved and after autoclaving cooled down to 40 ºC. Under sterile conditions, NA was poured on Petri dishes and left to solidify. On solidification, plates were incubated for 24 hours to check for contamination before use.

3.2.7. Recovery of Lyophilized Cultures

The ampoules of Gram (+) and Gram (-) bacteria procured were disinfected by wiping with 70% Ethanol. Initially, the end of the outer vial was heated with a flame and then cooled by squirting a few drops of water to generate a crack. Once the tip was extracted, the inner vial was taken out using forceps. The contents were aspirated several times to mix the suspension with the aseptically added sterile water. After 15-30 minutes the suspensions were inoculated onto 2mL MHB. After the growth of lyophilized cultures, 0.5 mL aliquots were poured in 20 mL MHB and incubated at 37 ºC until turbidity appeared. The bacterial cultures were used for glycerol stock preparation.

3.2.8. Glycerol Stock Preparation

40% glycerol was prepared by taking 40 mL glycerol and 60 mL distilled water and autoclaving the mixture. Actively growing bacteria were mixed with 40% glycerol in a ratio of 1:1 in a 50 mL falcon tube (15 mL culture + 15 mL of 40% Glycerol). The mixtures were vortexed. 1 mL aliquots of the solutions were dispensed in 2 mL Eppendorf tubes labelled with the name of bacterial strains and date. Tubes were sealed with Parafilm and stored at -80ºC till further use, prepared for all the bacterial strains under study.

3.2.9. Revival of Glycerol Stocks

The glycerol stocks of Gram (+) bacteria, *S. aureus*, *E. faecalis*, *B. cereus*, MRSA and Gram (-) bacteria, *E. coli*, MDR *Escherichia coli*, *P. aeruginosa*, *K. pneumoniae* were thawed before use. Under sterile conditions, the 15 mL Falcon tubes were labelled with the name of bacteria and date and arranged in a test tube stand. Each tube was filled with 10 mL of MHB, and then, 1 mL

of the corresponding bacterial strains was introduced into the tubes for inoculation. The tubes were sealed and incubated along with a Media control tube for 24 hours at 37 ºC.

3.2.10. Subculture on Nutrient Agar

The bacteria were sub-cultured on NA using a sterile inoculating loop using the streaking method.

Fig.-3.1: Revival of glycerol stocks and media preparation.

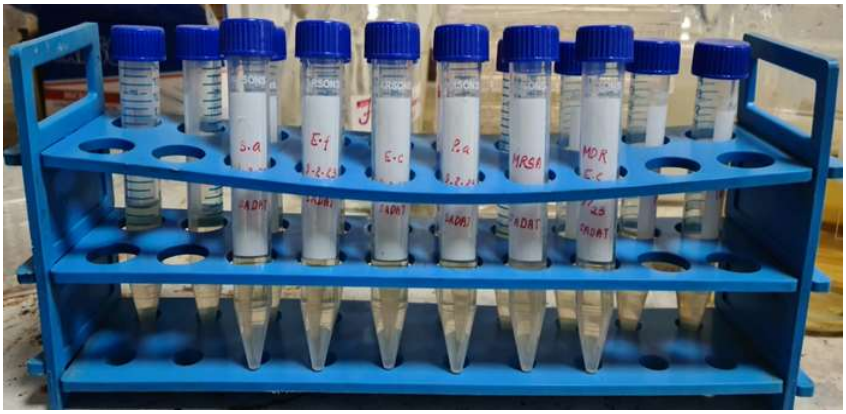

Fig.-3.2: Liquid subculture of Gram (+) and Gram (-) bacteria in Mueller Hinton Broth. Control tubes are used for quality control (Contamination).

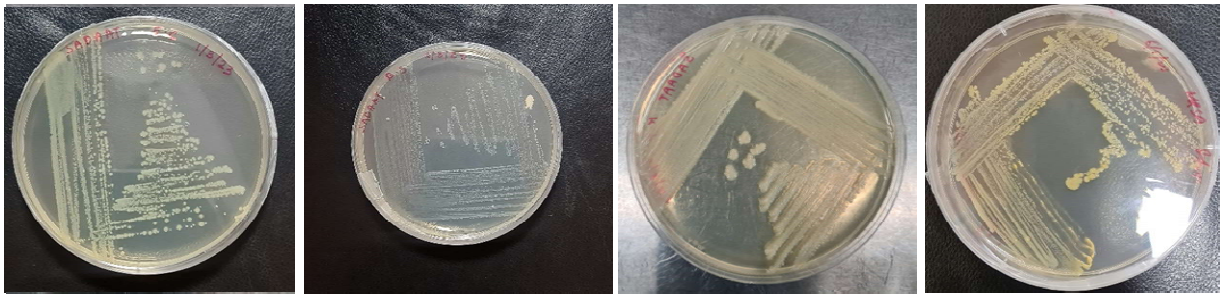

Fig.-3.3: Subculture of Gram (+) bacteria on Nutrient Agar Media; *S. aureus*, *B. cereus*, *E. faecalis* and MRSA.

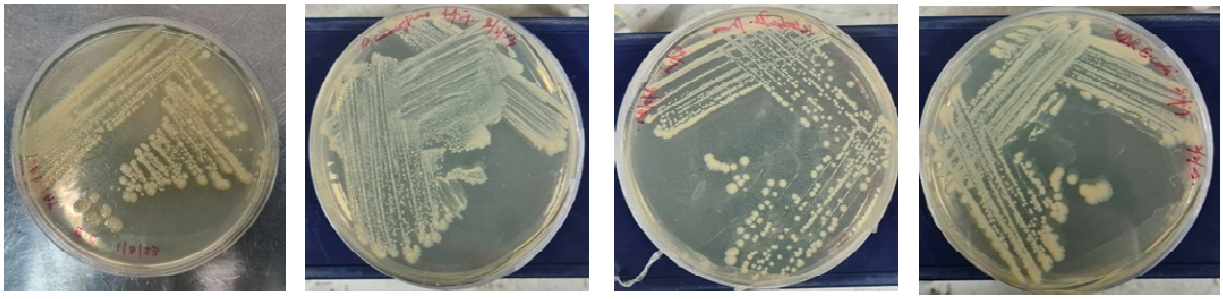

Fig.-3.4: Subculture of Gram (-) bacteria on Nutrient Agar Media; *E. coli*, *P. aeruginosa*, *K. pneumonia* and MDRE.

Table 3.1: Mueller Hinton Broth recommended for determination of the susceptibility of bacteria to antimicrobial agents by broth dilution method.

Mueller Hinton Broth- General Purpose Media	
Ingredients	**Grams/Litre**
HM infusion B	300.000
Acicase	17.500
Starch	1.500

Table 3.2: Composition of nutrient agar media used as general-purpose media for cultivation of less fastidious microorganisms.

Nutrient Agar Media- General Purpose Media	
Ingredients	**Grams/Litre**
Peptone	5.000
NaCl	5.000
HM Peptone B	1.500
Yeast Extract	1.500
Agar	15.000
Final pH	7.4 ± 0.2

3.2.11. Antimicrobial Susceptibility Testing

The broth microdilution method was used to ascertain the susceptibility and MIC values of the series of compounds against Gram (+) and Gram (-) bacteria under the guidelines of the CLSI guidelines 2016 (CSLI, 2016). CIP, AMK, and STR of known MIC values were used as control drugs. For determining the MIC following steps were followed:

3.2.11.1. Preparation of Stock solution and working solutions

Stock solutions of test compounds and control drugs (powdered form) at a concentration of 10 mg/mL were prepared by dissolving them in DMSO. 1 mg/mL and working solutions were further prepared using the formula $C_1V_1=C_2V_2$.

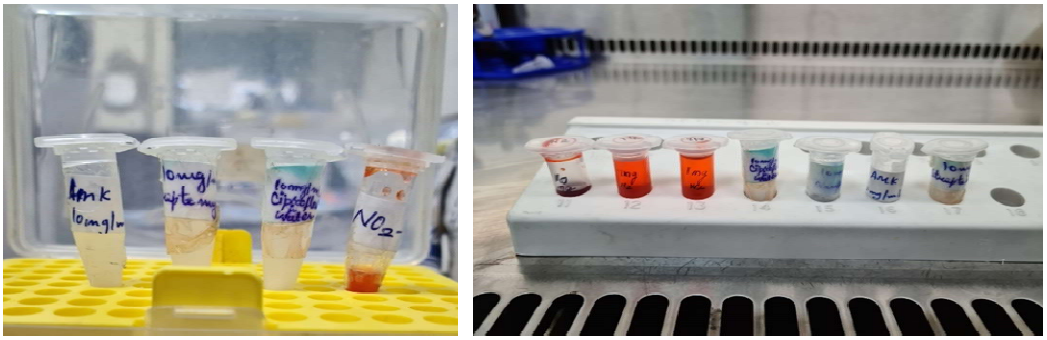

Fig.-3.5: Preparation of stock and working solutions of drugs.

3.2.11.2. Inoculum Preparation

The bacterial strains sub-cultured in MHB were grown to reach the log phase and adjusted to achieve turbidity equivalent to 0.5 McFarland turbidity standard (equivalent to 10^8 CFU/mL OD600 ranging between 0.3-0.6). The 0.5 McFarland suspension of the respective bacterial strains was diluted appropriately (1:150), resulting in a final inoculum containing 10^5 CFU/mL. The inoculum was plated on NA media as a quality control measure to ascertain the presence of 10^5 CFU/mL of colonies.

3.2.11.3. Susceptibility Testing: Broth Microdilution Method

The 96-well plates were labelled with the compound name, reference antibiotics (two wells/compound), and name of bacterial strains. 200 µL of MHB were dispensed into the wells except for the 1st column. 200 µL of the respective compounds and drugs (CIP, AMK, and STR) were pipetted into the first column with a concentration equal to 128 µg/mL. 2-fold serial dilution was performed so that the concentration from the 1st to 10th well ranges from 128 µg/mL-0.25 µg/mL. This was followed by inoculation of 50 µL of 10^5 CFU/mL cells of *S.*

aureus, *E. faecalis*, *B. cereus*, MRSA, MDRE, *P. aeruginosa,* and *K. pneumoniae* to wells in individual 96-well plates. The last two wells were taken as GC and MC, one lacking the drug and the other lacking both drug and compound as an indicator of contamination. The plates were sealed with parafilm. After incubating the plates for 24 hours at 37 °C, an examination was conducted to ascertain whether visible growth was present or absent by comparing them with the CC and MC wells which also act as indictors of contamination. MIC was defined as the lowest concentration of the compound where no visible bacterial growth was observed.

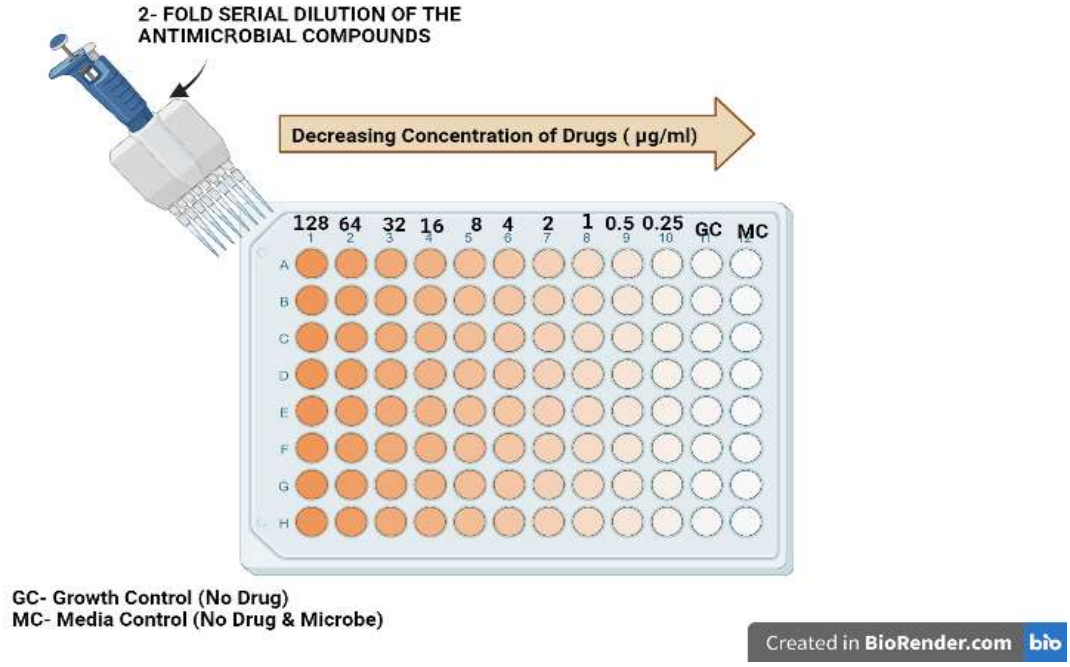

Fig.-3.6: Diagrammatic representation for serial two-fold dilution of compound library.

3.2.12. Determination of MIC

To determine the MIC, the broth microdilution technique was employed, as described previously [1, 2]. The 96-well plates were labeled with the compound name, reference antibiotics (two wells/compound), and name of bacterial strains. 200 µL of MHB were dispensed into the wells except for the 1st column. 200 µL of the respective compounds and drugs (CIP, AMK, and STR) were pipetted into the first column with a concentration equal to 128 µg/mL. 2-fold serial dilution was performed so that the concentration from the 1st to 10th well ranges from 128 µg/mL-0.25 µg/mL. This was followed by inoculation of 50 µL of 10^5 CFU/mL cells of *S. aureus*, *E. faecalis*, *B. cereus, E. coli*, *P. aeruginosa,* and *K. pneumoniae* to wells in individual

96-well plates. The last two wells were taken as GC and MC, one lacking the drug and the other lacking both drug and compound as an indicator of contamination. The plates were sealed with parafilm. Following a 24-hour incubation period at 37 °C, the plates were examined to determine whether visible growth was present or absent by comparing them with the CC and MC Wells which also act as indictors of contamination.

3.2.12.1. Spectrophotometric Analysis

The OD of each well was measured at 600 nm using a microplate reader. The OD values for each well were recorded and the calculation of growth inhibition percentage was carried out as described. In the calculation of percentage inhibition, the control well containing the bacterial culture but without any compound, GC was used as the reference for comparison. This control well was used to determine the baseline OD value of the bacterial culture and considered as 100% growth or metabolic activity. The OD value of each well was then compared to the OD value of the control well to calculate the percentage inhibition of bacterial growth or metabolic activity. The percentage of growth inhibition in each well was calculated by comparing the OD of each well to that of the growth control wells using the following formula:

Percentage inhibition = [(OD control – OD treated)/OD control] x 100

The data was plotted to determine the percentage of inhibition (plotting the percentage of inhibition versus the concentration of the antibiotic). The IC_{50} value was determined from the curve as the antibiotic concentration that hinders 50% of bacterial growth.

3.2.13. Determination of MBC

To ascertain if the compounds are bactericidal, the MBC assay was performed as per CSLI, 2016 guidelines [3, 4]. MBC is the minimum concentration of compound that leads to a 3 log10-fold decrease in CFU units or the lowest drug concentration that results in 99.9% killing of bacterial cells in initial inoculums. It is important to determine MBC as it provides insights into the optimal dosing regimen and identifies potential resistance mechanisms. The MBC was performed by broth micro dilution. The experiment was performed in duplicates. Briefly, 2 sterile 96-well plates were filled with MHB containing serial two-fold dilutions ranging from 1x-4x MIC of compounds and Ampicillin (4-16 µg/mL) as standard in a set of 2. Drug-free controls were also included. The plates were inoculated with 50 µL of *S. aureus* and *E. faecalis*

respectively with a final density equal to 10^5 CFU. The initial CFU of inoculums was verified by plating onto NA media. After 24 hours, the drug-containing wells showing no sign of growth compared to growth culture tubes were appropriately diluted to sub-MIC levels by 10-fold serial dilution in MHB. 100 µL of each dilution was plated onto NA plates in duplicates. CFU was enumerated following a 24-hour incubation period at 37 ºC. CFU/mL was calculated using the formula: **No. of Colonies × Dilution Factor ÷ Volume of Culture Plated**, then $\log_{10}$ values of an average number of colonies and log reduction were calculated using log calculator Omni Calculator to determine if there is a 3-log reduction in cell number. Ampicillin (AMP) was used as a control drug. Colonies ranging from 30-300 were considered countable. The lowest concentration of the drug which caused 99.9% killing with a 3-log reduction in CFU was taken as MBC of the drug.

3.2.14. Time-kill kinetics

To ascertain the bactericidal mechanism *i.e.* the Time v/s Concentration dependent-killing of the lead compound **2d**, the kill curve kinetics assay, was performed using the CFU/mL method as per CSLI guidelines with slight modifications. Another method adapted from the protocol described by Wang was also used to study the kill curve to provide insights into the extent of killing (concentration-dependence) and rate of killing (time-dependence) [5, 6].

3.2.14.1. Assessment of 24-Hour Time-Kill Kinetics via CFU/mL Evaluation

To determine the kill kinetics of lead **2d** compound, *E. faecalis* and *S. aureus* cultures with cell density 1×10^5 CFU/mL (confirmed by plate count) were exposed to 8 µg/mL MIC, 16 µg/mL (2xMIC) and 32 µg/mL (4xMIC) of **2d**. A growth control CC was included as a negative control (devoid of the compound). 2x MIC of AMP was taken as a standard drug. The log CFU/mL for all groups was determined at time 0 and at a subsequent time interval of 4 hours (taken up to 24 hours). Aliquots (100 µL) of drug-exposed cultures were pipetted out at predetermined time intervals of 4 hours in one day i.e., at 0, 4, 8, 9, 12, 16, 20, and 24 hours and serially diluted, then plated onto NA for CFU enumeration. First, the colonies at different dilutions for each concentration were enumerated then the average colony count at dilutions $10^{-1,}$ $10^{-2,}$ $10^{-3,}$ and 10^{-4} was calculated and then converting the value into $\log_{10}$ (Note: the colonies on plates showing 30-300 colonies were only considered). The curve was generated by plotting Log10 CFU values for each concentration against time. Time-kill curves were constructed and assessed to gauge the

speed and magnitude of bacterial eradication. The rate of bacterial reduction was calculated from the initial time point at 0 hours to the point of maximum decrease in log10 CFU/mL.

3.2.14.2. Evaluation of Time-Kill Kinetics based on MTT-reduction on a 360-Minute Scale

For this assay, working solutions of **2d** were prepared in a series of conical tubes containing MIC, 2xMIC, and 4xMIC in 5 mL MHB. For each concentration, a set of tubes labeled with the time point were taken. 100 µL of 10^5 CFU/mL of *E. faecalis* and *S. aureus* were dispensed in their respective set of tubes and incubated at 37 ºC. At the various time points 0, 60, 120, 180, 240, 300, and 360 minutes, the incubated tubes containing culture-molecule mixtures were treated with 150 µL of MTT and incubated for 20 minutes. After incubation, the tubes were centrifuged at 10,000 rpm at 10 ºC for 10 minutes. The supernatant was discarded and the pellet containing formazan crystals at the bottom was dissolved in 1.5 mL of Isopropanol and absorption was measured at 550 nm. For positive control, the cells were treated with 2xMIC of STR. The untreated cultures were taken as a negative control. MTT can be reduced to purple formazan crystals by a dehydrogenase system of active cells which can be quantified through spectrophotometric analysis by dissolving in organic solvent Isopropanol. OD550 nm can be directly correlated to the number of metabolically active cells and this was used to determine the bacterial killing at various concentrations over time.

3.2.15. Post-Antibiotic Effect

The PAE was determined as per the described protocol [7, 8]. Bacterial samples can have persistent subpopulations that remain dormant under antibiotic treatment and lead to disease recurrence following cessation of antibiotic therapy. The PAE was evaluated using the viable count method and the procedure adopted was the slight modification of protocol as reported previously. Briefly, an exponentially grown culture of *E. faecalis* and *S. aureus* with a final density of 10^6 CFU/mL was exposed to the compound and control drug Ampicillin (AMP) at x, 2x, and 4xMIC for 2 hours. Following drug exposure, the drugs were removed through three rounds of centrifugation at 10,000 rpm for 10 minutes each. The resulting pellet was then reconstituted in MHB. Antibiotics were removed immediately after drug exposure (2 hours) and taken as 0-hour readings and then after 1, 2, 3, 4, 5, 6, 7, 8, 12, and 24 hours by centrifugation. Aliquots removed at predetermined time points were serially diluted 10-fold (N, $10^{-1,}$ 10^{-2}, $10^{-3,}$ 10^{-4}, $10^{-5,}$ and 10^{-6}) and plated on NA media in triplicates. GC with inoculums but no antibiotics

were similarly processed and included to monitor the killing effect due to antibiotics to avoid any error in CFUs during processing.

The calculation of PAE followed the protocol described by Craig and Gudmundsson, expressed as **PAE = T-C**. In this context, 'T' represents the duration it takes for the viability count of a culture exposed to antibiotics to increase by 1 log10 unit compared to the count immediately after dilution, while 'C' represents the corresponding time for the growth control.

3.2.16. Fluorescent Microscopy

DAPI and PI staining are commonly used to assess cell viability and the effect of antibiotics on cells. DAPI is a fluorescent dye that binds to DNA and emits blue fluorescence upon excitation by ultraviolet light. PI is also a fluorescent dye that binds to DNA, but it emits red fluorescence upon excitation by ultraviolet light. In live cells, the DAPI stain enters the nucleus and binds to DNA, whereas PI is excluded from the cell. However, in dead or damaged cells, the cell membrane becomes permeable to PI, which enters the cell and binds to DNA, causing it to emit red fluorescence. When using DAPI and PI staining to assess cell viability and the effect of antibiotics on cells, the cells are typically treated with the antibiotic and then stained with DAPI and PI. Live cells will appear blue, whereas dead cells will appear red. The staining was done as per the described protocol [9, 10]. This staining technique was used to investigate the impact of lead compounds on the viability of *E. faecalis* and *S. aureus* using DAPI and PI stains. Bacterial cells were grown to an OD600 of 0.5. 1 mL of the actively growing cultures was pipetted into Eppendorf tubes with MIC and 2xMIC of compound. After incubation of 2 hours at 37 ºC, the cultures in tubes containing the compound were centrifuged at 10,000 rpm for 10 minutes supernatant was decanted and the pellet was resuspended in 200 µL Normal Saline Solution (NSS). 20 µL of PI (5 µg/mL) were added to the tubes and incubated for 15 minutes at 0 ºC in the dark. The unbound PI was removed by centrifuging the tubes at 10,000 rpm for 10 minutes and washing the pellet thrice with 200 µL of NSS. This was followed by a 15-minute incubation with 2 µL of DAPI (10 µg/mL) at 0 ºC in the dark. Finally, 100 µL of cultures were mounted onto the clean well-labeled slides, left to dry, and methanol fixed. For negative controls, the corresponding bacterial cells that did not receive compound treatment were processed under similar conditions. The stained bacterial cells were visualized under a fluorescent microscope and photographed using an inbuilt digital camera.

3.2.17. Microtiter Plate Biofilm Inhibition Assay

To determine whether the compound can inhibit the formation of biofilms, the Microtiter Plate Biofilm Assay was utilized as per described procedure [11, 12]. Firstly, the compound was prepared as a working stock (200 µL of compound in 1st well) and was serially diluted two-fold to obtain a concentration ranging from 0.25-128 µg/mL in 8 individual 96-well plates (1 plate for inoculation of each bacterium) already containing 100 µL MHB (final volume of 200 µL). 50 µL of bacterial suspension containing 10^5 CFU/mL bacteria cells were added to the wells of their respective plates (*S. aureus, E. faecalis, B. cereus, E. coli, P. aeruginosa, K. pneumoniae*). Culture control and Media control were included, in which only bacterial culture and growth media were dispensed respectively. Following this, the plates were incubated at 37 °C for 24 hours to facilitate bacterial growth and to assess whether the presence of the compounds hindered the development of biofilm, as specified. No visible growth was observed in wells that correspond to the MIC of the compound for the bacterial strains tested. After the incubation period, the planktonic bacterial cells in the wells were removed by washing three times with PBS, and aliquots from the wells were serially diluted and plated onto NA to correlate further findings. Subsequently, 125 µL of a 30% solution containing 0.5% CV and methanol was added to all the wells of the 96-well plates. The plate was placed in an incubator for 20 minutes at 37 ºC to stain the biofilm formed by microorganisms that are adherent to the abiotic surface of a microtiter plate. Any unbound CV was eliminated by rinsing the wells with distilled water, and the wells were left to air-dry at room temperature. The wells were then visualized and photographed under a microscope to quantify the extent of biofilm formation. To quantify the amount of biofilm formed, 200 µL of 30% [aqueous] acetic acid was added to each well to dissolve the CV. The OD of the dissolved CV was assessed at a wavelength of 470 nm utilizing a microplate reader. This protocol was repeated thrice to achieve optimal results and correct any background interference that may be present. The calculation of biofilm formation inhibition percentage was performed using the following formula**:**

$$\mathbf{[100-(TreatedOD_{470}nm \div Growth\ ControlOD_{470}nm) \times 100]}$$

This formula compares the optical density of the treated wells to that of the culture control wells and expresses the result as a percentage of inhibition.

3.2.18. Biofilm Eradication Assay

A modified methodology incorporating diverse methods used earlier was implemented to determine the potential of the compound for biofilm eradication and assess the minimum concentration required for biofilm eradication [13, 14]. 12 well plates were employed for this assay. To begin with, the bacterial strains (*S.aureus*, *E. faecalis*, *B. cereus*, *P. aeruginosa*, *E. coli*, and *K. pneumoniae*) were grown to the mid-log phase and diluted to obtain 10^5 CFU/mL of cells. 3 mL of MHB was pipetted into the 12 well plates and subsequently inoculated with 100 µL of the bacterial suspension. Media Control was taken as a positive control containing only MHB. For each bacterial strain, separate plates were utilized and subjected to incubation for 24, 48, and 72 hours to assess the effect of different concentrations on various stages of bacterial biofilm formation. After the incubation at given time points the plates were washed thrice with PBS to get rid of the planktonic bacterial cells. After washing x, 2x, 4x, 8x, and 16xMIC concentrations of the compound were added to the wells and incubated for 24 hours at 37 ºC. Culture Control well taken as a negative control was not incubated with the compound. After incubation, the drug-containing plates were washed with PBS. This was followed by the addition of 30% of 0.5% CV stain. The plates were subsequently left to incubate further for 1 hour at room temperature. In the next step, the CV was removed by thorough washing. Each well was observed under a microscope and photographed. To quantify the percentage of eradication 30% [aqueous] acetic acid was added to the wells to dissolve CV-staining adherent cells. This was done by recording the OD at 470 nm using a spectrophotometer. The calculation of the biofilm eradication percentage was performed according to the formula:

[100-(Treated OD470nm ÷ Growth Control OD470nm) ×100]

The percentages were calculated by taking the mean of three OD readings obtained for each concentration.

3.2.19. Cytotoxicity Assay

The critical factor that allows any compound to proceed successfully during drug discovery is selective toxicity to pathogens and non-toxicity to human cells. The assay was performed under the standards set by the ISO and OECD, to ensure accurate and reproducible results. The cytotoxicity of the lead compound was evaluated against HEK-293. Before evaluating the cytotoxicity of the compound, the cells were grown to reach a confluency of 70-80%. The

culture techniques used were following the cell culture technique guidelines regulated by the ICLAC, ATCC, and ECACC.

3.2.19.1. Cell Lines

HEK-293 cell lines were purchased from the NCCS, Pune, India. The cell lines were cultured in DMEM (supplemented with 10% foetal bovine serum) in a CO_2 incubator with 98% humidity and 5% CO_2 at 37 ºC.

3.2.19.2. Cytotoxicity Assay using MTT

The method was carried out as described earlier [15, 16]. The 100 µL of HEK-293 cells were placed into the 96-well microtiter plate and left to incubate for 24 hours at a temperature of 37 °C with 5% CO_2. The cells were treated with 6 concentrations of the compound 4, 8, 16, 32, 64, and 128 µg/mL dissolved in DMSO for time points 24, 48, and 72 hours to determine the time and dose-dependent effect of the compound on cell viability. Untreated control wells received only DMSO. Following the designated time intervals, the count of viable cells was determined as follows: The culture medium from the 96-well plate was first aspirated and replaced with 100 µL of fresh medium. Subsequently, 20 µL of the MTT stock solution (consisting of 5 mg of MTT in 1 mL of PBS) was introduced into each well, including the untreated control wells. Subsequently, the 96-well plates were incubated at 37 °C under a 5% CO_2 environment for 4 hours. After this incubation period, 85 µL of the medium was taken out from each well, and 150 µL of DMSO was added to dissolve the insoluble formazan crystals formed by viable cells. The mixture was thoroughly homogenized using a pipette and further incubated at 37 °C for 10 minutes. The number of live cells was ascertained using a microplate reader to measure optical density at 590 nm. This evaluation was made based on the distinct capacity of live cells to lessen the tetrazolium component of MTT, resulting in the formation of purple-colored formazan crystals. The intensity of this colored formazan was measured at an absorbance of 570 nm using the microplate reader, and the following formula was used to calculate the percentage of growth inhibition:

$$\textbf{Mean } OD_{570} \textbf{ Treated Well} \div \textbf{Mean } OD_{570} \textbf{ Control well} \times 100$$

The results expressed were the average values of three experiments (± SD). Reduction of MTT to formazan crystals is mediated by the mitochondrial enzyme succinate dehydrogenase cells in the viable cells. The color of the formazan crystals that form after the reduction of MTT by viable

cells indicates the level of cell viability and, hence, the cytotoxicity of the test compound. The formazan crystals appear as purple or dark blue precipitates in viable cells. The number of viable cells present in the culture directly correlates with the colour intensity. Conversely, a decrease in colour intensity denotes a reduction in the number of viable cells, which in turn denotes an increase in cytotoxicity. A complete absence of color indicates that all the cells in the culture have died, and the test compound is highly cytotoxic to the cells.

3.3. Anti-TB activity using Alamar Blue Dye

3.3.1. Procedure

To assess the effectiveness of the compounds against *Mycobacterium Tuberculosis*, we utilized the Microplate Alamar Blue assay, a reliable technique using a thermally stable reagent, which exhibits a robust association with proportional and BACTEC radiometric methods. The process entailed the use of sterile 96-well plates, where 200 µL of sterile deionized water was placed in the outermost wells to prevent the medium from evaporating in the experimental wells during incubation. In every well, 100 µL of Middlebrook 7H9 broth was added, and the compounds were subsequently diluted directly on the plate, leading to a variety of final drug concentrations assessed, ranging from 100 to 0.2 µg/mL. Subsequently, the plates were sealed using parafilm and placed in an incubator at 37 °C for five days. Following the incubation period, a mixture of Alamar Blue reagent and 10% tween 80 in a 1:1 ratio (25 µL) was added to each well and incubated for an additional 24 hours. The color change within the wells was observed, where a blue color signified the absence of bacterial growth, while a pink color indicated the presence of bacterial growth. The MIC was defined as the minimum drug concentration that inhibited the change from blue to pink, indicating the inhibition of bacterial growth [17, 18].

3.3.2. Standard Strain used

Mycobacteria tuberculosis (Vaccine strain, H37 RV strain): ATCC No- 27294.

3.4. DPPH Radical Scavenging Activity Assay

The evaluation of the ability of compounds to neutralize free radicals was carried out following a previous study [19]. In this process, the compounds and standard antioxidant was introduced into test tubes at concentrations of 10, 20, and 30 µg/mL. Subsequently, the total volume in each test tube was adjusted to 600 µL by adding DMSO. To these solutions, 200 µL of a DPPH radical solution was introduced. Following thorough mixing through vortexing, the samples were

incubated for 30 minutes. Following the completion of the incubation period, absorbance measurements were taken at 517 nm using a spectrophotometer. Reduced absorbance suggests increased DPPH-radical scavenging activity. The following equation was used to calculate the percentage inhibition:

DPPH radical scavenging = **[(Ac-As)/Ac) 100]**

Where '**Ac**' represents the absorbance of the control and '**As**' represents the absorbance of the sample.

The positive control was L-ascorbic acid.

3.5. Computational Studies

3.5.1. Data Collection

Active synthetic organic compounds were drawn by chemdraw and saved in sdf format while receptor DprE1 (PDB-ID: 4FEH), Polyketide synthase (Pks13) (PDB-ID: 5V3Y) and Protein kinase B (PknB) (PDB-ID: 5U94) was downloaded from Protein Data bank in pdb format (www.pdb.org/pdb).

3.5.2. Protein Preparation

Receptor proteins were opened in discovery studio software, 2021 (https://discover.3ds.com/discovery-studio-visualizer-download) to remove undesired substances. All the Hetaatom, water molecules, and bounded ligands were removed from the protein; Hydrogen atoms were added and were saved as in pdb format [20].

3.5.3. Ligand Preparation

All synthetic drug candidate structures were drawn using Chemdraw and were saved in sdf format so they were uploaded in Open Babel GUI and were converted into pdb format as well as to smiles format for further study [21].

3.5.4. Molecular Docking

To evaluate the Drug-protein interaction of twelve organically synthetic drug compounds against DprE1, Polyketide synthase (Pks13), and Protein kinase B (PknB) molecular docking approach was applied using PyRx bioinformatics tool [22]. DprE1, Polyketide synthase (Pks13), and Protein kinase B (PknB) as receptor proteins were uploaded in PyRx one-by-one and were converted into a macromolecule. Using the Open Babel window, all ligand molecules were uploaded; the energy was minimized and was then converted into pdbqt format. Docking was run after creating a grad box using vina wizard. The grad box dimension for Protein kinase B (PknB)

X: 62.7592, Y: 48.9203, Z: 42.7956, for DprE1, X: 61.4444, Y: 60.1809, Z: 51.3220, and for Polyketide synthase (Pks13) X: 68.0260, Y: 82.8894, Z: 71.4195 were followed. Discovery studio 2021 was used for results visualization including 2D structure, hydrogen bonding, and other type of bonds [23].

3.5.5. Drug-Likeness and ADME

SwissADME online software (http://www.swissadme.ch/) was used for checking drug-likeness and also for ADME analysis. ADME is absorption, distribution, metabolism, and excretion [24]. Canonical smiles of ligand compounds were retrieved from PubChem and were pasted in swissADME to analyze drug-likeness and ADME parameters.

3.5.6. Toxicity

Canonical smiles of all the ligands were retrieved from PubChem database and were pasted one-by-one in Protox-II online web server (http://tox.charite.de/protox_II) and admetSAR (http://lmmd.ecust.edu.cn/admetsar2) for toxicity determination [25]. Protox-II online and admetSAR were run to check hepatotoxicity, mutagenicity and cytotoxicity, AMES toxicity, carcinogenicity, and acute oral toxicity of the compounds.

3.5.7. Molecular Dynamics Simulation

MDS Studies can provide a valuable means to attain insights into the intricate protein-ligand binding behaviour, a critical aspect in the field of drug design and discovery, serving as an effective current technological tool in medicinal chemistry. Therefore, the lead compounds from docking studies, **5a**, **5f**, and **5g** were next exposed to MDS for 100 ns using GROMACS 2021.3 [26], carried out in the same way as previously reported by K. Jangid [27]. CHARMM36-Mar2019 force field was employed to construct the complex topology, using the TIP3P model for water solvation. The design of the water box aimed to encompass a distance of at least 1.5 nm beyond the protein's surface. To maintain system neutrality, counter ions (Na+ and Cl-) were added as needed to balance the composition of the system, which included both the protein and the ligand. Subsequently, three consecutive steps, *viz.* energy minimization, NVT equilibration, and NPT equilibration, were executed to reduce the system's overall energy and stabilize it. Initially, the process commenced with energy minimization using the steepest descent algorithm, followed by NVT equilibration lasting 500 ps. During this equilibration, the protein was restrained, and a constant temperature of 310 K was maintained by employing the velocity-rescaling algorithm with a coupling constant of 0.1 ps. The system was subjected to NPT

equilibration for 500 ps at a pressure of 1 bar, employing the Berendsen barostat algorithm with a coupling constant of 1 ps [28]. Finally, the conclusive 100 ns of MD production were executed. In the meantime, the simulation process utilized a consistent time step of 2 fs. The LINCS algorithm was utilized to impose constraints on bond lengths [29]. Furthermore, the PME method was employed, employing a cut-off radius of 1.2 nm and a grid spacing of 0.16 nm. Furthermore, the Van der Waals cut-off distance was established at 1 nm. Using the GROMACS analytic tools like RMS, gyrate, and RMSF, for RMSD, the RGy, and RMSF were computed respectively to analyze the trajectory [30].

References

1. Ali, A., Corrêa, A.G., Alves, D., Zukerman-Schpector, J., Westermann, B., Ferreira, M.A. and Paixão, M.W., 2014. An efficient one-pot strategy for the highly regioselective metal-free synthesis of 1, 4-disubstituted-1, 2, 3-triazoles. *Chemical Communications*, *50*(80), pp.11926-11929.
2. Espinel-Ingroff, A., Colombo, A.L., Cordoba, S., Dufresne, P.J., Fuller, J., Ghannoum, M., Gonzalez, G.M., Guarro, J., Kidd, S.E., Meis, J.F. and Melhem, T.M.S.C., 2016. International evaluation of MIC distributions and epidemiological cutoff value (ECV) definitions for Fusarium species identified by molecular methods for the CLSI broth microdilution method. *Antimicrobial agents and chemotherapy*, *60*(2), pp.1079-1084.
3. Mir, M.A., Altuhami, S.A., Mondal, S., Bashir, N., Dera, A.A. and Alfhili, M.A., 2023. Antibacterial and Antibiofilm Activities of β-Lapachone by Modulating the Catalase Enzyme. *Antibiotics*, *12*(3), p.576.
4. Fernandes, A.W.C., dos Anjos Santos, V.L., Araújo, C.R.M., de Oliveira, H.P. and da Costa, M.M., 2020. Anti-biofilm effect of β-lapachone and lapachol oxime against isolates of Staphylococcus aureus. *Current Microbiology*, *77*, pp.204-209.
5. Tsuji, B.T., Yang, J.C., Forrest, A., Kelchlin, P.A. and Smith, P.F., 2008. In vitro pharmacodynamics of novel rifamycin ABI-0043 against Staphylococcus aureus. *Journal of Antimicrobial Chemotherapy*, *62*(1), pp.156-160.
6. Trampuz, A., Murphy, C.K., Rothstein, D.M., Widmer, A.F., Landmann, R. and Zimmerli, W., 2007. Efficacy of a novel rifamycin derivative, ABI-0043, against Staphylococcus aureus in an experimental model of foreign-body infection. *Antimicrobial agents and chemotherapy*, *51*(7), pp.2540-2545.
7. Proma, F.H., Shourav, M.K. and Choi, J., 2020. Post-Antibiotic Effect of Ampicillin and Levofloxacin to Escherichia coli and Staphylococcus aureus Based on Microscopic Imaging Analysis. *Antibiotics*, *9*(8), p.458.
8. Gottfredsson, M., Erlendsdóttir, H., Sigfússon, A. and Gudmundsson, S., 1998. Characteristics and dynamics of bacterial populations during postantibiotic effect determined by flow cytometry. *Antimicrobial agents and chemotherapy*, *42*(5), pp.1005-1011.

9. Zotta, T., Guidone, A., Tremonte, P., Parente, E. and Ricciardi, A., 2012. A comparison of fluorescent stains for the assessment of viability and metabolic activity of lactic acid bacteria. *World Journal of Microbiology and Biotechnology*, *28*, pp.919-927.
10. Bunthof, C.J., van den Braak, S., Breeuwer, P., Rombouts, F.M. and Abee, T., 1999. Rapid fluorescence assessment of the viability of stressed Lactococcus lactis. *Applied and Environmental Microbiology*, *65*(8), pp.3681-3689.
11. O'Toole, G.A., 2011. Microtiter dish biofilm formation assay. *JoVE (Journal of Visualized Experiments)*, (47), p.e2437.
12. Kragh, K.N., Alhede, M., Kvich, L. and Bjarnsholt, T., 2019. Into the well—A close look at the complex structures of a microtiter biofilm and the crystal violet assay. *Biofilm*, *1*, p.100006.
13. Kreth, J., Merritt, J., Shi, W. and Qi, F., 2005. Competition and coexistence between Streptococcus mutans and Streptococcus sanguinis in the dental biofilm. *Journal of bacteriology*, *187*(21), pp.7193-7203.
14. Kreth, J., Zhang, Y. and Herzberg, M.C., 2008. Streptococcal antagonism in oral biofilms: Streptococcus sanguinis and Streptococcus gordonii interference with Streptococcus mutans. *Journal of bacteriology*, *190*(13), pp.4632-4640.
15. Adan, A., Kiraz, Y. and Baran, Y., 2016. Cell proliferation and cytotoxicity assays. *Current pharmaceutical biotechnology*, *17*(14), pp.1213-1221.
16. Aslantürk, Ö.S., 2018. In vitro cytotoxicity and cell viability assays: principles, advantages, and disadvantages. *Genotoxicity-A predictable risk to our actual world*, *2*, pp.64-80.
17. Lourenco, M.C., de Souza, M.V., Pinheiro, A.C., Ferreira, M.D.L., Gonçalves, R.S., Nogueira, T.C.M. and Peralta, M.A., 2007. Evaluation of the anti-tubercular activity of nicotinic and isoniazid analogues. *Arkivoc*, *15*, pp.181-191.
18. Ancizu, S., Moreno, E., Solano, B., Villar, R., Burguete, A., Torres, E., Pérez-Silanes, S., Aldana, I. and Monge, A., 2010. New 3-methylquinoxaline-2-carboxamide 1, 4-di-N-oxide derivatives as anti-Mycobacterium tuberculosis agents. *Bioorganic & medicinal chemistry*, *18*(7), pp.2713-2719.
19. Savcı, A., Turan, N., Buldurun, K., Alkış, M.E. and Alan, Y., 2022. Schiff base containing fluorouracil and its M (II) complexes: Synthesis, characterization, cytotoxic and antioxidant activities. *Inorganic Chemistry Communications*, *143*, p.109780.

20. Bhadra, P., 2020. In-silico Analysis of Effects of Stevia Extracts on Diabetes. *Indian Journal of Natural Sciences*, *10*(60), pp.20710-20719.
21. Bhadra, P., 2020. Cinnamon: In silico Analysis targeted Therapy for Gastric Cancer. *Indian Journal of Natural Sciences*, *10*(60), pp.20662-20669.
22. Gomha, S.M., Abdelhady, H.A., Hassain, D.Z., Abdelmonsef, A.H., El-Naggar, M., Elaasser, M.M. and Mahmoud, H.K., 2021. Thiazole-Based Thiosemicarbazones: Synthesis, Cytotoxicity Evaluation and Molecular Docking Study. *Drug design, development, and therapy*, pp.659-677.
23. Rahman, F., Tabrez, S., Ali, R., Alqahtani, A.S., Ahmed, M.Z. and Rub, A., 2021. Molecular docking analysis of rutin reveals possible inhibition of SARS-CoV-2 vital proteins. *Journal of traditional and complementary medicine*, *11*(2), pp.173-179.
24. Pagadala, N.S., Syed, K. and Tuszynski, J., 2017. Software for molecular docking: a review. *Biophysical reviews*, *9*, pp.91-102.
25. Abdellatif, K.R., Abdelall, E.K., Elshemy, H.A., Lamie, P.F., Elnahaas, E. and Amin, D.M., 2021. Design, and synthesis of new anti-inflammatory agents with a pyrazole core: COX-1/COX-2 inhibition assays, anti-inflammatory, ulcerogenic, histopathological, molecular Modeling, and ADME studies. *Journal of Molecular Structure*, *1240*, p.130554.
26. Das, B., Mathew, A.T., Baidya, A.T., Devi, B., Salmon, R.R. and Kumar, R., 2023. Artificial intelligence assisted identification of potential tau aggregation inhibitors: ligand-and structure-based virtual screening, in silico ADME, and molecular dynamics study. *Molecular Diversity*, pp.1-19.
27. Dwivedi, A.R., Kumar, V., Yadav, R.P., Kumar, N., Jangid, K., Anand, P., Sharma, D.K., Barnawal, S. and Kumar, V., 2022. Design, synthesis, and evaluation of 4-phenyl-1, 2, 3-triazole substituted pyrimidine derivatives as antiproliferative and tubulin polymerization inhibitors. *Journal of Molecular Structure*, *1267*, p.133592.
28. Hess, B., 2008. P-LINCS: A parallel linear constraint solver for molecular simulation. *Journal of chemical theory and computation*, *4*(1), pp.116-122.
29. Jangid, K., Devi, B., Sahoo, A., Kumar, V., Dwivedi, A.R., Thareja, S., Kumar, R. and Kumar, V., 2023. Virtual screening and molecular dynamics simulation approach for the identification of potential multi-target directed ligands for the treatment of Alzheimer's disease. *Journal of Biomolecular Structure and Dynamics*, pp.1-19.

30. Kumar, A., Kalra, S., Jangid, K. and Jaitak, V., 2022. Flavonoids as P-glycoprotein inhibitors for multidrug resistance in cancer: An in-silico approach. *Journal of Biomolecular Structure and Dynamics*, pp.1-13.

CHAPTER-4

Design, Synthesis, and Unraveling the Antibacterial and Antibiofilm Potential of 2-Azidobenzothiazoles: Insights from a Comprehensive in Vitro Study

4.1. Introduction

Aromatic azides are most frequently used as reagents for the photoaffinity labeling of biomolecules despite their unusual uses in synthetic organic chemistry. A relatively small number of transformations are used to synthesize aryl azides. This chemistry, while helpful for relatively straightforward ligands, is not necessarily permissive to additional functional groups. It has been investigated to use other techniques, such as *p*-tosylazide reacting with lithium reagents or aryl Grignard made from the appropriate aryl halides. Similarly to this, it has been demonstrated that *p*-tosylazide can react with aryl amide salts to produce the required azides. The general application of this transformation has been constrained by somewhat harsh conditions. In contrast to aromatic azides, aliphatic azides can be made using a variety of ways. A high-yielding reaction with triflyl azide can easily transform aliphatic amines into the corresponding azides, apart from simple substitution reactions utilizing the azide ion and different electrophiles (TfN_3). This reaction, recently popularized by Wong, has drawn a lot of attention and found several uses. It has been discovered that aryl azides can be produced from organoboron compounds employing a copper (II) catalyst. The diazotization of $[ArN_2]$ $[BF_4]$ salts immobilized in [BMIM][PF_6] ionic liquid is an effective way to produce azido-derivatives. However, only a small number of transformations are used in the synthesis of aryl azides. They are frequently made from the equivalent amines using the diazonium salts of those amines. Depending on whether or not there are incompatible functional groups present, this could occasionally be an issue. Alternative approaches have been researched, such as interactions between organometallic aryls and *p*-tosyl azides, which have been studied (derived from the corresponding aryl halide). More recently, Liu and Tor have successfully prepared aryl azides using Wong's (TfN_3) technique. Even though it works, this approach has several shortcomings. First, the highly reactive Tf_2O is used. Second, it has been discovered that TfN_3 is explosive on its own. Tertbutyl nitrite (*t*-BuONO) and NaN_3 have recently been reported to be used in the synthesis of aromatic azides by Das *et al*. Phenyl hydrazine derivatives can also be used as a starting material in various processes to produce aromatic azides. Using diazonium salt and sulfonamide, Dutt *et al*. described the synthesis of aryl azide; however, a significant drawback of this technique is the production of sulfonic acid as a byproduct [1-8].

This study involves the design and synthesis of novel 2-azidobenzothiazoles, and their subsequent evaluation for antibacterial efficacy and antioxidant activity. It represents an

important contribution to the field of medicinal chemistry, highlighting the potential of 2-azidobenzothiazoles as promising candidates for addressing bacterial infections and combating oxidative stress-related conditions.

4.2. Results & Discussion

4.2.1. Chemistry

This study presents a simple approach for the synthesis of 2-azidobenzothiazoles through the transformation of substituted 2-aminobenzothiazoles. The method involves the utilization of sodium nitrite and sodium azide as key reagents under ambient reaction conditions (**Scheme-4.1**). The introduction of azide groups into organic molecules, facilitated by sodium nitrite and sodium azide, is a significant chemical transformation that opens doors to diverse functionalization and subsequent applications. The mild reaction conditions employed, in conjunction with these reagents, contribute to the synthesis's accessibility and potential applicability across a range of substrates. The synthesis of 2-azidobenzothiazoles (**Fig.-4.1**) via this methodology adds to the toolbox of functional group transformations. The ability to incorporate azide functionality onto the benzothiazole scaffold is noteworthy due to the versatile reactivity of azides, which can be harnessed for further derivatization and diversification of the synthesized compounds. Additionally, the utilization of substituted 2-aminobenzothiazoles as starting materials allows for the introduction of specific substituents that can influence the resulting compound's properties and behaviors. The mild conditions employed in this synthesis are advantageous for maintaining the integrity of sensitive functional groups and minimizing unwanted side reactions. This feature is particularly beneficial when working with complex or delicate molecules, where harsher conditions might lead to undesired chemical transformations or yield losses. Further analysis of the equal amounts of sodium nitrite, sodium acetate, and sodium azide necessary for the reaction revealed that 4 equivalents of each were suitable to achieve the desired product in high yields. The synthesis of 2-azidobenzothiazoles in an isolated yield of 80-95% results from the smooth, rapid, and quantitative progression of the reaction. It is evident that both EDG and EWG are acceptable for this transformation and produced high yields of the intended product in 1 hour, demonstrating the further scope of the reaction. It was intriguing to learn that free ester and halogen groups might withstand the conditions of a reaction without producing hydrazide.

The choice of substituents and substitution patterns in the synthesis of 2-azidobenzothiazoles, as well as the subsequent antibacterial activity studies, seems to be guided by specific factors aimed at enhancing the antibacterial potential of the compounds while minimizing cytotoxicity. The selection of certain substituents and substitution patterns has been inspired by previous studies or analogs that have shown promising antimicrobial activities. The presence of EWG like -NO_2 at the *Meta* position increases the antibacterial activity by influencing interactions with bacterial targets. In this context, the introduction of a -NO_2 group on the benzothiazole ring might enhance antibacterial potential. Replacement of the *meta* substituent of benzothiazole ring with methoxy group (**2b**), carboxylate (**2c**), hydrogen (**2e**), or ethoxy (**2g**) decreased the activity. Conversely, introducing a 4, 6-difluoro group (**2a**) on the benzothiazole ring did not show any enhancement in the activity. Furthermore, the activity is not significantly influenced by the halogen group positioned *ortho* to the benzothiazole ring and the presence of a methyl group at the *para* position. The capability of 2-azido-6-nitro-benzothiazole to inhibit biofilm formation is noteworthy. This indicates potential interference with bacterial adhesion and colonization, an important factor in bacterial pathogenicity. The study's focus on extended exposure of a human cell line (Human Embryonic Kidney-293) to higher concentrations of 2-azido-6-nitro-benzothiazole suggests an attempt to determine the compound's selectivity for bacterial cells over human cells. The fact that the compound demonstrates selective cytotoxicity towards bacterial cells even at higher concentrations is promising for potential therapeutic applications.

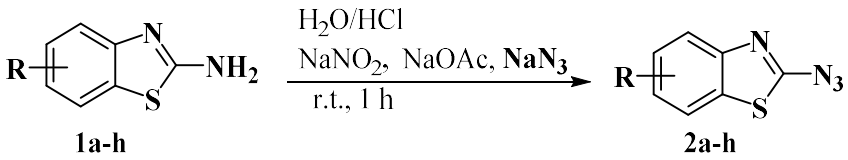

R = H; 6-NO_2; 6-OCH_3; 6-OC_2H_5; 5-Br; 4-CH_3; 6-COOEt; 4,6-F

Scheme-4.1: 2-aminobenzothiazoles converted into 2-azidobenzothiazoles using sodium nitrite and sodium azide.

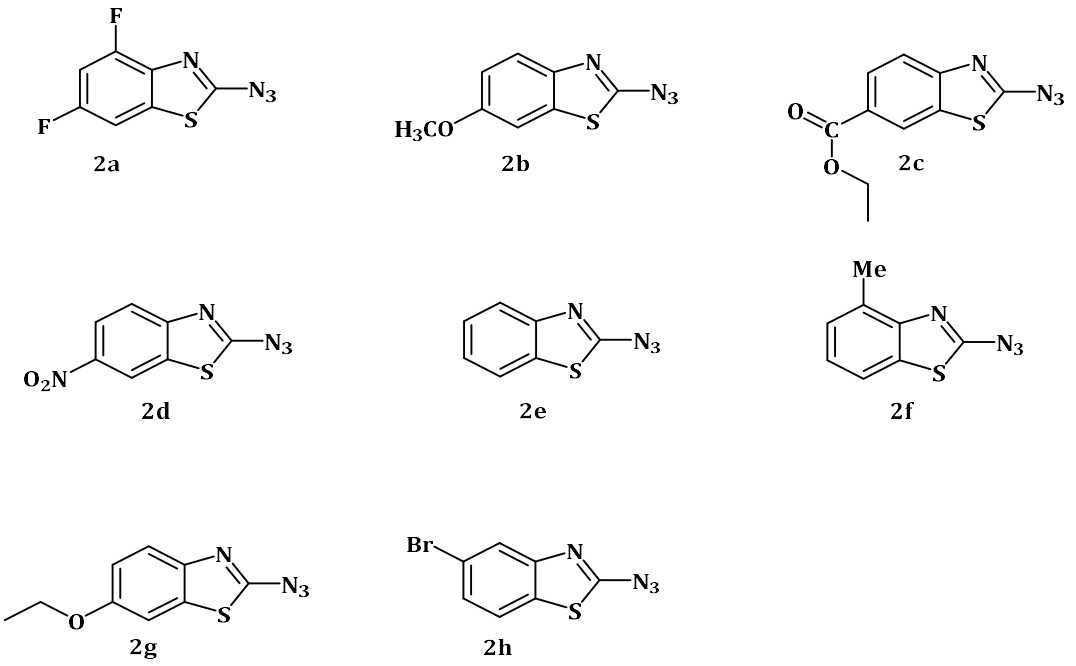

Fig.-4.1: Depiction of the synthesized 2-azidobenzothiazoles.

Reaction conditions: Substrate (0.5mmol, 1equiv), $NaNO_2$ (2mmol, 4equiv), NaOAc (2mmol, 4equiv), NaN_3 (2mmol, 4equiv), H_2O/HCl, r.t., 1 h.

Isolated yield and structure were confirmed by comparison of IR, mp, MS, and ^1H NMR.

(**Note:** Although we have not experienced any problem in handling this compound, precautions should be taken due to its explosive nature)

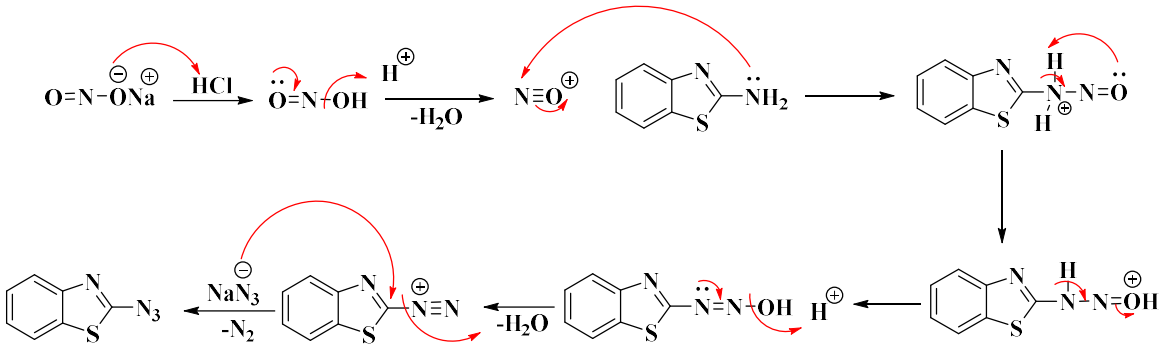

Fig.-4.2: Mechanistic pathway for the synthesis of 2-azidobenzithiazoles (**2a-h**).

4.2.2. *In vitro* Antibacterial Activity

4.2.2.1. Minimum Inhibitory Concentration (MIC)

The antibacterial activity and MIC of all the synthesized compounds were evaluated using the Broth Micro dilution technique as described in the methodology. All the synthesized compounds were evaluated for their antibacterial effectiveness against the American Type Culture Collection (ATTC) strains of *S. aureus, E. faecalis, B. cereus, K. pneumoniae, P. aeruginosa* and *E. coli* and clinical isolates of MRSA and MDRE. It was found that compound **2d** showed good antibacterial activity against the Gram (+) bacterial strains. It was elucidated that the compounds are more active against the Gram (+) bacterial strains, *E. faecalis,* and *S. aureus* with MIC of 8 µg/mL (**Table 4.1**). However, it was moderately active against Gram (-) bacteria *P. aeruginosa* and Gram (+) bacteria *B. cereus* with a MIC value of 64 µg/mL. Substantially the compound displayed activity even against the Resistant strains, MRSA, and MDR *E. coli* of clinical origin with a MIC value of 128 µg/mL (**Table 4.1, 4.2**). These results were found to be consistent with several other benzothiazole derivatives, which inhibited the growth of Gram (+) and Gram (-) bacteria [9]. The MIC values of control drugs against the bacterial strains were also similar to the range given by CSLI.

Table 4.1: MIC (µg/mL) of the compounds and antibiotics tested against Gram (+) bacterial strains. Amikacin (AMK), Streptomycin (STR) and Ciprofloxacin (CIP) were used as controls.

S. No.	Compound	*S. aureus*	*E. faecalis*	*B. cereus*	*MRSA*
1	2a	128	64	128	128
2	2b	128	128	128	128
3	2c	64	64	128	128
4	2d	8	8	64	128
5	2e	128	32	64	128
6	2f	128	>128	128	128
7	2g	128	128	128	128
8	2h	128	128	128	128
9	AMK	2.5	2.5	1.25	>128
10	STR	2.5	2.5	2.5	>128
11	CIP	1.25	0.3125	2.5	>128

Table 4.2: MIC (µg/mL) of the compounds and antibiotics tested against Gram (-) bacterial strains. Amikacin (AMK), Streptomycin (STR) and Ciprofloxacin (CIP) were used as controls.

S. No.	Compound	*P. aeruginosa*	*K. pneumoniae*	*E. coli*	*MDR E. Coli*
1	2a	128	128	128	128
2	2b	128	64	64	128
3	2c	128	128	64	128
4	2d	64	128	128	128
5	2e	64	128	128	128
6	2f	128	128	128	128
7	2g	128	128	128	128
8	2h	128	128	128	128
9	AMK	2.5	2.5	2.5	>128
10	STR	2.5	2..5	2.5	>128
11	CIP	5	1.25	0.015	>128

(a) ***Staphylococcus aureus***

(2d) MIC- 8 µg/mL

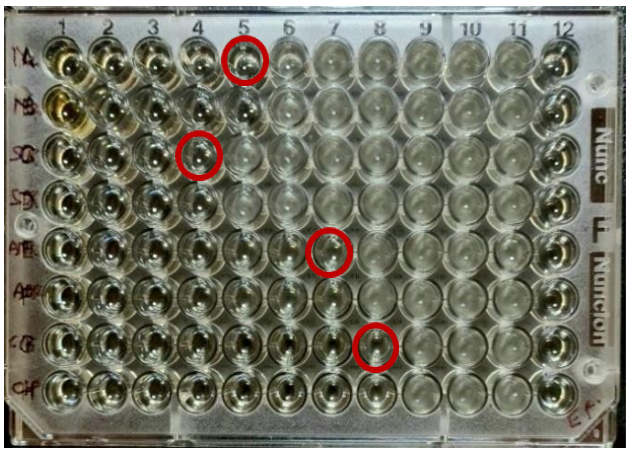

(b) ***Enterococcus faecalis***

(2d) MIC- 8 µg/mL

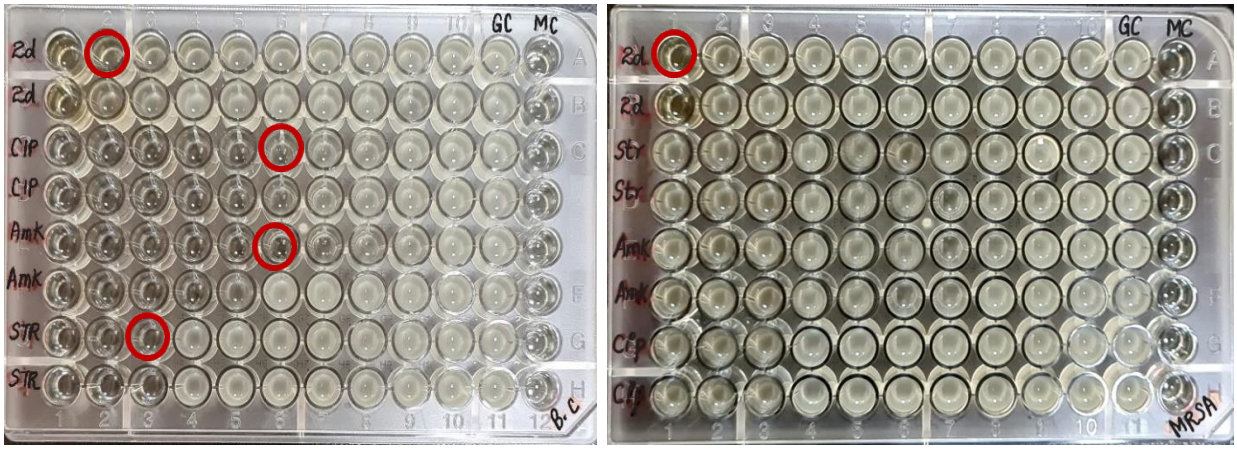

(c) *Bacillus cereus*

(2d) MIC – 64 µg/mL

(d) *Methicillin* Resistant *S. aureus*

(2d) MIC - 128 µg/mL

Fig.-4.3: Minimum inhibitory concentration of **2d**, STR, AMK, and CIP against Gram (+) bacteria, (a) *S. aureus,* (b) *E. faecalis,* (c) *B. cereus* and (d) Methicillin Resistant *S. aureus*. CIP (Represented by red-circled wells showing no visible growth compared to growth control well).

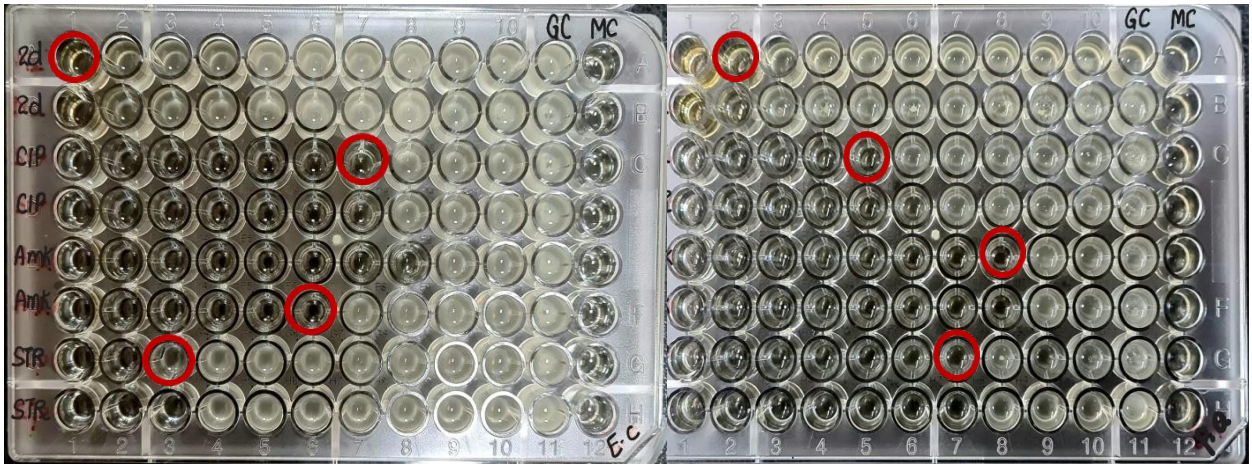

(a) *Escherichia coli*

(2d) MIC- 128 µg/mL

(b) *Pseudomonas aeruginosa*

(2d) MIC- 64 µg/mL

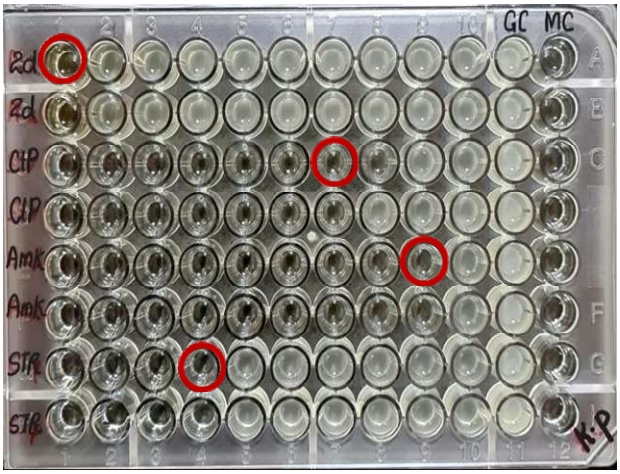

(c) *Klebsiella pneumoniae*

(2d) MIC- 128 µg/mL

(d) Multi-Drug Resistant *E. coli*

(2d) MIC- 128 µg/mL

Fig.-4.4: Minimum inhibitory concentration of **2d**, STR, AMK, and CIP against Gram (-) bacteria, *E. coli, P. aeruginosa, K. pneumoniae,* and Multi-Drug Resistant *E. coli*. (Represented by red-circled wells showing no visible growth compared to growth control well).

4.2.2.1.1. Percentage Inhibition of Growth

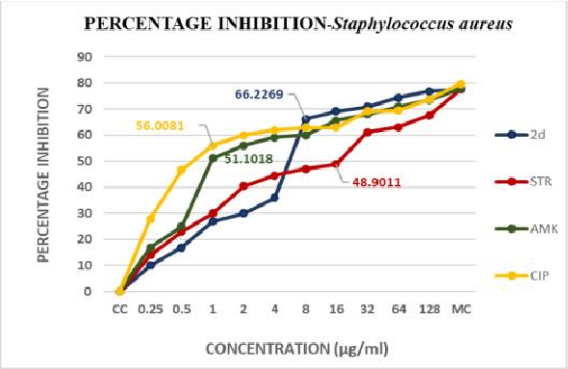

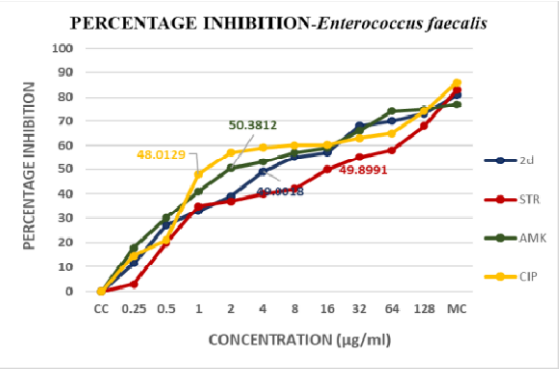

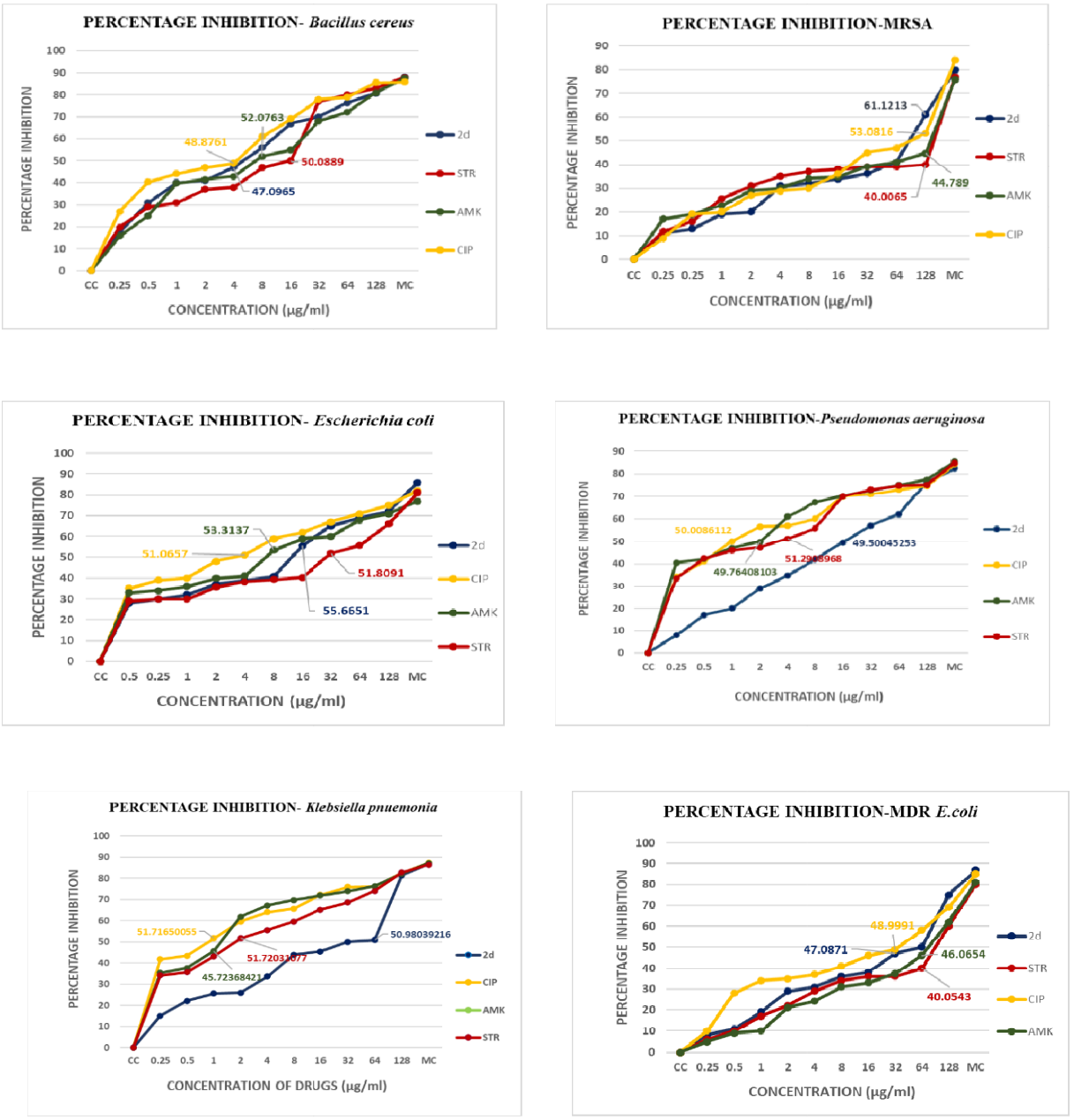

Fig.-4.5: Spectrophotometric Analysis: Figure showing percentage inhibition in growth of Gram (+) and Gram (-) bacteria in the presence of antibacterial compounds and concentrations at which 50% of the growth is inhibited by comparing with OD600 of growth control wells. (%) calculated by taking the mean of 3 OD values.

4.2.2.2. Minimum Bactericidal Concentration (MBC)

As MIC only measures the ability of antimicrobial agents to inhibit bacterial growth, we performed an MBC assay which determines the lowest concentration of antimicrobial compound that can kill 99.9% of bacterial cells. MBC is required by regulatory agencies for approval of new antimicrobials. The MBC of the series of compounds **2a-h** was assessed against the Gram (+) bacterial strains *E. faecalis and S. aureus* as the compounds exhibited comparatively better MIC values against these strains compared to other strains. The MBC values must not be more than four times the MIC, which is consistent with our results [10]. For both *S. aureus* and *E. faecalis* MBC of the lead compound **2d**, was equal to 2xMIC *i.e.,* 16 µg/mL. The other compounds tested had bactericidal effects (led to 99.9% killing) rather than bacteriostatic effects, with MBC values of 128 µg/mL. Compound **2a** showed bactericidal activity at 2xMIC (128 µg/mL) against *E. faecalis*. Compound **2b** exhibited bactericidal activity at its MIC values, indicating their potential as promising antimicrobial agents that can effectively inhibit and kill bacterial pathogens. **2c** showed bactericidal potential against both Gram (+) bacteria at 2xMIC. **2e** showed bactericidal potential only against *E. faecalis* at 4x MIC. Ampicillin was used as a control drug and its MIC and MBC values against *S. aureus* were found to be 4 and 8 µg/mL and for *E. faecalis* the MIC and MBC values were 2 and 4 µg/mL. Negative controls for both strains, devoid of compounds were used to validate the CFU counts. CFU enumeration indicated a 3-log reduction, 99.9% killing in both Gram (+) bacteria compared to the CFU count of Growth control which is indicative of the MBC. Overall, these findings suggest that the tested compounds have potent bactericidal activity against *E. faecalis* and *S. aureus*, which could be crucial in eradicating bacterial infections. The MBC values obtained after the enumeration of the CFU/mL are given in **Table 4.3.**

Table 4.3: MBC (µg/mL) of 2-azidobenzothiazoles against *S. aureus* and *E. faecalis.*

S. No.	Compound	*E. faecalis*	*S. aureus*
1	2a	128	128
2	2b	128	128
3	2c	128	128
4	2d	16	16
5	2e	128	>128
6	2f	128	128

7	2g	128	128
8	2h	128	128
9	Ampicillin	4	8

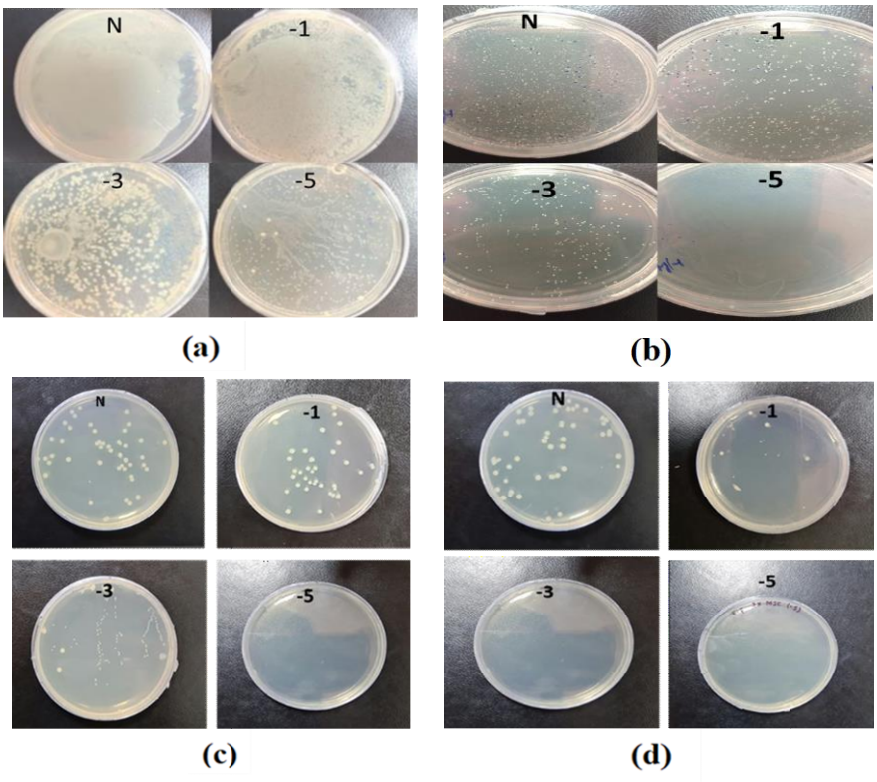

Fig.-4.6: Result of CFU enumeration of *E. faecalis* on nutrient agar plates after incubation for 24 hours at 37 ºC (a) untreated control plates (b) **2a** treated plates (MIC) (c) **2b** treated (MIC) (d) **2e** (2x) MIC treated plates showing 99.9% killing (more than 3 log reduction in CFU count) compared to untreated.

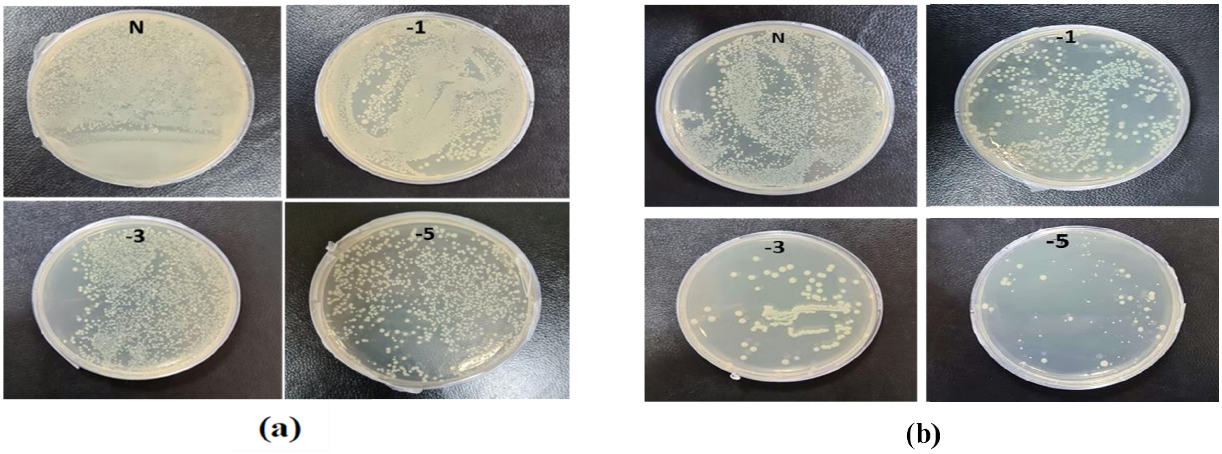

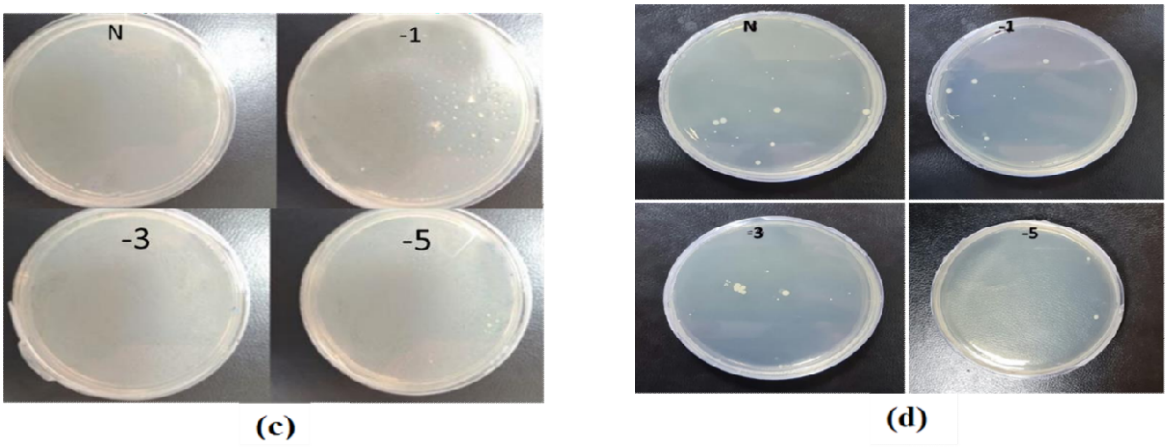

Fig.-4.7: Result of CFU enumeration as represented by circular colonies of *S. aureus* on nutrient agar plates after incubation for 24 hours at 37 ºC (a) untreated control plates (b) **2d** treated plates (MIC) (c) **2d** treated plates showing 99.9% killing (more than 3 log reduction in CFU count) compared to untreated (d) Ampicillin treated (2x) MIC.

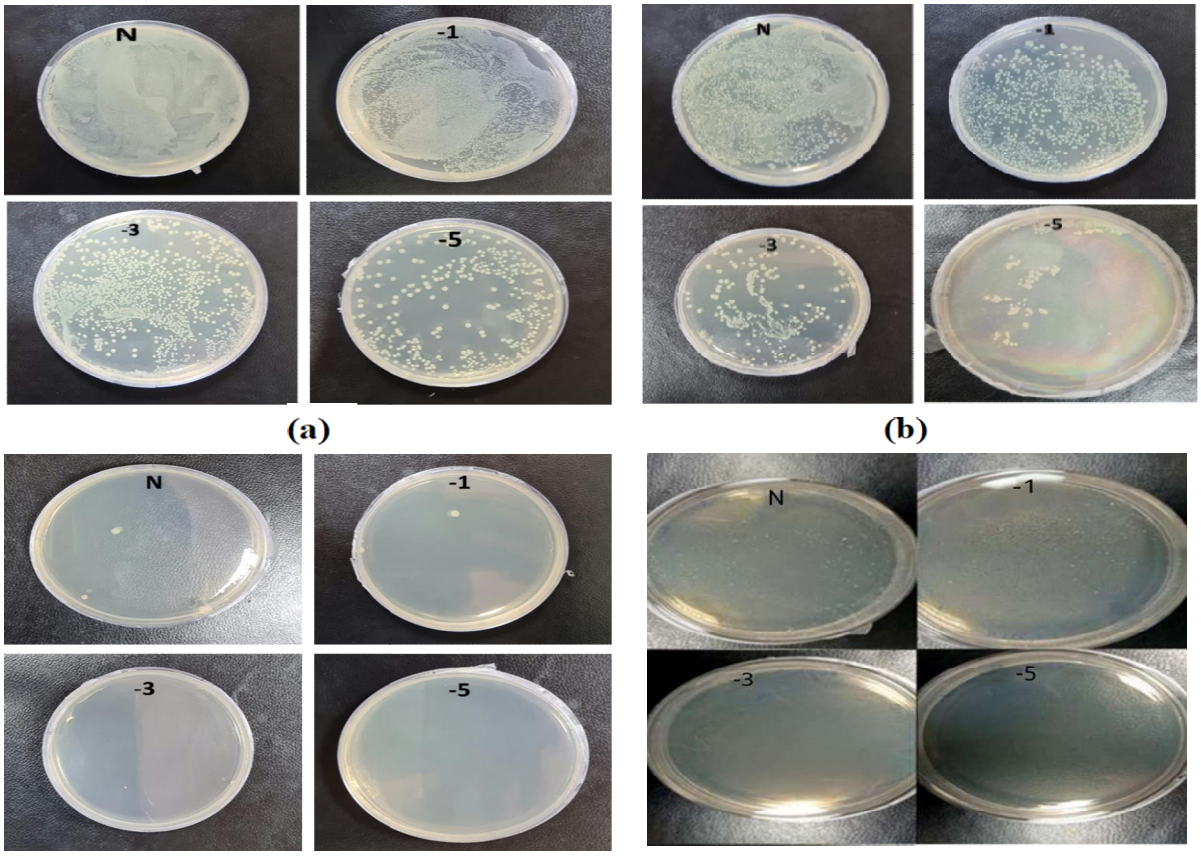

Fig.-4.8: Result of CFU enumeration as represented by circular colonies of *E. faecalis* on nutrient agar plates after incubation for 24 hours at 37 ºC (a) untreated control plates (b) **2d** treated plates (MIC) (c) **2d** treated plates showing 99.9% killing(more than 3 log reduction in CFU count) compared to untreated (d) Ampicillin treated (2x) MIC.

4.2.2.3. Time-Kill Kinetics

To study the dynamics of *in vitro* activity, we assessed the kill curve kinetics of our lead compound **2d** against *S. aureus* and *E. faecalis* at concentrations of MIC (8 µg/mL), 2xMIC (16 µg/mL) and 4xMIC (32 µg/mL) for 24 hours at seven-time points (0, 4, 8, 12, 16, 20 and 24 hours of exposure) using the two methods as described in methodology.

4.2.2.3.1. Assessment of 24-Hour Time-Kill Kinetics via CFU/mL Evaluation

Staphylococcus aureus

Fig.-4.9a represents the time-kill curve of compound **2d** against *S. aureus* at different concentrations (MIC, 2xMIC, and 4xMIC) at the given time points, compared to ampicillin (2xAMP) and growth control (GC). The colonies were counted and converted into log10 values in Excel. At time zero, all cultures showed similar bacterial counts ranging from 5.08 to 5.10 log10 CFU/mL. As time progressed, the bacterial counts decreased in all cultures except GC. The compound **2d** at 4xMIC showed the most potent activity, reducing the bacterial counts to 0.08 log10 CFU/mL after 12 hours of incubation (more than 3 log reductions). In comparison, at 2xMIC, compound **2d** reduced the bacterial counts to 0.4 log10 CFU/mL within 16 hours, and at MIC, the reduction was modest, with bacterial counts remaining at 2.403 log10 CFU/mL after 24 hours of incubation indicating the bacteriostatic nature of the compound at a lower concentration. When comparing the activity of compound **2d** to ampicillin (2xAMP), the results showed that at 4xMIC and 2xAMP, the bacterial counts reduced to similar levels after 12 hours of incubation. Moreover, at the time interval of 4-12 hours maximum killing was observed at all three concentrations. In conclusion, compound **2d** showed a concentration-dependent as well as time-dependent bactericidal activity against *S. aureus*, with the highest bactericidal activity observed at 4xMIC within 12 hours.

Enterococcus faecalis

Fig.-4.9b represents the time-kill curve of *E. faecalis*, with various concentrations of **2d**, MIC, 2xMIC, 4xMIC, and 2xAMP at different time points. The bacteria appear to be highly

susceptible to the compound as evidenced by the significant decrease in the growth rate at higher concentrations over time. After an interval of 4 hrs, a significant reduction in the growth rate was observed at all concentrations (approximately 2-log reduction across all concentrations). After 8 hours, there was a significant decrease in CFU/mL count, at higher concentrations of 2x and 4xMIC, while as for MIC the activity remained static. 4xMIC exhibited bactericidal activity achieving 99.9% killing within 8 hours. At MIC the compound exhibited a bacteriostatic activity at all time points. At 2xMIC the bactericidal activity was achieved after 12 hours which is similar to that of Ampicillin. The results suggest that *E. faecalis* was highly susceptible to the compound at higher concentrations and the bactericidal effect was observed at 2xMIC and 4xMIC within 12 and 8 hours respectively. Overall, we can deduce from the results that the activity of compound **2d** is concentration-dependent as well as time-dependent killing.

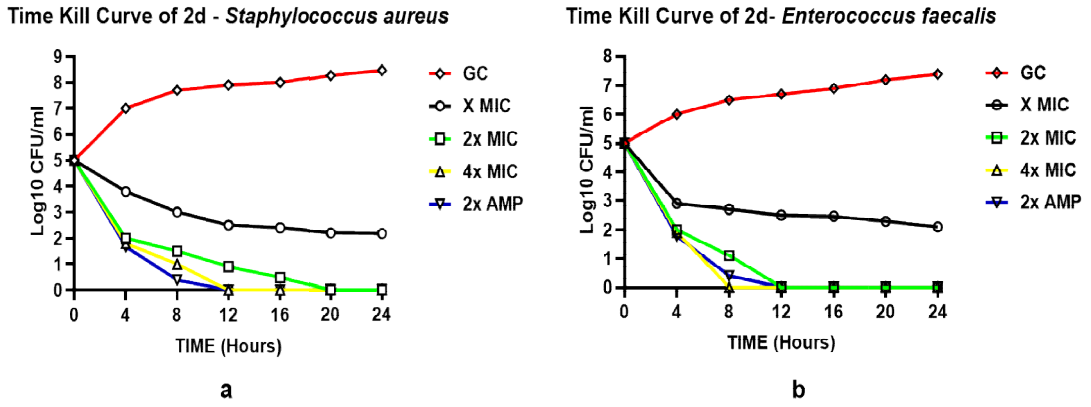

Fig.-4.9: Time-kill curves of compound **2d**. The killing activity of **2d** against two bacteria against two bacterial strains *S. aureus* **(A)** and E. *faecalis* **(B)** monitored for 24 hours by the CFU enumeration method. The compound concentrations used in the experiment were MIC (green), 2xMIC (pink), and 4xMIC (blue). Ampicillin indicated by the yellow line was used as a positive control. For negative control (Black line), the cultures were incubated under similar conditions without any drug.

4.2.2.3.2. Evaluation of Time-Kill Kinetics based on MTT-reduction on a 360-Minute Scale

To ascertain whether the impact of compound **2d** on the growth of *S. aureus* and *E. faecalis* is dose-dependent, the time-kill kinetic assay was carried out using MTT on the minute scale as described in the methodology. Both the bacterial strains were incubated individually with compound **2d** at its final concentration of MIC, 2xMIC, and 4xMIC. The optical density of the

cultures was recorded at time intervals of 60 minutes. It is clear from **Fig.-4.10** that the compound showed bactericidal activity against both strains in a dose-dependent manner. The killing pattern of compound **2d** against *S. aureus* was comparable to that of Streptomycin with over 75% of bacterial death within 4 hours of the treatment. For *E. faecalis*, however, the compound showed a similar rate of death after 2 hours of treatment compared to Streptomycin.

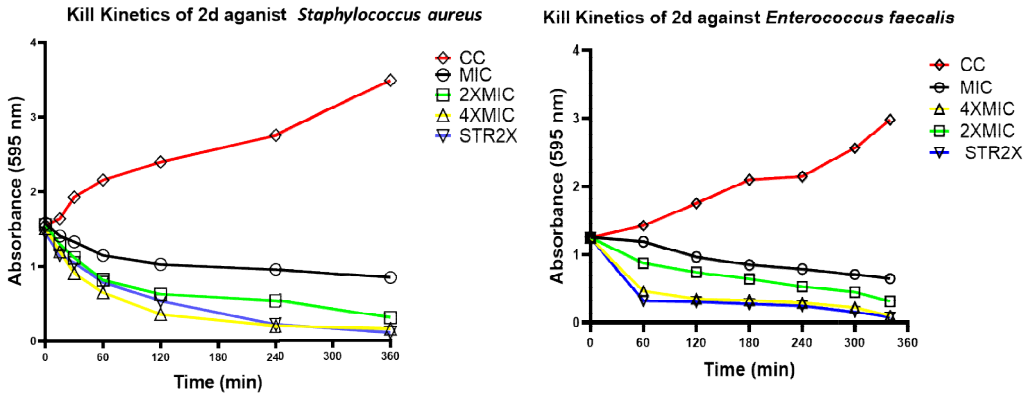

Fig.-4.10: The killing activity of **2d** against two bacterial strains *S. aureus* (a) and *E. faecalis* (b) was monitored for 360 minutes. The compound concentrations used in the experiment were MIC (Black), 2xMIC (Green), and 4xMIC (Yellow). Streptomycin (STR) indicated by the Blue line was used as a positive control. For negative control (Red line), the cultures were incubated under similar conditions without any drug.

Fig.-4.11: 2d treated cells unable to convert MTT into formazan crystals due to the absence of a dehydrogenase system of viable cells compared to untreated cells (GC).

4.2.2.4. Post-Antibiotic Effect (PAE)

To investigate the effect of compound **2d**, post its withdrawal, and assess whether the suppression in the growth of bacterial cells, *S. aureus* and *E. faecalis* persist after this brief exposure, the PAE was calculated. The determination of PAE was derived using the viable count method as described. *S. aureus* and *E. faecalis* were individually treated with MIC (8 µg/mL), 2xMIC (16 µg/mL), and 4xMIC (32 µg/mL) concentrations of the compound **2d** and MIC of Ampicillin for 2 hours. The growth was monitored by CFU enumeration after a time interval of 1 hour. The PAE results represented here are determined at a higher inoculum size of 1×10^6 CFU/mL as against the routine inoculum size of 1×10^5 CFU/mL more commonly used for susceptibility testing (MIC). To avoid the ambiguity in PAE results owing to the higher inoculum effect, MIC assay was first performed at a higher inoculum size (1×10^6 CFU/mL) to select the correct concentrations of antibacterial agents (**2d** & AMP) for PAE determination. No change in MIC of **2d** as well as Ampicillin was determined at higher inoculum size. PAE was calculated using the formula: **PAE= T-C** as described in the methodology.

Staphylococcus aureus

The cells took an average of 5.33 hours to increase their CFU by 1 $\log_{10}$ post-withdrawal of compound **2d**, irrespective of the concentration of compound **2d**. After treatment and removal of 8 and 32 µg/mL of **2d**, the growth was suppressed for around 6 hours. The recovery period after **2d** treatment was almost identical to that of MIC of Ampicillin treatment. The PAE results indicate that compound **2d**, at concentrations ranging from 8, 16, and 32 µg/mL, demonstrates a significant and sustained inhibitory effect on bacterial regrowth even after the removal of the antibiotic. The consistent PAE duration across the tested concentrations suggests that compound **2d** exhibits a concentration-independent PAE (**Table 4.4**).

Enterococcus faecalis

In the case of *E. faecalis*, the cells took an average of 5.66 hours to increase their CFU by 1 $\log_{10}$ post-withdrawal of compound **2d**, which was comparable to that of Ampicillin. In this case, the results indicate that the post-compound effect is independent of drug concentration as there is not

much variation in the time taken by the bacteria to increase their CFU by 1 $\log_{10}$ at all three concentrations tested (**Table 4.5**).

The results reveal that both *S. aureus* and *E. faecalis* exhibited similar post-treatment growth characteristics in response to compound **2d**. The average time required for a 1 log10 CFU increase was 5.33 hours (± 0.577) for *S. aureus* and 5.66 hours (± 0.617) for *E. faecalis* when treated with MIC, 2xMIC, and 4xMIC concentrations of compound **2d (Fig.-4.12)**. These results suggest a consistent and predictable post-treatment effect independent of the drug concentration, indicating the potential effectiveness of compound **2d**. The sustained inhibitory effect of concentration-independent PAE can reduce the selection pressure for antibiotic-resistant bacterial strains. By maintaining a prolonged suppression of bacterial growth even after sub-MIC levels, the development and spread of resistance mechanisms may be hindered, preserving the effectiveness of the antibiotic over an extended period. Concentration-independent PAE offers advantages in terms of flexibility in dosing, extended suppression of bacterial regrowth, reduced resistance development, and optimized antibiotic therapy. These benefits contribute to the potential improvement in treatment outcomes and the management of bacterial infections.

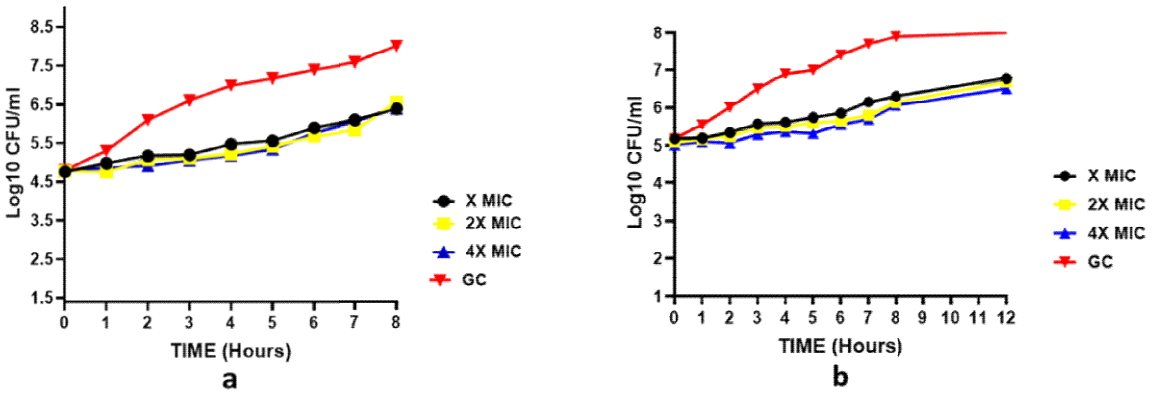

Fig.-4.12: Post-antibiotic effect of compound **2d** at various concentrations against (a) *S. aureus* (b) *E. faecalis* indicating the time points at which a 1 log10 CFU/ml increase was observed for *S. aureus* and *E. faecalis* after a brief exposure (2 hours) to compound **2d** at different concentrations (x, 2x, and 4xMIC) and subsequent removal of the antimicrobial agent.

Table 4.4: Post-antibiotic activity of **2d** at MIC, 2xMIC, and 4xMIC and Ampicillin against *S. aureus*.

Compound	MIC	Time (hours)	PAE= T-C
2d	1x	6	5.00
	2x	7	6.00
	4x	6	5.00
Ampicillin	2x	6	5.00
The culture controls took, **C= 1.00** hours to grow in the absence of the antimicrobial agent. The average of the PAE of 2d at different concentrations was around **5.33 hours**			

Table 4.5: Post-antibiotic activity of **2d** at MIC, 2xMIC, and 4xMIC and Ampicillin against *E. faecalis.*

Compound	MIC	Time (hours)	PAE= T-C
2d	1x	7	5.00
	2x	8	6.00
	4x	8	6.00
Ampicillin	2x	8	6.00
The culture controls took, **C= 2** hours to grow in the absence of the antimicrobial agent. The average of the PAE of **2d** at different concentrations was around **5.66 hours**			

4.2.2.5. Fluorescent Microscopy

To further explore the mechanism by which the compound targeted the bacterial cells, fluorescent microscopy was performed on the bacterial cells treated with the compound. Post **2d** treatment, *E. faecalis,* and *S. aureus* were treated with two fluorescent dyes 4', 6-diamidino-2-phenylindole (DAPI), and propidium iodide (PI). DAPI is a fluorescent dye that binds to DNA and emits blue fluorescence upon excitation by ultraviolet light and PI is also a fluorescent dye that binds to DNA, but it emits red fluorescence upon excitation by ultraviolet light. PI is a membrane-impermeable DNA-binding fluorescent dye whereas DAPI is a membrane-permeable

DNA-binding dye. PI only enters cells with compromised membranes and stains the nucleic acid of dead cells. DAPI is permeable to the cell wall and fluoresces upon binding to chromosomal DNA, whether the cells are dead or alive. For control, the cells were treated with DAPI and PI without prior treatment with compound **2d**. The DAPI/PI staining results revealed the presence of red fluorescence in both *S. aureus* and *E. faecalis* bacterial strains. The red fluorescence observed in the bacterial cells indicates the uptake and binding of PI, suggesting compromised cell membrane integrity. This red fluorescence was visually distinguishable from the blue fluorescence emitted by DAPI, which stains the DNA of both live and dead bacteria. The identification of compromised membrane integrity is of significance as it can indicate the susceptibility of *S. aureus* and *E. faecalis* strains to antimicrobial treatments. The presence of red fluorescence provides evidence of cell damage and potential loss of viability, suggesting that these strains may be more susceptible to the effects of **2d** targeting the cell membrane. From **Figs.-4.13A & 4.13B**, it is evident that the antibacterial activity of compound **2d** was due to damage to the cell wall of the bacterial cells. These findings suggest that compound **2d** targets the cell wall of bacterial cells, leading to compromised membrane integrity and ultimately cell death.

Conducting cell membrane-related studies on synthesized derivatives is a reasonable approach to understanding their mechanisms of action. The cell membrane has a pivotal function in regulating the passage of molecules and ions in and out of the cell, as well as in cell signaling and communication. Therefore, studying how the synthesized derivatives interact with the cell membrane can offer valuable insights into their potential mechanisms of action. However, we understand it is worth emphasizing that cell membrane-related studies alone may not provide a comprehensive understanding of the mechanisms of action of the synthesized derivatives. There could be additional mechanisms involved in their effects on cell viability that are independent of the cell membrane but DAPI and PI are commonly used fluorescent dyes that can be used to assess cell viability and membrane integrity. DAPI stains the nuclei of both live and dead cells, while PI is excluded from live cells but stains the DNA of dead or damaged cells with compromised membrane integrity. DAPI/PI staining allows for the differentiation between live cells (DAPI-positive, PI-negative). By using DAPI/PI staining, we wanted to assess the overall cell viability and determine whether the synthesized derivative has any detrimental effects on cell membrane integrity, which may lead to cell death.

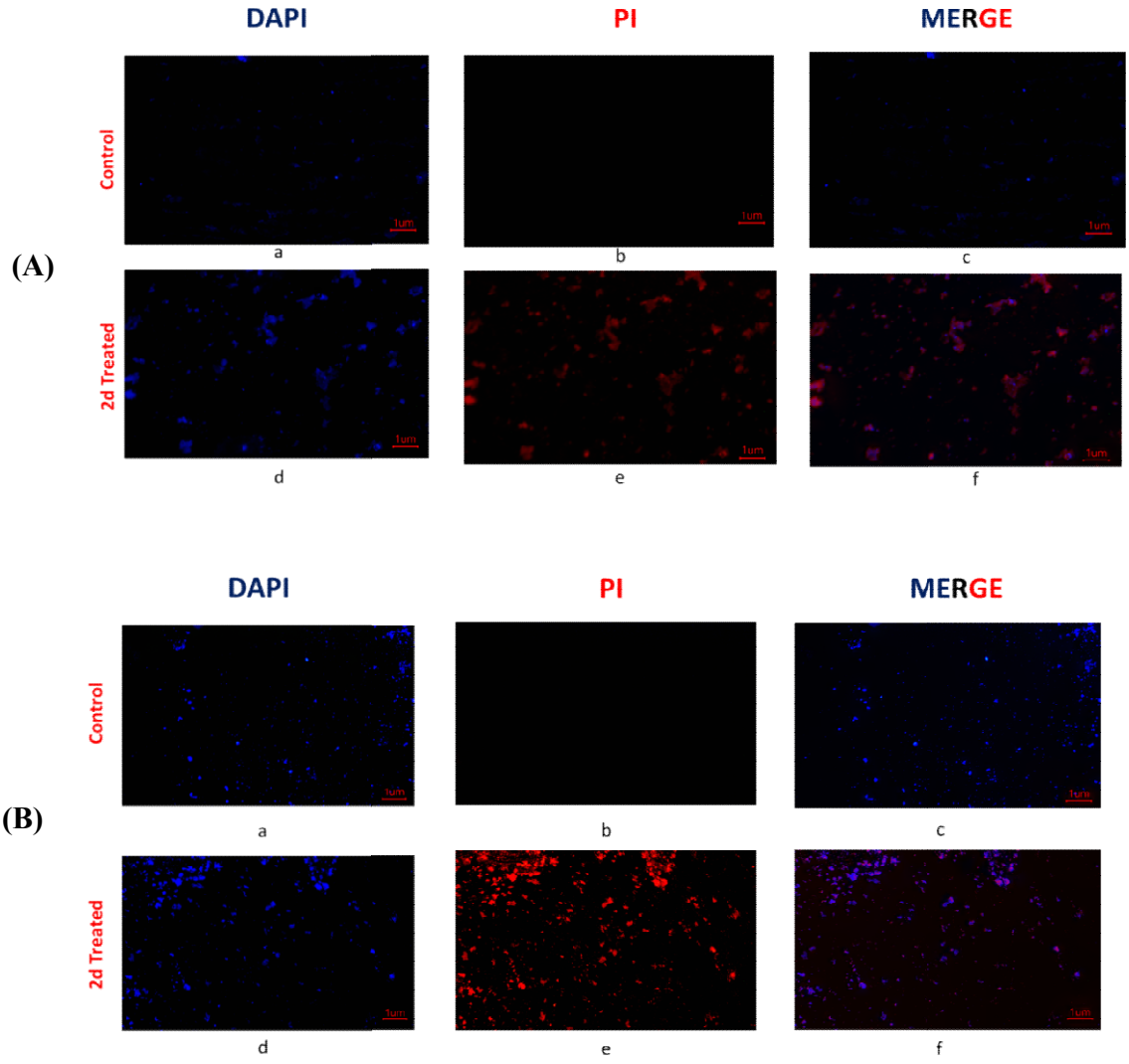

Fig.-4.13: (A) Fluorescent images of *S. aureus*: The untreated cells were stained with DAPI and PI and visualized under a fluorescent microscope. The photographed images of cells for DAPI (a) and PI (b) were merged (c). Under similar conditions **2d** (2x) treated *S. aureus cells* were photographed for DAPI (d) and PI (e) and the images were merged using Image (f); (B) Fluorescent microscopy images of *E. faecalis:* The untreated cells were stained with DAPI and PI and visualized under a fluorescent microscope (Magnus). The photographed images of cells for DAPI (a) and PI (b) were merged (c). Under similar conditions, **2d** (2x) treated *E. faecalis* cells were photographed for DAPI (d) and PI (e), and the images were merged using Image (f).

4.2.2.6. Biofilm Inhibition Assay

The compound **2d**, with the strong antibacterial activity, was tested against American Type Culture Collection (ATCC) strains of biofilm-forming Gram (+) bacteria, *S. aureus, E. faecalis, B. cereus* and Gram (-) bacteria, *E. coli, P. aeruginosa, K. pneumoniae*. The Quantitative assessment of biofilm inhibition was done by calculating the percentage inhibition of the compound through spectrophotometric analysis for each bacterial strain by Microtiter Plate Biofilm Assay. The Quantitative assessment of biofilm inhibition was done by calculating the percentage inhibition of the compound through spectrophotometric analysis for each bacterial strain by Microtiter Plate Biofilm Assay. The Qualitative assessment was done by CV staining and visualization under the microscope. The percentage of biofilm inhibition was quantified by spectrophotometric analysis by taking the mean of three OD values (± SD) of [aqueous] acetic acid solubilized crystal-violet stained biofilms using the formula:

[100-(Treated OD470nm ÷ Growth Control OD470nm) ×100]

The percentage of biofilm inhibition was determined at various concentrations of compound **2d** (0.25-128 µg/mL), and the values reported are the means of three optical density (OD) measurements to ensure more reliable and accurate results. Compound **2d** exhibited significant biofilm inhibitory activity against all tested bacterial strains in a concentration-dependent manner. The percentage of biofilm inhibition varied across different concentrations and bacterial species. For *S. aureus*, compound **2d** displayed increasing biofilm inhibition percentages with higher concentrations. At the highest tested concentration of 128 µg/mL, the biofilm inhibition was 70.30%. Similarly, for *E. faecalis*, the biofilm inhibition reached 73.04% at the same concentration. *B. cereus* showed a distinct trend, with biofilm inhibition percentages of 61.23% and 53.09% at the highest concentration (128 µg/mL) and half that concentration (64 µg/mL), respectively. However, the inhibitory effect decreased significantly at lower concentrations. Among the Gram (-) bacteria, Pseudomonas aeruginosa demonstrated substantial biofilm inhibition, with percentages ranging from 62.07% at 128 µg/mL to 35.47% at 0.25 µg/mL. *E. coli* and *K. pneumoniae* exhibited lower biofilm inhibition percentages, ranging from 19.73% to 49.41% and from 14.07% to 45.59%, respectively, across the tested concentrations. Overall, these results indicate that compound **2d** possesses significant biofilm inhibitory activity against a

range of biofilm-forming bacterial strains with the most significant inhibitory potential against *S. aureus* and *E. faecalis*.

The percentage of biofilm inhibition at different concentrations of compound **2d** was consistent with the qualitative analysis conducted using light microscopy. Microscopic examination revealed disrupted biofilm architecture and reduced biofilm biomass in the presence of compound **2d**, supporting the quantitative findings. The microscopic analysis provided visual confirmation of the biofilm inhibitory potential of compound **2d**. The growth control revealed a thick and compact biofilm structure, indicating the successful formation of mature biofilms by the tested bacterial strains. In contrast, the microscopic images of the biofilms treated with compound **2d** at different concentrations displayed notable differences compared to the growth control. The biofilms exposed to compound **2d** exhibited reduced biomass and disrupted biofilm architecture. The qualitative analysis corroborated the quantitative results, confirming that compound **2d** has a significant impact on biofilm formation across different bacterial strains. The visual evidence of reduced biomass and disrupted biofilm architecture shown in the figures at various concentrations supports the notion that compound **2d** interferes with the crucial steps of biofilm development (**Figs.-4.14-4.17**).

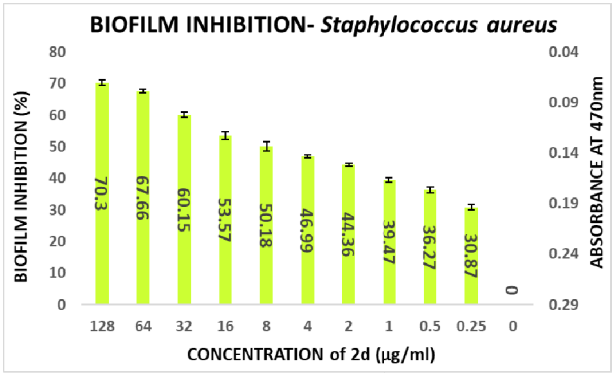

(A)

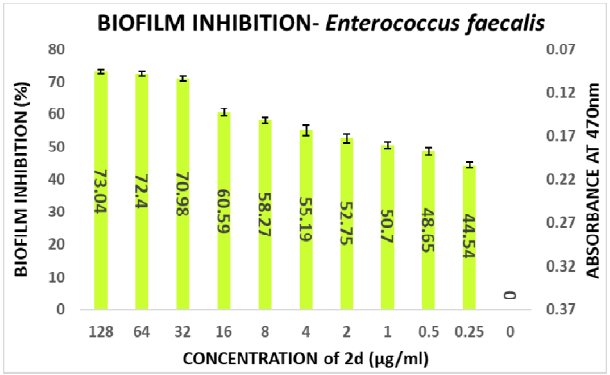

(B)

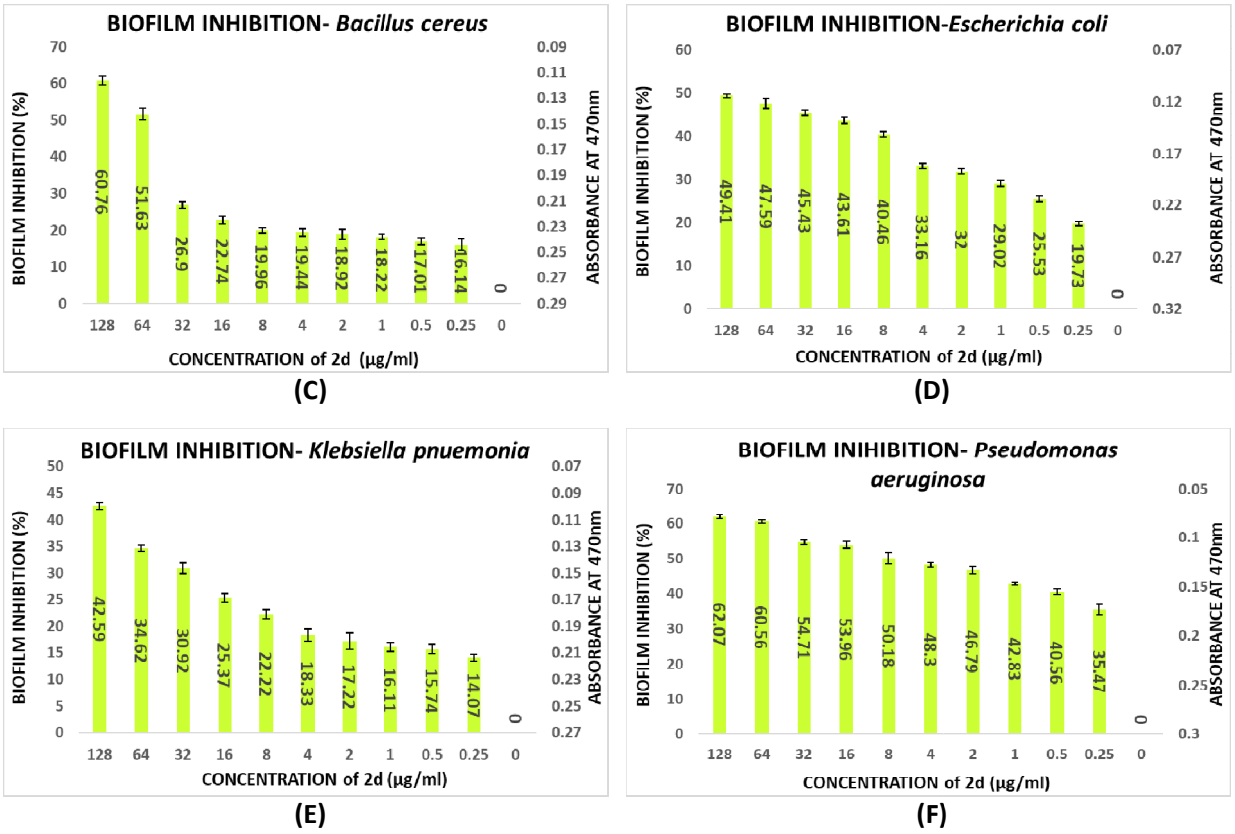

Fig.-4.14: Quantitative analysis of biofilm percentage inhibition- (A) *S. aureus;* (B) *E. faecalis;* (C) *B. cereus;* (D) *E. coli;* (E) *P. aeruginosa;* (F) *K. pneumoniae.*

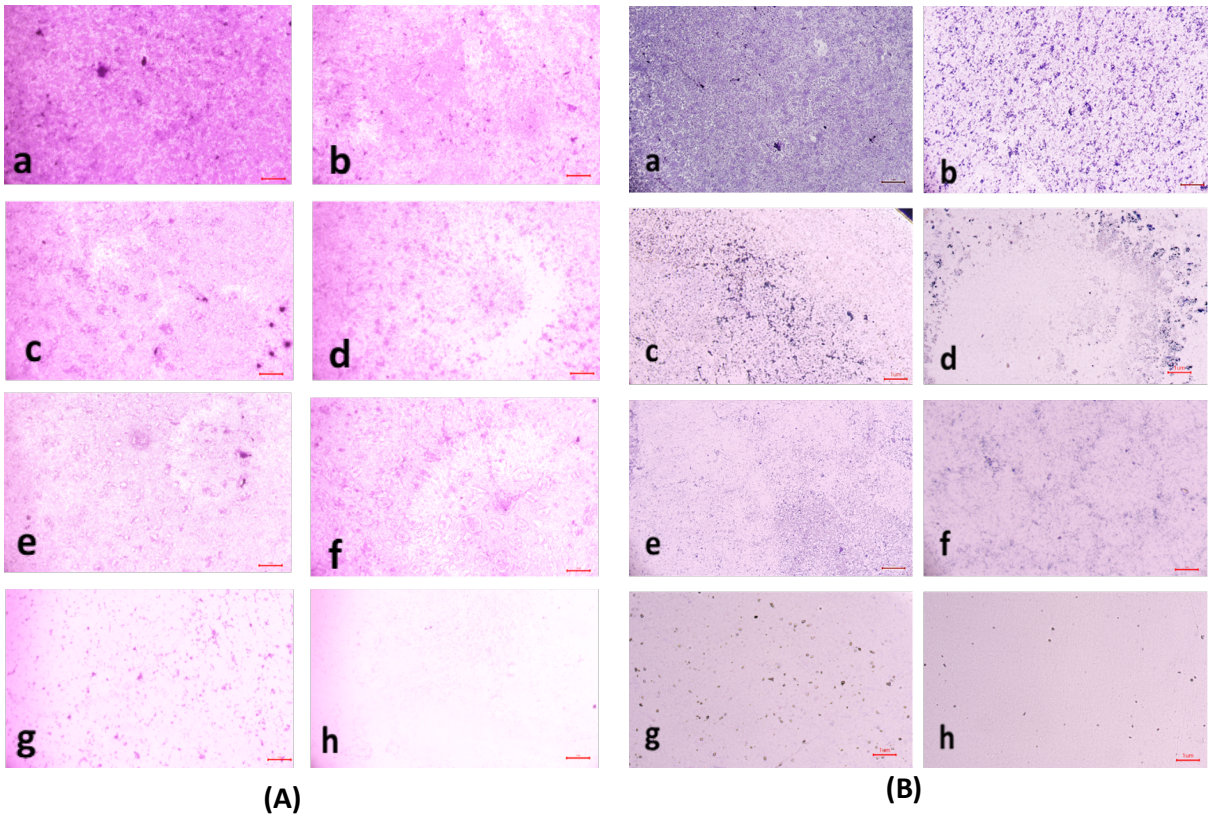

Fig.-4.15: (A) Light microscopic images of biofilm (10x- Magnus) in *S. aureus* at (a) GC (b) 4 µg/mL (c) 8 µg/mL (d) 16 µg/mL (e) 32 µg/mL (f) 64 µg/ml (g) 128 µg/ml treated wells (h) MC; (B) Light microscopic images of biofilm (10x- Magnus) in *E. faecalis* at (a) GC (b) 4 µg/mL (c) 8 µg/mL (d) 16 µg/mL (e) 32 µg/mL (f) 64 µg/mL (g) 128 µg/mL treated wells (h) MC.

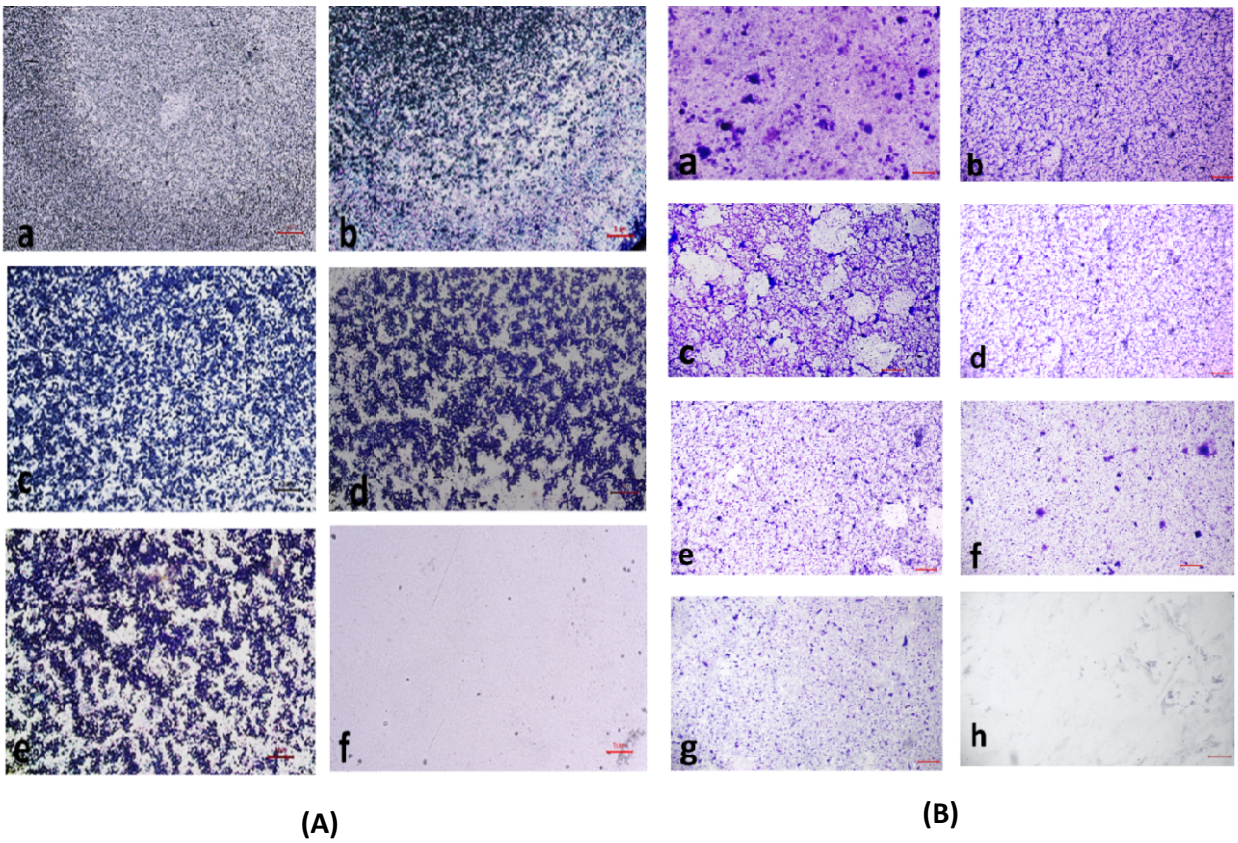

Fig.-4.16: (A) Light microscopic images of biofilm (10x- Magnus) in *B. cereus* at (a) GC (b) 4 µg/mL (c) 16 µg/mL (d) 32 µg/mL (e) 128 µg/mL (f) MC; (B) Light microscopic images of biofilm (10x- Magnus) in *E. coli* at (a) GC (b) 4 µg/mL (c) 8 µg/mL (d) 16 µg/mL (e) 32 µg/mL (f) 64 µg/mL (g) 128 µg/mL treated wells (h) MC.

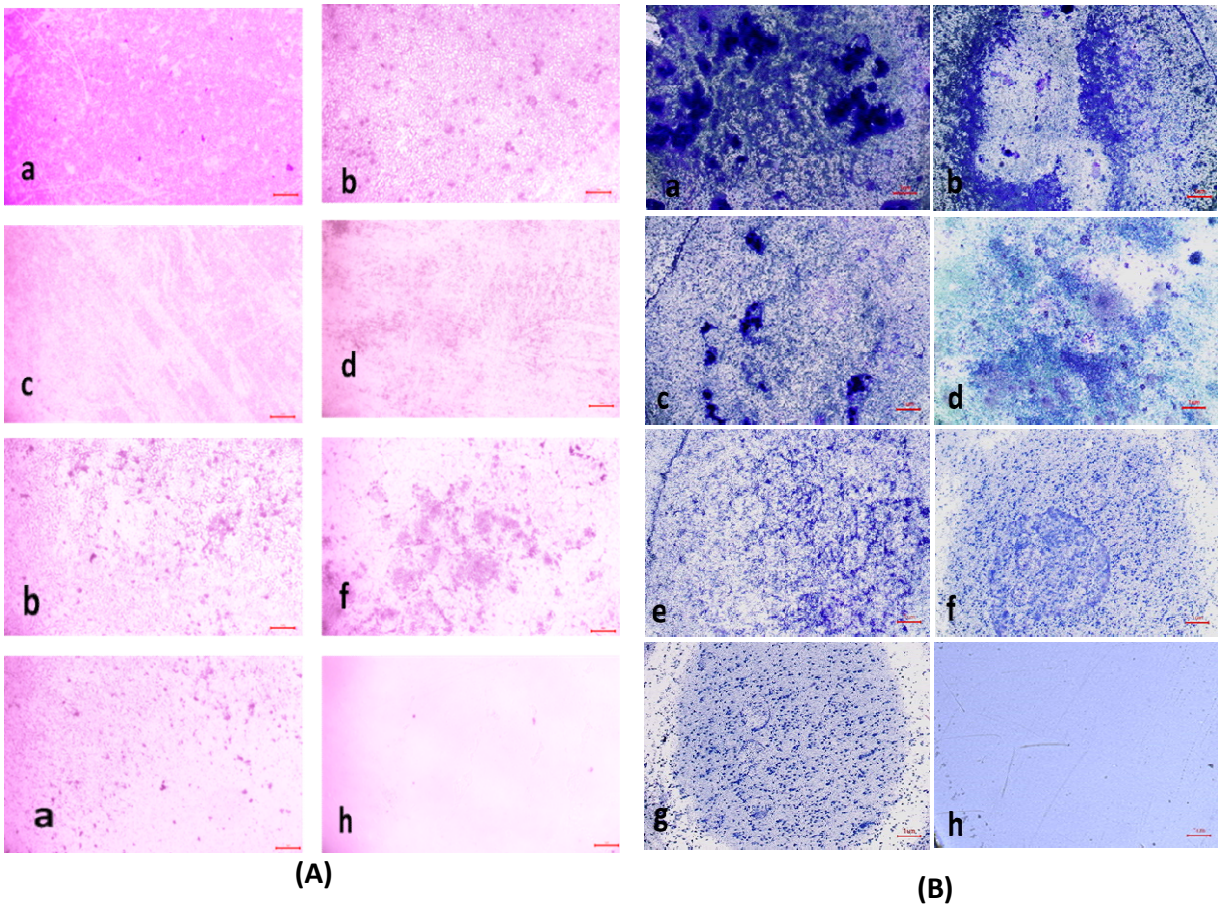

Fig.-4.17: (A) Light microscopic images of biofilm (10x- Magnus) in *P. aeruginosa* at (a) GC (b) 4 µg/mL(c) 8 µg/mL (d) 16 µg/mL (e) 32 µg/mL (f) 64 µg/mL (g) 128 µg/mL treated wells (h) MC; (B) Light microscopic images of biofilm (10x- Magnus) in *K. pneumoniae* at (a) GC (b) 4 µg/mL(c) 8 µg/mL (d) 16 µg/mL (e) 32 µg/mL (f) 64 µg/mL (g) 128 µg/mL treated wells (h) MC.

4.2.2.7. Biofilm Eradication Assay

The compound **2d** exhibited strong biofilm inhibition potential against both *E. faecalis* and *S. aureus* prompting the evaluation of Biofilm Eradication potential against these two strains. The antibiofilm effect of the compound was evaluated both qualitatively and quantitatively by Light Microscopy and Crystal Violet method at concentrations 8, 16, 32, 64, and 128 µg/mL to evaluate the effect of the compound on various stages of biofilm formed at 24, 48 and 72 hours. Light microscopic images revealed that the growth control wells exhibited significant biofilm formation at all three-time points. At 24 hours, cell attachment was observed, followed by cell

aggregation at 36 hours, and extensive biofilm formation or mat formation at 48 hours. However, in wells incubated with compound **2d** at different concentrations, non-aggregation of cells was observed during all stages of biofilm formation for both bacterial strains. This indicates the compound's ability to inhibit cell aggregation, a critical step in biofilm development.

This qualitative finding was further investigated with the crystal violet staining method by comparing the absorbance between the growth control wells and the wells incubated with the compound. The percentage of biofilm Eradication at various concentrations is shown (**Figs.-4.18A & 4.18B)** which indicates a strong antibiofilm potential of the compound eradicating up to more than 40% of the biofilm at all concentrations. The crystal violet staining method confirmed the qualitative findings, demonstrating the compound's antibiofilm potential. The absorbance measurements showed that compound **2d** eradicated over 40% of the biofilm at all tested concentrations. Notably, at higher concentrations, the compound exhibited substantial eradication potential against both *E. faecalis* and *S. aureus*, eliminating 70-77% of the preformed biofilm at all three-time points. These results suggest that compound **2d** has a strong biofilm eradication capability. The qualitative and quantitative evaluation of biofilm eradication correlated with each other. The eradication potential of the compound on the densely pre-biofilm at 72 hours against both bacterial strains indicates that the compound can be a promising agent for biofilm eradication. The quantitative evaluation of the percentage of biofilm eradication was done as per the formula mentioned in the methodology and the results represented are the mean values of the three OD readings taken for each concentration in different wells. The compound effectively inhibited cell aggregation and eradicated preformed biofilms in a dose-dependent manner.

The biofilm eradication percentages of compound **2d** against 24-hour formed *S. aureus* biofilms were found to be 59% at 8 µg/mL, 67% at 16 µg/mL, 69% at 32 µg/mL, 74% at 64 µg/mL, and 76% at 128 µg/mL. For 48-hour biofilms, the eradication percentages were 59%, 65%, 70%, 71%, and 74% at the corresponding concentrations. In the case of mature biofilms formed for 72 hours, compound **2d** exhibited eradication percentages of 50%, 54%, 62%, 68%, and 73% at the respective concentrations.

The biofilm eradication percentages of compound **2d** against 24-hour formed *E. faecalis* biofilms were found to be 42% at 8 µg/mL, 52% at 16 µg/mL, 61% at 32 µg/mL, 69% at 64 µg/mL, and 72% at 128 µg/mL. For 48-hour biofilms, the eradication percentages were 58%, 59%, 67%,

70%, and 72% at the corresponding concentrations. In the case of mature biofilms formed for 72 hours, compound **2d** exhibited eradication percentages of 40%, 42%, 48%, 55%, and 66% at the respective concentrations.

These values represent the mean average derived from three distinct experiments conducted independently. The outcomes of this research underscore the strong antibiofilm efficacy of compound **2d** against *S. aureus* and *E. faecalis*. The compound exhibited remarkable efficacy in eradicating biofilms at various time points and concentrations. Compound **2d** effectively eradicated a significant proportion of the 24-hour formed biofilms. Even at the lowest concentration tested (8 µg/mL), the compound achieved a substantial eradication percentage. As the concentration increased the eradication percentages also increased, reaching 72-76% at the highest concentration (128 µg/mL). These findings highlight the concentration-dependent efficacy of compound **2d** in disrupting and eliminating early-stage *S. aureus* and *E. faecalis* biofilms. Furthermore, compound **2d** demonstrated consistent efficacy in eradicating biofilms formed over 48 hours. The eradication percentages indicated its ability to penetrate and disrupt biofilm structures at various concentrations. Notably, even at lower concentrations, the compound achieved eradication percentages above 50-65%, demonstrating its potency against established biofilms in both bacteria. Compound **2d** also exhibited substantial efficacy in eradicating mature biofilms formed over 72 hours. The eradication percentages ranged from 50% to 73% for *S. aureus* and 40-66% for *E. faecalis*, indicating its ability to target and disrupt the mature biofilm matrix. These results suggest that compound **2d** possesses strong biofilm-eradicating properties, even in the presence of a mature biofilm structure. The findings of this study emphasize the capability of compound **2d** to serve as a promising antibiofilm agent against *S. aureus* and *E. faecalis*. The ability of the compound to significantly reduce biofilm density and disrupt biofilm architecture is consistent with the qualitative observations made during the study. The strong correlation between the qualitative and quantitative evaluations supports the robustness of the antibiofilm activity of compound **2d**. The compound effectively inhibited cell adhesion, auto-aggregation, and mat formation, as observed under light microscopy. These findings suggest that compound **2d** may target key stages of biofilm development and inhibit biofilm formation (**Fig.-4.19-4.21**).

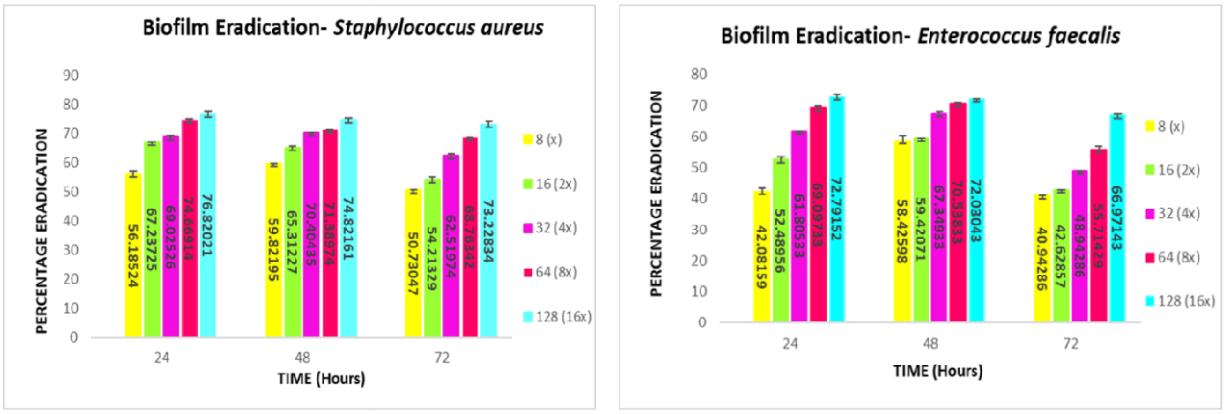

(A) **(B)**

Fig.-4.18: Quantitative Analysis: Biofilm eradication percentage (A) *S. aureus* (B) *E. faecalis* at different concentrations of compound **2d** affecting the preformed 24-, 48- and 72-hour biofilms.

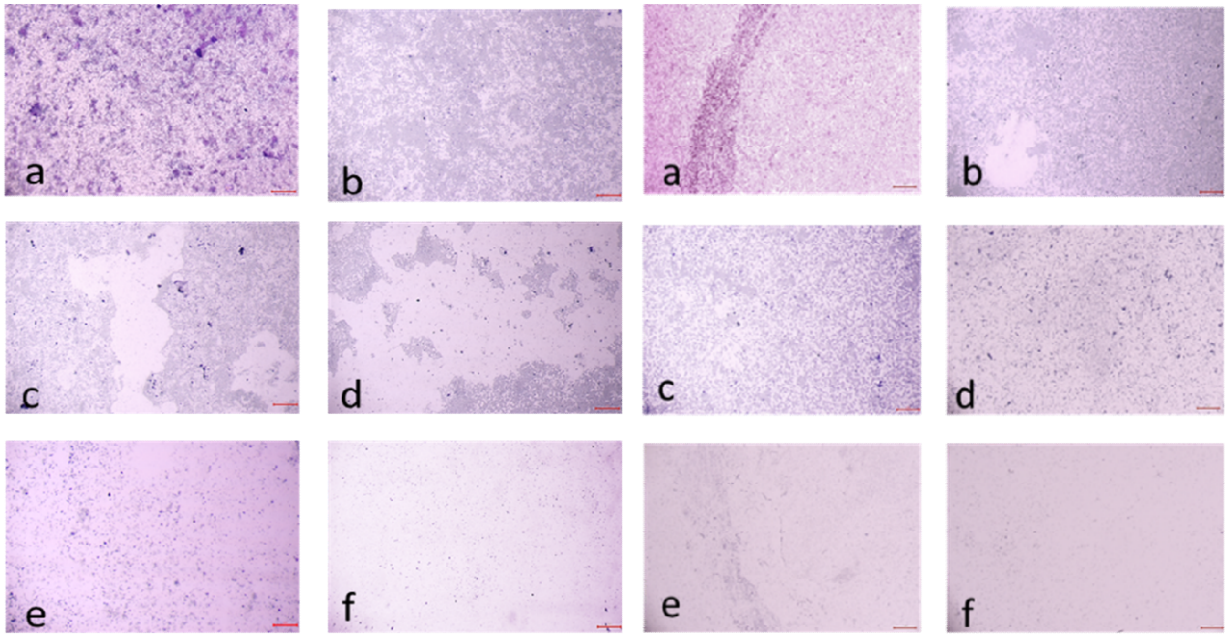

(A) **(B)**

Fig.-4.19: (A) Light microscopic images (20X) of biofilm eradication in 24 hour-preformed biofilms of *S. aureus* by compound **2d**, (a) GC-showing initial attachment to surface (devoid of compound exhibiting biofilm formation after 24 hours) (b) 8 µg/mL (c) 16 µg/mL (d) 32 µg/mL (e) 64 µg/mL (f) 128 µg/mL; (B) Biofilm of *S. aureus* by compound 2d, (a) GC-showing aggregation of cells (devoid of compound exhibiting biofilm formation after 48 hours) (b) 8 µg/mL (c) 16 µg/mL (d) 32 µg/mL (e) 64 µg/mL (f) 128 µg/mL.

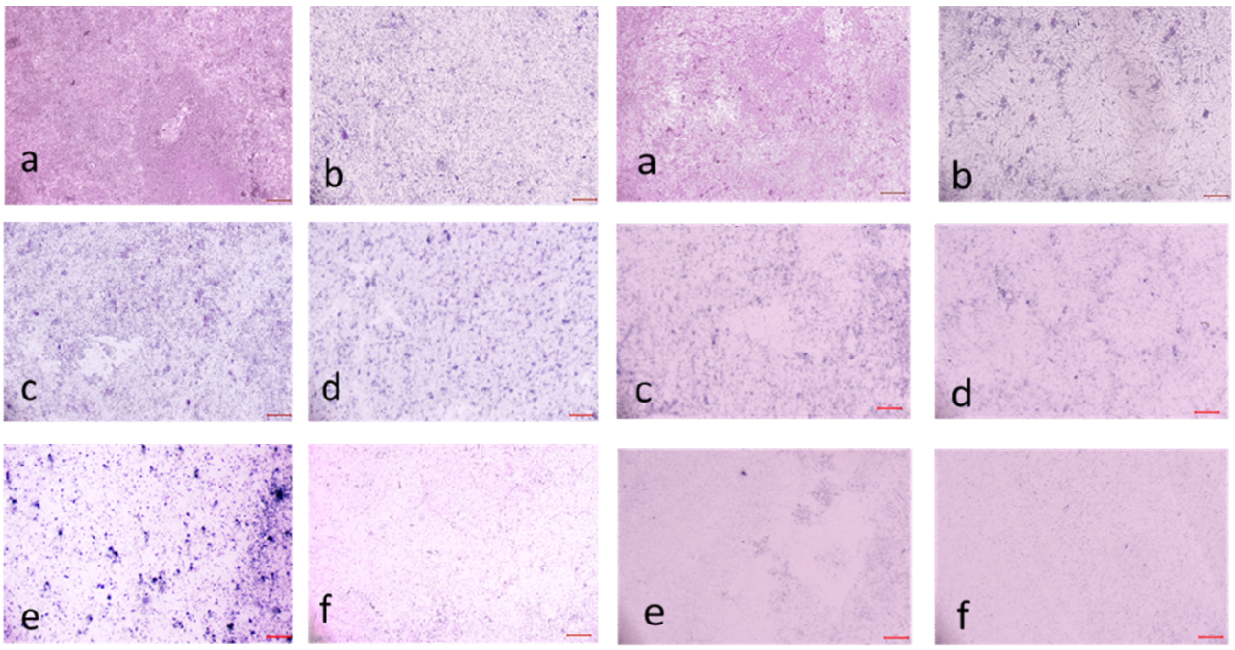

Fig.-4.20: (A) Light microscopic images (20X) of biofilm eradication in 72 hour-preformed biofilm of *S.aureus* by compound **2d**, (a) GC-showing mat formation (devoid of compound exhibiting biofilm formation after 72 hours) (b) 8 µg/mL (c) 16 µg/mL (d) 32 µg/mL (e) 64 µg/mL (f) 128 µg/mL. (B) Light microscopic images (20X) of biofilm eradication in the 24-hour-preformed biofilm of *E. faecalis* by compound **2d**, (a) GC-showing initial attachment to the surface (devoid of compound exhibiting biofilm formation after 24 hours) (b) 8 µg/mL (c) 16 µg/mL (d) 32 µg/mL (e) 64 µg/mL (f) 128 µg/mL.

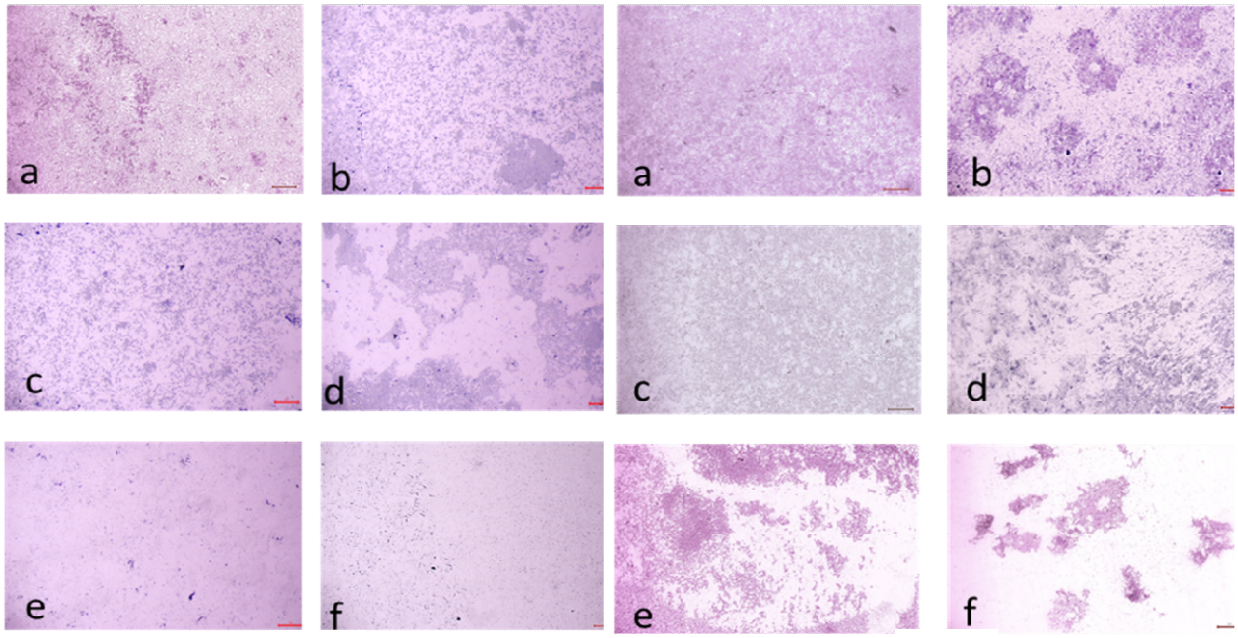

Fig.-4.21: (A) Light microscopic images (20X) of biofilm eradication in 48 hour-preformed biofilm of *E. faecalis* by compound **2d**, (a) GC-showing aggregation of cells (devoid of compound exhibiting biofilm formation after 48 hours) (b) 8 µg/mL (c) 16 µg/mL (d) 32 µg/mL (e) 64 µg/mL (f) 128 µg/mL. (B) Light microscopic images (20X) of biofilm eradication in 72 hour-preformed biofilm of *E. faecalis* by compound **2d**, (a) GC-showing mat formation (devoid of compound exhibiting biofilm formation after 72 hours) (b) 8 µg/mL (c) 16 µg/mL (d) 32 µg/mL (e) 64 µg/mL (f) 128 µg/mL.

4.2.2.8. Cytotoxicity Assay

The MTT-based cell viability assay performed on HEK-293 verified that cells exposed to **2d** compound at varying concentrations for different time durations have a non-toxic effect on the human embryonic kidney cell lines. The results of the MTT-based cell viability assay were conducted on HEK-293 cells. Surprisingly, the findings indicate that the cells exposed to **2d** exhibited a non-toxic response, demonstrating higher percentages of viable cells even at higher concentrations and longer exposure durations (**Fig.-4.22**). This suggests that the **2d** compound is cytocompatible and does not have a concentration- or time-dependent effect on cell viability. The results from the MTT assay indicated that cell viability remained notably elevated, even

within the higher concentration range of 16 to 128 µg/mL. The percentage of viability was determined using the formula:

Mean OD570 Treated Well ÷ Mean OD570 Control well× 100

The data presented in **Table 6** demonstrate the favorable impact of the **2d** compound on HEK-293 cell viability. At the lowest concentration tested (4 µg/mL), the average viability percentages remained consistently high across all concentration and time point combinations. At the highest concentration tested (128 µg/mL), the average viability percentage after 72 hours of exposure was 88.15 ± 0.005774%, indicating that even at this relatively elevated concentration, the **2d** compound did not significantly compromise cell viability. This trend of high viability percentages persisted throughout the experiment, irrespective of the exposure duration. It is important to note that these results are specific to HEK-293 cells and should not be generalized to other cell types without further experimentation.

Table 4.6: Percentage of HEK-293 cell viability after treatment with different concentrations **2d** for different time points (percentages expressed are the average values of three experiments ± SD).

Average Percentage of Viable Cells after Exposure with 2d for Different Time Durations			
Conc. (µg/mL)	**24 hours**	**48 hours**	**72 hours**
4	99.96±2.532	98.59± 0.501	99.52±0.001
8	97.62±0.475	96.85±1.269	95.35±0.010017
16	94.54±0.989	96.22±0.173	94.36±0.006429
32	90.30±0.557	91.74±0.289	88.48±0.002309
64	87.29±0.428	90.24±0.765	91.23±0.024664
128	85.32±0.164	87.06±0.153	88.15±0.005774

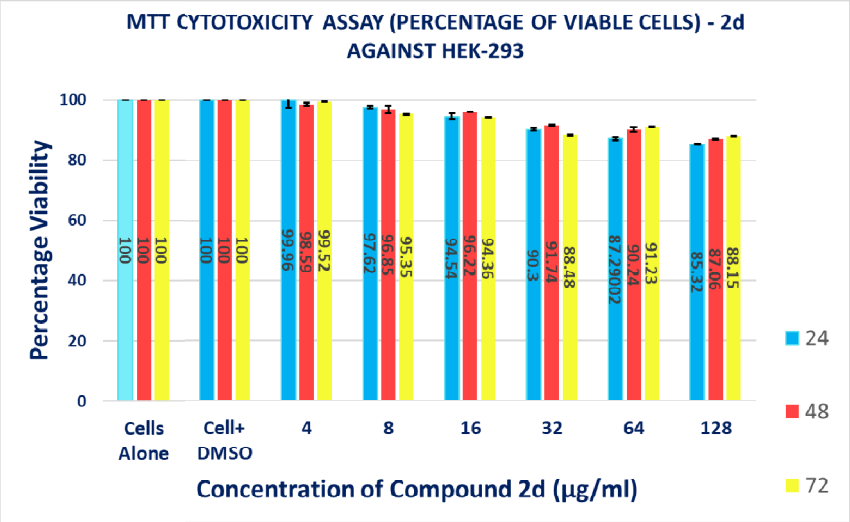

Fig.-4.22: Graphical representation of the results of MTT cytotoxicity assay.

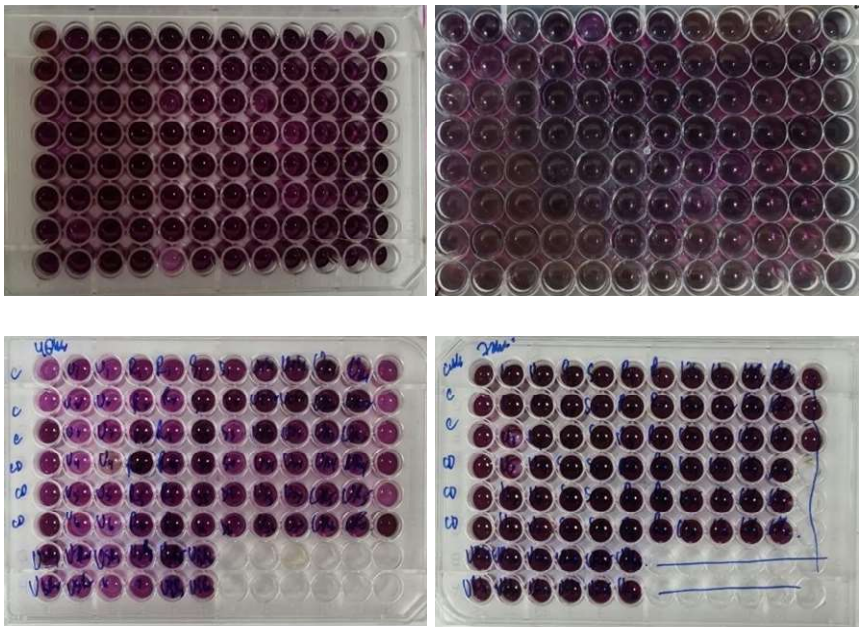

Fig.-4.23: 96-well plate showing cell lines with treated different concentrations of **2d** for different time points showing colour change on the addition of MTT (due to reduction of MTT to formazan crystals) by viable cells indicating a non-toxic effect of the compound even at higher concentrations.

4.2.3. Assessment of Antioxidant Characteristics of Synthesized 2-azidobenzothiazoles

The DPPH radical scavenging assay is a widely used method to assess the antioxidant properties of various chemical compounds. In this study, the antioxidant capabilities of 2-azidobenzothiazoles were evaluated using this assay. The results indicated that these compounds exhibited significant antioxidant activity across different concentrations of 10, 20, and 30 µg/mL. This suggests that 2-azidobenzothiazoles have the potential to effectively scavenge free radicals, thereby contributing to their potential use as antioxidants in various applications. The assessment of antioxidant activity was based on the changes in the absorption behavior of the DPPH radical, a stable free radical with a characteristic deep purple color. When this radical encounters an antioxidant, it undergoes a reduction in its free radical form, leading to a change in color from purple to pale yellow. The extent of this color change is directly related to the antioxidant activity of the tested compounds. Notably, the results revealed a concentration-dependent increase in the percentage of antioxidant activity for all tested concentrations of 2-azidobenzothiazoles. As a reference, ascorbic acid was employed, and it demonstrated inhibitions of 52.74%, 62.33%, and 78.57% at concentrations. This demonstrates that the antioxidant activity of ascorbic acid also increased with higher concentrations, in line with the expected behavior. The percentage inhibition range for the different 2-azidobenzothiazole compounds was as follows: **2a** (40.25-71.34%), **2b** (30.56-59.24%), **2c** (62.33-92.79%), **2d** (56.25-80.75%), **2e** (46.46-68.06%), **2f** (67.61-83.28%), **2g** (49.43-77.27%), and **2h** (67.11-79.55%). These results indicate that the various 2-azidobenzothiazole compounds possess a wide range of antioxidant activities, with some exhibiting particularly high levels of inhibition at the highest tested concentration. This suggests that 2-azidobenzothiazoles may be promising candidates for further exploration as antioxidants.

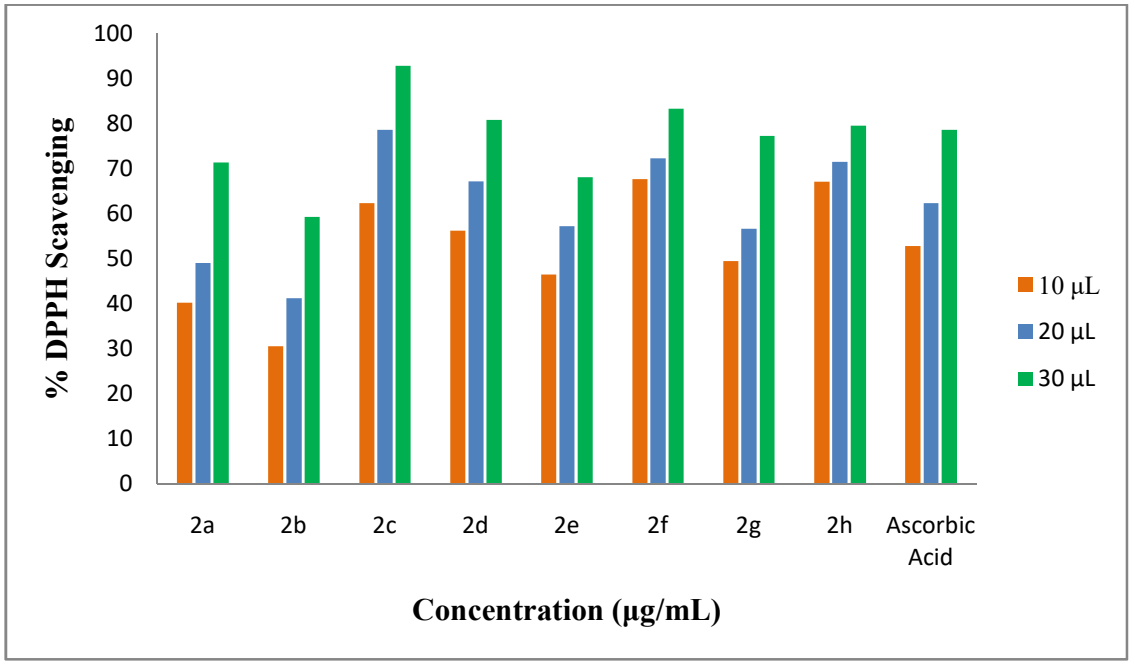

Fig.-4.24: Relative absorption of the compounds (**2a-h**) at different concentrations with respect to ascorbic acid.

4.3. Conclusion

This study focused on the synthesis 2-azidobenzothiazoles using a rapid protocol involving sodium nitrite and sodium azide, establishing a straightforward, effective, and high-yielding method. Motivated by the promising antibacterial activity of benzothiazole derivatives, we conducted *in vitro* antibacterial tests on the synthesized compounds. Results demonstrated that compound **2d** exhibited potent antibacterial activity against various strains, positioning it as a potential antimicrobial target for drug-resistant microorganisms. Our comprehensive *in vitro* study holds significant implications for addressing antibiotic resistance, shedding light on the potency of 2-azidobenzothiazoles against both Gram-(+) and Gram-(-) bacteria, including drug-resistant strains. Notably, our findings reveal the efficacy of lead compound **2d** in inhibiting and eradicating biofilms formed by diverse bacterial strains, addressing a major challenge in clinical settings. This discovery underscores the compound's selective cytotoxicity towards bacterial cells while sparing human cells, offering promising prospects for safe and effective antimicrobial treatments. The identification of compound **2d** as a potent lead highlights its potential for therapeutic applications, emphasizing the importance of ongoing drug discovery efforts in combating antibiotic resistance and biofilm-associated infections. Further optimization and

exploration of this lead compound, along with others in the series, may pave the way for the development of novel antibiotics or antimicrobial agents.

References

1. Singh, M.K., Tilak, R., Nath, G., Awasthi, S.K. and Agarwal, A., 2013. Design, synthesis and antimicrobial activity of novel benzothiazole analogs. *European journal of medicinal chemistry*, *63*, pp.635-644.
2. Nicholls, D., Gescher, A. and Griffin, R.J., 1991. Medicinal azides. Part 8. The in vitro metabolism of p-substituted phenyl azides. *Xenobiotica*, *21*(7), pp.935-943.
3. Zhilitskaya, L.V., Shainyan, B.A. and Yarosh, N.O., 2021. Modern approaches to the synthesis and transformations of practically valuable benzothiazole derivatives. *Molecules*, *26*(8), p.2190.
4. Lima, C.G., Ali, A., van Berkel, S.S., Westermann, B. and Paixão, M.W., 2015. Emerging approaches for the synthesis of triazoles: beyond metal-catalyzed and strain-promoted azide–alkyne cycloaddition. *Chemical Communications*, *51*(54), pp.10784-10796.
5. Ali, A., Corrêa, A.G., Alves, D., Zukerman-Schpector, J., Westermann, B., Ferreira, M.A. and Paixão, M.W., 2014. An efficient one-pot strategy for the highly regioselective metal-free synthesis of 1, 4-disubstituted-1, 2, 3-triazoles. *Chemical Communications*, *50*(80), pp.11926-11929.
6. de la Torre, A.F., Ali, A., Westermann, B., Schmeda-Hirschmann, G. and Pertino, M.W., 2018. An efficient cyclization of lapachol to new benzo [h] chromene hybrid compounds: a stepwise vs. one-pot esterification-click (CuAAC) study. *New Journal of Chemistry*, *42*(24), pp.19591-19599.
7. Faraji, L., Shahkarami, S., Nadri, H., Moradi, A., Saeedi, M., Foroumadi, A., Ramazani, A., Haririan, I., Ganjali, M.R., Shafiee, A. and Khoobi, M., 2017. Synthesis of novel benzimidazole and benzothiazole derivatives bearing a 1, 2, 3-triazole ring system and their acetylcholinesterase inhibitory activity. *Journal of Chemical Research*, *41*(1), pp.30-35.
8. Almehmadi, M.A., Aljuhani, A., Alraqa, S.Y., Ali, I., Rezki, N., Aouad, M.R. and Hagar, M., 2021. Design, synthesis, DNA binding, modeling, anticancer studies and DFT calculations of Schiff bases tethering benzothiazole-1, 2, 3-triazole conjugates. *Journal of Molecular Structure*, *1225*, p.129148.
9. Catalano, A., Carocci, A., Defrenza, I., Muraglia, M., Carrieri, A., Van Bambeke, F., Rosato, A., Corbo, F. and Franchini, C., 2013. 2-Aminobenzothiazole derivatives: search for new antifungal agents. *European Journal of Medicinal Chemistry*, *64*, pp.357-364.

10. Gonzalez, N., Sevillano, D., Alou, L., Cafini, F., Gimenez, M.J., Gomez-Lus, M.L., Prieto, J. and Aguilar, L., 2013. Influence of the MBC/MIC ratio on the antibacterial activity of vancomycin versus linezolid against methicillin-resistant Staphylococcus aureus isolates in a pharmacodynamic model simulating serum and soft tissue interstitial fluid concentrations reported in diabetic patients. *Journal of Antimicrobial Chemotherapy*, *68*(10), pp.2291-2295.

CHAPTER-5

Catalyst and Solvent-free, Ultrasound Promoted Rapid Protocol for the One-pot Synthesis of Benzothiazole Amide Derivatives: Synthesis, Crystallography, In Vitro, and In Silico Studies

5.1. Introduction

In the realm of organic chemistry, the relentless pursuit of more efficient and environmentally friendly synthetic methodologies has become a hallmark of contemporary research. Traditional chemical synthesis often involves the use of catalytic agents and organic solvents, which not only add complexity to the process but also contribute to environmental pollution and safety concerns. As a response to these challenges, the scientific community is in a perpetual quest to discover novel, more sustainable approaches to chemical synthesis. The elimination of catalysts and solvents from the synthetic process not only simplifies the procedure but also significantly reduces the environmental footprint of the entire synthesis. Traditional catalysts often require the use of toxic or hazardous substances, making their removal a paramount objective for chemists striving for greener chemistry. The absence of solvents is equally noteworthy, as it addresses concerns about solvent waste, which is a common byproduct in chemical processes. This solvent-free aspect not only aligns with the principles of green chemistry but also has the potential to mitigate the risks associated with solvent handling. Furthermore, the utilization of ultrasound as a promoter introduces a novel and efficient dimension to the synthesis. The application of ultrasound waves in chemical reactions, known as sonication, has garnered increasing attention for its ability to enhance reaction rates, increase yields, and promote more uniform mixing, all of which lead to expedited and improved synthetic outcomes. This innovation, in conjunction with the removal of catalysts and solvents, offers a powerful combination of benefits that paves the way for a more sustainable and effective methodology.

The most prevalent cause of death worldwide is tuberculosis (TB), which is brought on by the contagious mycobacteria MTB. It is a major public health problem worldwide, with an estimated 10 million people with emerging TB and 1.4 million dying from the disease in 2019. The WHO recommends a standard six-month treatment consisting of four drugs: isoniazid, ethambutol, rifampicin, and pyrazinamide. However, treatment may be extended if the patient has drug-resistant TB. In recent times, there have been notable advancements in TB treatment. Among these, the emergence of novel medications like bedaquiline and delamanid has proven to be particularly significant in managing drug-resistant forms of TB. There has also been progress in the development of shorter treatment regimens, which could help to improve treatment adherence and reduce the burden of TB. The appearance of drug-resistant variants such as MDR-TB (resistant to isoniazid and rifampicin), XDR-TB (resistant to all initial and certain second-

line drugs), and the recently recognized fully TDR-TB strains represents a substantial and alarming public health concern. Aside from the risk of TB becoming incurable, the expansion of MDR-TB might cause the cost of the present treatments to grow by 100 to 1400 times. Currently, MDR-TB causes 5.3% of TB cases. The WHO says that each year there are 490,000 new cases of MDR-TB, which result in over 110,000 fatalities. The majority of first-line TB medications were developed in the 1950s and 1960s. Before bedaquiline, which was introduced in the last of 2012 for treating MDR-TB, there had been a roughly 50-year gap in the availability of new drugs for TB treatment. The re-manufacturing and re-positioning of synthetic bioactive are required because of the aforementioned facts to create novel anti-TB medications [1-3].

It is widely known that the standard treatment for TB is lengthy and often problematic due to non-compliance and severe side effects. Therefore, it is urgent to focus on drug discovery efforts to find safe drug candidates that target new pathways and work quickly. These compounds should prevent resistance and effectively clear the TB-causing pathogen, reducing the chances of disease reactivation. In recent times, there has been a significant push to expand the limited range of anti-TB drugs with newer molecules. However, traditional target-based drug discovery approaches have faced challenges, as the identified inhibitors often lacked the desired growth-inhibiting effects. These failures could be attributed to issues with drug permeability, efflux, or vulnerability of the intended target, all of which present major obstacles to overcome. To overcome these challenges, researchers are revisiting cell-based phenotypic screens, which provide compounds with cellular potency, although they may sometimes exhibit toxicity-related characteristics. Therefore, when prioritizing compounds from this approach, it is crucial to implement a series of stringent assays to evaluate their properties thoroughly. This process ensures that only promising leads progress further, possessing positive attributes like *in vivo* efficacy and safety without undesirable features. Furthermore, it is essential to establish a connection with a specific target whose inhibition leads to the antimycobacterial effect. This knowledge enables the prediction of potential cross-reactivity with host-associated proteins, reducing the risk of adverse effects. Recently, a screening method of a fragment library containing a total of 1000 compounds led to the discovery of 10 benzothiazole derivatives. These compounds demonstrated a strong binding affinity to MTB transaminase enzyme. Surprisingly, only one of these derivatives exhibited inhibitory activity against the transaminase enzyme. Two fascinating issues are brought up by this discovery. To begin with, the active site of MTB DAPA

displays a notable attraction to the benzothiazole scaffold. Additionally, the enzyme's activity can be impeded through two distinct mechanisms: either by disrupting the interaction between Lys 283 and PLP or by establishing a direct interaction with hydrophobic residues located at the site [4-7].

This comprehensive study focuses on the green synthesis of benzothiazole amide derivatives and explores their potential as antimycobacterial agents. The research includes detailed analysis, such as crystallography, antioxidant activity, *in vitro* experiments, and *in silico* studies, to elucidate the compounds' structural properties, antimycobacterial effectiveness, and the underlying mechanisms. The findings from this study provide valuable insights into the development of benzothiazole amide derivatives as potential candidates for combating mycobacterial infections, contributing to the ongoing efforts to address tuberculosis and related diseases.

5.2. Results & Discussion

5.2.1. Chemistry

The primary aim of this investigation was to synthesize target benzothiazole amide derivatives (**Fig.-5.1**). The synthesis of these compounds involved a two-step reaction sequence, starting with the cyclocondensation of diethyl oxalate with 2-aminothiophenol followed by further processing under reflux conditions. The first step of the reaction involved the cyclocondensation of diethyl oxalate with 2-aminothiophenol. This condensation reaction is a crucial step for the formation of the benzothiazole ring system. The reaction was performed under reflux conditions, which allowed for a controlled and consistent heating of the reaction mixture. During the reflux process, the temperature decreased gradually from 147 to 93 °C for 4 hours. The gradual decrease in temperature was essential to facilitate the formation of the target product and avoid any undesirable side reactions or product degradation. The reflux conditions ensured that the reaction reached completion, leading to a high yield of the desired intermediate product, which is a key intermediate for the subsequent step.

The desired amides (**5a-l**) resulted from the reaction between ethyl benzothiazole-2-carboxylate **3** and various secondary amines (**4a-l**) (**Scheme-5.1**). To achieve this, the reactions were conducted under neat conditions using Ultrasonication as the energy source. The use of Ultrasonication as a method for promoting chemical reactions has gained popularity in recent years due to its efficiency and ability to accelerate reactions under ambient conditions. The

reaction was carried out for 1 hour, and after its completion (TLC), the reaction mixture was subjected to separation. The organic layer was then concentrated on a rotatory evaporator, resulting in the formation of a solid product. Further purification of the obtained solid was accomplished through recrystallization from ethanol. Remarkably, the entire reaction process proved to be highly efficient, as the desired products (**5a-l**) were obtained in good yields without the need for any additional purification steps. The use of Ultrasonication facilitated rapid and efficient reaction kinetics, leading to the successful formation of the target compounds. The significance of this study lies in the convenient and green synthesis of a diverse set of amides, which are valuable building blocks in organic synthesis and pharmaceutical research. The use of neat conditions, where no solvent was required, further highlights the eco-friendly nature of the process. It is important to emphasize that the reaction's selectivity and efficiency can be attributed to the unique reactivity of ethyl benzothiazole-2-carboxylate **3** and the diverse set of cyclic amines (**4a-l**) employed in the study. The ability to obtain a diverse array of amides with varying substituents opens up new possibilities for the exploration and development of novel compounds with potential biological properties.

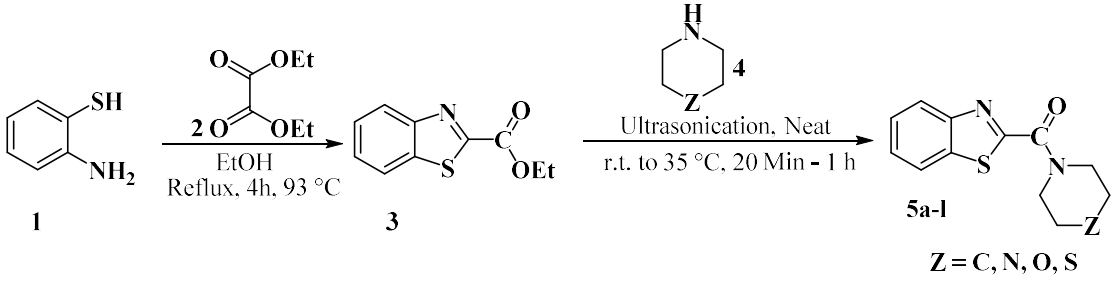

Scheme-5.1: Ultrasonic-assisted synthesis of benzothiazole amide derivatives.

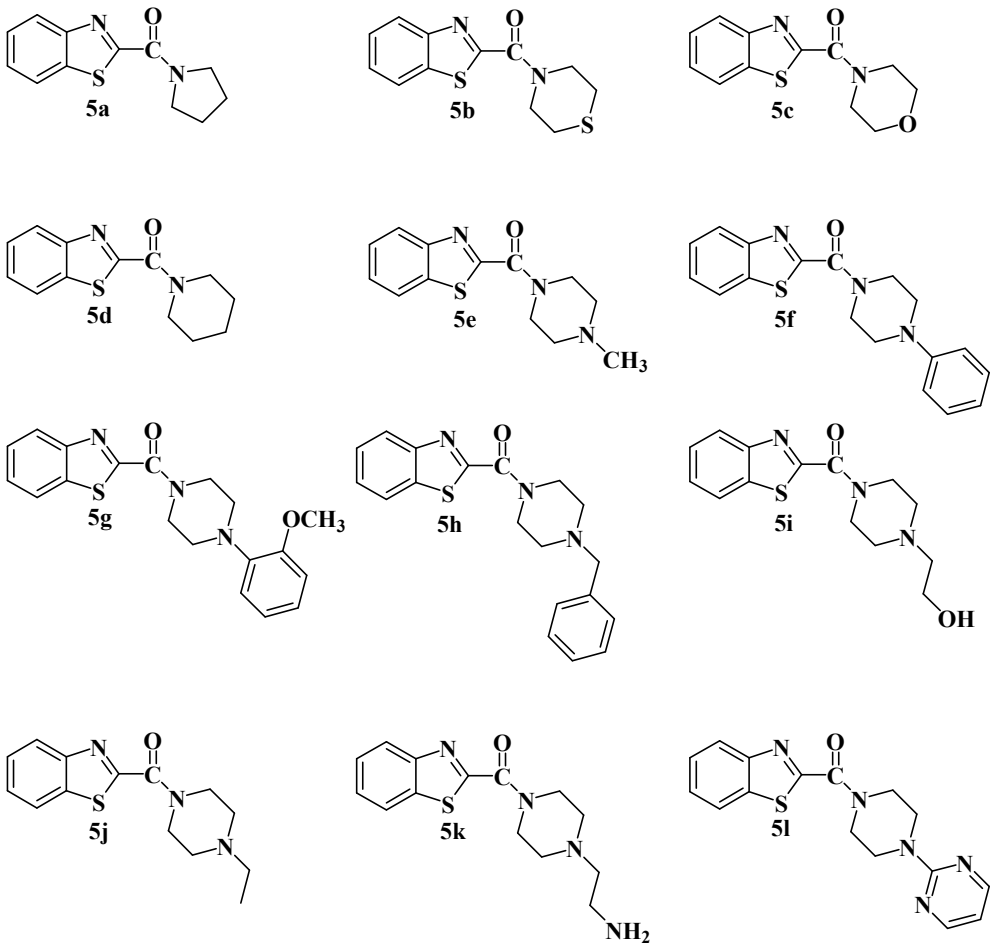

Fig.-5.1: Depiction of the benzothiazole scaffolds synthesized by green approach.

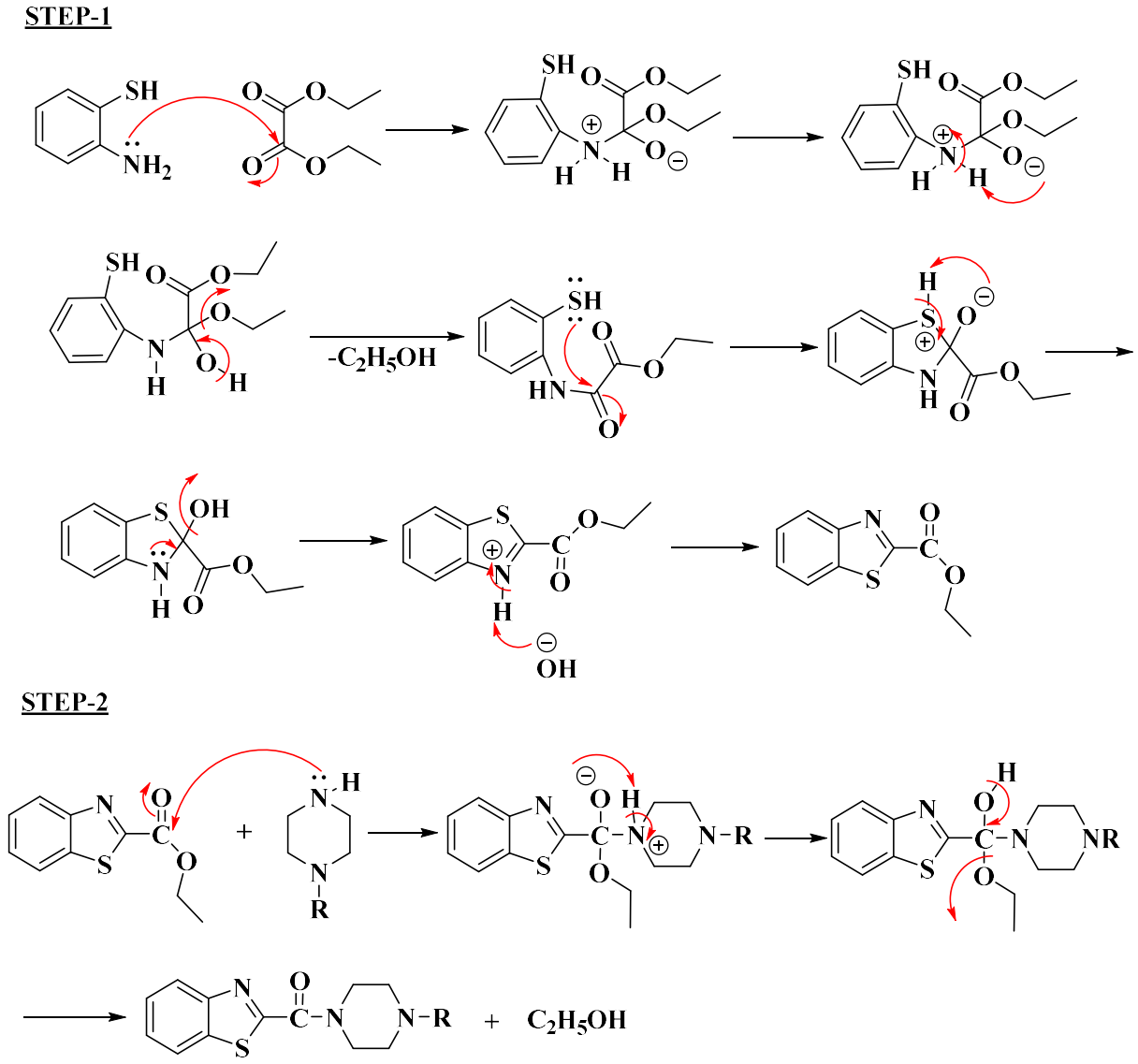

Fig.-5.2: Mechanistic pathway for the synthesis of benzothiazole amide derivatives (**5a-l**).

5.2.2. X-ray Crystallography

X-ray single-crystal diffraction stands as the most essential and accessible method for determining the structure of crystalline materials, which in turn plays a pivotal role in comprehending the intricate connections between a material's structure and its properties. This robust technique empowers researchers to visually examine the intricate structural details of compounds with a high degree of accuracy, providing invaluable insights into their makeup and arrangement. Following the examination of synthesized compounds using techniques such as FTIR, NMR, and HRMS, the structures of compounds **5a**, **5g**, and **5l** were subsequently verified

through the precise method of single crystal X-ray diffraction. This advanced analytical approach involves exposing these compounds to X-rays and scrutinizing the resulting diffraction patterns, allowing for an even more detailed and reliable assessment of their molecular structures. This comprehensive structural analysis enhances the credibility and understanding of these specific compounds in the context of the overall research.

Compound **5a** crystallizes in a monoclinic crystal system having space group Cc. Eight molecules are confined in the asymmetric unit. The structural framework gives rise to a 1-D network with the aid of hydrogen bonding interaction such as H02H---O6 having bond distance 2.664 Å, 127.03° and also due to H02H with H24A (2.161 Å, 140.36°). The edge-on interaction exhibited between S1 and H10B with a bond distance of 2.971Å, 146.90°gives rise to slipped 2D-arrangement of molecules placed anti-parallel with respect to each other. The overall 3D interpenetrating network is exhibited by the supramolecular interactions that exist between H03A with C020 having a bond distance of 2.786Å, 156.03°.

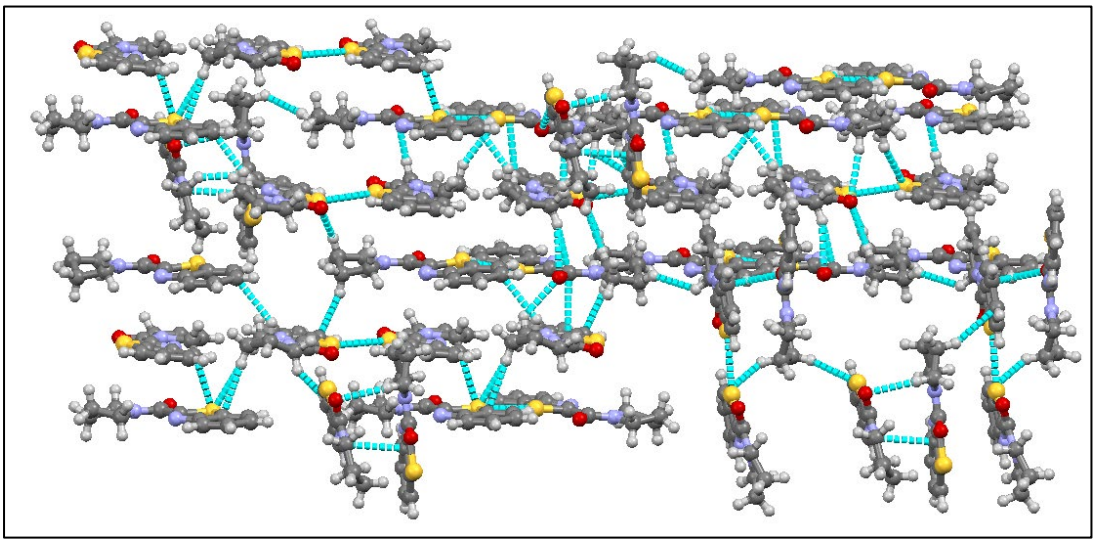

Fig.-5.3: Packing diagram of compound **5a**.

Compound **5g** crystallizes in an orthorhombic crystal system having space group $P2_1/c$. The molecule attains non-planarity due to aryl rings present in the molecule. The ID pattern is exhibited due to edge-on interaction through a bifurcated hydrogen bond between H17 with N3 and C13 having a bond distance of 2.725Å, 166.37°, and 2.725Å, 136.67°. Further, the molecules grow through the edge on interactions between S1 with H12B having a bond length of 2.86.6Å, 167.95° as well as S1 with O1 2.702Å, 145.47°. The 2D arrangement is observed

between C4 with H10, further, the slipped 3D arrangement is formed between C4 with H11B having bond distance of 3.125Å, 137.03°give rise to a zig-zag pattern.

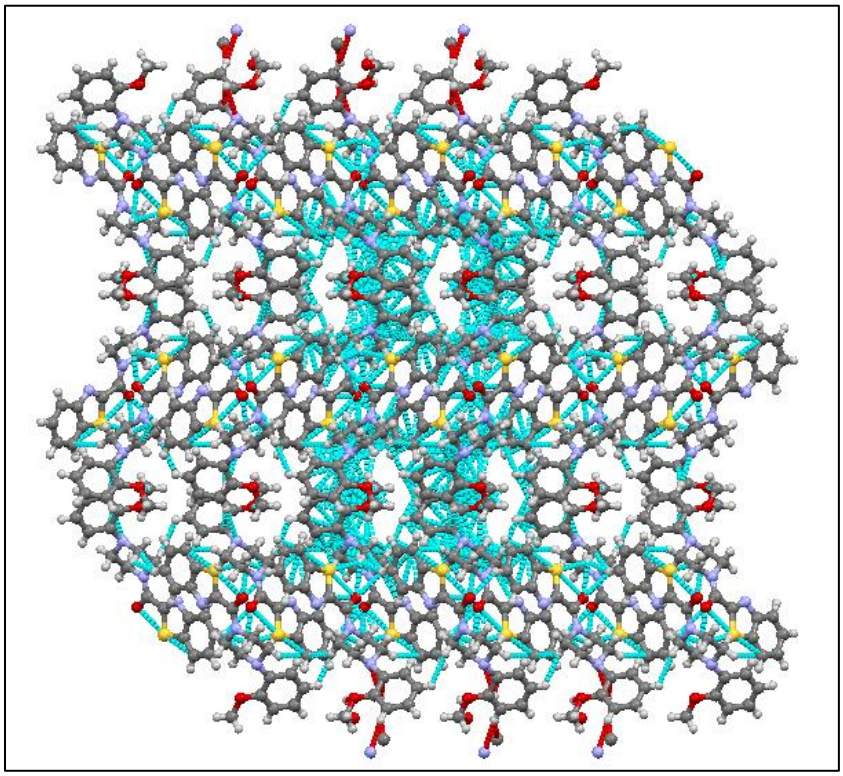

Fig.-5.4: Packing diagram of compound **5g**.

Compound **5l** crystallizes in a monoclinic crystal system having space group $P2_1/n$. Four molecules are confined in the asymmetric unit. The molecules are connected through various supramolecular interactions along the x-axis. The molecules attain slipped arrangement via S1-O1 interaction with a bond length of 3.2054 Å, 122.52° along a 1-dimensional arrangement. Further weak intermolecular interactions such as H2 with C14 covering a distance of 2.76 Å from hydrogen-bonded tapes give rise to chains along the X-axis. Further, the pi-pi interactions because of C11-C7, and N5-H7B having bond lengths of 3.38 Å and 2.54 Å give rise to the layered structures.

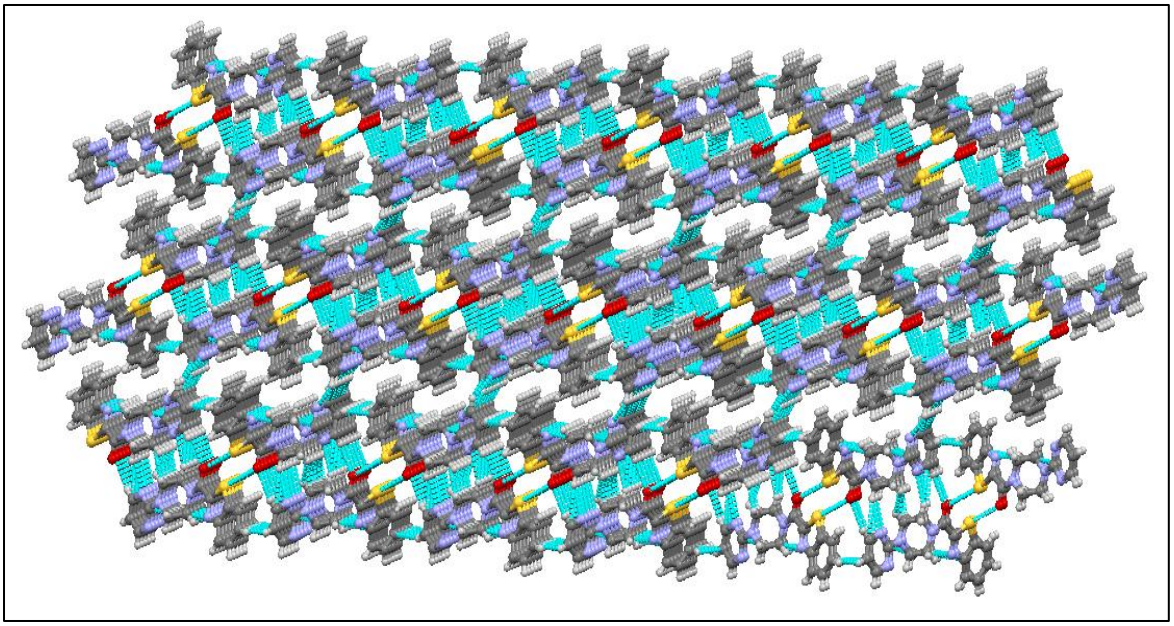

Fig.-5.5: Packing diagram of compound **5l**.

Table 5.1: Crystallographic data and structure refinement details for compounds **5a**, **5g**, and **5l**.

Parameters	**5a**	**5g**	**5l**
Empirical formula	$C_{12}H_{12}N_2OS$	$C_{19}H_{19}N_3O_2S$	$C_{16}H_{15}N_5OS$
Formula weight	232.30	353.43	325.39
Temperature	100(2) K	100(2) K	100(2) K
Wavelength	0.71073Å	0.71073 Å	0.71073Å
Crystal system	Monoclinic	Orthorhombic	Monoclinic
Space group	Cc	$P2_1/c$	$P2_1/n$
Unit cell dimensions	a = 21.214(3) Å b = 21.364(3) Å c = 19.348(3) Å α = 90° β = 102.062(5)° γ = 90°	a = 8.3843(5) Å b = 14.6864(8) Å c = 27.2708(16) Å α = 90° β = 90° γ = 90°	a = 12.7301(9) Å b = 5.0302(3) Å c = 23.7063(17) Å α = 90° β = 102.775(2)° γ = 90°
Volume	8575(2) $Å^3$	358.0(3) $Å^3$	1480.45(17)$Å^3$
Z	32	4	4

Density (calculated)	1.439g/cm^3	1.398g/cm^3	1.460 g/cm^3
Absorption coefficient	0.280 mm^{-1}	0.211 mm^{-1}	0.231 mm^{-1}
F (000)	3904	1488	680
Theta range for data collection	1.906° to 33.152°	2.038° to 33.193°	2.026° to 33.078°
Index ranges	-27<=h<=32, -32<=k<=32, -29<=l<=29	-11<=h<=12, -16<=k<=22, -41<=l<=41	-17<=h<=18, -7<=k<=7, -35<=l<=36
Reflection collected	118960	84696	23818
independent reflections	27102 [R(int) = 0.0379]	12046 [R(int) = 0.0622]	5142 [R(int) = 0.0421]
Data/restraints /parameters	27102 / 3 / 1153	12046 / 0 / 453	5142/0/208
Goodness-of-fit on F^2	1.037	1.026	1.041
Final R indices [I>2σ(I)]	R1 = 0.0380, wR2 = 0.0915	R1 = 0.0359, wR2 = 0.0963	R1 = 0.0451, wR2 = 0.0954
R indices (all data)	R1 = 0.0441, wR2 = 0.0938	R1 = 0.0426, wR2 = 0.1000	R1 = 0.0816, wR2 = 0.1125
Largest diff. peak and hole	0.905 and -0.779 eÅ^{-3}	0.512 and -0.407eÅ^{-3}	0.347 and -0.469 eÅ^{-3}

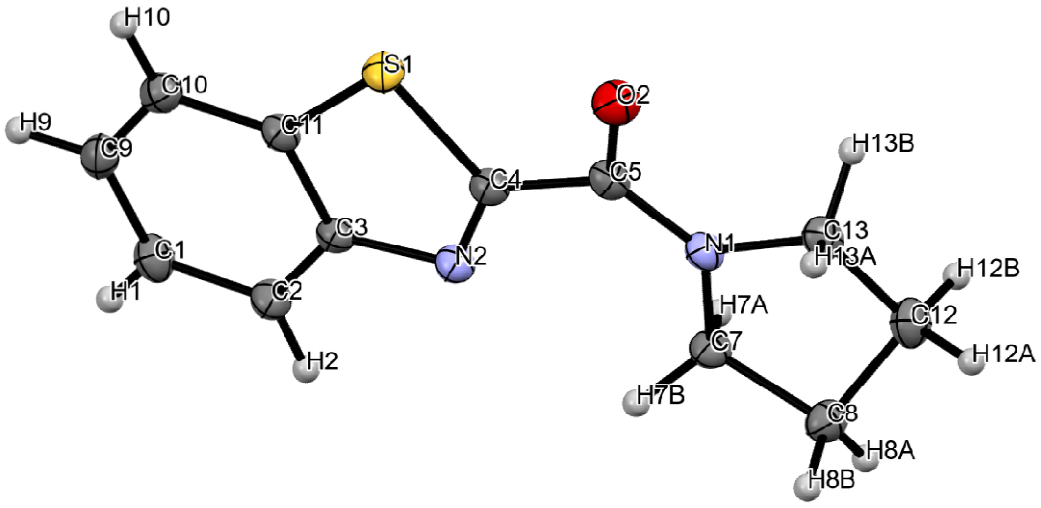

Fig.-5.6: ORTEP view of compound **5a**.

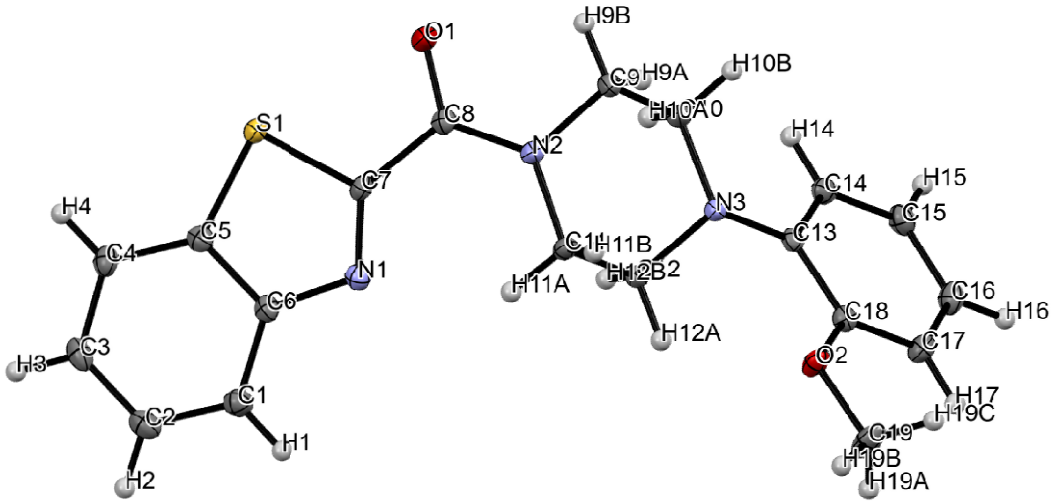

Fig.-5.7: ORTEP view of compound **5g**.

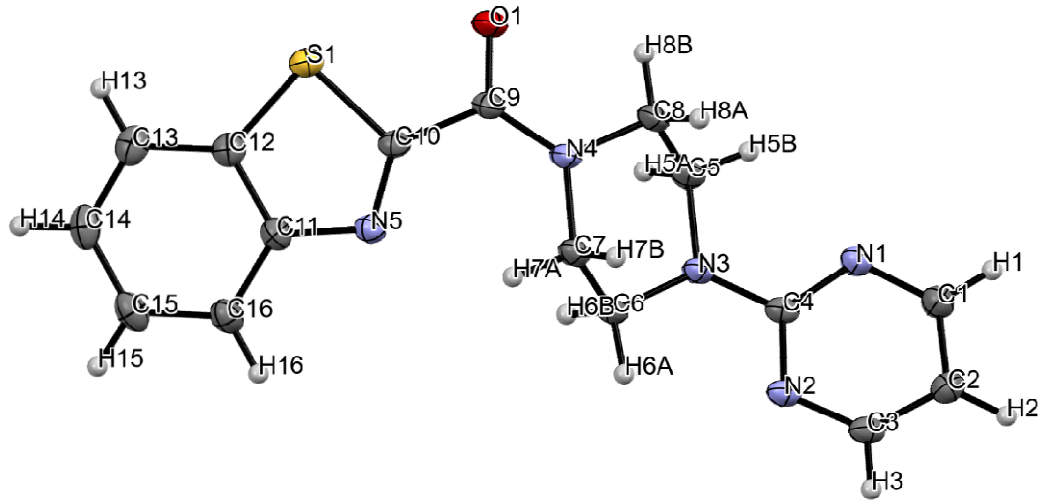

Fig.-5.8: ORTEP view of compound **5l**.

5.2.3. *In vitro* Antibacterial Activity

All the synthesized compounds (**5a-l**) were tested against Gram (+) bacteria *S. aureus* and Gram (-) bacteria *E. coli*. The MIC of each synthetic compound was ascertained for each bacterial strain using the broth dilution assay. Notably, our findings revealed that none of the compounds displayed any discernible antibacterial activity against either *S. aureus* or *E. coli*.

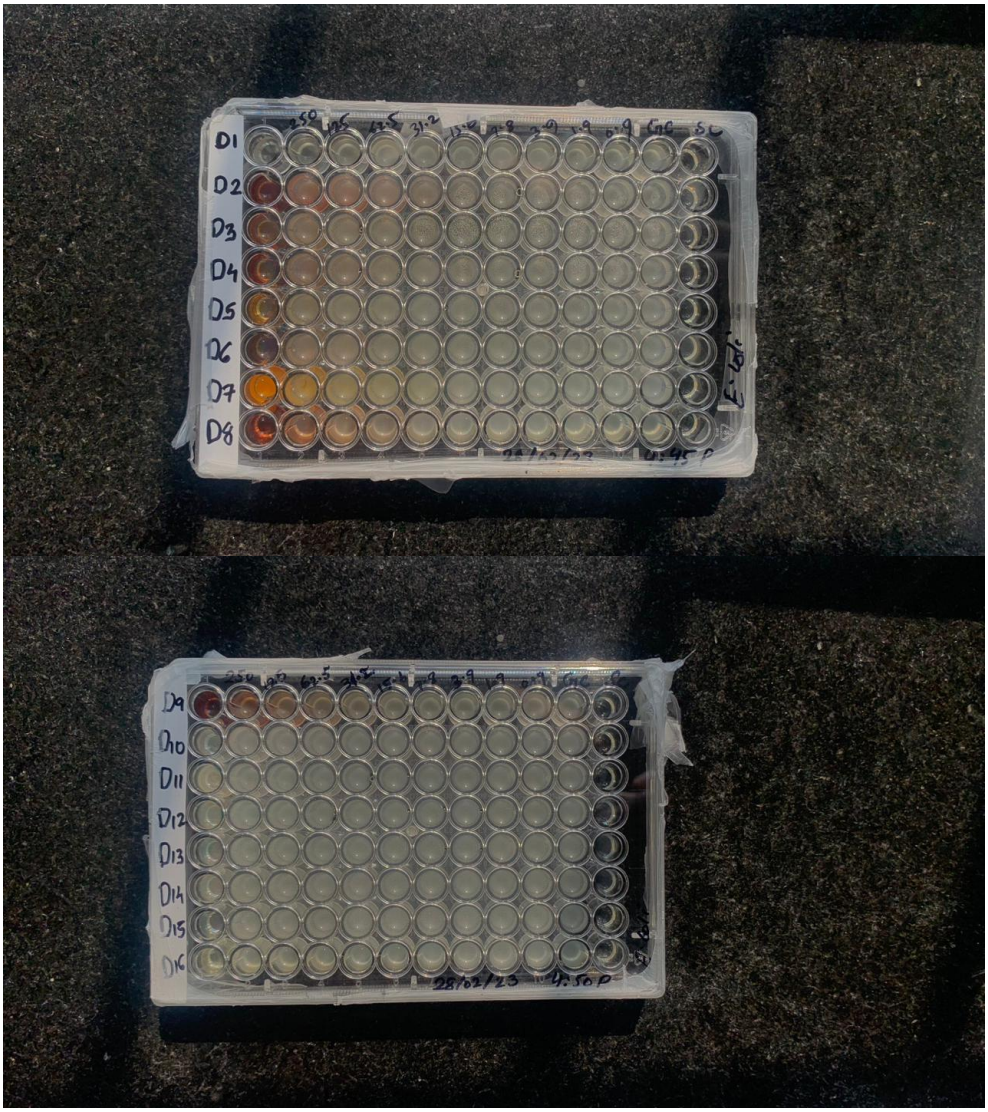
D1
D2
D3
D4
D5
D6
D7
D8
D9
D10
D11
D12
D13
D14
D15
D16
28/02/23

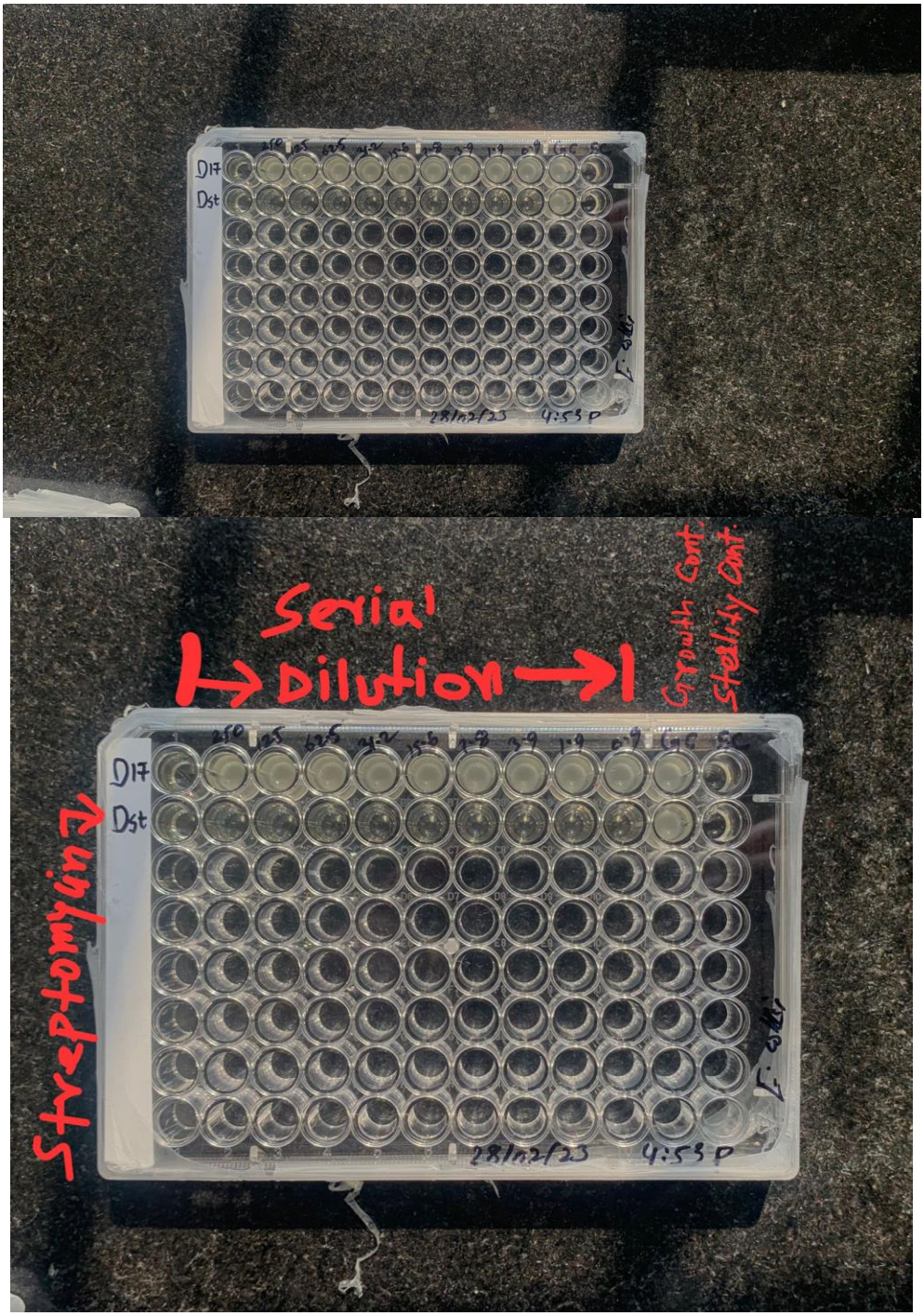

Fig.-5.9: MIC of compounds (**5a-l**) and STR against Gram (-) bacteria *E. coli.*

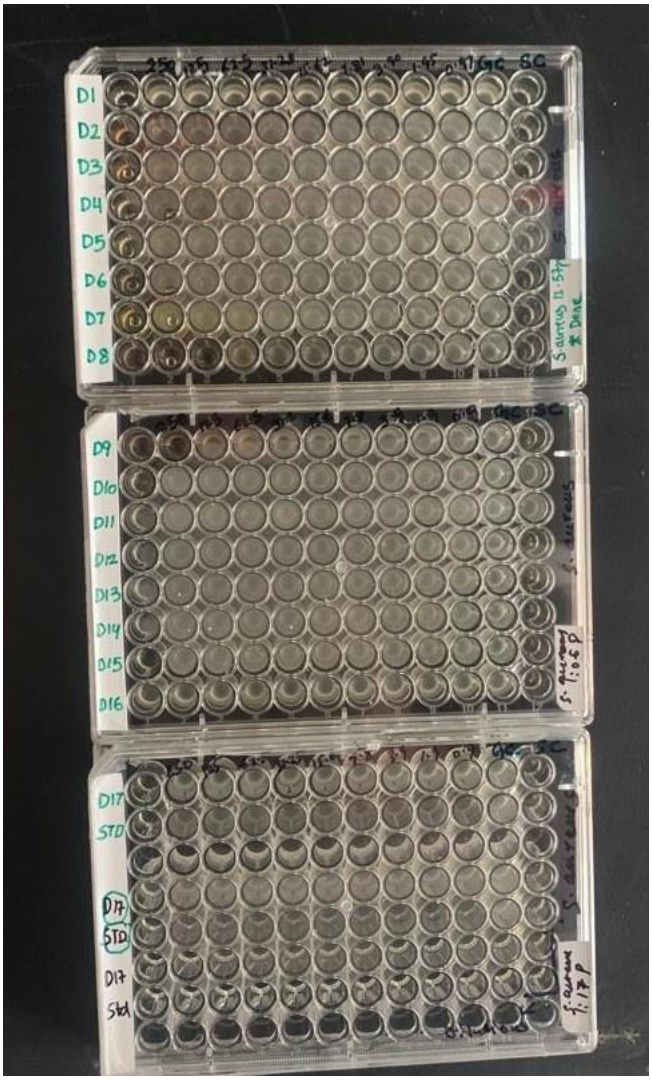

Fig.-5.10: MIC of compounds (**5a-l**) and STR against Gram (+) bacteria *S. aureus.*

5.2.4. Antituberculosis Activity

The effectiveness of benzothiazole-2-carboxamides in combating tuberculosis was assessed against *Mycobacterium tuberculosis* at various concentrations, including 100, 50, 25, 12.5, 6.25, 3.12, 1.6, and 0.8 μg/mL. The outcomes are detailed in **Table 5.2**. Ligands **5a** and **5l** demonstrated anti-TB activity at 1.6 μg/mL, while **5f**, **5g**, and **5e** exhibited activity at 3.12, 6.2, and 12.5 μg/mL, respectively. These activities closely resemble those of the second-line standard medications Isoniazid, Ethambutol, and Pyrazinamide, which exhibit MIC values of 1.6 and 3.125 μg/mL. In contrast, ligands **5b**, **5d**, **5i**, **5j**, **5k**, **5c**, and **5h** displayed significantly lower anti-TB activity, with concentrations of 25 and 50 μg/mL. These ligands effectively suppressed the growth of *Mycobacterium tuberculosis* at the specified concentrations. Notably, their

effectiveness in inhibiting TB bacteria at a concentration of 50 µg/mL was less pronounced compared to other compounds. It was observed that compounds containing a fused ring with a nitrogen hetero-atom (**5a**, **5e**, **5f**, **5g**, and **5l**) exhibited strong anti-TB activity. Conversely, compounds with a ring containing oxygen and sulphur heteroatoms (**5b** and **5c**) displayed reduced anti-TB activity, underscoring the significant influence of structural composition on their effectiveness against TB. Furthermore, the presence of a methylene group at the *N*-atom of the heterocyclic ring in **5h** did not enhance its anti-TB activity, suggesting that this specific modification did not contribute significantly to their effectiveness against *Mycobacterium tuberculosis*.

Table 5.2: Anti-tuberculosis activity of the synthesized compounds **(5a-l).**

S. No.	Compound	100 µg/mL	50 µg/mL	25 µg/mL	12.5 µg/mL	6.2 µg/mL	3.12 µg/mL	1.6 µg/mL	0.8 µg/mL
01	**5a**	S	S	S	S	S	S	S	R
02	**5b**	S	S	S	R	R	R	R	R
03	**5c**	S	S	R	R	R	R	R	R
04	**5d**	S	S	S	R	R	R	R	R
05	**5e**	S	S	S	S	R	R	R	R
06	**5f**	S	S	S	S	S	S	R	R
07	**5g**	S	S	S	S	S	R	R	R
08	**5h**	S	S	R	R	R	R	R	R
09	**5i**	S	S	S	R	R	R	R	R
10	**5j**	S	S	S	R	R	R	R	R
11	**5k**	S	S	S	R	R	R	R	R
12	**5l**	S	S	S	S	S	S	S	R

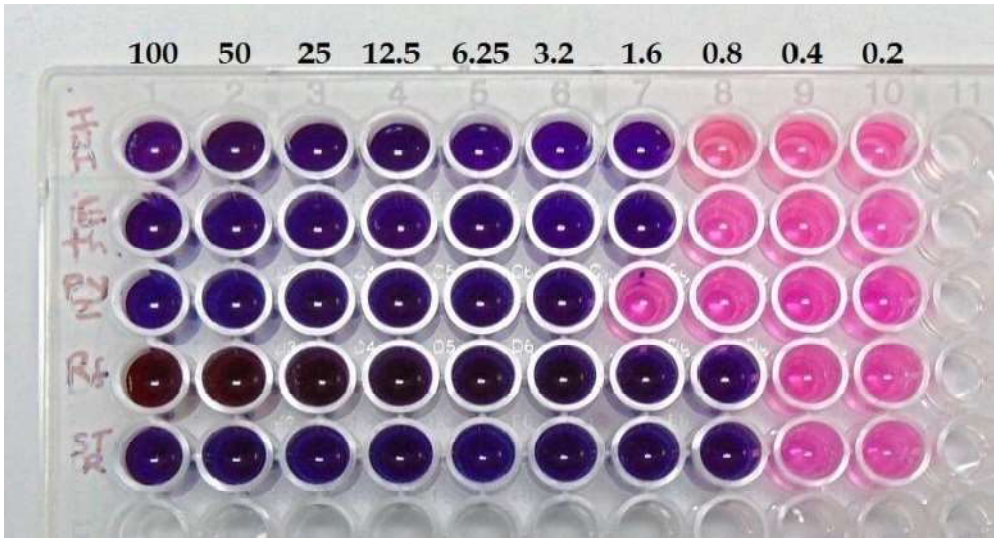

Fig.-5.11: MIC of control drugs: Isoniazid, Ethambutol, Pyrazinamide, Rifampicin, and Streptomycin.

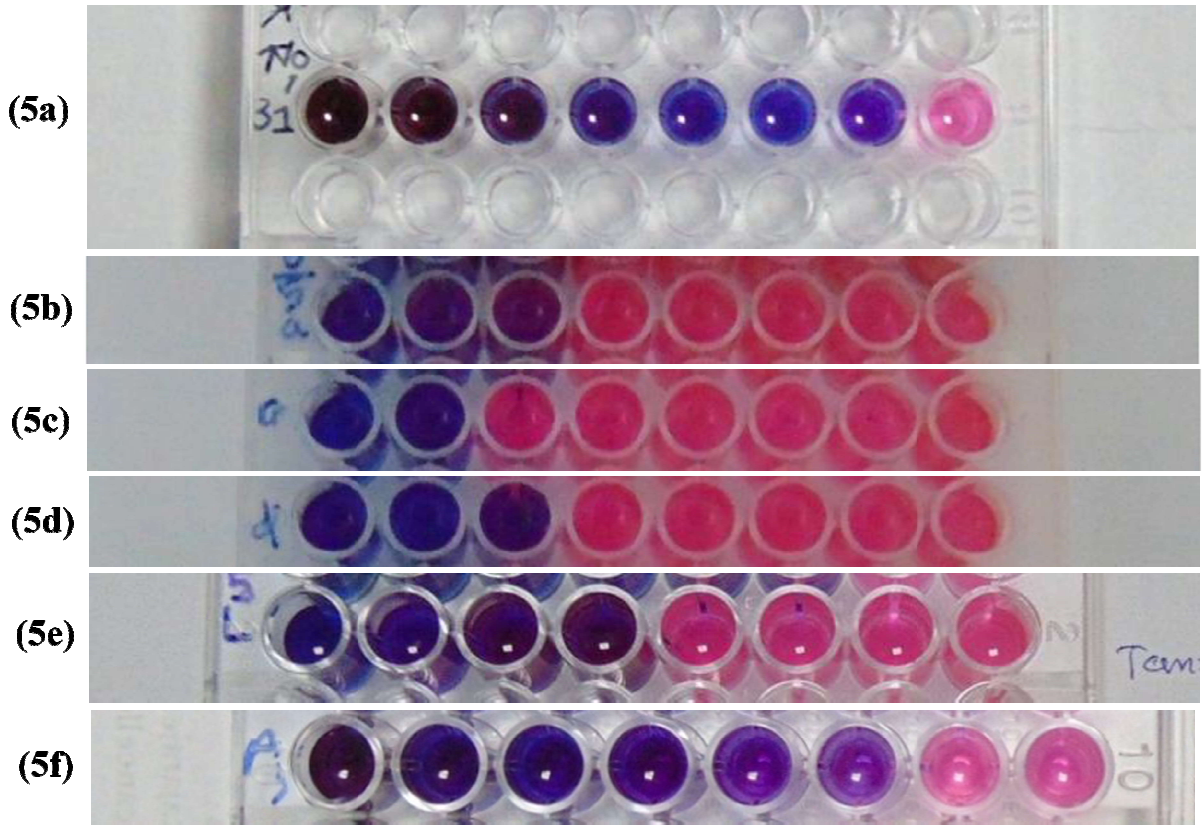

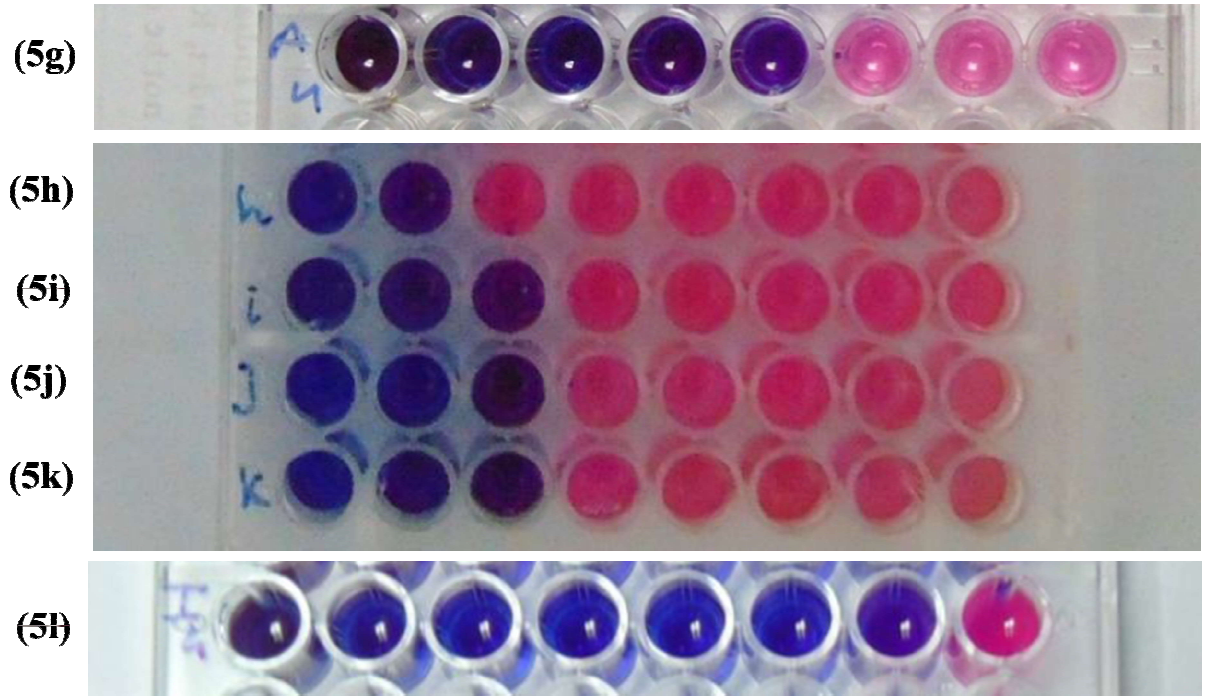

Fig.-5.12: MIC of the synthesized compounds against *Mycobacterium tuberculosis*.

5.2.5. Molecular Docking

Molecular docking was carried out for compounds (**5a-l**) against DprE1, Polyketide synthase (Pks13), and Protein kinase B (PknB) to evaluate their therapeutic potential as antimycobacterial chemotypes. Molecular docking has a key role in ligand-protein and protein-protein interaction to see for best pose and binding sites of receptors to which a ligand molecule binds and is extensively used in modern drug discovery [8]. Results shown in **Table 5.3** show that all the drug candidates have a strong binding affinity equal to or greater than -6.1kcal/mol. The binding affinities of drug candidates with DprE1 show that **5a, 5f, 5g, 5h, and 5l** has promising binding affinity score of -8.0, -8.9, -9.1, -8.9, and -8.8 kcal/mol respectively. The results of molecular docking with Polyketide synthase (Pks13) show that six of the selected drug candidates have a strong binding affinity of equal or greater than -7.0 kcal/mol including **5b, 5e**, which has a binding affinity of -7.1, -7.3 kcal/mol, **5f** and **5g** has 8.8 and 8.9 kcal/mol, while **5h** and **5l** has a strongest binding affinity of -8.4 kcal/mol respectively. The results for another targeted protein i.e. Protein kinase B (PknB), in **Table 5.3** shows that five drug candidates have a binding affinity

of equal or greater than -7.0 kcal/mol, including **5d**, **5f**, **5g, 5h, and 5l** having binding affinity of -7.0, -7.6, -7.3, -7.8, and -7.4 kcal/mol respectively.

It is evident from **Figs.-5.13-5.17** and **Table 5.4** that amino acid residues of DprE1 protein GLY124, ALA53, ALA64, ALA128, MET74, ILE184, ALA94, THR122 with **5a,** TYR314, VAL365, LYS134, HIS132, ALA417, GLN336 with **5f,** TYR60, TYR314, ALA417, ARG58, ILA131, VAL121, LYS367, VAL365, LYS314, HIS132 are interacting with **5g,** VAL365, ARG58, ALA417, LYS367, HIS132 and TYR60 of DprE1 protein interacts with **5h** while ARG58, HIS132, and VAL365 interact with **5l**. **Figs.-5.18-5.22** and **Table 5.4** shows that amino acid residues of Protein kinase B (PknB) i.e. GLU208, TYR182, VAL104, PRO141, LYS140, ALA142, ARG101 interacts with **5a,** ASP156, MET145, VAL95, LEU17, ALA38, VAL25, MET25, MET155 interacts with **5f,** while GLY20, SER23, VAL25, ASP138, ASP156, MET92, LYS40, ILE159, MET155 interact with **5g**, MET55, LEU17, ILE159, VAL25, LYS40, ASP138, GLY20, ASP156 interact with **5h** compound while MET145, LEU17 interacts with **5l**.

Figs.-5.23-5.27 and **Table 5.4** shows that amino acid residues of Polyketide synthase (Pks13) i.e. PHE1670, PHE1585, MET1669, TYR1582 interact with **5a,** VAL1515, ILE1544, ILE1507, ILE1648, ALA1541, ALA1511, ALA1541 interact with **5f and** TYR1637, PHE1670, ALA1667, ILE1643, TYR1674, HIS1699, TYR1663 interacts with **5g**, PHE1585, 1670, VAL1611 interact with **5h** while HIS1699, ALA1477, PRO1476, TRP1532 interacts with **5l**. The overall results based on molecular docking and experimental work show that five major compounds i.e. **5a, 5f**, **5g**, **5h**, **5l** have a promising potential as antituberculosis.

Table 5.3: Molecular docking of synthetic drug candidates with selected target proteins of *Mycobacterium tuberculosis.*

Compounds	4FEH (DprE1) Binding Affinity (kcal/mol)	5V3Y(Polyketide synthase (Pks13)) Binding Affinity (kcal/mol)	5u94(Protein kinase B (PknB)) Binding Affinity (kcal/mol)
5a	-8.0	-6.9	-6.4
5b	-7.2	-7.1	-6.8
5c	-7.3	-6.9	-6.8
5d	-7.7	-6.8	-7.0
5e	-7.4	-7.3	-6.5

5f	-8.9	-8.8	-7.6
5g	-9.1	-8.9	-7.3
5h	-8.9	-8.4	-7.8
5i	-7.8	-7.3	-6.9
5j	-7.6	-7.0	-6.1
5k	-7.8	-7.9	-6.7
5l	-8.8	-8.4	-7.4

Table 5.4: Amino acid residues of receptor proteins interaction with ligand compounds having strong binding affinity.

Compounds	**Amino Acid Residues Interaction (DpER1)**	**Amino Acid Residues Interaction (5V3Y)**	**Amino Acid Residues Interaction (5U49)**
5a	Hydrogen Bond: THR122	Other Bond: PHE1670, PHE1585, MET1669, TYR1582	Hydrogen Bond: GLU208, ARG101
	Other Bond: GLY124, ALA53, ALA64, ALA128, MET74, ILE184,ALA94		Other Bond: TYR182, VAL104, PRO141, LYS140, ALA142,ARG101
5f	Hydrogen Bond: GLN336	Hydrogen Bond: ALA1541	Other Bond: ASP156, MET145, VAL95, LEU17, ALA38, VAL25, MET25, MET155
	Other Bond: TYR314, VAL365, LYS134, HIS132, ALA417	Other Bond: VAL1515, ILE1544, ILE1507, ILE1648, ALA1541, ALA1511, ALA1541	
5g	Hydrogen Bond: HIS132	Other Bond: TYR1637, PHE1670, ALA1667, ILE1643, TYR1674, HIS1699, TYR1663	Hydrogen Bond: ASP156(2), GLY20, SER23
	Other Bond: TYR60, TYR314, ALA417, ARG58, ILA131, VAL121, LYS367, VAL365, LYS314, HIS132		Other Bond: VAL25, ASP138, ASP156, MET92, LYS40, ILE159, MET155

5h	Hydrogen Bond: TYR60	Other Bond: PHE1585, 1670, VAL1611	Hydrogen Bond: GLY20, ASP156
	Other Bond: VAL365, ARG58, ALA417, LYS367, HIS132		Other Bond: MET55, LEU17, ILE159, VAL25,LYS40, ASP138,156
5i	Hydrogen Bond: SER228, HIS132, GLY133	Hydrogen Bond: TRP1579, GLN1633, TYR1586	Hydrogen Bond: GLY20, SER23
	Other Bond: ILE131, PRO116	Other Bond: PHE1670, TYR1637, SER1636	Other Bond: MET92, 145,155, VA25, 95, LEU17, ALA38
5j	Other Bond: VAL121, CYS129, ARG58, ILE131, ALA417, ALA64	Other Bond: TYR1637, TRP1579, VAL1611, PHE1670, 1585	Hydrogen Bond: GLY20, ASP156
			Other Bond: ASP138,156
5k	Hydrogen Bond:TYR314, SER228, HIS132, GLY117	Hydrogen Bond: GLY1478, HIS1632, 1699,1664, SER1533, ALA1477	Hydrogen Bond: SER23
	Other Bond: ILE131, PRO116	Other Bond:HIS1699,1664 TYR1674,1663 SER1533, ILE1643, ALA1667	Other Bond: MET92, 145,155, VAL25, 95, LEU17, ALA38,
5l	Hydrogen Bond: ARG58, HIS132	Hydrogen Bond: HIS1699, ALA1477	Other Bond: MET145, LEU17
	Other Bond: VAL365	Other Bond: PRO1476, TRP1532	

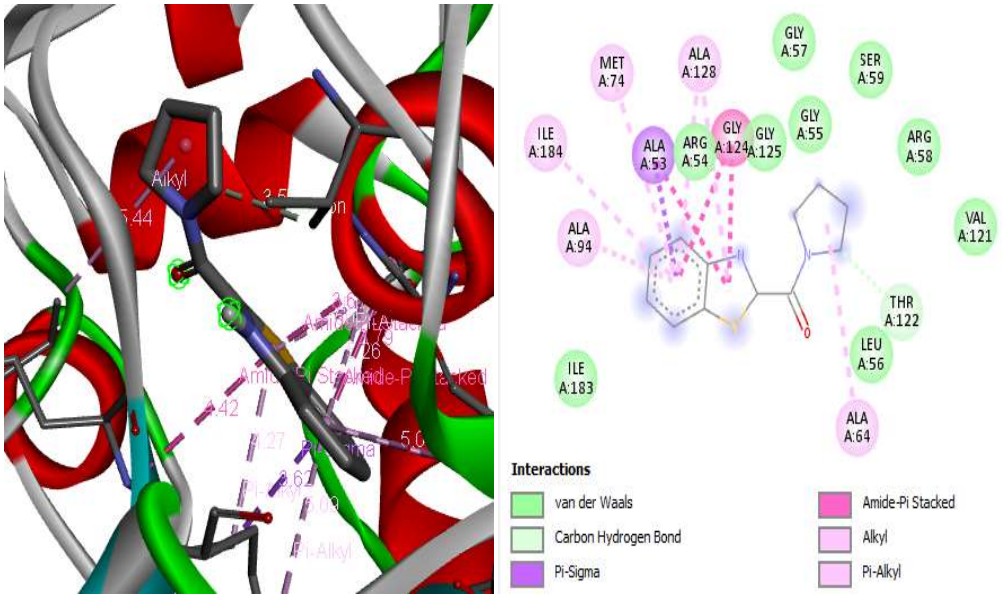

Fig.-5.13: The interaction between compound **5a** and the DprE1 receptor protein, represented in both 3D and 2D forms.

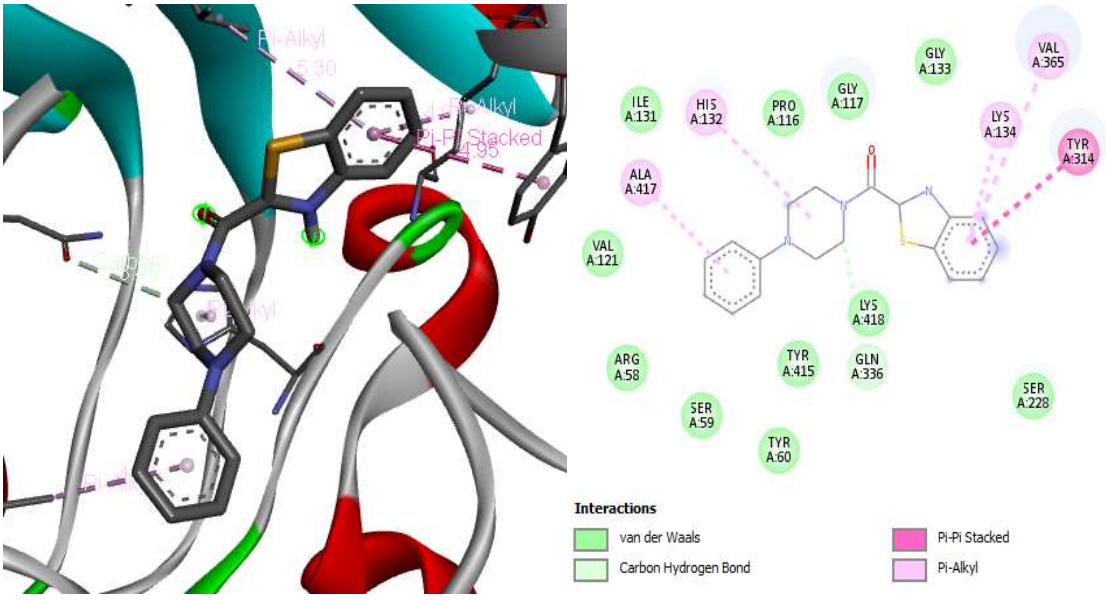

Fig.-5.14: The interaction between compound **5f** and the DprE1 receptor protein, represented in both 3D and 2D forms.

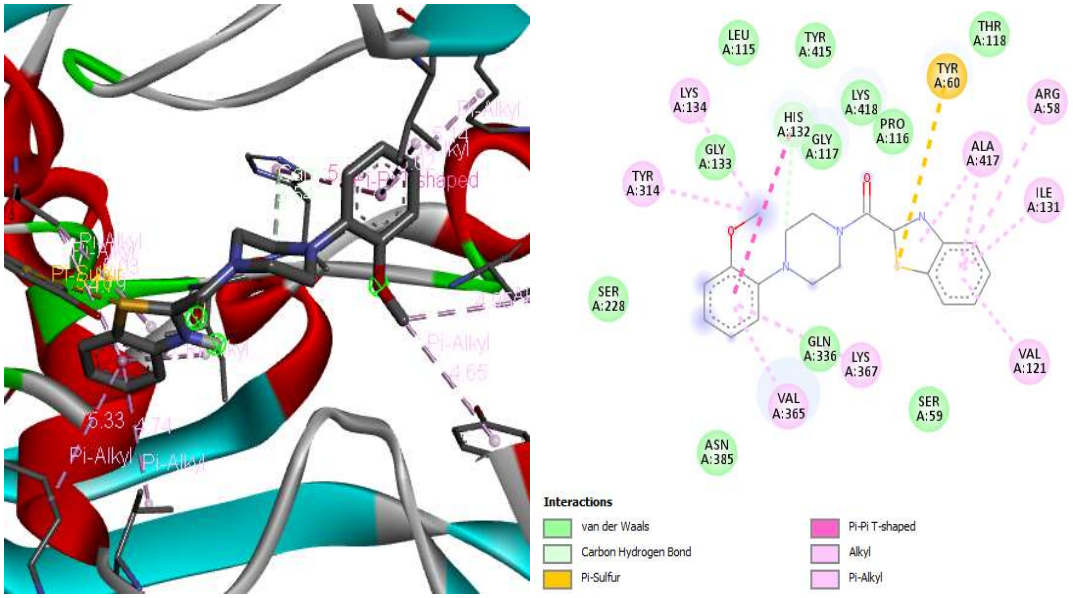

Fig.-5.15: The interaction between compound **5g** and the DprE1 receptor protein, represented in both 3D and 2D forms.

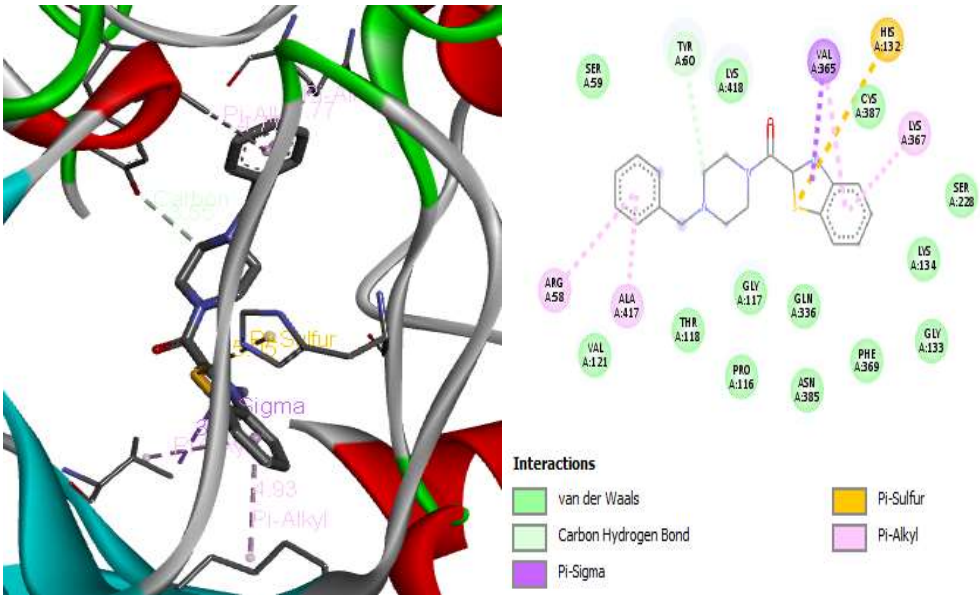

Fig.-5.16: The interaction between compound **5h** and the DprE1 receptor protein, represented in both 3D and 2D forms.

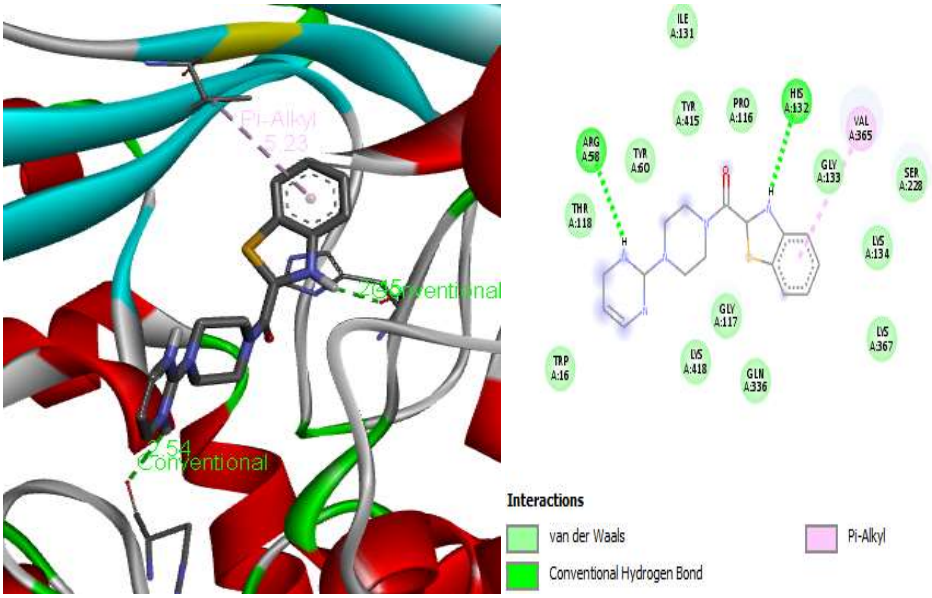

Fig.-5.17: The interaction between compound **5l** and the DprE1 receptor protein, represented in both 3D and 2D forms.

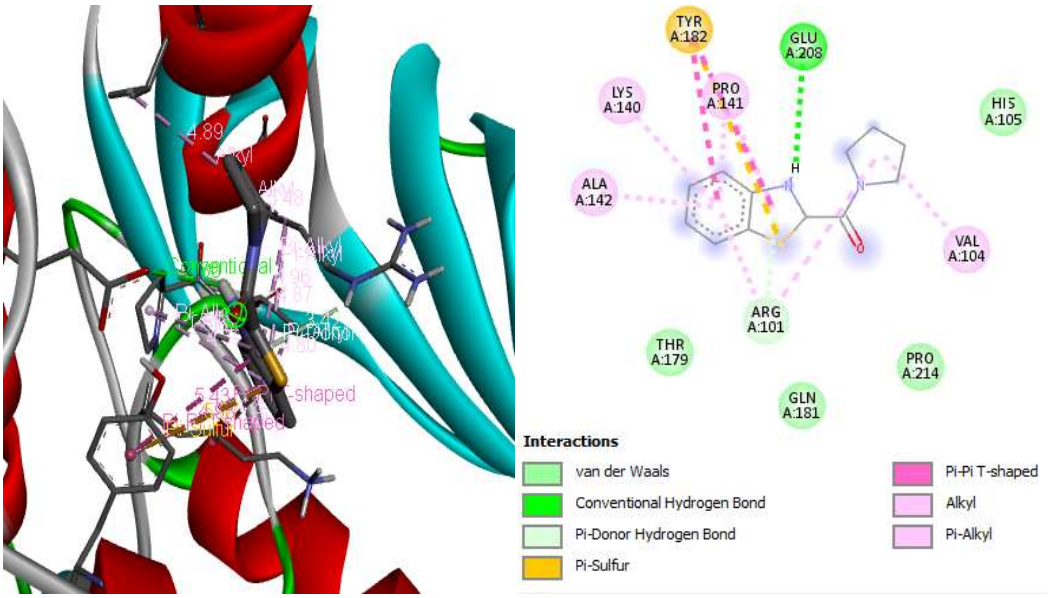

Fig.-5.18: The interaction between compound **5a** and the Protein kinase B (PknB) receptor protein, represented in both 3D and 2D forms.

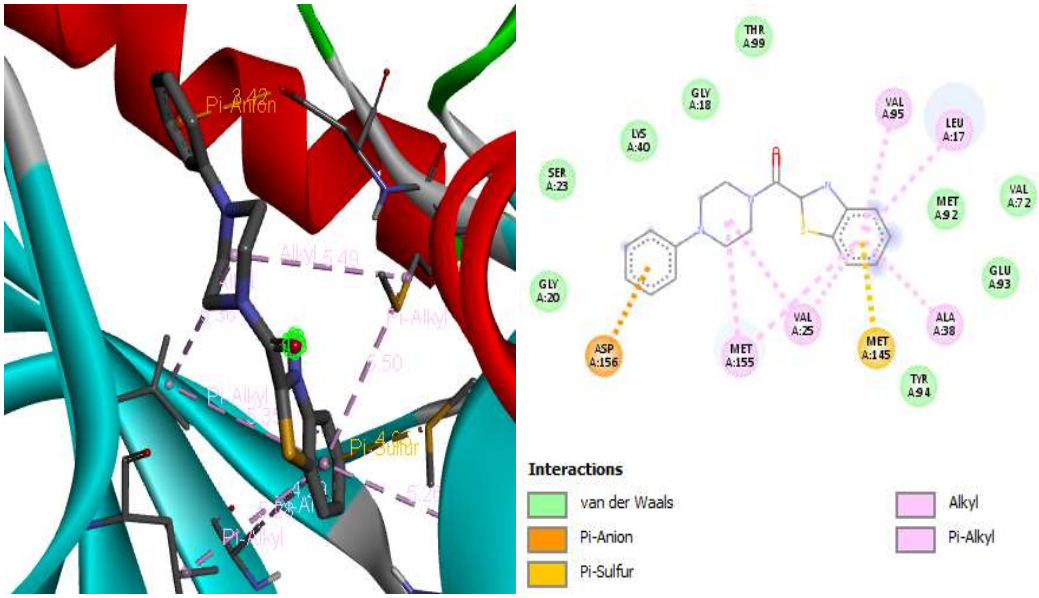

Fig.-5.19: The interaction between compound **5f** and the Protein kinase B (PknB) receptor protein, represented in both 3D and 2D forms.

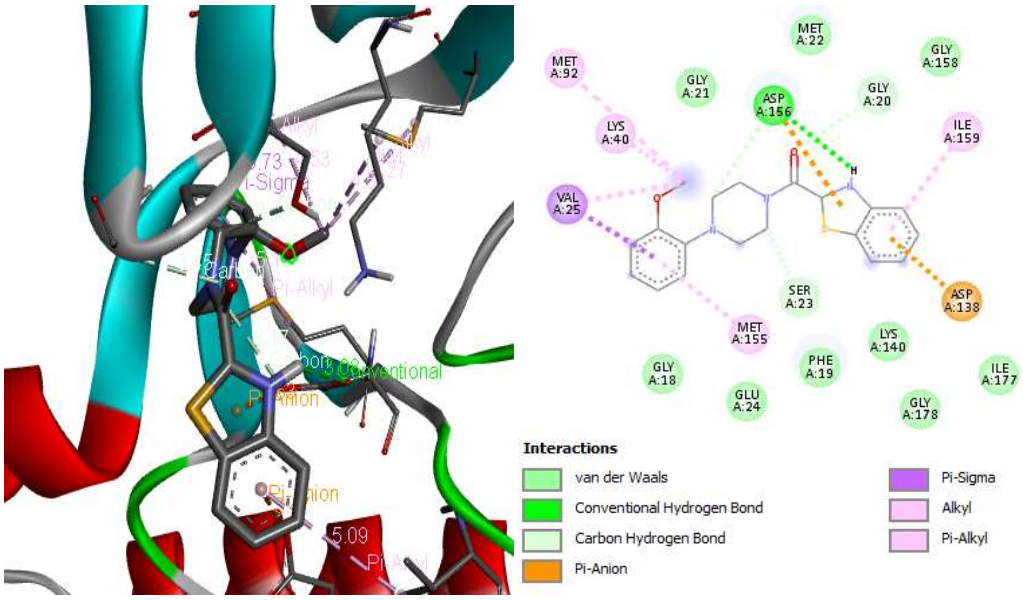

Fig.-5.20: The interaction between compound **5g** and the Protein kinase B (PknB) receptor protein, represented in both 3D and 2D forms.

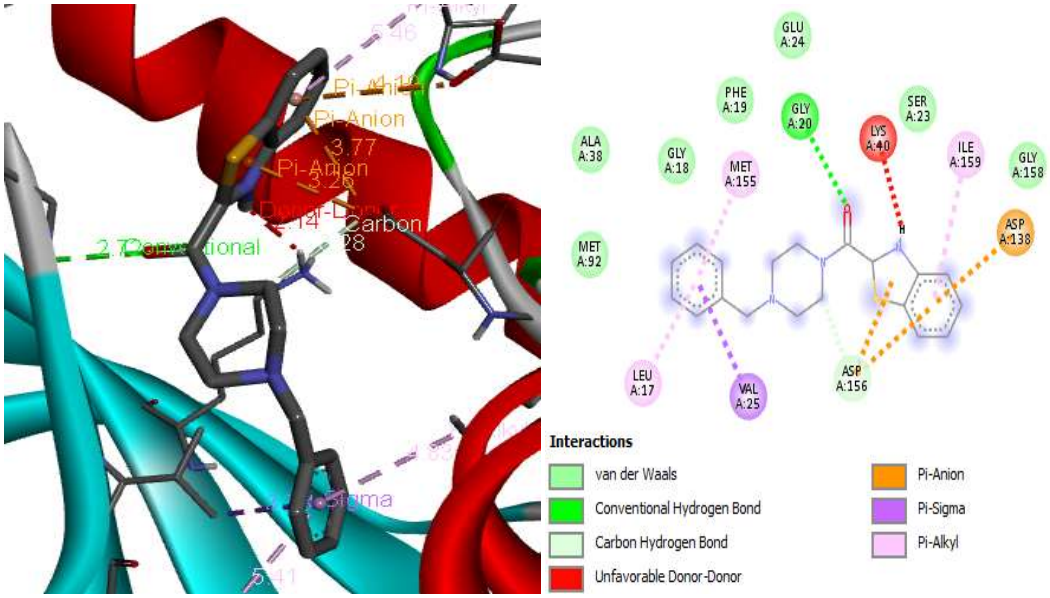

Fig.-5.21: The interaction between compound **5h** and the *Protein kinase B* (PknB) receptor protein, represented in both 3D and 2D forms.

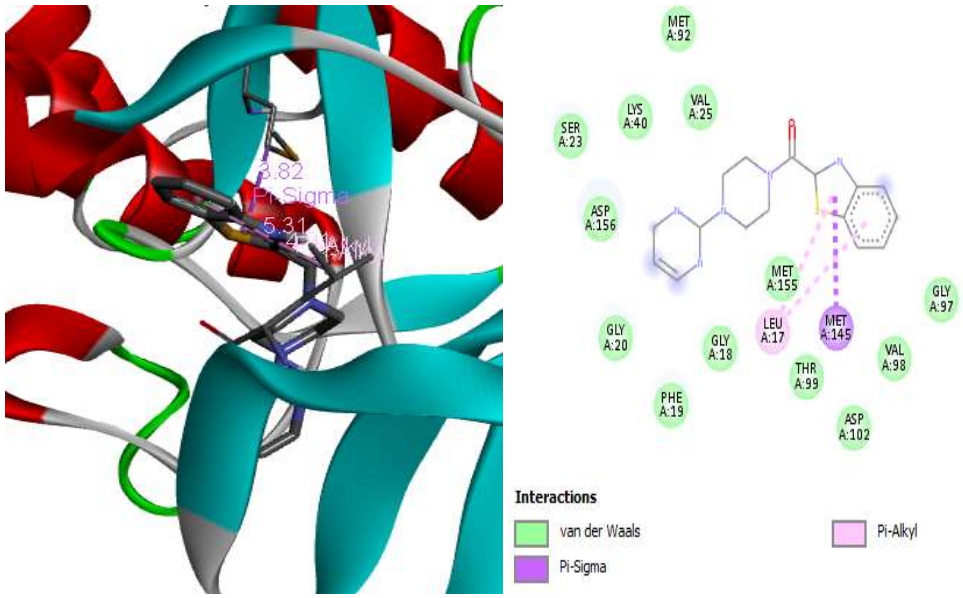

Fig.-5.22: The interaction between compound **5l** and the Protein kinase B (PknB) receptor protein, represented in both 3D and 2D forms.

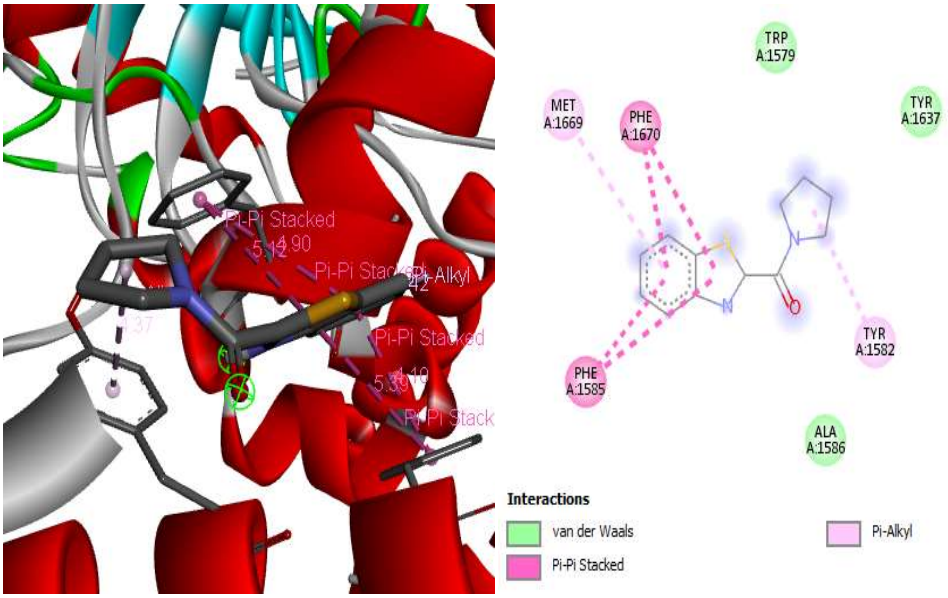

Fig.-5.23: The interaction between compound **5a** and the Polyketide synthase (Pks13) receptor protein, represented in both 3D and 2D forms.

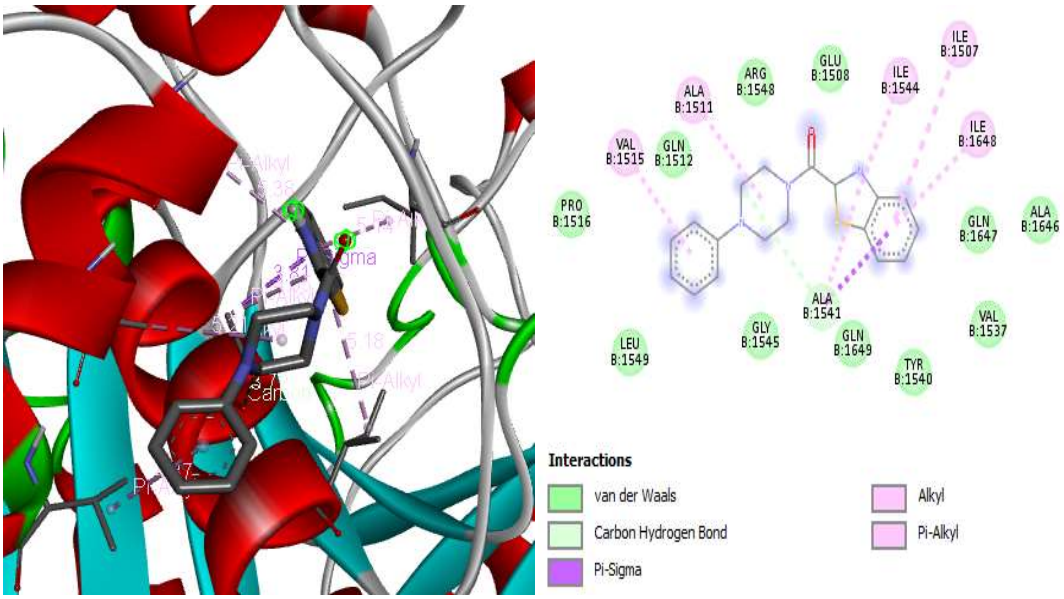

Fig.-5.24: The interaction between compound **5f** and the Polyketide synthase (Pks13) receptor protein, represented in both 3D and 2D forms.

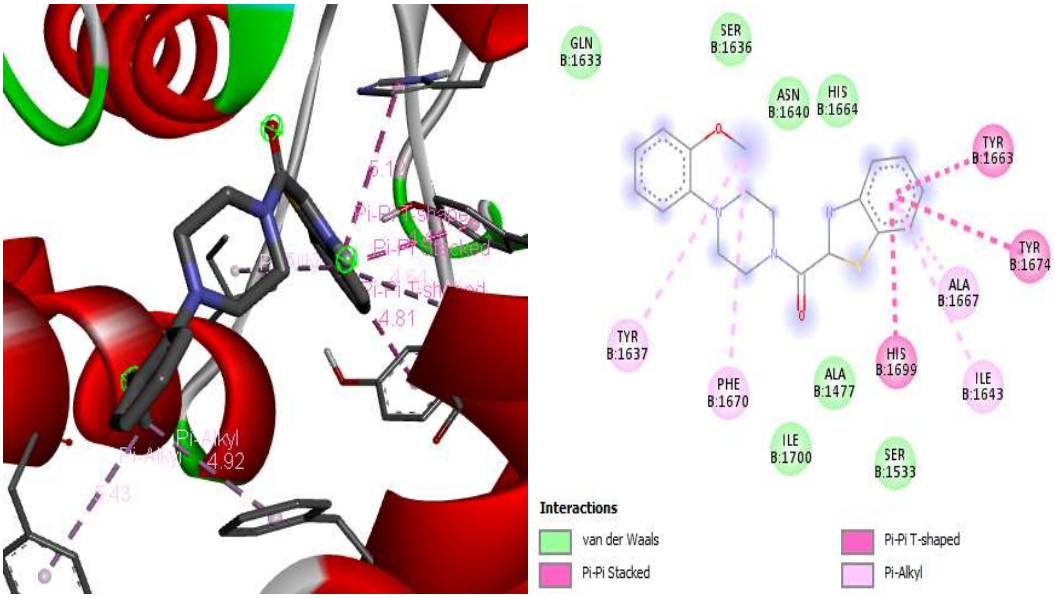

Fig.-5.25: The interaction between compound **5g** and the Polyketide synthase (Pks13) receptor protein, represented in both 3D and 2D forms.

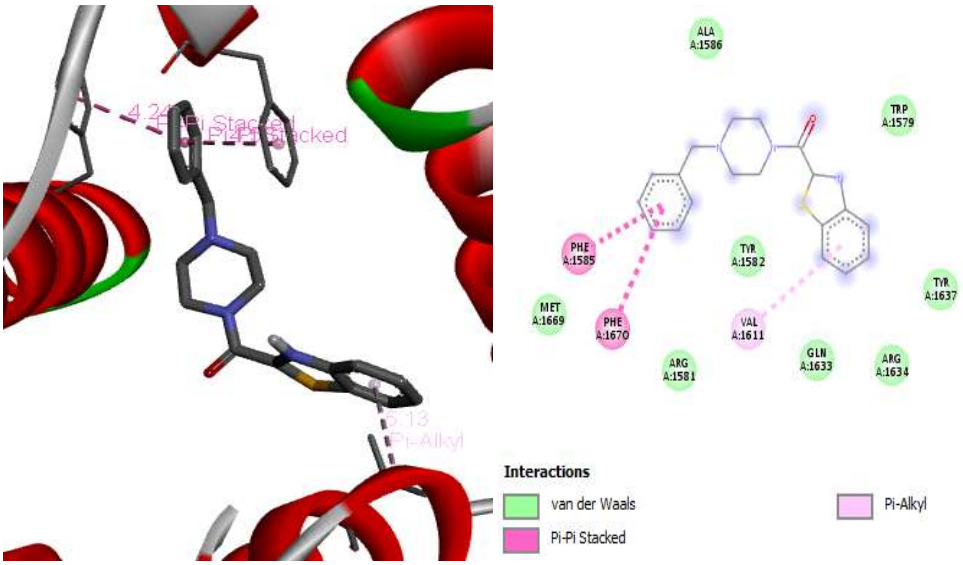

Fig.-5.26: The interaction between compound **5h** and the Polyketide synthase (Pks13) receptor protein, represented in both 3D and 2D forms.

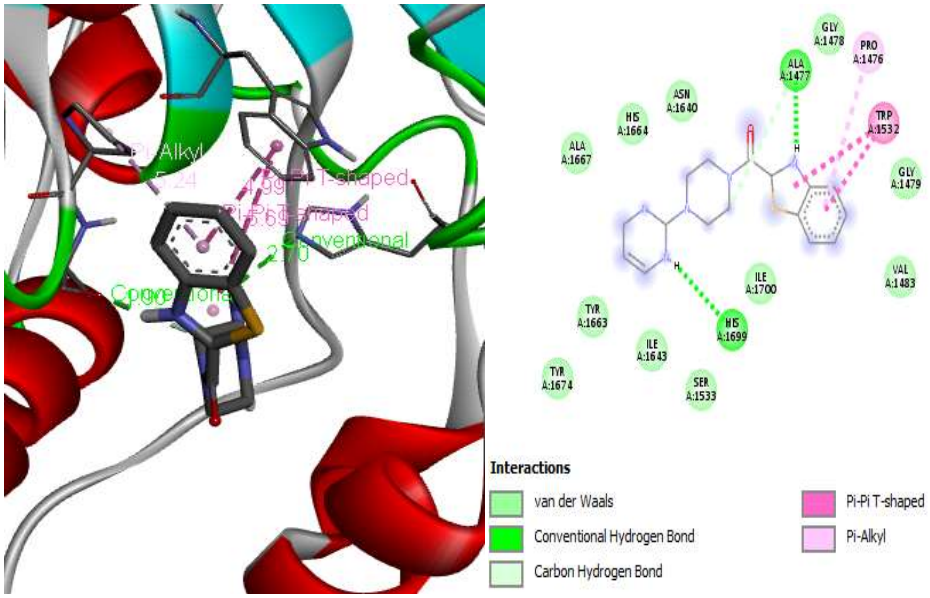

Fig.-5.27: The interaction between compound **5l** and the Polyketide synthase (Pks13) receptor protein, represented in both 3D and 2D forms.

5.2.6. ADME Analysis of Synthetic Drug Candidates

To discover various factors, including physical properties, lipophilicity, Lipinski, and solubility of bioactive components, an ADME study was conducted using swissADME [9]. As many medication candidates fail a clinical trial, ADME is crucial to the development of any therapy. Candidates taking an orally administered medication may not have more than two violations [10]. Lipinski rule of five (≤5 H-bond donor, ≤10 H-bond acceptor, Molecular weight ≤500Da, Molar Refractivity 40-130 and ≤5logP)[8] was followed for selected compounds to analyze whether these may act as drugs or not. The drug compounds with high binding affinity score was further analyzed for ADME and the results in **Table 5.5** demonstrate that all selected compounds pass the Lipinski rule of five and has no violation showed by any of our drug candidate. Gastrointestinal absorption shows that all compounds are highly soluble. For water solubility Logs values ranges from -10 to 0 which indicates different category of solubility i.e. -10, -6, -4, -2 and 0 for insoluble, poorly soluble, soluble, very soluble and highly soluble respectively [6]. Table 2 shows that all compounds are in the range of high solubility and no one is insoluble in the selected candidates.

Table 5.5: ADME analysis of synthetic drug candidates.

Properties	Features	5a	5f	5g	5h	5l
Physiochemical Properties	MW(g/mol)	232.3	323.41	353.44	337.44	325.39
	H.B Donor	0	0	0	0	0
	H.B Acceptor	2	2	3	3	4
	MR	68.93	100.79	107.28	105.04	96.38
	Arom. Heavy Atom	9	15	15	15	15
	Rotatable Bonds	2	3	4	4	3
	TPSA	61.44	64.68	73.91	64.68	90.46
Lipophilicity	LogP(SILICOS-IT)	3.33	3.55	3.57	3.92	2.44
Water Solubility	Logsw(SILICOS-IT)	-3.37	-5.19	-5.3	-5.59	-4.45
Pharmacokinetics	GI Absorption	High	High	High	High	High
Drug-likeness	Lipinski	0	0	0	0	0

5.2.7. Toxicity Analysis

The toxicity of each ingredient, including its potential for hepatotoxicity, carcinogenicity, mutagenicity, Immunogenicity, and cytotoxicity was examined using the online Protox-II server. Toxicology prediction is now a crucial phase in drug designs to ascertain the negative effects of a specific molecule on humans, plants, and the ecosystem. Traditional methods require several animal studies to determine the toxicity of the substances, which is a notorious process for its high cost and time-consuming but also raises significant ethical issues. Comparatively, toxicity prediction provided by computational tools requires less time, costs less money, produces results more often, and minimizes the need for biological experimentation. It is shown in (**Table 5.6)** that all our drug candidates are non-toxic and inactive while considering hepatotoxicity, carcinogenicity, mutagenicity, Immunogenicity, and cytotoxicity. Using admetSAR, selected chemicals' toxicity was validated and double-checked which shows all selected compounds to be

AMES Non-toxic, and Non-Carcinogenic (**Table 5.7**). Additionally, it was found that all drug compounds exhibited low inhibition activity against the human hERG and demonstrated only mild acute toxicity in rats, with a median LD_{50} of 2.401 mol/kg. As per the anticipated acute oral toxicity classification, all of our chosen drug candidates fall into the 'class III' category. The substances of class III have LD_{50} values of less than 5000mg/kg and were regarded as appropriate from a druggable perspective.

Table 5.6: Toxicity analysis of synthetic drug candidates using Protx-II online web server.

Compounds	Hepatotoxicity	Carcinogenicity	Immunotoxicity	Mutagenicity	Cytotoxicity
5a	Inactive	Inactive	Inactive	Inactive	Inactive
5f	Inactive	Inactive	Inactive	Inactive	Inactive
5g	Inactive	Inactive	Inactive	Inactive	Inactive
5h	Inactive	Inactive	Inactive	Inactive	Inactive
5l	Inactive	Inactive	Inactive	Inactive	Inactive

Table 5.7: Toxicity analysis of synthetic drug candidates using AdmetSAR online web server.

Compounds	heggr	AMES Toxicity	Carcinogenicity	Acute Oral Toxicity	Carcinogenicity (Three Class)	Rat Acute Toxicity(LD_{50}, mol/kg)
5a	Weak	Non	Non	III	Non-Required	2.1701
5f	Weak	Non	Non	III	Non-Required	2.4025
5g	Weak	Non	Non	III	Non-Required	2.6884
5h	Weak	Non	Non	III	Non-Required	2.2592
5l	Weak	Non	Non	III	Non-Required	2.4892

5.2.8. Molecular Dynamics Simulation

The MDS study is crucial for a clear estimation of the stability and conformational variations occurring within the targeted protein-ligand complex. Therefore, we have successfully conducted simulation investigations on the protein-docked complexes involving compounds **5a**, **5f**, and **5g** for 100 ns. **Fig.-5.28** depicts the analysis results from the MD trajectory of a protein-ligand complex of all the three above-mentioned compounds. The RMSD plot (**Fig.-5.28A**) for all the complexes was found to be swapping between 0.2-0.36 nm without any major hike, indicating that all the complexes were stable throughout the MD simulation. Additionally, the protein's radius of gyration was computed to determine its compactness within the MD structure and to visualize the protein's overall dimensions. This analysis further underscores the remarkable stability of the entire complex, as there were no observed alterations in the RGy value, lying stable for complete trajectory time at ~2.18 nm (**Fig.-5.28B**). Stability and the flexibility of several amino acids present in the protein structure were noticed using RMSF throughout the simulation study to assess the dynamic properties of amino acid residues.

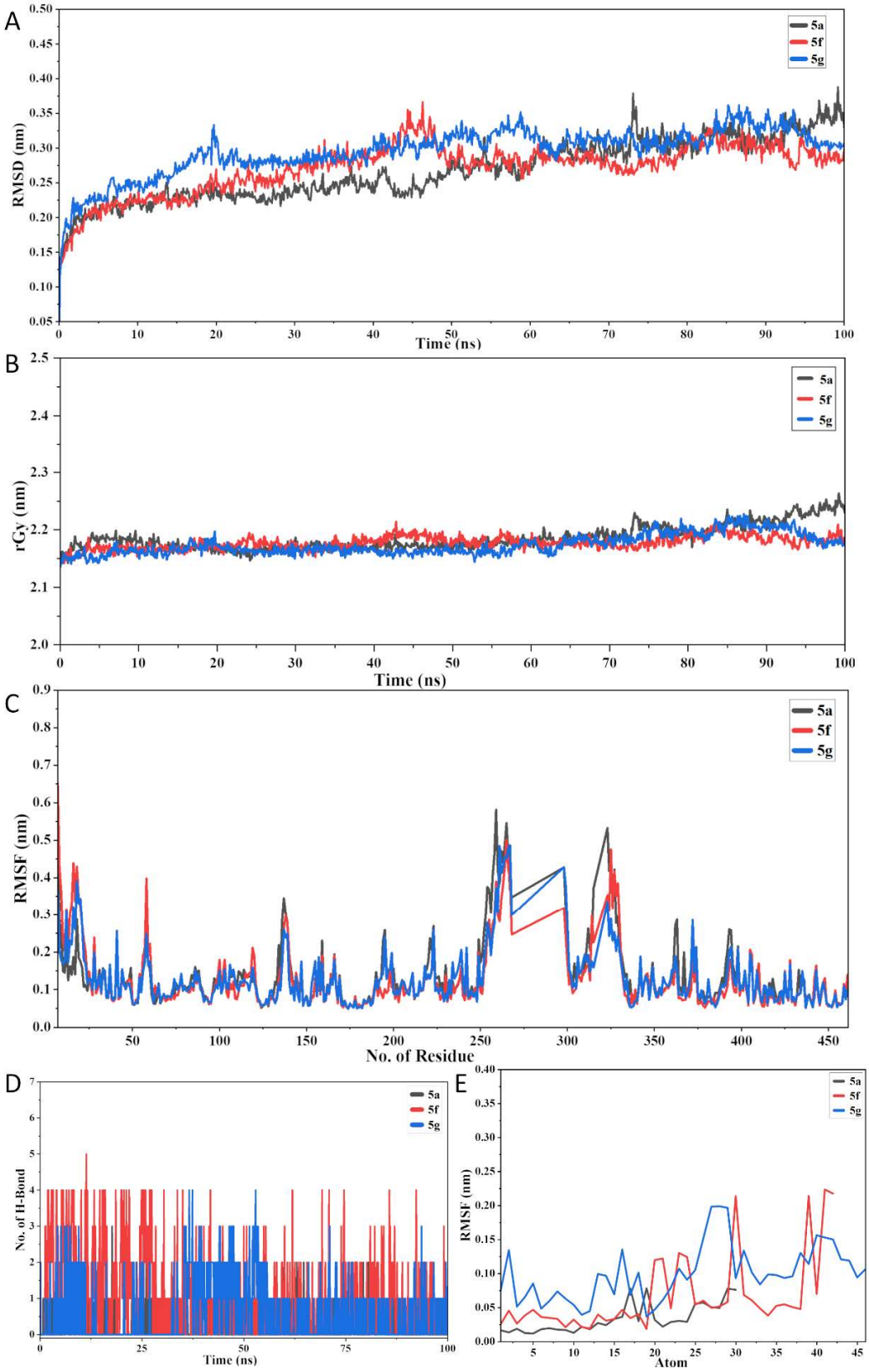
A
RMSD (nm)
Time (ns)
5a
5f
5g
B
rGy (nm)
Time (ns)
5a
5f
5g
C
RMSF (nm)
No. of Residue
5a
5f
5g
D
No. of H-Bond
Time (ns)
5a
5f
5g
E
RMSF (nm)
Atom
5a
5f
5g

Fig.-5.28: MD trajectory analysis of the **5a**, **5f**, and **5g**-protein complexes. A) Protein-ligand RMSD; B) RGy for complex, C) RMSF for protein, D) H-bond of complex & E) RMSF for ligand.

Fig.-5.28C, RMSF plot was examined, and the results specified that the region between 260-300 and 320-335 residues fluctuated at higher values than other residues, indicating the presence of loop regions. Overall, no internal fluctuations were detected throughout the simulation, and the protein's RMSF value remains within the acceptable range of 0.05 to 0.43 nm. The ligand **5a** exhibits a lower RMSF value in the range of 0.02-0.08 nm, indicating its stable positioning within the catalytic pocket with minimal variations (**Fig.-5.28E**). RMSF for **5f** and **5g** had higher fluctuations in the range of 0.02-0.2 nm but within the acceptable range, indicating that ligands were trying to stabilize inside the protein's binding pocket. Hydrogen bonds were calculated throughout the trajectory using a cut-off value of 0.35nm to assess the contribution of hydrogen bonding in complex formation. The results revealed that **5a**, **5f**, and **5g**; all the complexes contained 70, 80, and 90% of hydrogen bond occupancy, signifying the importance of hydrogen bonds for complex formation (**Fig.-5.28D**).

5.2.9. Antioxidant Activity

The study aimed to assess the antioxidant properties of benzothiazole amide derivatives using the DPPH radical scavenging assay at various concentrations (10, 20, and 30 μg/mL). The DPPH assay is a widely recognized method for evaluating the ability of compounds to scavenge free radicals. Notably, the results of the study revealed a concentration-dependent increase in the percentage of antioxidant activity for all tested concentrations. This suggests that as the concentration of the benzothiazole amide derivatives increased, their capacity to inhibit free radical activity also increased. This is a significant finding as it demonstrates the concentration-dependent behavior of these compounds, indicating their potential as effective antioxidants. To provide a point of reference, ascorbic acid, a well-known antioxidant, was used in the study. Ascorbic acid displayed inhibitions of 52.74%, 68.33%, and 70.57% at concentrations of 10, 20, and 30 μg/mL, respectively. This indicates that ascorbic acid's antioxidant activity also increased with higher concentrations. The percentage inhibition range for all the tested benzothiazole amide derivatives was as follows: **5a** (28.09-44.33%), **5b** (29.63-48.91%), **5c** (32.99-51.65%), **5d** (21.71-39.09%), **5e** (31.25-47.05%), **5f** (28.12-41.25%), **5g** (36.94-44.16%), **5h** (27.67-

36.49%), **5i** (25.22-41.16%), **5j** (23.06-59.23%), **5k** (36.23-58.37%), and **5l** (33.17-63.25%). These findings underscore the varying degrees of antioxidant activity among the different benzothiazole amide derivatives. While some compounds demonstrated lower inhibition percentages, others exhibited significantly higher percentages of inhibition, suggesting that certain derivatives may have more robust antioxidant properties.

In summary, the results of this study indicate that benzothiazole amide derivatives have the potential to act as effective antioxidants, with their activity being concentration-dependent. The variations in inhibition percentages among the different compounds suggest that further research and investigation are warranted to determine the specific mechanisms and potential applications of these derivatives in the context of oxidative stress-related diseases and conditions.

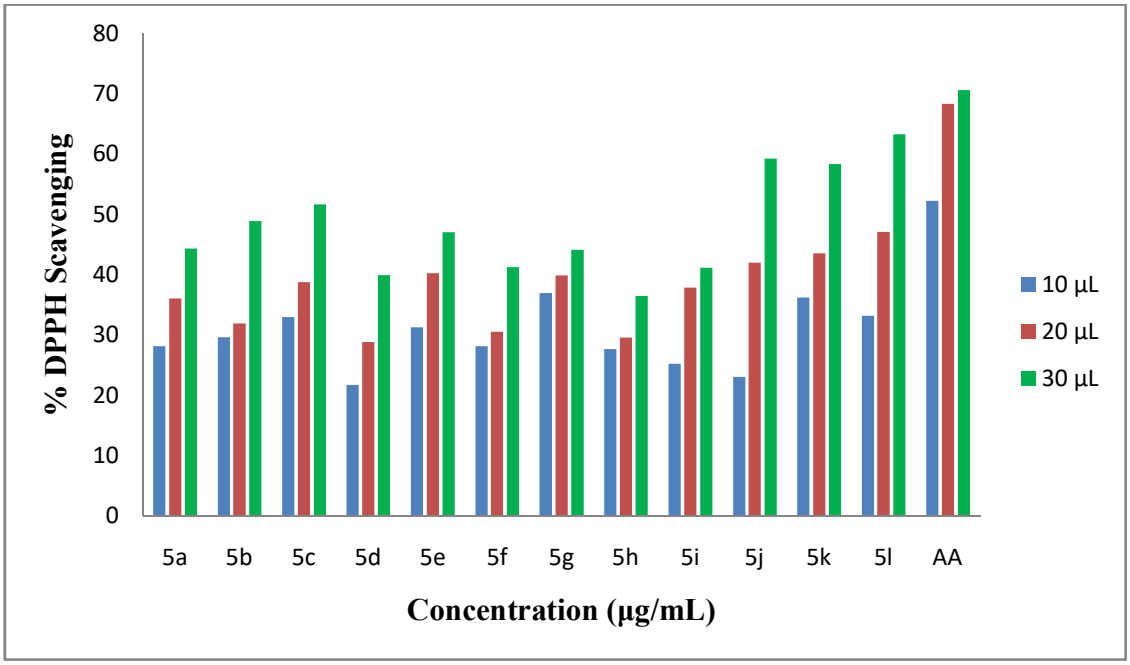

Fig.-5.29: Relative absorption of the compounds (**5a-l**) at different concentrations with respect to ascorbic acid.

5.3. Conclusion

This study focused on synthesizing a series of benzothiazole amide derivatives using a combination of ethyl benzothiazole-2-carboxylate and alicyclic piperazines through molecular hybridization. A total of twelve varied analogues were synthesized by coupling ethyl

benzothiazole-2-carboxyalte (**3a)** with different secondary amines (**4a-l**). This coupling was achieved without the need for a catalyst or solvent, and Ultrasonication was used to promote the reaction, resulting in high selectivity within just one hour. Notably, this reaction adheres to the principles of green chemistry design, being the first of its kind to do so comprehensively. The versatility of the reaction was demonstrated across a wide array of substrates with various substitutions and functionalities. The disclosed protocol is remarkable for its straightforward reaction conditions, lack of catalyst requirement, sustainability, and selectivity. To evaluate their effectiveness against *Mycobacterium tuberculosis* H37Rv (Mtb) strain, all twelve derivatives were subjected to *in vitro* testing using the MABA assay. The results revealed that each of the synthesized compounds displayed anti-tubercular activity, with potency ranging from 1.6 to 12.5 µg/mL. These findings underline the potential promise of benzothiazole amide derivatives as agents for combating tuberculosis. Furthermore, molecular docking studies demonstrated that five compounds *i.e.,* **5a, 5f, 5g**, **5h, and 5l** have strong binding affinity to interact with tuberculosis protein and also follow guidelines of ROF i.e. Lipinski rules. The findings show that the five major compounds are non-toxic and are safe, and may act as safe drug compounds.

References

1. Chakraborti, A.K., Rudrawar, S., Jadhav, K.B., Kaur, G. and Chankeshwara, S.V., 2007. "On water" organic synthesis: a highly efficient and clean synthesis of 2-aryl/heteroaryl/styryl benzothiazoles and 2-alkyl/aryl alkyl benzothiazolines. *Green Chemistry*, *9*(12), pp.1335-1340.
2. Breen, R.A., Swaden, L., Ballinger, J. and Lipman, M.C., 2006. Tuberculosis and HIV co-infection: a practical therapeutic approach. *Drugs*, *66*, pp.2299-2308.
3. Harding, E., 2020. WHO global progress report on tuberculosis elimination. *The Lancet Respiratory Medicine*, *8*(1), p.19.
4. Migliori, G.B., De Iaco, G., Besozzi, G., Centis, R. and Cirillo, D.M., 2007. First tuberculosis cases in Italy resistant to all tested drugs. *Weekly releases (1997–2007)*, *12*(20), p.3194.
5. Velayati, A.A., Masjedi, M.R., Farnia, P., Tabarsi, P., Ghanavi, J., ZiaZarifi, A.H. and Hoffner, S.E., 2009. Emergence of new forms of totally drug-resistant tuberculosis bacilli: super extensively drug-resistant tuberculosis or totally drug-resistant strains in Iran. *Chest*, *136*(2), pp.420-425.
6. Udwadia, Z.F., Amale, R.A., Ajbani, K.K. and Rodrigues, C., 2012. Totally drug-resistant tuberculosis in India. *Clinical Infectious Diseases*, *54*(4), pp.579-581.
7. Caminero, J.A., 2006. Treatment of multidrug-resistant tuberculosis: evidence and controversies. *The International Journal of Tuberculosis and Lung Disease*, *10*(8), pp.829-837.
8. Pagadala, N.S., Syed, K. and Tuszynski, J., 2017. Software for molecular docking: a review. *Biophysical reviews*, *9*, pp.91-102.
9. Abdellatif, K.R., Abdelall, E.K., Elshemy, H.A., Lamie, P.F., Elnahaas, E. and Amin, D.M., 2021. Design, synthesis of new anti-inflammatory agents with a pyrazole core: COX-1/COX-2 inhibition assays, anti-inflammatory, ulcerogenic, histopathological, molecular Modeling, and ADME studies. *Journal of Molecular Structure*, *1240*, p.130554.
10. Bhadra, P., 2020. In-silico Analysis of Effects of Stevia Extracts on Diabetes. *Indian Journal of Natural Sciences*, *10*(60), pp.20710-20719.

CHAPTER-6

Base-Catalysed Synthesis of (E)-N-(benzo[d]thiazol-2-yl)-1-(1H-indol-3-yl)methanimine

6.1. Introduction

Schiff bases, a class of compounds typically derived from the reaction of primary amines with aldehydes or ketones under controlled conditions, have gained prominence owing to their diverse applications. These compounds have exhibited notable potential as active agents against a range of ailments, including tumors, viruses, fungi, and bacterial infections. For instance, Schiff bases derived from indole-3-carboxaldehyde have demonstrated antimicrobial and antitumor properties, showcasing their therapeutic relevance. Moreover, these compounds are instrumental in stabilizing metal cations, thereby enhancing their applications in catalysis, industry, and biology. Traditionally, the synthesis of Schiff bases has employed catalysts such as organic and inorganic bases or Lewis acids. However, the environmental impact and difficulty in the recovery of these catalysts have raised concerns. Consequently, there is a growing interest in the use of recoverable heterogeneous catalysts, as they offer effective catalysis while mitigating environmental risks. For example, catalysts like FeCu@N-doped carbon have proven efficient under UV light, facilitating the conversion of amines and alcohols into Schiff bases. Similarly, Co/Zn-incorporated mesoporous silica nanoparticles have been employed for the synthesis of Schiff bases from aryl amines and benzyl alcohol. Additionally, a mixture of P_2O_5 and Al_2O_3 has been utilized to catalyze Schiff base formation from carbonyl compounds and primary amines, obviating the need for solvents. In a parallel development, Co nanoparticles embedded in mesoporous nitrogen-doped carbon have demonstrated efficacy in converting $–NO_2$ groups into amino groups, followed by coupling with carbonyl compounds in the presence of formic acid at elevated temperatures. Schiff bases are not only crucial in medicinal applications but also hold significant promise in diverse fields such as photovoltaic solar cells, sensors, and OLEDs due to their unique emission properties. Recent advancements have led to the creation of straightforward Schiff bases with white luminescent properties derived from a single chromophore. Investigating the excited state and its relationship with molecular structure or aggregation can provide valuable insights into the optical characteristics of these materials [1-12].

In the present study, piperidine, an organic base catalyst, was employed to synthesize novel benzothiazole-indole based Schiff bases. The yields of the synthesized products were compared with those obtained using conventional methods. Various spectroscopic techniques, including IR, ^{1}H NMR, ^{13}C NMR, and mass spectrometry, were used to characterize the synthesized Schiff

bases. Furthermore, the recoverability and reusability of the piperidine catalyst were assessed over multiple reaction cycles.

In this study, the primary focus was on the design and synthesis of benzothiazole-indole based Schiff bases. Compound **3b**, in particular, was examined for its antimycobacterial activity, shedding light on its potential in combating mycobacterial infections. Additionally, the study investigates the antioxidant properties of these compounds. By systematically assessing these aspects, the research contributes valuable information regarding the therapeutic potential of benzothiazole-indole based Schiff bases, serving as a stepping stone for the development of agents with dual roles in antimycobacterial and antioxidant therapies.

6.2. Results and Discussion

6.2.1. Chemistry

A series of Schiff bases were synthesized using a simple and efficient methodology as depicted in **Scheme-6.1**. The starting materials, indole-3-carbaldehyde and 2-phenyl indole-3-carboxaldehyde were subjected to react with various benzothiazole amines. Piperidine was employed as a homogeneous catalyst, and the reaction was conducted under reflux conditions for a minimum of 1 hour in methanol. The resulting products, designated as **3a-3f**, were consistently obtained in impressive yields. Remarkably, all the tested benzothiazole amines exhibited compatibility with this transformation, effectively leading to the preparation of the targeted compounds in high yields. The IR spectra showed the appearance of new bands at approximately 1621-1640 cm^{-1}, signifying the presence of the imine group (C=N). Interestingly, the absorption peak at 1661 cm^{-1}, linked to the C=O group in the initial aldehyde, disappeared in the spectra. This absence of the C=O absorption band indicated the successful condensation between the NH_2 and C=O groups of the amine and aldehyde respectively, resulting in the formation of Schiff bases. Further supporting evidence was obtained through complementary ^{1}H-NMR, which disclosed evident signals within the chemical shift range of 9.1−9.3 ppm, corresponding to the CH=N protons in all the synthesized products.

To explore the synthetic versatility of the protocol, a base-free alternative approach was investigated. Initially, 2-amino-benzothiazole derivatives were employed as model substrates for the reaction with indole-3-carbaldehyde and 2-phenyl-indole-3-carboxaldehyde, utilizing ethanol as the solvent. It's important to highlight that when the catalyst was not present, product formation did not occur, even when the reaction temperature was increased to 90 °C. The

introduction of piperidine as a catalyst under similar conditions yielded products in moderate yields after 3 hours of reaction in ethanol. Interestingly, increasing the amount of catalyst to 20% did not produce a substantial improvement in the reaction's yield. In contrast, employing methanol as a solvent led to comparable yields of desired products, indicating its efficacy as a solvent. Further optimization revealed that employing piperidine catalyst under reflux conditions in methanol for 1 hour resulted in excellent product yield. These discoveries led to the identification of an optimal procedure for Schiff base synthesis, involving the use of ethanol or methanol using piperidine as the catalyst. Expanding the substrate scope and longer reaction times proved advantageous for boosting the reaction yield. Solvent investigations highlighted the superiority of methanol in terms of reaction yield, outperforming ethanol where only a moderate yield was obtained. Notably, benzothiazole amines were compatible with the reaction, affording the desired ligands in high yields. Comparative analysis of the two synthetic methodologies revealed the base-free approach as a viable alternative, demonstrating comparable yields to the conventional method utilizing piperidine as an organic base. This approach holds potential for various Schiff base syntheses and could be extended to other reactions that necessitate organic bases, including Knoevenagel and Aldol condensations. The ease of catalyst separation further underscores the practicality of this approach, enabling its reuse for multiple cycles without significant reduction in product yield. The catalyst retrieval process involved dissolving the synthesized Schiff bases, followed by a sequence of filtration, washing, and subsequent drying at 80 °C.

In summary, the synthesized Schiff bases through this methodology represent a versatile and efficient approach, as evidenced by high yields and compatibility with diverse amine substrates. This study opens avenues for further exploration and applications in various synthetic endeavors, harnessing the advantages of base-free catalysis for the design of novel reactions and compound libraries.

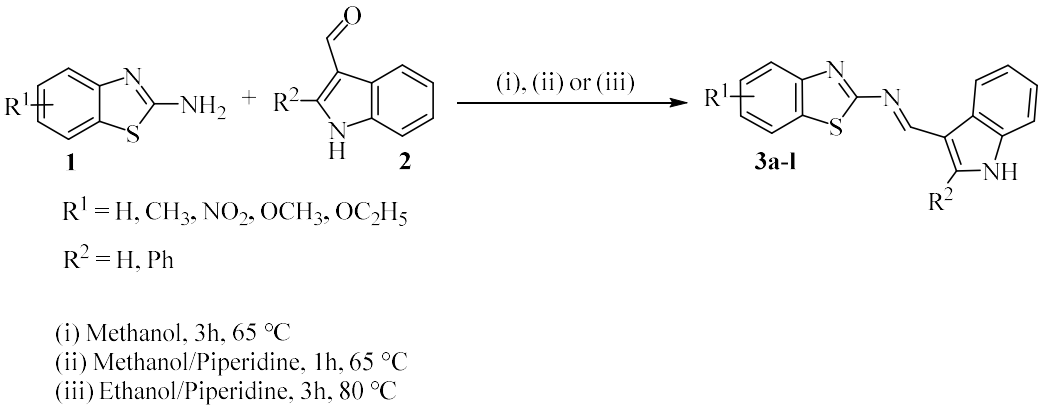

Scheme-6.1: Base-Catalyzed Synthesis of Benzothiazole-Indole Schiff bases.

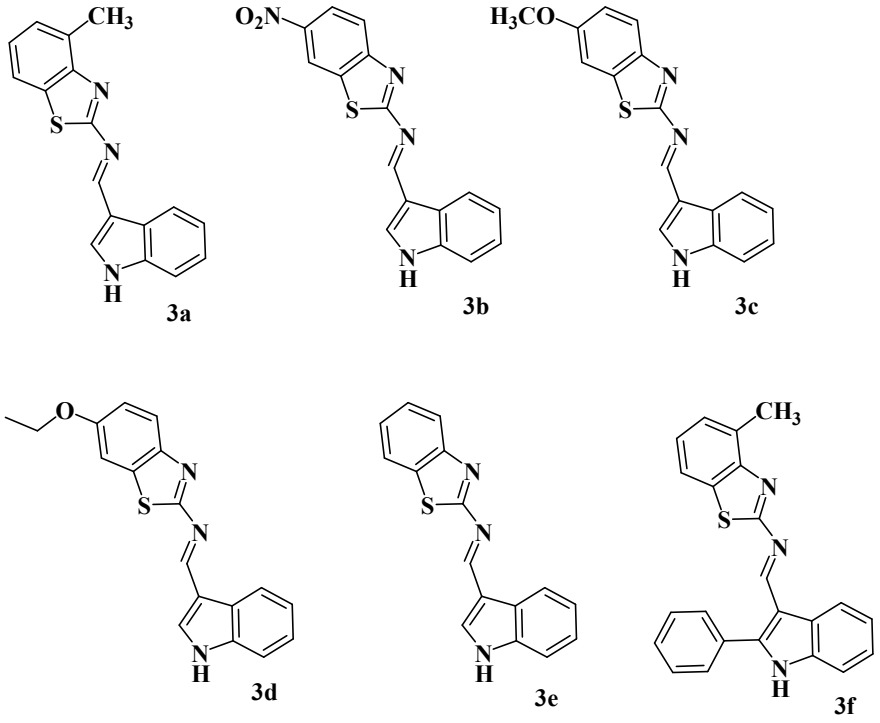

Fig.-6.1: Depiction of the synthesized Benzothiazole-Indole Schiff bases.

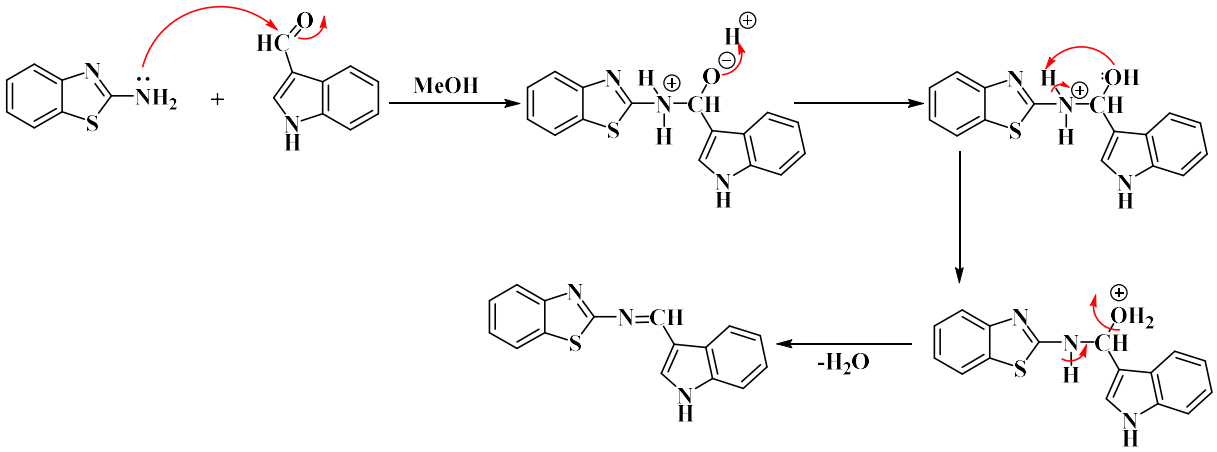

Fig.-6.2: General mechanistic pathway for the synthesis of benzothiazole-indole schiff bases.

6.2.2. Representative *in Vitro* Anti-TB Activity of (E)-1-(1H-indol-3-yl)-N-(6-nitrobenzo[*d*]thiazol-2-yl)methanimine

The effectiveness of (E)-1-(1H-indol-3-yl)-N-(6-nitrobenzo[*d*]thiazol-2-yl)methanimine (**3b**) against *Mycobacterium tuberculosis* was assessed at various concentrations, including 100, 50, 25, 12.5, 6.25, 3.12, 1.6, and 0.8 µg/mL. The outcome is detailed in **Table 6.1**. Compound **3b** demonstrated anti-TB activity at 1.6 µg/mL, which resemble those of the second-line standard medications Isoniazid, and Ethambutol, which exhibit MIC value of 1.6 µg/mL. This ligand effectively suppressed the growth of *Mycobacterium tuberculosis* at the specified concentration (1.6 µg/mL).

Table 6.1: Anti-TB activity of compound **3b.**

S. No.	Compound	100 µg/mL	50 µg/mL	25 µg/mL	12.5 µg/mL	6.2 µg/mL	3.12 µg/mL	1.6 µg/mL	0.8 µg/mL
01	**3b**	S	S	S	S	S	S	S	R

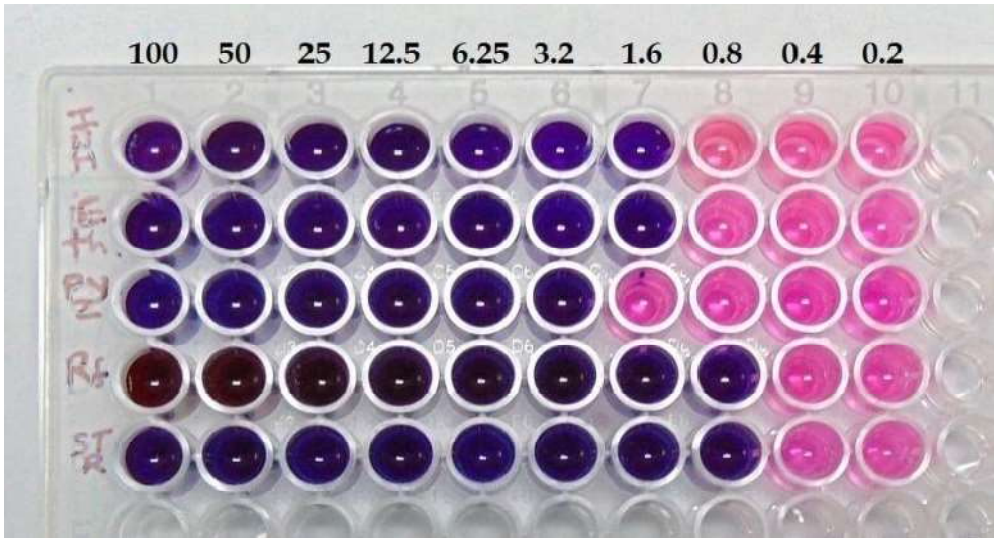

Fig.-6.3: MIC of control drugs: Isoniazid, Ethambutol, Pyrazinamide, Rifampicin, and Streptomycin.

Fig.-6.4: MIC of compound **3b** against *Mycobacterium tuberculosis.*

6.2.3. Assessment of Antioxidant Characteristics of Synthesized Schiff Bases

Synthetic compounds with antioxidant properties have garnered significant attention in recent research. In this study, the antioxidant characteristics of synthesized Schiff bases were evaluated by employing the DPPH radical scavenging test. The Schiff bases under investigation were tested at three different concentrations. As a reference, ascorbic acid, a well-known antioxidant, was used. In this study, a total of tested six synthesized Schiff bases (**3a**, **3b**, **3c**, **3d**, **3e**, and **3f**) at three different concentrations (10, 20, and 30 µg/mL) and compared their performance to that of the standard antioxidant, ascorbic acid. The results of the DPPH radical scavenging test revealed that all tested Schiff bases exhibited antioxidant activity comparable to that of standard ascorbic acid across different concentrations. Notably, there was a concentration-dependent increase in the percentage of antioxidant activity for all the compounds, suggesting their active involvement in free radical scavenging. As a reference, ascorbic acid exhibited inhibitions of 52.74%, 62.33%, and 78.57% at concentrations of 10, 20, and 30 µg/mL, respectively. In

contrast, the synthesized Schiff bases displayed varying degrees of antioxidant activity, as summarized as follows: **3a** (67.52-70.24%), **3b** (86.34-91.70%), **3c** (55.70-86.98%), **3d** (80.04-92.51%), **3e** (87.43-94.04%), **3f** (60.65-76.43%). The findings of this study suggest that the synthesized Schiff bases exhibited significant antioxidant activity across different concentrations. Their performance was comparable to that of ascorbic acid, a well-known antioxidant. These findings underscore the potential of Schiff bases as effective antioxidants, with Schiff bases **3b**, **3d**, and **3e** showing the most promise. Further research into the applications and mechanisms of these compounds is warranted, as they may have a significant impact on health and food science.

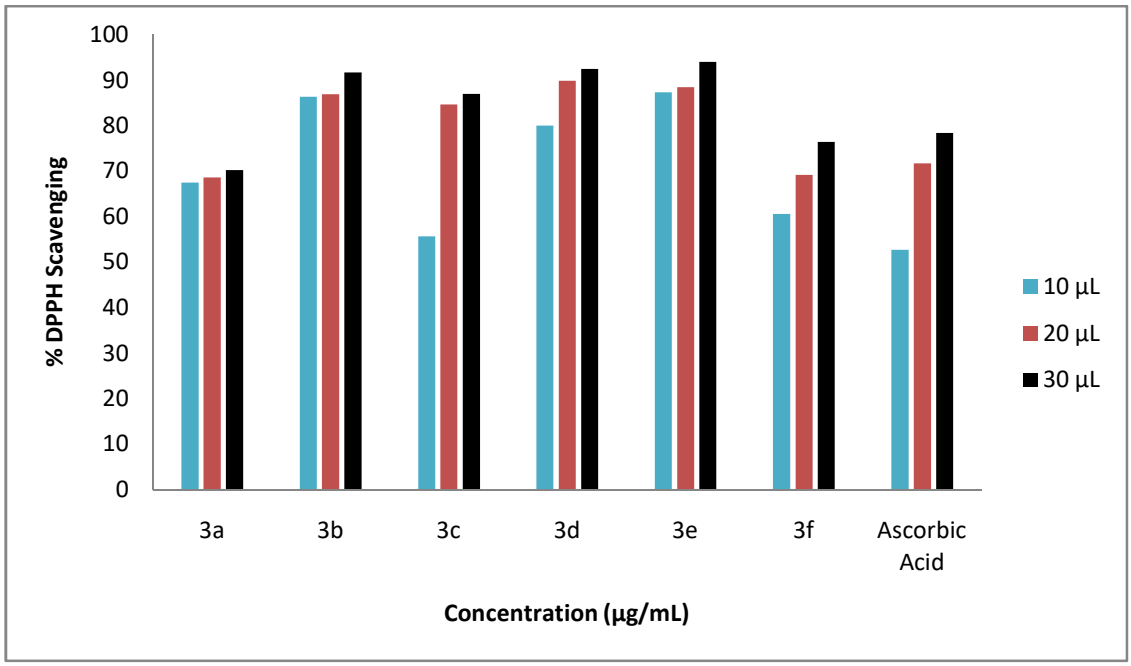

Fig.-6.5: Relative absorption of the compounds (**3a-f**) at different concentrations with respect to ascorbic acid.

6.3. Conclusion

The synthesis of benzothiazole-based Schiff base ligands, incorporating indole components, was successfully achieved through two methods: conventional piperidine-catalyzed synthesis and a base-free heterogeneous catalysis approach. Both methods demonstrated high efficiency in yielding products, as confirmed by thorough spectroscopic analyses. The synthesized compounds exhibited potent antioxidant activity, highlighting their potential as effective agents against oxidative stress. Furthermore, compound **3b**, derived from this synthesis, demonstrated

exceptional antimycobacterial efficacy with a minimum inhibitory concentration (MIC) of 1.6 μg/mL against the *Mycobacterium Tuberculosis* H37Rv strain. This notable finding not only underscores the diverse biological activities of the synthesized Schiff bases but also positions compound **3b** as a promising candidate for novel antimycobacterial treatments, thereby offering valuable insights for future pharmaceutical research and development. The study showcases the versatility of Schiff bases and the potential of their derivatives in addressing various health-related challenges.

References

1. Vamsikrishna, N., Kumar, M.P., Ramesh, G., Ganji, N., Daravath, S. and Shivaraj, 2017. DNA interactions and biocidal activity of metal complexes of benzothiazole Schiff bases: Synthesis, characterization and validation. *Journal of Chemical Sciences*, *129*, pp.609-622.
2. Gabr, M.T., El-Gohary, N.S., El-Bendary, E.R., El-Kerdawy, M.M. and Ni, N., 2016. Synthesis, in vitro antitumor activity and molecular modeling studies of a new series of benzothiazole Schiff bases. *Chinese Chemical Letters*, *27*(3), pp.380-386.
3. Mishra, N., Kumar, K., Pandey, H., Anand, S.R., Yadav, R., Srivastava, S.P. and Pandey, R., 2020. Synthesis, characterization, optical and anti-bacterial properties of benzothiazole Schiff bases and their lanthanide (III) complexes. *Journal of Saudi Chemical Society*, *24*(12), pp.925-933.
4. Chauhan, K., Singh, P., Kumari, B. and Singhal, R.K., 2017. Synthesis of new benzothiazole Schiff base as selective and sensitive colorimetric sensor for arsenic on-site detection at ppb level. *Analytical Methods*, *9*(11), pp.1779-1785.
5. Chauhan, K., Singh, P., Kumari, B. and Singhal, R.K., 2017. Synthesis of new benzothiazole Schiff base as selective and sensitive colorimetric sensor for arsenic on-site detection at ppb level. *Analytical Methods*, *9*(11), pp.1779-1785.
6. Vicini, P., Geronikaki, A., Incerti, M., Busonera, B., Poni, G., Cabras, C.A. and La Colla, P., 2003. Synthesis and biological evaluation of benzo [d] isothiazole, benzothiazole and thiazole Schiff bases. *Bioorganic & medicinal chemistry*, *11*(22), pp.4785-4789.
7. Rao, N.N., Gopichand, K., Nagaraju, R., Ganai, A.M. and Rao, P.V., 2020. Design, synthesis, spectral characterization, DNA binding, photo cleavage and antibacterial studies of transition metal complexes of benzothiazole Schiff base. *Chemical Data Collections*, *27*, p.100368.
8. Al-Hamdani, U.J., Abbo, H.S., Fadhl, A.A. and Titinchi, S.J., 2022. Chloro-benzothiazole Schiff base ester liquid crystals: synthesis and mesomorphic investigation. *Liquid Crystals*, *49*(13), pp.1866-1877.
9. Daravath, S., Vamsikrishna, N., Ganji, N. and Venkateswarlu, K., 2018. Synthesis, characterization, DNA binding ability, nuclease efficacy and biological evaluation studies of Co (II), Ni (II) and Cu (II) complexes with benzothiazole Schiff base. *Chemical Data Collections*, *17*, pp.159-168.

10. Mishra, V.R., Ghanavatkar, C.W., Mali, S.N., Chaudhari, H.K. and Sekar, N., 2019. Schiff base clubbed benzothiazole: synthesis, potent antimicrobial and MCF-7 anticancer activity, DNA cleavage and computational study. *Journal of Biomolecular Structure and Dynamics*.
11. Kassem, M.A. and Shah, R.K., 2023. Nano-sized cadmium-benzothiazole Schiff base complexes: Synthesis, characterization, and the impact of surfactants for cadmium determination. *Applied Organometallic Chemistry*, *37*(4), p.e7047.
12. Malik, S., Miana, G.A., Ata, A., Kanwal, M., Maqsood, S., Malik, I. and Kazmi, Z., 2023. Synthesis, characterization, in-silico, and pharmacological evaluation of new 2-amino-6-trifluoromethoxy benzothiazole derivatives. *Bioorganic Chemistry*, *130*, p.106175.

CHAPTER-7

EXPERIMENTAL SECTION

7.1. Experimental Procedure for the Synthesis of 2-Azidobenzothiazoles

2-aminobenzothiazole (0.5 mmol) was dissolved in water in a 50 mL round-bottom flask at room temperature, using a magnetic stirrer. Hydrochloric acid was then carefully added drop by drop until the complete dissolution of 2-aminobenzothiazole in water was achieved. In the next step solutions of sodium nitrite, (2 mmol), sodium acetate (2 mmol), and sodium azide (2 mmol) were added dropwise after every 5 minutes respectively and the reaction was stirred for further 30 minutes. The progression of the reaction was monitored using TLC, which confirmed its completion within 1 hour. The solid precipitate was filtered, washed with water, and recrystallized from ethanol which did not require any further purification. (Note: *$NaNO_2$, $NaOAc$, and NaN_3 were first dissolved in water, and then added dropwise to the reaction mixture respectively. Also, the role of sodium acetate is to neutralize the acidic medium*).

7.2. Spectroscopic Data

2-Azido-4, 6-difluorobenzothiazole (2a)

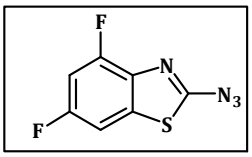

Brown solid, yield: 93%, mp 170–173 °C, IR (neat) υ: 2124 cm^{-1} (-N_3). ^{1}H-NMR (400 MHz, DMSO-d_6) δ (ppm): 7.98 (m, 1H), 7.63 (m, 1H). HRMS (ESI) *m/z*: $[M + Na]^+$ calcd for $C_7H_2F_2N_4S$, 234.9866; found, 234.8841.

2-Azido-6-methoxybenzothiazole (2b)

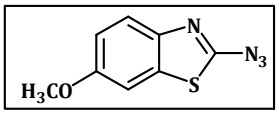

Brown solid, yield: 93%, mp 155–158 °C, IR (neat) υ: 2113 cm^{-1} (-N_3). ^{1}H-NMR (400 MHz, DMSO-d_6) δ (ppm): 8.25 (d, J = 12 Hz, 1H), 7.94 (d, 1H), 7.35 (dd, J = 8 Hz, 1H), 3.93 (s, 3H). HRMS (ESI) *m/z*: $[M + H]^+$ calcd for $C_8H_6N_4OS$, 207.0341; found, 207.0337.

Ethyl 2-azidobenzothiazole-6-carboxylate (2c)

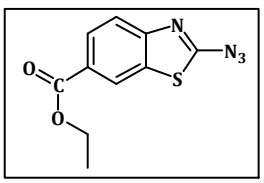

White solid, yield: 89%, mp 145–148 °C, IR (neat) υ: 2126 cm^{-1} (-N_3). ^{1}H-NMR (400 MHz, $CDCl_3$) δ (ppm): 8.08 (d, J = 4 Hz, 1H), 7.47 (m, 1H), 7.39 (d, J = 4 Hz, 1H), 3.74 (q, J = 4 Hz, 2H), 1.28 (t, J = 8 Hz, 3H).

2-Azido-6-Nitro-benzothiaole (2d)

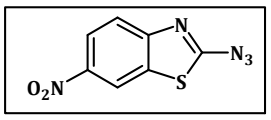

Creamy white solid, yield: 95%, mp 190–193 °C, IR (neat) υ: 2120 cm^{-1} (-N_3). ^{1}H-NMR (400 MHz, $CDCl_3$) δ (ppm): 8.77 (d, 1H), 8.40 (dd, *J* = 4 Hz, 1H), 8.10 (d, *J* = 8 Hz, 1H). HRMS (ESI) *m/z*: $[M + H]^+$ calcd for $C_7H_3N_5O_2S$, 222.0086; found, 222.0326.

2-Azidobenzothiazole (2e)

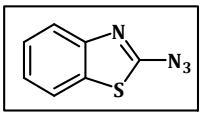

Brown solid, yield: 80%, mp 153–156 °C, IR (neat) υ: 2119 cm^{-1} (-N_3). ^{1}H-NMR (400 MHz, $CDCl_3$) δ (ppm): 8.22 (d, *J* = 8 Hz, 1H), 7.74 (d, *J* = 8 Hz, 1H), 7.70 – 7.58 (m, 2H). GCMS: *m/z* calcd for $C_7H_4N_4S$, 176; found, 176.

2-Azido-4-methylbenzothiazole (2f)

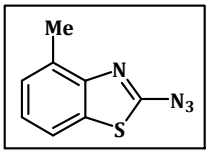

Orange solid; yield: 80%, mp 117–120 °C, IR (neat) υ: 2120 cm^{-1} (-N_3). ^{1}H-NMR (400 MHz, $CDCl_3$) δ (ppm): 7.73 (d, *J* = 8 Hz, 1H), 7.30 (d, *J* = 8 Hz, 1H), 7.18 (t, *J* = 8 Hz, 1H), 2.40 (s, 3H).

2-Azido-6-ethoxybenzothiazole (2g)

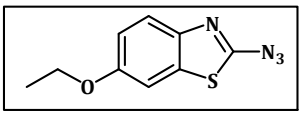

Brown solid, yield: 92%, mp 161–164 °C, IR (neat) υ: 2107 cm^{-1} (-N_3). ^{1}H-NMR (400 MHz, $CDCl_3$) δ (ppm): 8.07 (d, *J* = 8 Hz, 1H), 7.70 (d, *J* = 12 Hz, 1H), 7.02 (dd, *J* = 4 Hz, 1H), 4.06 (q, *J* = 8 Hz, 2H), 1.44 (t, *J* = 8 Hz, 3H). GCMS: *(m/z)* calcd for $C_9H_8N_4OS$, 220; found, 221.

2-Azido-5-bromobenzothiazole (2h)

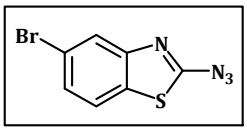

Brown solid; yield: 82%, mp 180–183 °C, IR (neat) υ: 2110 cm^{-1} (-N_3). ^{1}H-NMR (400 MHz, DMSO-d_6) δ (ppm): 8.32 (d, *J* = 4 Hz, 1H), 8.16 (d, *J* = 8 Hz, 1H), 7.66 (dd, 1H).

7.3. Representative Spectra

^{1}H-NMR Spectrum of Compound 2a:

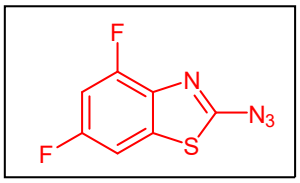

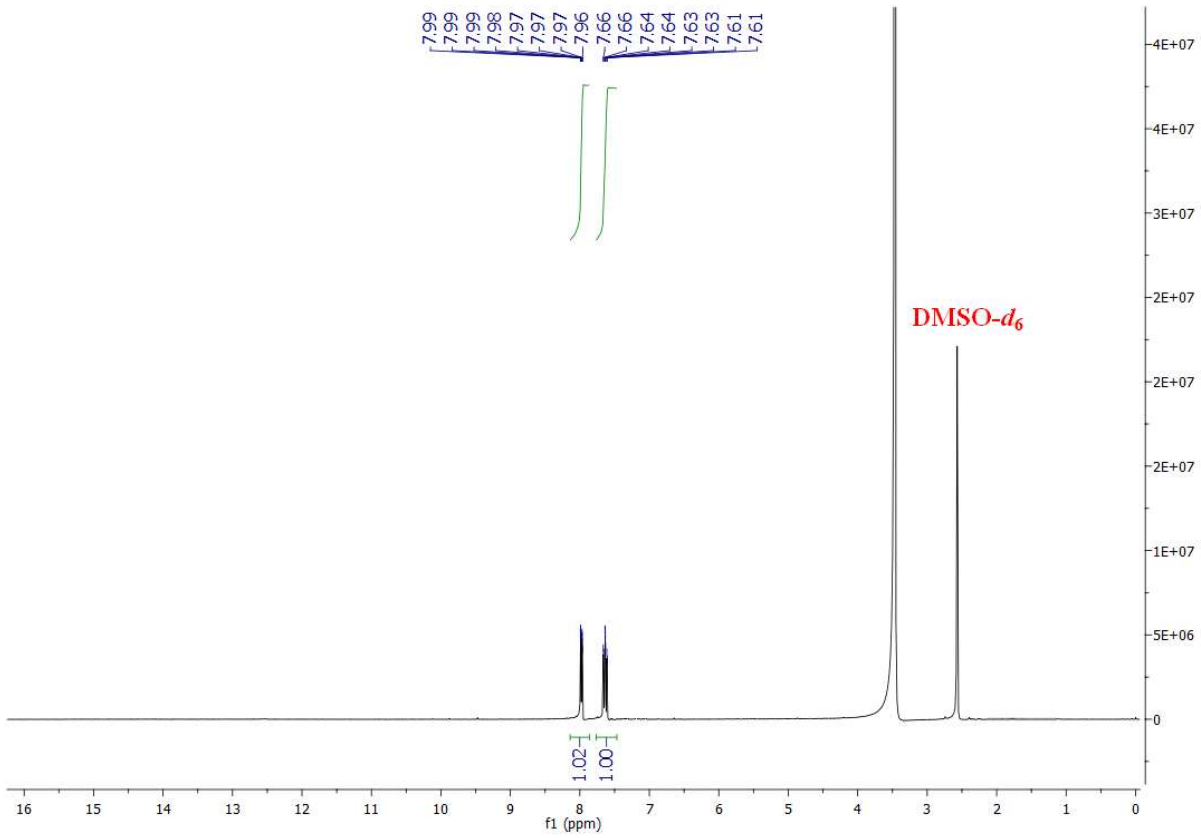

^{19}F-NMR Spectrum of Cpmpound 2a:

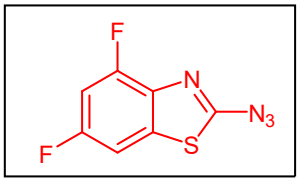

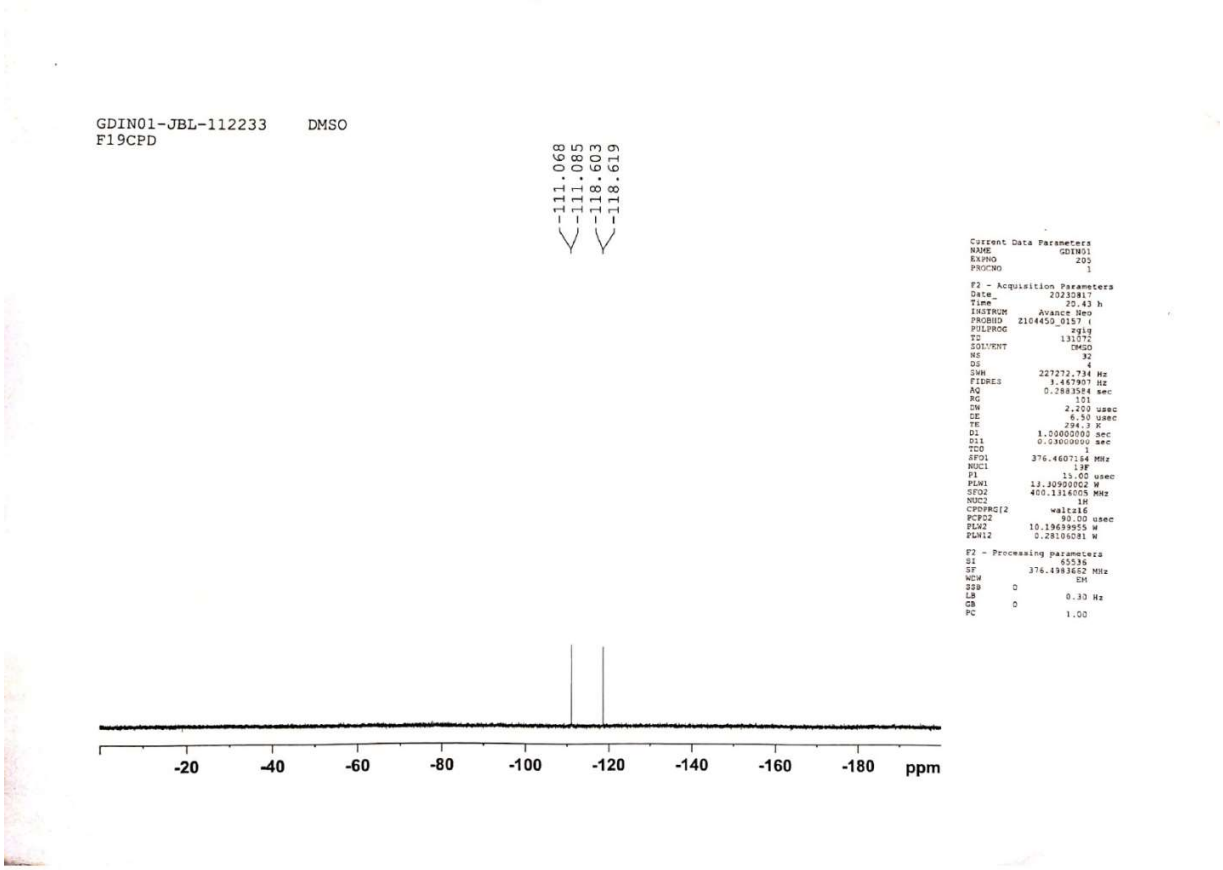

^{1}H-NMR Spectrum of Compound 2b:

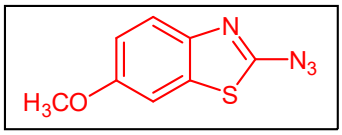

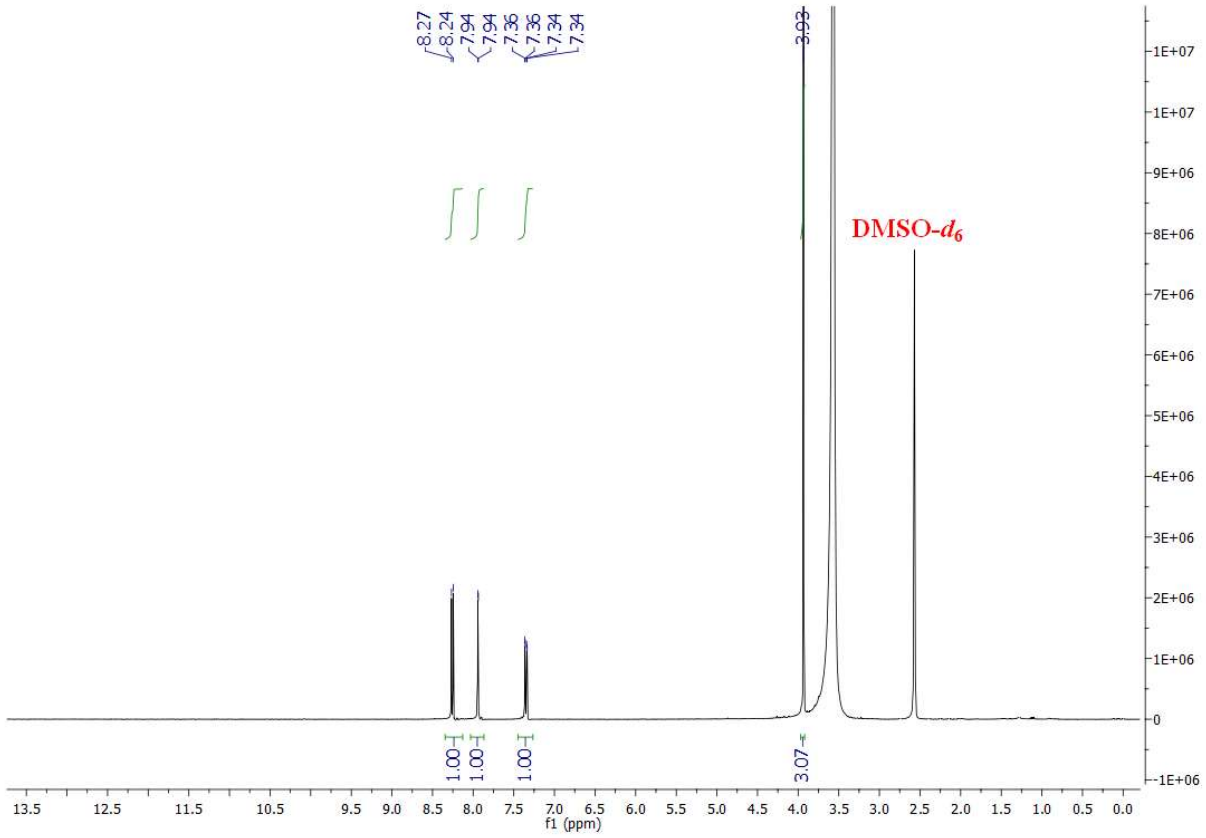

[1]H-NMR Spectrum of Compound 2d:

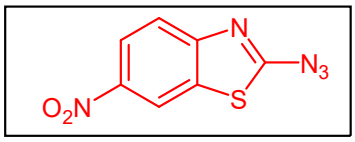

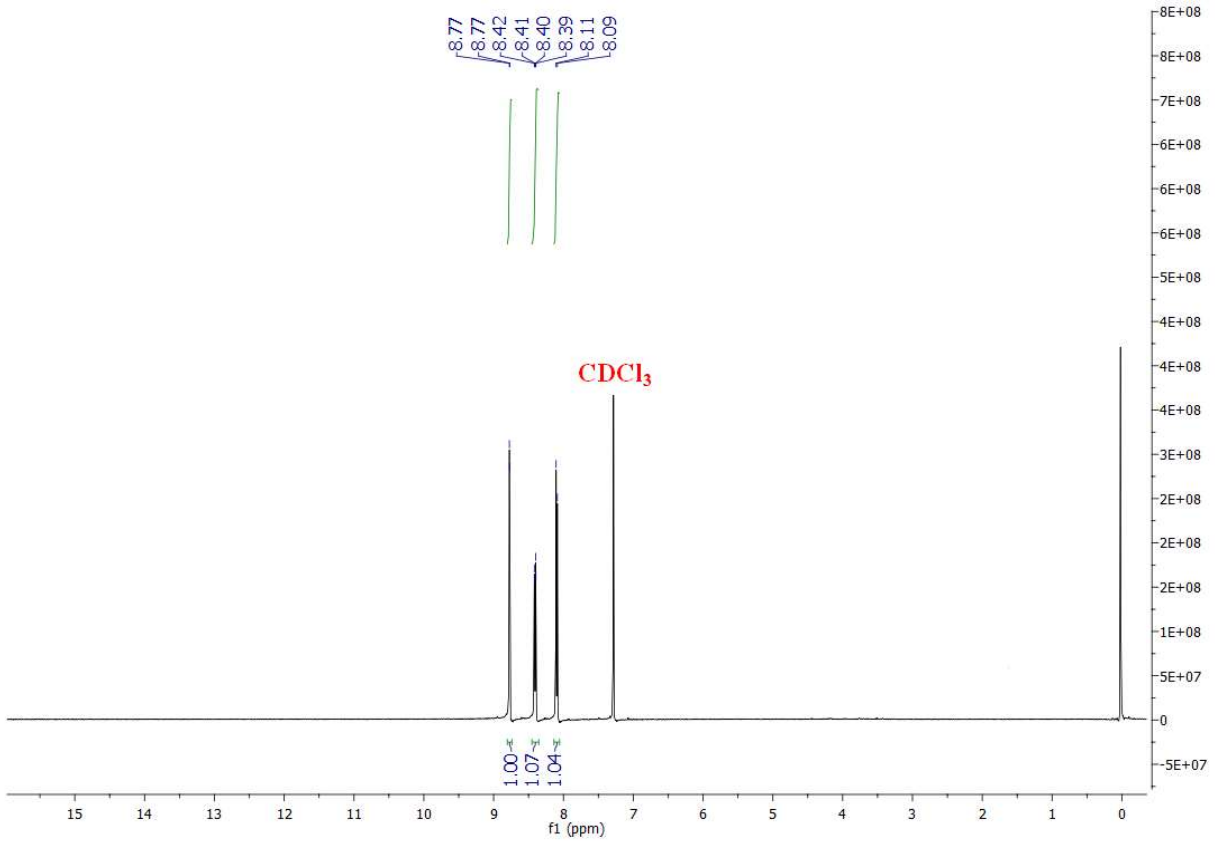

IR Spectrum of Compound 2a:

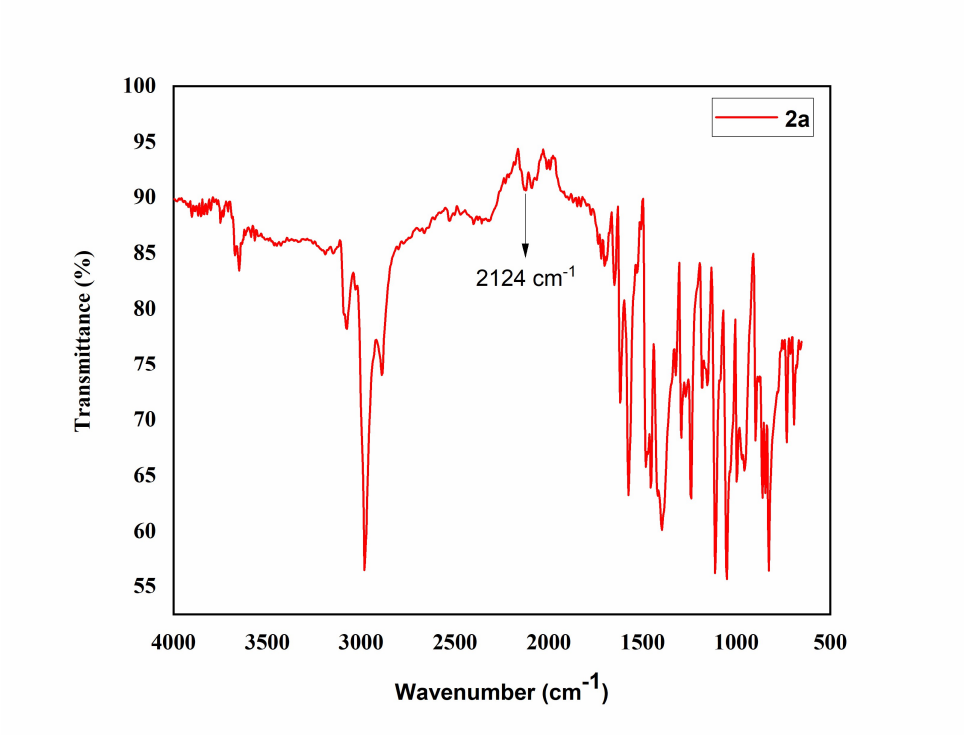

IR Spectrum of Compound 2d:

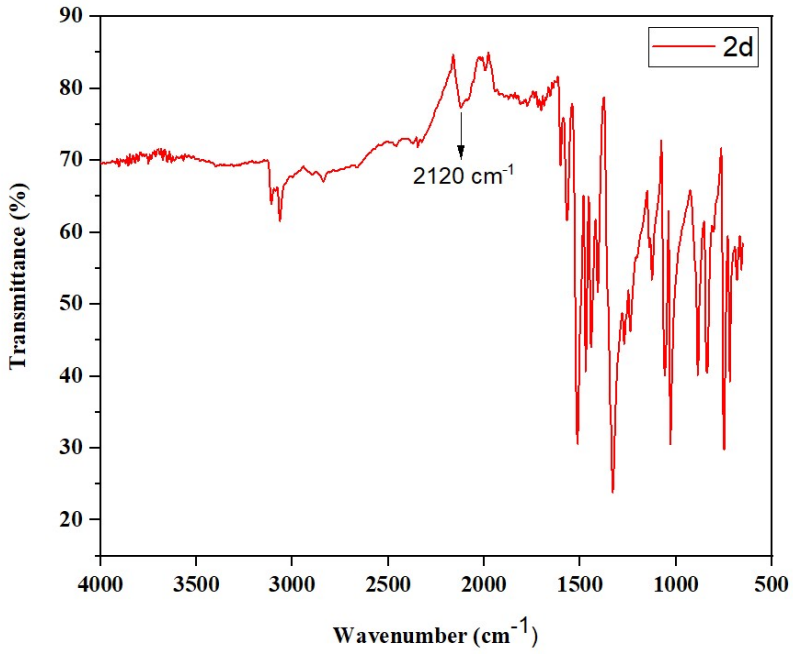

IR Spectrum of Compound 2f:

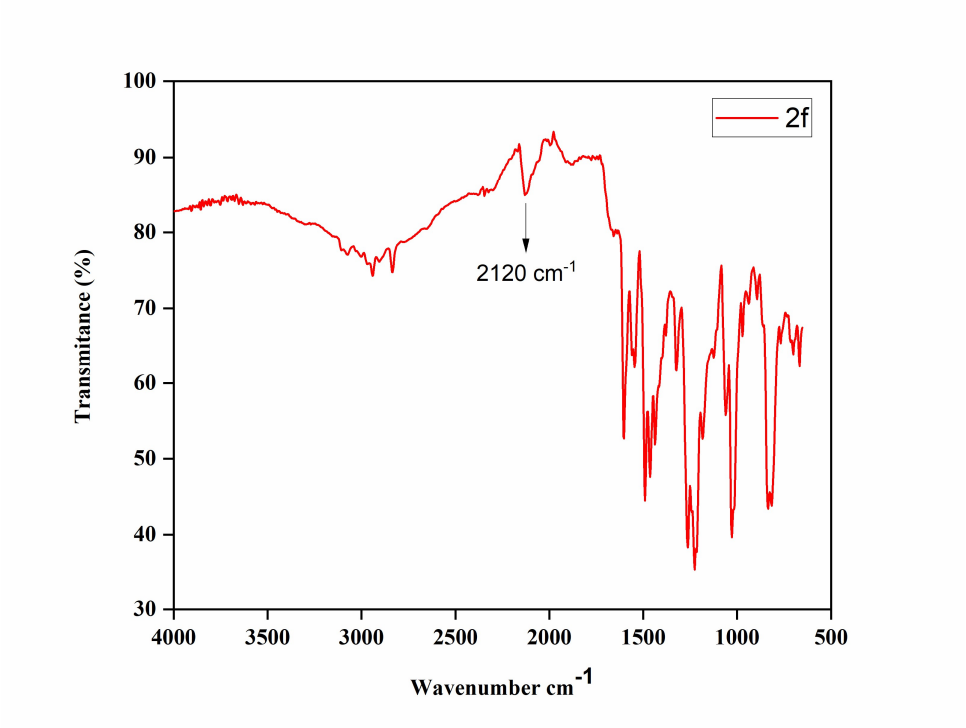

7.4. Experimental Procedure for the Synthesis of Benzothiazole Amide Derivatives

7.4.1. General Procedure for the Synthesis of ethyl benzothiazole-2-carboxylate (3)

A mixture of o-aminothiophenol (1 mmol) and diethyl oxalate (1 mmol) was prepared in a round-bottom flask. The reaction mixture was subjected to mild reflux using a heating mantle for 4 hours. During this time, the temperature gradually decreased from 147 to 93 °C. Following the completion of the reaction (TLC), the reaction mixture was permitted to cool at room temperature. The cooled mixture was then poured slowly into a solution composed of 50 mL of concentrated HCl, 150 mL of H_2O, and 70 mL of C_2H_5OH. Continuous stirring was maintained during this step. This led to the dissolution of the oily substance and the formation of a solid precipitate. The resulting mixture was allowed to cool further for a sufficient period to ensure complete precipitation of the product. The solid product was separated by vacuum filtration using a Buchner funnel. The obtained solid was washed with aqueous ethanol to remove impurities and residual reagents. The washed product was then dried, typically under vacuum or at a controlled temperature, until a constant weight was attained. The dried product was ultimately crystallized from ethanol to obtain ethyl benzothiazole-2-carboxylate. The yield of ethyl benzothiazole-2-carboxylate was determined by measuring the weight of the purified and

dried product. The reaction temperature during reflux should be carefully monitored to ensure a controlled reaction and prevent overheating.

7.4.2. General Procedure for the Synthesis of Benzothiazole Amide Derivatives

Ethyl benzothiazole-2-carboxylate (1 mmol) was accurately weighed and placed in a 10 mL round bottom flask. The corresponding amine (1 equiv) was added to the flask, and the reaction mixture was prepared. Ultrasonication was employed to initiate the reaction at room temperature, and the temperature was gradually raised to 35 °C over a specified duration (ranging from 15 minutes to 1 hour, depending on the specific reaction conditions). This gradual temperature increase was crucial for the success of each reaction. The progress of the reaction was observed by employing TLC. Following the completion of the reaction, the mixture was allowed to cool down to room temperature. To isolate the desired product, the cooled mixture was dissolved in an appropriate volume of ethyl acetate. The ethyl acetate solution was washed with H_2O to remove any water-soluble impurities. This step was repeated as necessary until a clear organic layer was obtained. The organic layer was separated from the aqueous layer and concentrated using a rotary evaporator to remove the solvent. The resulting solid obtained after solvent removal was subjected to recrystallization from ethanol to purify the product. The obtained crystals were isolated by filtration, air-dried, and subsequently analyzed using appropriate techniques (*e.g.,* IR, NMR, and mass spectrometry) to confirm their identity and purity. This experimental procedure was repeated for each reaction with specific variations as needed, such as reaction time and choice of amines, to synthesize the desired compounds.

7.5. Spectroscopic Data

Ethyl benzothiazole-2-carboxylate (3)

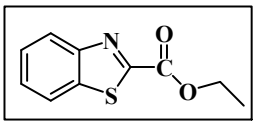

White solid, yield: 83%, mp 68–72 °C, IR (neat) υ: 1750 cm^{-1} (C=O). ^{1}H-NMR (400 MHz, $CDCl_3$) δ (ppm): 8.26 (d, *J* = 8 Hz, 1H), 7.98 (d, *J* = 8 Hz, 1H), 7.61-7.52 (m, 2H), 4.56 (q, *J* = 8 Hz, 2H), 1.50 (t, *J* = 8 Hz, 3H). ^{13}C-NMR (100 MHz, $CDCl_3$) δ (ppm): 160.77, 158.66, 153.32, 136.88, 127.64, 127.18, 125.62, 122.17, 63.22, 14.39. HRMS (ESI) *m/z*: $[M + H]^+$ calcd for $C_{10}H_9NO_2S$, 208.0432; found, 208.0432.

Benzothiazol-2-yl(pyrrolidin-1-yl)methanone (5a)

Creamy white solid, yield: 92%, mp 99–103 °C, IR (neat) υ: 1621 cm^{-1} (C=O). ^{1}H-NMR (400 MHz, $CDCl_3$) δ (ppm): 8.08 (d, *J* = 4 Hz, 1H), 7.95 (d, *J* = 8 Hz, 1H), 7.53–7.45 (m, 2H), 4.22 (t, *J* = 4 Hz, 2H), 3.74 (t, *J* = 4 Hz, 2H), 2.06-1.93 (m, 4H). ^{13}C NMR (100 MHz, $CDCl_3$) δ (ppm): 165.93, 159.54, 153.88, 136.54, 126.72, 126.54, 124.86, 122.14, 49.28, 48.02, 26.80, 23.95. HRMS (ESI) *m/z*: $[M + H]^+$ calcd for $C_{12}H_{12}N_2OS$, 233.0749; found, 233.0746.

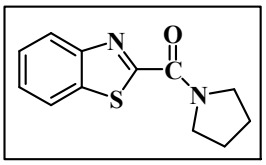

Benzothiazol-2-yl(thiomorpholino)methanone (5b)

Yellowish solid, yield: 88%, mp 112–115 °C, IR (neat) υ: 1618 cm^{-1} (C=O). ^{1}H-NMR (400 MHz, $CDCl_3$) δ (ppm): 8.00 (d, *J* = 8 Hz, 1H), 7.88 (d, *J* = 8 Hz, 1H), 7.48–7.39 (m, 2H), 4.55 (t, *J* = 4 Hz, 2H), 4.01 (t, *J* = 4 Hz, 2H), 2.72 (q, *J* = 8 Hz, 4H). ^{13}C-NMR (100 MHz, $CDCl_3$) δ (ppm): 164.34, 160.07, 152.98, 136.14, 126.77, 126.61, 124.66, 121.85, 49.43, 46.35, 28.52, 27.54. HRMS (ESI) *m/z*: $[M + Na]^+$ calcd for $C_{12}H_{12}N_2OS_2$, 287.0289; found, 287.0283.

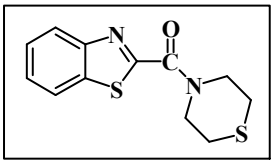

Benzothiazol-2-yl(morpholino)methanone (5c)

White solid, yield: 84%, mp 103–106 °C, IR (neat) υ: 1621 cm^{-1} (C=O). ^{1}H-NMR (400 MHz, $CDCl_3$) δ (ppm): 8.10 (d, *J* = 8 Hz, 1H), 7.98 (d, *J* = 8 Hz, 1H), 7.58–7.50 (m, 2H), 4.54 (t, *J* = 4 Hz, 2H), 3.87–3.83 (m, 6H). ^{13}C-NMR (100 MHz, $CDCl_3$) δ (ppm): 164.50, 159.75, 153.09, 136.21, 126.79, 126.61, 124.65, 121.87, 67.24, 66.91, 47.20, 43.93. HRMS (ESI) *m/z*: $[M + H]^+$ calcd for $C_{12}H_{12}N_2O_2S$, 249.0698; found, 249.0699.

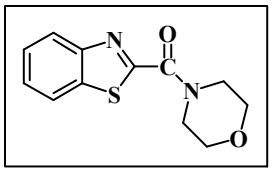

Benzothiazol-2-yl(piperidin-1-yl)methanone (5d)

Brownish yellow solid, yield: 87%, mp 80–83 °C, IR (neat) υ: 1615 cm^{-1} (C=O). ^{1}H-NMR (400 MHz, $CDCl_3$) δ (ppm): 8.10 (d, *J* = 8 Hz, 1H), 7.95 (d, *J* = 8 Hz, 1H), 7.56–7.46 (m, 2H), 4.26 (t, *J* = 4 Hz, 2H), 3.79 (t, *J* = 4 Hz, 2H), 1.74 (s, 6H). ^{13}C-NMR (100 MHz, $CDCl_3$) δ (ppm): 164.92, 159.91, 153.05, 136.09, 126.47, 126.42, 124.51, 121.80, 47.69, 44.75, 26.76, 25.80, 24.58. HRMS (ESI) *m/z*: $[M + H]^+$ calcd for $C_{13}H_{14}N_2OS$, 247.0905; found, 247.0908.

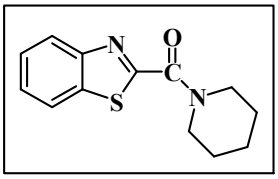

Benzothiazol-2-yl(4-methylpiperazin-1-yl)methanone (5e)

White solid, yield: 72%, mp 146–148 °C, IR (neat) υ: 1630 cm^{-1} (C=O). ^{1}H-NMR (400 MHz, $CDCl_3$) δ (ppm): δ (ppm) 8.10 (d, *J* = 4 Hz, 1H), 7.98 (d, *J* = 4 Hz, 1H), 7.57–7.49 (m, 2H), 4.47 (t, *J* = 4 Hz, 2H), 3.90 (t, *J* = 4 Hz, 2H), 2.56 (t, *J* = 4 Hz, 4H), 2.37 (s, 3H).

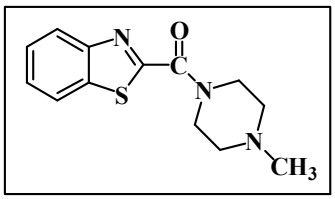

^{13}C-NMR (100 MHz, $CDCl_3$) δ (ppm): 164.65, 159.65, 153.02, 136.11, 126.64, 126.50, 124.56, 121.79, 55.44, 54.70, 46.36, 45.94, 43.43. HRMS (ESI) *m/z*: $[M + H]^+$ calcd for $C_{13}H_{15}N_3OS$, 262.1014; found, 262.1010.

Benzothiazol-2-yl(4-phenylpiperazin-1 -yl)methanone (5f)

Pale yellow solid, yield: 91%, mp 95–98 °C, IR (neat) υ: 1622 cm^{-1} (C=O). ^{1}H-NMR (400 MHz, $CDCl_3$) δ (ppm): 8.11 (d, *J* = 4 Hz, 1H), 7.97 (d, *J* = 8 Hz, 1H), 7.57–7.49 (m, 2H), 7.39 (t, *J* = 8 Hz, 2H), 7.14 (d, *J* = 4 Hz, 2H), 7.12 (t, *J* = 8 Hz, 1H), 4.67 (t, *J* = 4 Hz, 2H), 4.03 (t, *J* = 4 Hz, 2H), 3.38 (t, *J* = 4 Hz, 4H). ^{13}C-NMR

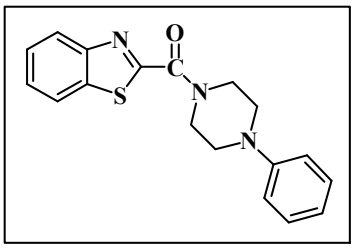

(100 MHz, $CDCl_3$) δ (ppm): 164.57, 159.82, 153.18, 151.10, 136.32, 129.82, 126.90, 126.72, 124.75, 121.96, 119.36, 116.80, 49.60, 49.03, 46.22, 43.46. HRMS (ESI) *m/z*: $[M + Na]^+$ calcd for $C_{18}H_{17}N_3OS$, 346.0990; found, 346.3317.

Benzothiazol-2-yl(4-(2-methoxyphenyl) piperazin-1-yl)methanone (5g)

Pale yellow solid, yield: 93%, mp 128–130 °C, IR (neat) υ: 1614 cm^{-1} (C=O). ^{1}H-NMR (400 MHz, $CDCl_3$) δ (ppm): 8.10 (d, *J* = 8 Hz, 1H), 7.96 (d, *J* = 8 Hz, 1H), 7.54–7.49 (m, 2H), 7.07– 7.03 (m, 1H), 6.96 – 6.89 (m, 3H), 4.65 (t, *J* = 8 Hz, 2H), 4.05 (t, *J* = 4 Hz, 2H), 3.90 (s, 3H), 3.20 (t, *J* = 4 Hz, 4H). ^{13}C-NMR (100

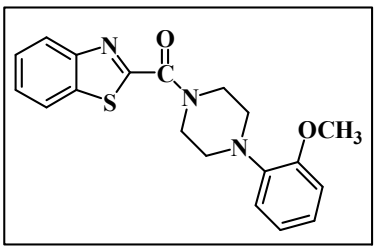

MHz, $CDCl_3$) δ (ppm): 164.82, 159.74, 153.12, 152.30, 140.62, 136.22, 126.69, 126.56, 124.63, 123.61, 121.87, 121.10, 118.52, 111.34, 55.47, 51.34, 50.72, 46.84, 43.87. HRMS (ESI) *m/z*: $[M + H]^+$ calcd for $C_{19}H_{19}N_3O_2S$, 354.1276; found, 354.1271.

Benzothiazol-2-yl(4-benzylpiperazin-1-yl)methanone (5h)

Yellow solid, yield: 91%, mp 155–157 °C, IR (neat) υ: 1619 cm^{-1} (C=O). ^{1}H-NMR (400 MHz, $CDCl_3$) δ (ppm): 8.09 (dd, *J* = 4 Hz, 1H), 7.96 (d, *J* = 4 Hz, 1H), 7.56–7.47 (m, 2H), 7.36–7.28 (m, 5H), 4.46 (t, *J*

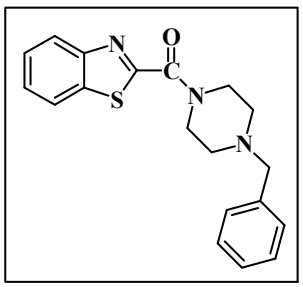

= 4 Hz, 2H), 3.89 (t, *J* = 4 Hz, 2H), 3.59 (s, 2H), 2.60 (m, 5H). ^{13}C-NMR (100 MHz, $CDCl_3$) δ (ppm): 164.79, 159.70, 153.09, 137.62, 136.18, 129.18, 128.37, 127.32, 126.63, 126.51, 124.59, 121.82, 62.88, 53.52, 52.82, 46.56, 43.65. HRMS (ESI) *m/z*: $[M + H]^+$ calcd for $C_{19}H_{19}N_3OS$, 338.1327; found, 338.1324.

Benzothiazol-2-yl(4-(2-hydroxyethyl)piperazin-1-yl)methanone (5i)

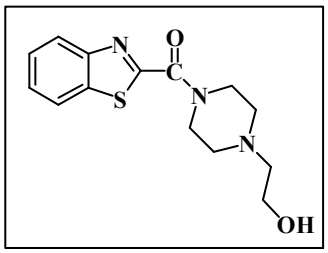

Brown solid, yield: 84%, mp 133–135 °C, IR (neat) υ: 1609 cm^{-1} (C=O), 3335 cm^{-1} (OH). ^{1}H-NMR (400 MHz, $CDCl_3$) δ (ppm): 8.07 (d, *J* = 8 Hz, 1H), 7.94 (d, *J* = 4 Hz, 1H), 7.53–7.45 (m, 2H), 4.46 (t, *J* = 4 Hz, 2H), 3.87 (t, *J* = 4 Hz, 2H), 3.68 (t, *J* = 4 Hz, 2H), 3.21 (s, 1H), 2.63 (m, 6H). ^{13}C-NMR (100 MHz, $CDCl_3$) δ (ppm): 164.50, 159.69, 153.00, 136.11, 126.73, 126.58, 124.59, 121.84, 59.48, 57.96, 53.48, 52.72, 46.41, 43.49. HRMS (ESI) *m/z*: $[M + H]^+$ calcd for $C_{14}H_{17}N_3O_2S$, 292.1120; found, 292.1133.

Benzothiazol-2-yl(4-ethylpiperazin-1-yl)methanone (5j)

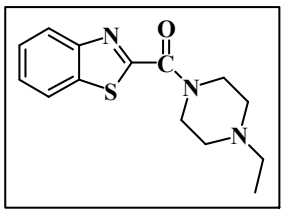

Brown solid, yield: 79%, mp 150–152 °C, IR (neat) υ: 1622 cm^{-1} (C=O). ^{1}H-NMR (400 MHz, $CDCl_3$) δ (ppm): 8.08 (d, *J* = 8 Hz, 1H), 7.95 (d, *J* = 4 Hz, 1H), 7.54–7.46 (m, 2H), 4.48 (t, *J* = 4 Hz, 2H), 3.89 (t, *J* = 4 Hz, 2H), 2.59 (t, *J* = 4 Hz, 4H), 2.49 (q, *J* = 4 Hz, 2H), 1.13 (t, *J* = 4 Hz, 3H). ^{13}C-NMR (100 MHz, $CDCl_3$) δ (ppm): 164.69, 159.63, 153.05, 136.15, 126.65, 126.52, 124.58, 121.81, 53.23, 52.43, 52.18, 46.37, 43.44, 11.82. HRMS (ESI) *m/z*:$[M + H]^+$ calcd for $C_{14}H_{17}N_3OS$, 276.1171; found, 276.1171.

(4-(2-Aminoethyl)piperazin-1-yl)(benzothiazol-2-yl)methanone (5k)

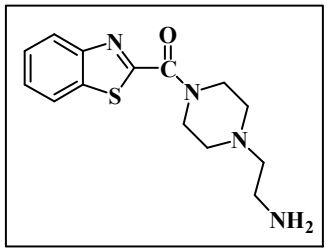

Creamy white solid, yield: 81%, mp 138–140 °C, IR (neat) υ: 1614 cm^{-1} (C=O). ^{1}H-NMR (400 MHz, $CDCl_3$) δ (ppm): 8.10 (d, *J* = 8 Hz, 1H), 7.98 (d, *J* = 4 Hz, 1H), 7.57–7.47 (m, 2H), 3.63 (t, *J* = 4 Hz, 2H), 3.02 (t, *J* = 4 Hz, 2H), 2.67 (t, *J* = 4 Hz, 2H), 2.60 (t, *J* = 4 Hz, 6H), 1.27 (s, 2H). ^{13}C-NMR (100 MHz, $CDCl_3$) δ (ppm): 163.98, 159.99, 152.98, 137.06, 126.76, 126.67, 124.34, 122.38, 57.00, 56.61, 53.21, 53.00, 45.27, 36.36. HRMS (ESI) *m/z*: $[M + H]^+$calcd for $C_{14}H_{18}N_4OS$, 291.1280; found, 291.1270.

Benzothiazol-2-yl(4-(pyrimidin-2-yl)piperazin-1-yl)methanone (5l)

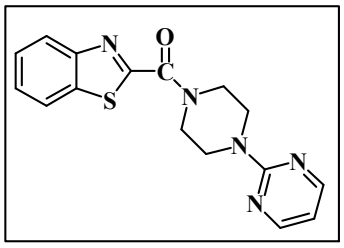

White solid, yield: 91%, mp 125–127 °C, IR (neat) υ: 1619 cm^{-1} (C=O). ^{1}H-NMR (400 MHz, $CDCl_3$) δ (ppm): 8.37 (d, *J* = 4 Hz, 2H), 8.13 (d, *J* = 8 Hz, 1H), 7.99 (d, *J* = 8 Hz, 1H), 7.58–7.50 (m, 2H), 6.57 (t, *J* = 4 Hz, 1H), 4.55 (t, *J* = 4 Hz, 2H), 4.01 (t, *J* = 4 Hz, 4H), 3.95 (t, *J* = 4 Hz, 2H). ^{13}C-NMR (100 MHz, $CDCl_3$) δ (ppm): 164.57, 161.55, 160.02, 157.82, 153.10, 136.22, 126.77, 126.60, 124.70, 121.87, 110.53, 46.40, 44.26, 43.55, 43.50. HRMS (ESI) *m/z*: $[M + H]^{+}$calcd for $C_{16}H_{15}N_5OS$, 326.1076; found, 326.1076.

7.6. Representative Spectra

^{1}H and ^{13}C-NMR Spectra of Compound 3a:

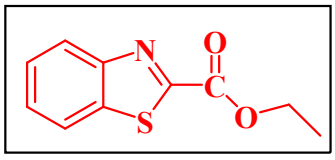

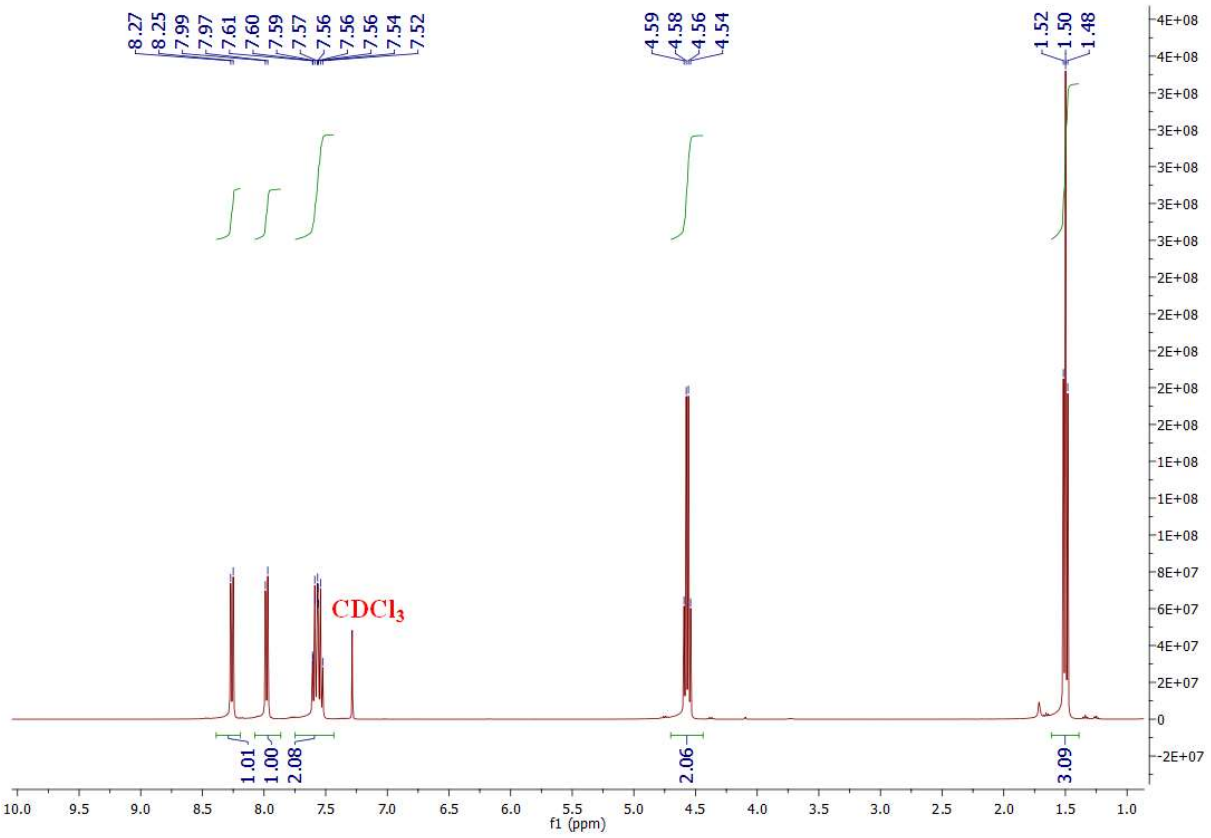
8.27
8.25
7.99
7.97
7.61
7.60
7.59
7.57
7.56
7.56
7.56
7.54
7.52
4.59
4.58
4.56
4.54
1.52
1.50
1.48
CDCl3
1.01
1.00
2.08
2.06
3.09
f1 (ppm)

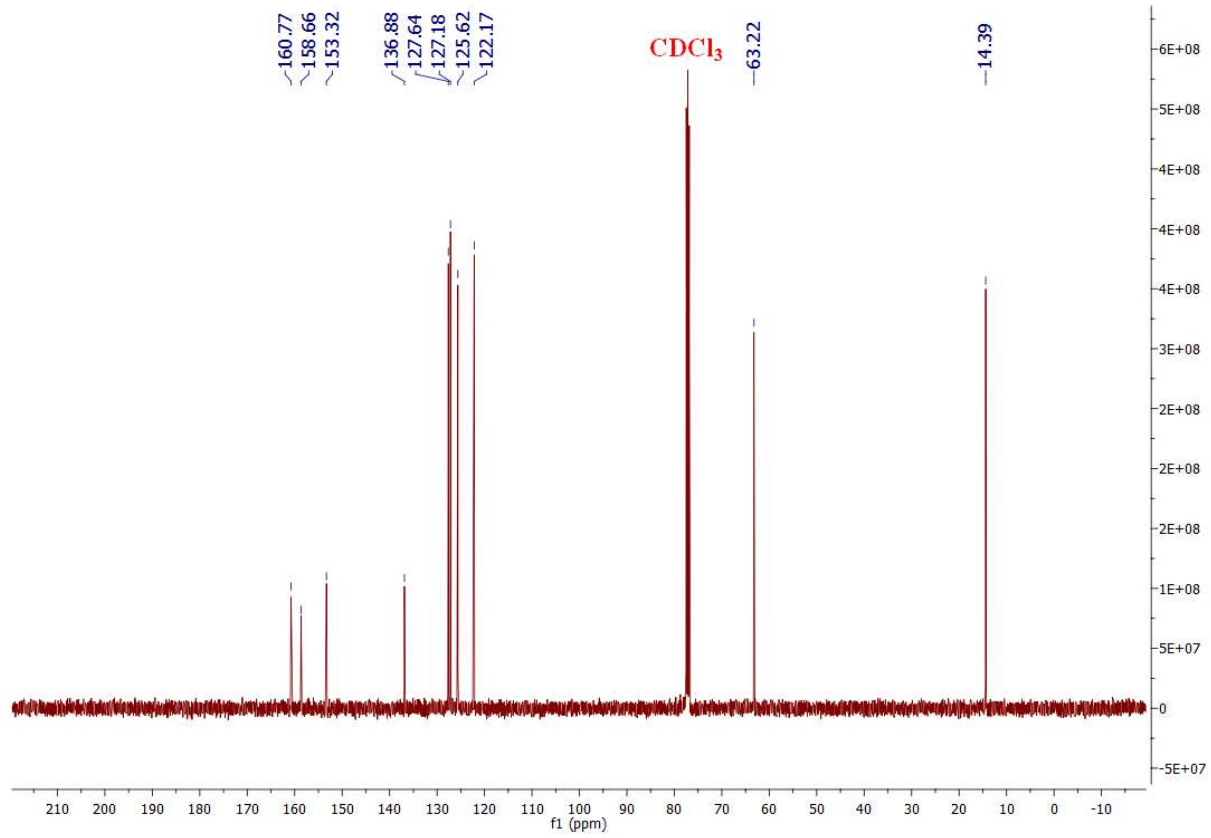

^{1}H and ^{13}C-NMR Spectra of Compound 5a:

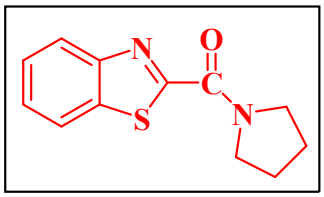

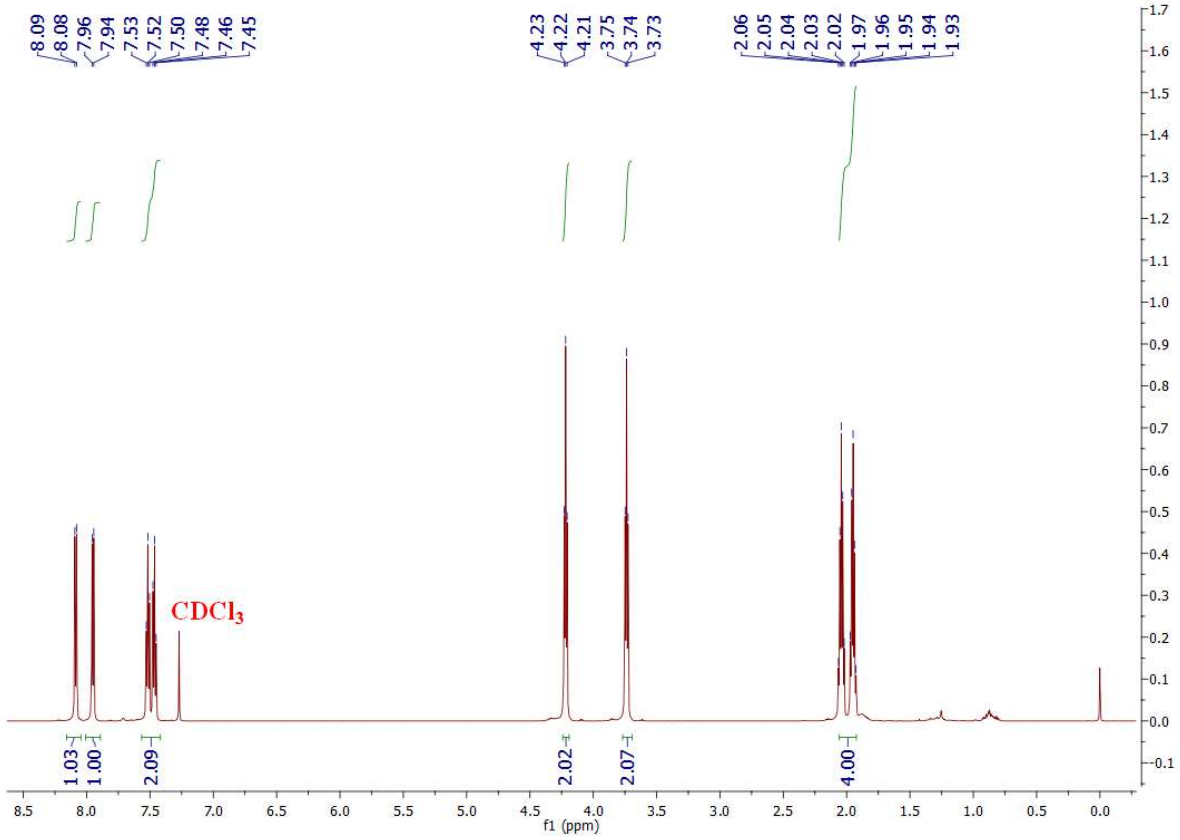
8.09
8.08
7.96
7.94
7.53
7.52
7.50
7.48
7.46
7.45
4.23
4.22
4.21
3.75
3.74
3.73
2.06
2.05
2.04
2.03
2.02
1.97
1.96
1.95
1.94
1.93
CDCl3
1.03
1.00
2.09
2.02
2.07
4.00
f1 (ppm)

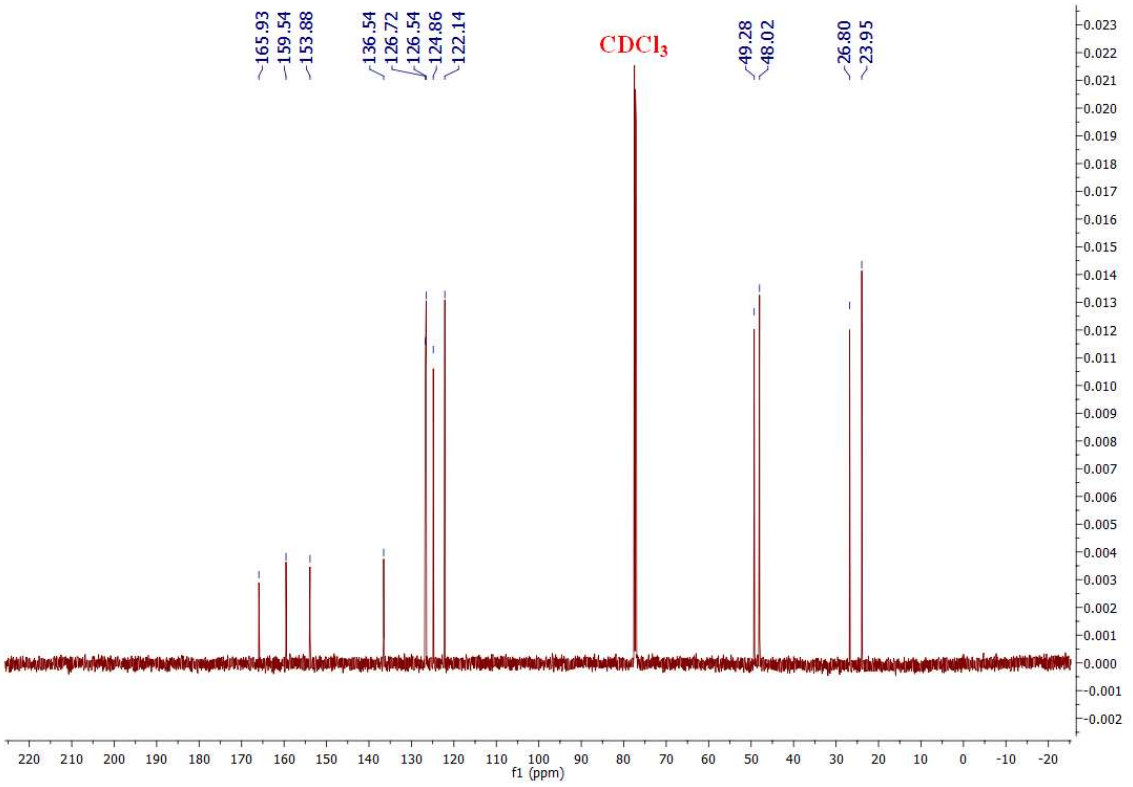
165.93
159.54
153.88
136.54
126.72
126.54
124.86
122.14
CDCl3
49.28
48.02
26.80
23.95
f1 (ppm)

^{1}H and ^{13}C-NMR Spectra Compound 5f:

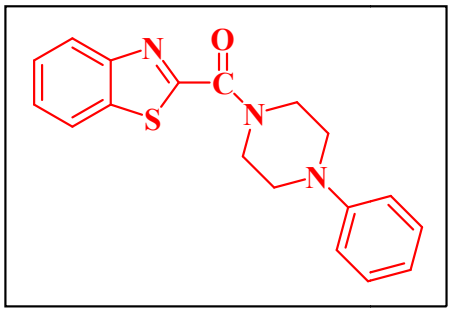

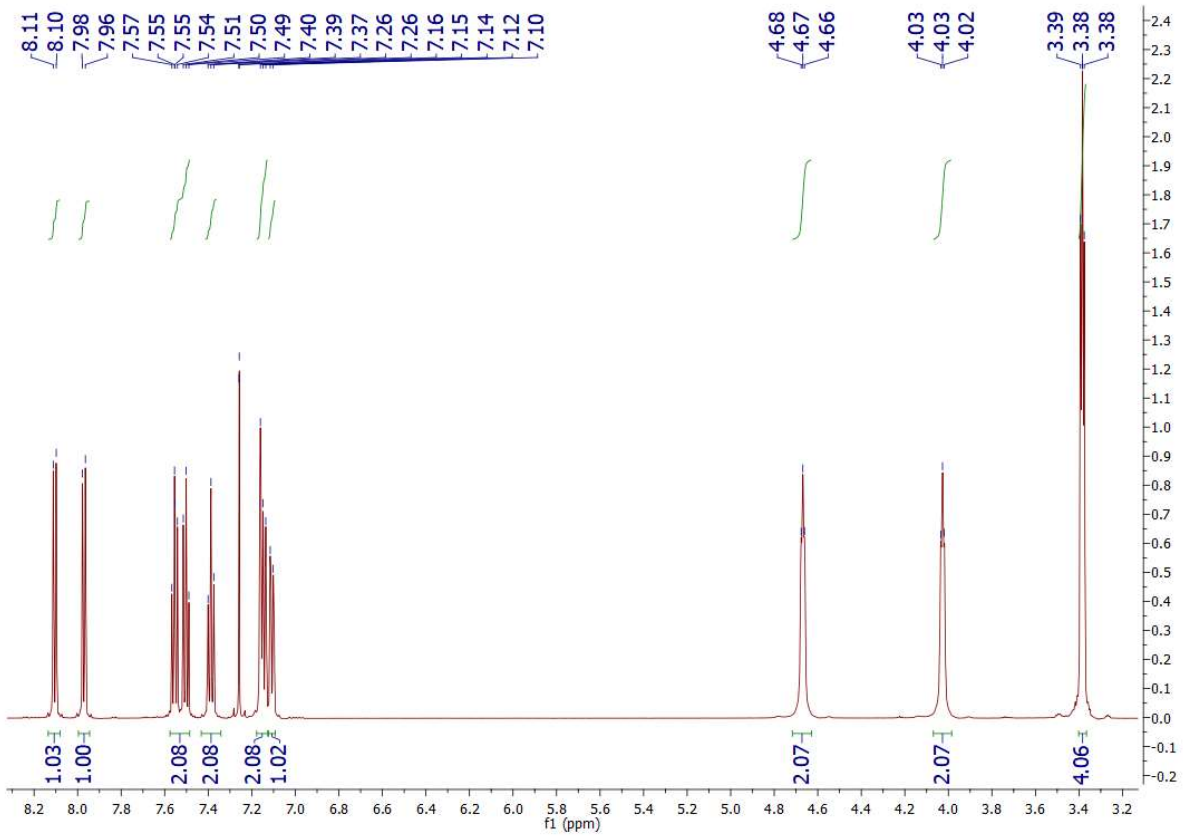

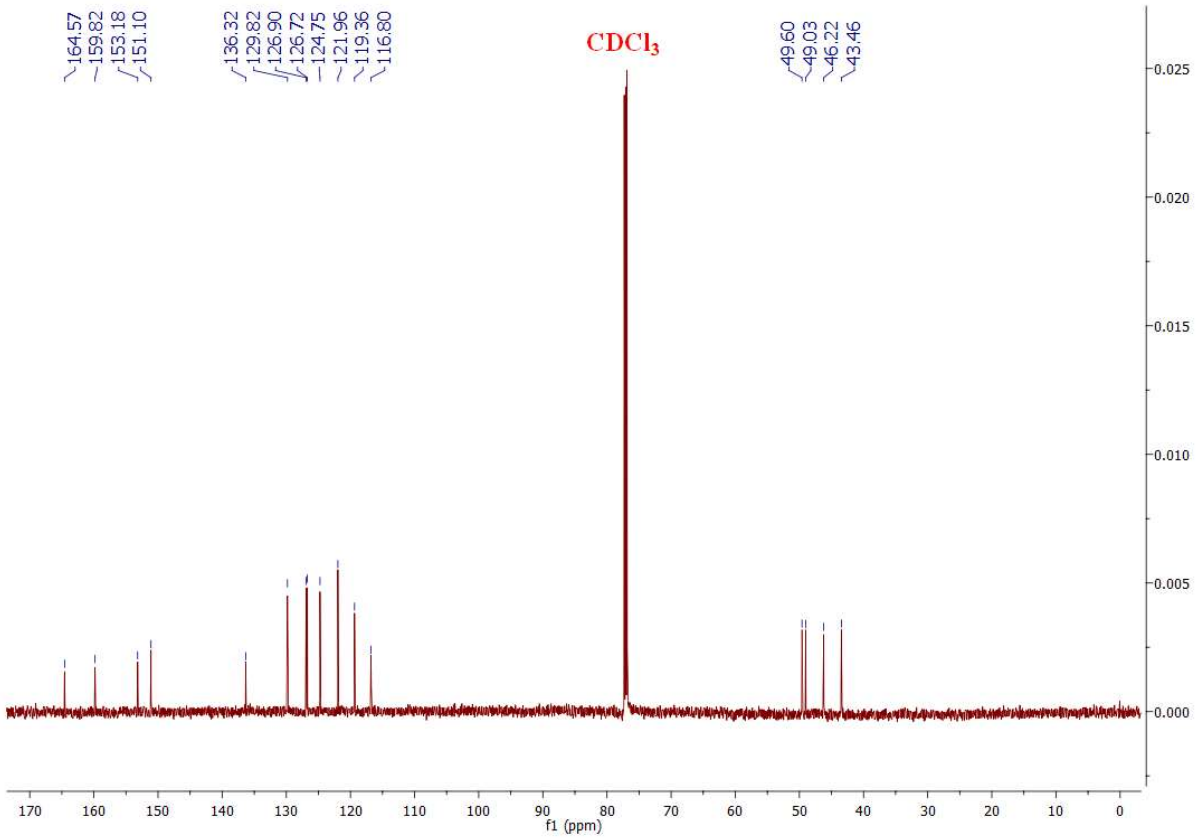

^{1}H and ^{13}C-NMR Spectra of Compound 5l:

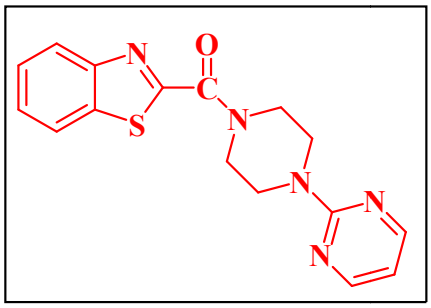

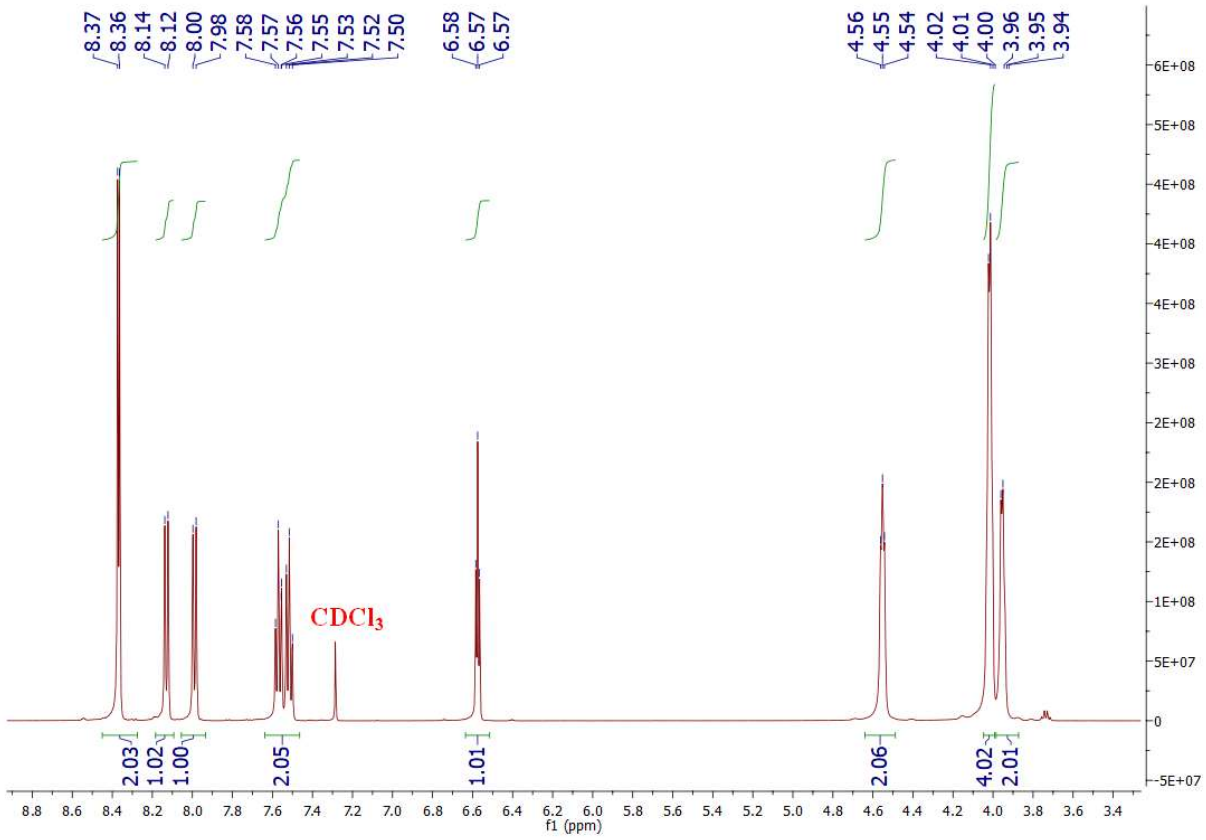
8.37
8.36
8.14
8.12
8.00
7.98
7.58
7.57
7.56
7.55
7.53
7.52
7.50
6.58
6.57
6.57
4.56
4.55
4.54
4.02
4.01
4.00
3.96
3.95
3.94
CDCl3
2.03
1.02
1.00
2.05
1.01
2.06
4.02
2.01
f1 (ppm)

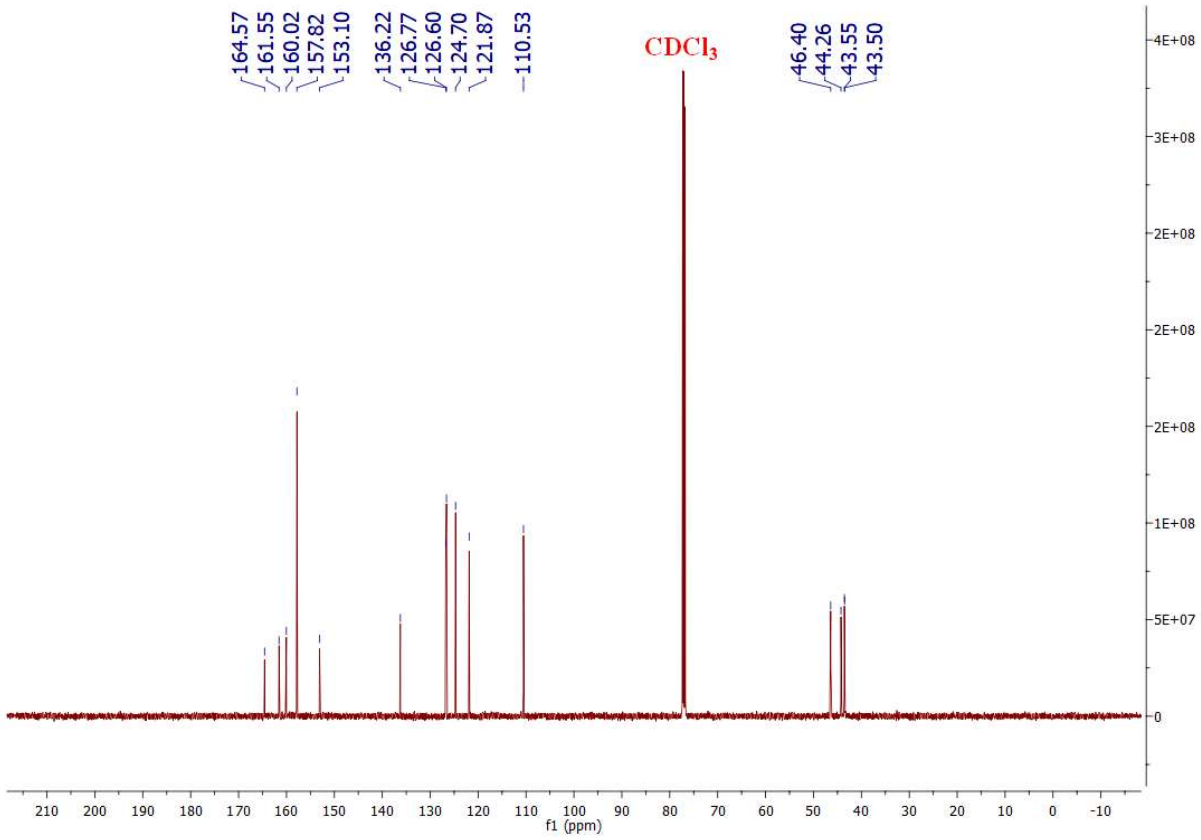

IR Spectrum of Compound 5g:

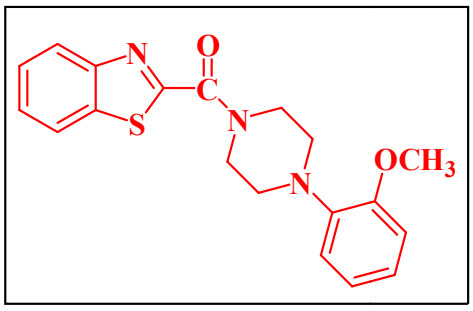

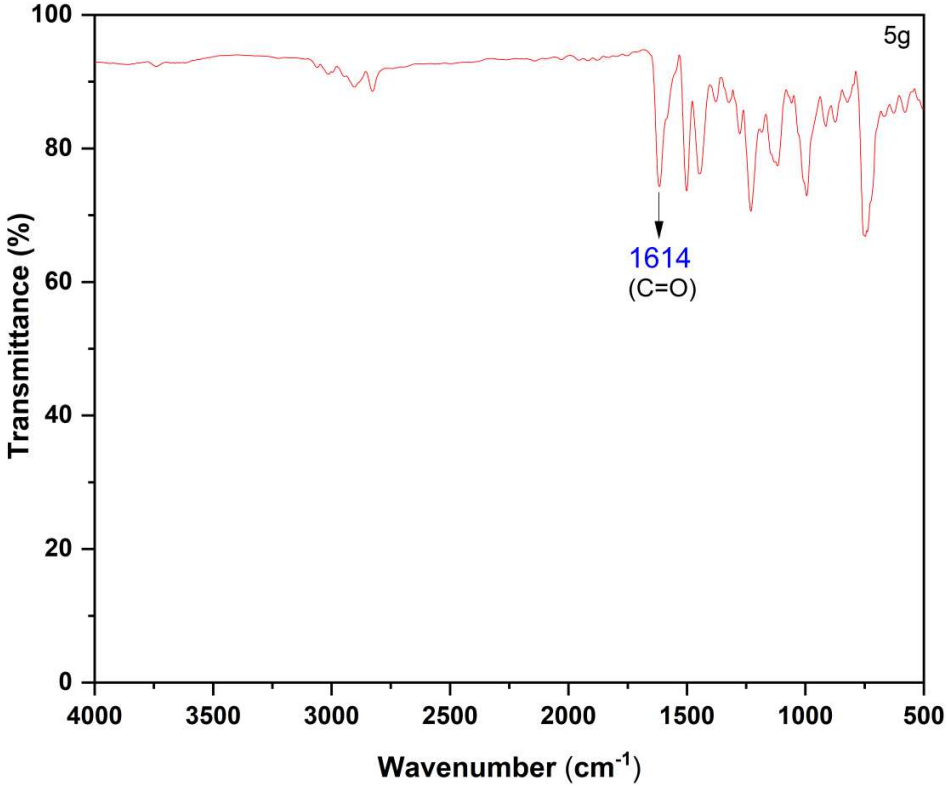

IR Spectrum of Compound 5h:

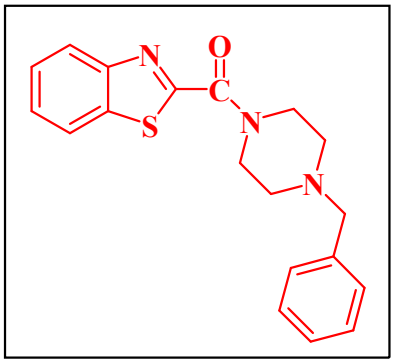

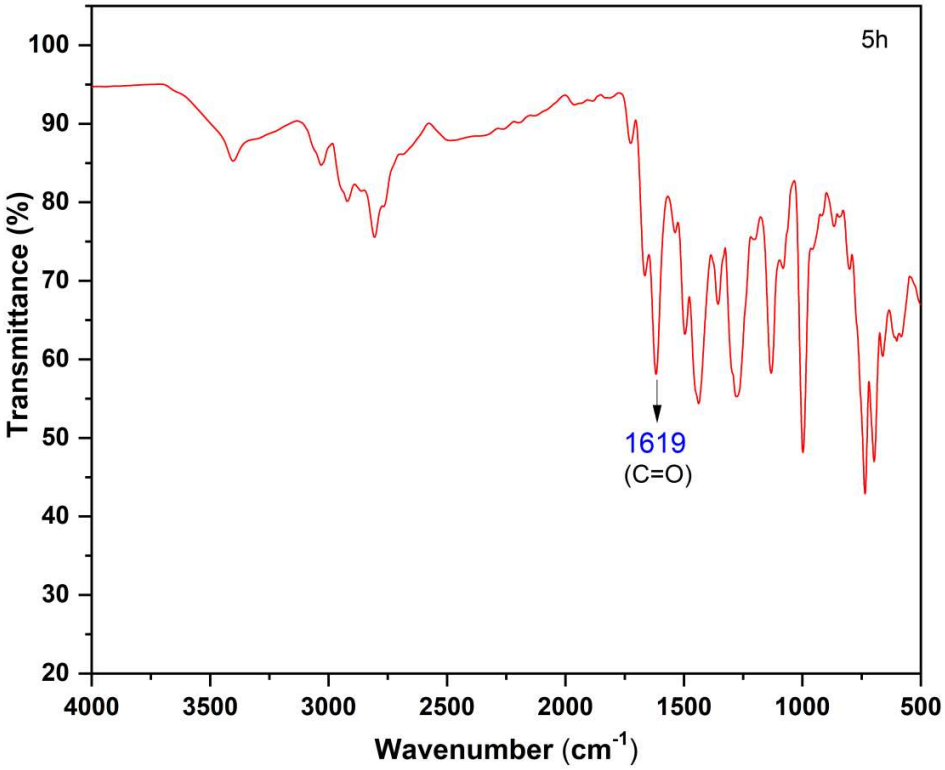

IR Spectrum of Compound 5l:

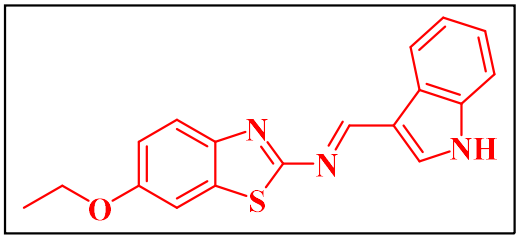

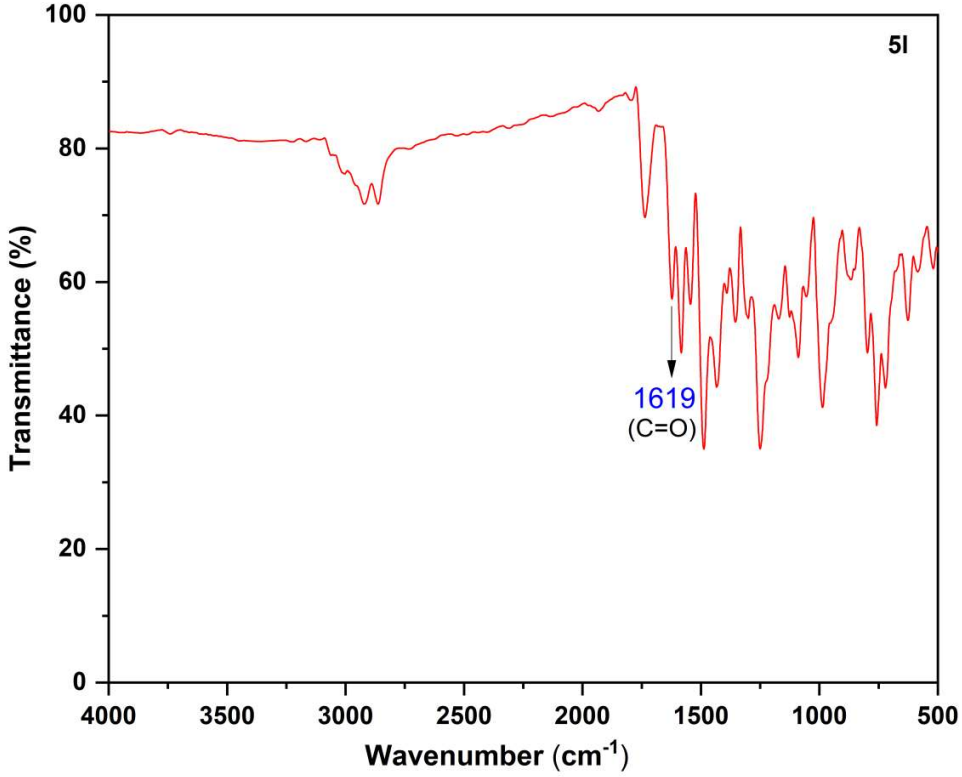

7.7. Experimental Procedure for the Synthesis of Benzothiazole-Indole Schiff Bases

7.7.1. Base-Catalyzed Synthesis of Schiff Bases: A solution of indole-3-carbaldehyde or 2-phenyl-indole-3-carboxaldehyde and 2-aminobenzothiazoles in a 1:1 stoichiometric ratio was prepared in either ethanol or methanol. The reaction mixture was refluxed at 65 °C (for methanol and 80 °C for ethanol) for the specified duration while being catalyzed by five drops of piperidine. After completion of the refluxing period, the reaction mixture was allowed to cool, resulting in the formation of a solid precipitate. This precipitate was separated by filtration, and the obtained solid was subjected to drying. Subsequently, the dried solid was recrystallized from ethanol, yielding the desired pure compounds.

7.7.2. Base-Free Synthesis of Schiff Bases: Into a 50 mL round bottom flask, indole-3-carbaldehyde or 2-phenyl-indole-3-carboxaldehyde, the corresponding amine, and either ethanol or methanol (15 mL) as the solvent was added. This mixture was then stirred at 65 °C (for methanol) (80 °C in case of ethanol) using an oil bath for 3 hours. Once the reaction's completion

was confirmed by TLC, the hot reaction mixture was cautiously transferred into ice-cold water. After cooling, the resulting solid precipitate was isolated through filtration. The collected solid was subsequently dried and subjected to recrystallization in ethanol, ultimately yielding the desired pure compounds.

7.8. Spectroscopic Data

(E)-1-(1H-indol-3-yl)-N-(4-methylbenzo[*d*]thiazol-2-yl)methanimine (3a)

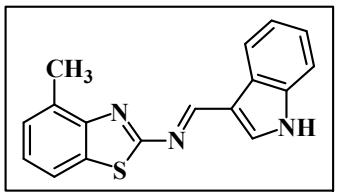

Yellow solid, yield: 90%, mp: 175-177 °C, IR (neat) υ: 1635 cm^{-1} (-CH=N), 3498 cm^{-1} (NH). ^{1}H-NMR (500 MHz, $CDCl_3$) δ (ppm): 12.27 (s, 1H), 9.21 (s, 1H, -CH=N), 8.39-8.36 (m, 2H), 7.80 (d, *J* = 8 Hz, 1H), 7.55 (dd, *J* = 4 Hz, 1H), 7.33-7.23 (m, 4H), 3.33 (s, 3H). ^{13}C-NMR (125 MHz, DMSO) δ (ppm): 172.19, 161.07, 151.62, 137.52, 133.03, 131.29, 130.33, 126.90, 126.70, 124.52, 122.08, 120.78, 119.37, 118.27, 114. 38, 112.52, 18. 24. LC-MS *m/z*: [M + H] calcd for $C_{17}H_{13}N_3S$, 291.08; found, 292.00.

(E)-1-(1H-indol-3-yl)-N-(6-nitrobenzo[*d*]thiazol-2-yl)methanimine (3b)

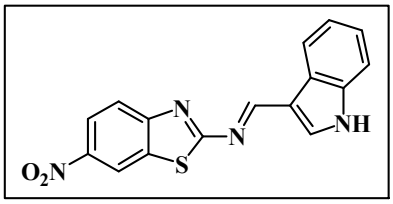

Reddish yellow solid, yield: 95%, mp: 180-183 °C, IR (neat) υ: 1640 cm^{-1} (-CH=N), 1567 and 1329 cm^{-1} (N-O), 3498 cm^{-1} (NH). ^{1}H-NMR (500 MHz, DMSO) δ (ppm): 9.32 (s, 1H, -CH=N), 9.05 (d, *J* = 4 Hz, 1H), 8.48 (s, 1H), 8.36 (d, *J* = 4 Hz, 1H), 8.30 (d, *J* = 8 Hz, 1H), 7.99 (d, *J* = 8 Hz, 1H), 7.57 (d, *J* = 4 Hz, 1H), 7.33 (m, 2H). ^{13}C-NMR (125 MHz, DMSO) δ (ppm): 179.58, 163.19, 156.81, 143.76, 138.26, 138.07, 134.51, 125.01, 124.53, 123.08, 122.58, 122.30, 122.09, 119.50, 115.19, 113.31. HRMS (ESI) *m/z*: $[M + H]^+$ calcd for $C_{16}H_{10}N_4O_2S$, 323.0603; found, 323.0599. HRMS *m/z*: $[M + H]^+$ calcd for $C_{16}H_{10}N_4O_2S$, 322.0524; found, 323.0599.

(E)-1-(1H-indol-3-yl)-N-(6-methoxybenzo[*d*]thiazol-2-yl)methanimine (3c)

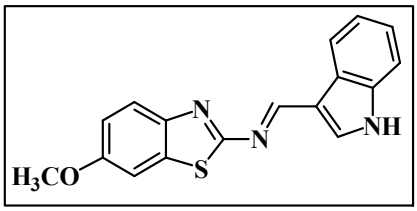

Yellow solid, yield: 88%, mp 190-192 °C, IR (neat) υ: 1630 cm^{-1} (-CH=N), 3498 cm^{-1} (NH). ^{1}H-NMR (500 MHz, DMSO) δ (ppm): 12.22 (s, 1H), 9.19 (s, 1H, -CH=N), 8.35 (dd, *J* = 4 Hz, 2H), 7.75 (d, *J* = 8 Hz, 1H), 7.59 (d, *J* = 4 Hz, 1H), 7.55 (dd, *J* = 4 Hz, 1H), 7.32 – 7.27 (m, 2H), 7.07 (dd, *J* = 4 Hz, 1H), 3.84 (s, 3H). ^{13}C-NMR (125 MHz, DMSO) δ (ppm): 171.46, 160.87, 157.19, 146.34, 138.68, 138.01, 135.15,

125.02, 124.11, 122.87, 122.50, 122.46, 115.57, 114.88, 113.00, 105.65, 56.15. LC-MS *m/z*: [M + H] calcd for $C_{17}H_{13}N_3OS$, 307.07; found, 308.00.

(E)-N-(6-ethoxybenzo[*d*]thiazol-2-yl)-1-(1H-indol-3-yl)methanimine (3d)

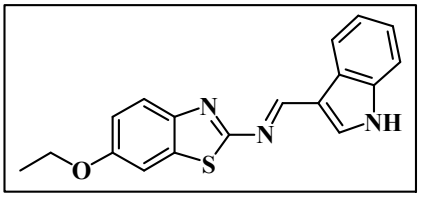

Yellow solid, yield: 90%, mp 172-175 °C, IR (neat) υ: 1630 cm^{-1} (-CH=N), 3498 cm^{-1} (NH). ^{1}H-NMR (500 MHz, DMSO) δ (ppm): 12.21 (s, 1H), 9.19 (s, 1H, -CH=N), 8.35 (m, 2H), 7.73 (d, *J* = 8 Hz, 1H), 7.56 (dd, *J* = 4 Hz, 2H), 7.32 – 7.26 (m, 2H), 7.05 (dd, *J* = 4 Hz, 1H), 4.10 (q, *J* = 4 Hz, 2H), 1.37 (t, *J* = 8 Hz, 3H). ^{13}C-NMR (125 MHz, DMSO) δ (ppm): 171.41, 160.80, 156.42, 146.29, 138.64, 138.02, 135.16, 125.04, 124.09, 122.87, 122.47, 115.93, 114.90, 112.99, 106.26, 64.14, 15.15. LC-MS *m/z*: [M + H] calcd for $C_{18}H_{15}N_3OS$, 321.09; found, 322.00.

(E)-N-(benzo[*d*]thiazol-2-yl)-1-(1H-indol-3-yl)methanimine (3e)

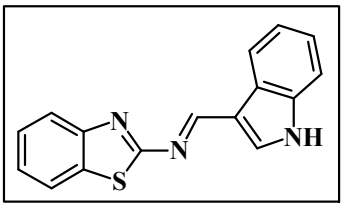

Yellow solid, yield: 81%, mp: 188-190 °C, IR (neat) υ: 1621 cm^{-1} (-CH=N), 3498 cm^{-1} (NH). ^{1}H-NMR (500 MHz, $CDCl_3$) δ (ppm): 9.26 (s, 1H, -CH=N), 8.60 (d, *J* = 4 Hz, 1H), 7.99 (d, *J* = 8 Hz, 1H), 7.95 (s, 1H), 7.85 (d, *J* = 4 Hz, 1H), 7.49 (t, *J* = 8 Hz, 2H), 7.39 – 7.35 (m, 3H). LC-MS *m/z*: [M + H] calcd for $C_{16}H_{11}N_3S$, 277.06; found, 278.00.

(E)-N-(4-methylbenzo[*d*]thiazol-2-yl)-1-(2-phenyl-1H-indol-3-yl)methanimine (3f)

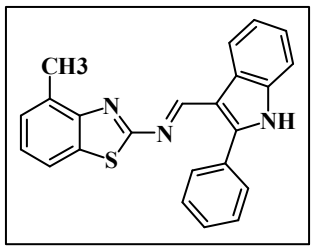

Yellow solid, yield: 88%, mp 192-194 °C, IR (neat) υ: 1621 cm^{-1} (-CH=N), 3498 cm^{-1} (NH). ^{1}H-NMR (500 MHz, $CDCl_3$) δ (ppm): 10.11 (s, 1H), 9.13 (s, 1H, -CH=N), 8.72 (d, *J* = 8 Hz, 1H), 7.66 – 7.62 (m, 3H), 7.58 – 7.55 (m, 3H), 7.46 (d, *J* = 4 Hz, 1H), 7.36 – 7.31 (m, 2H), 7.26 – 7.21 (m, 2H), 2.74 (s, 3H). ^{13}C-NMR (125 MHz, DMSO) δ (ppm): 173.06, 161.42, 147.98, 136.15, 133.57, 132.44, 130.47, 129.90, 129.46, 129.27, 129.15, 126.79, 126.31, 124.55, 124.31, 123.83, 122.94, 118.90, 112.21, 111.06, 18.61. LC-MS *m/z*: [M + H] calcd for $C_{23}H_{17}N_3S$, 367.11; found, 368.00.

7.9. Representative Spectra

^{1}H and ^{13}C-NMR Spectra of Compound 3b:

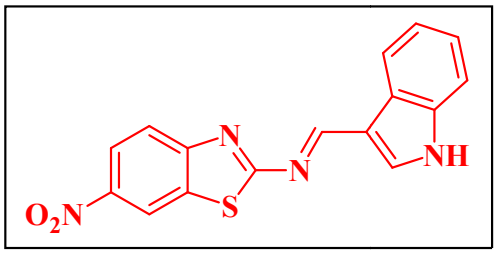
O2N
S
N
N
NH

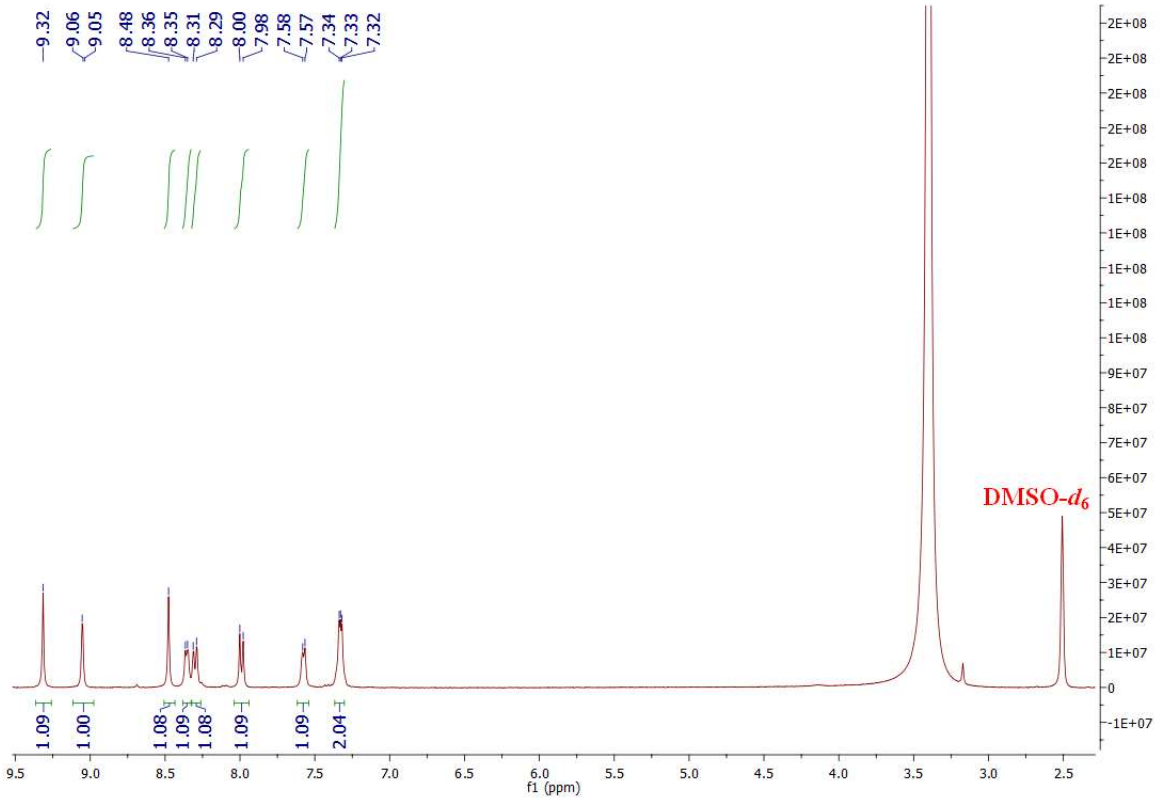
9.32
9.06
9.05
8.48
8.36
8.35
8.31
8.29
8.00
7.98
7.58
7.57
7.34
7.33
7.32
DMSO-d6
1.09
1.00
1.08
1.09
1.08
1.09
1.09
2.04
f1 (ppm)

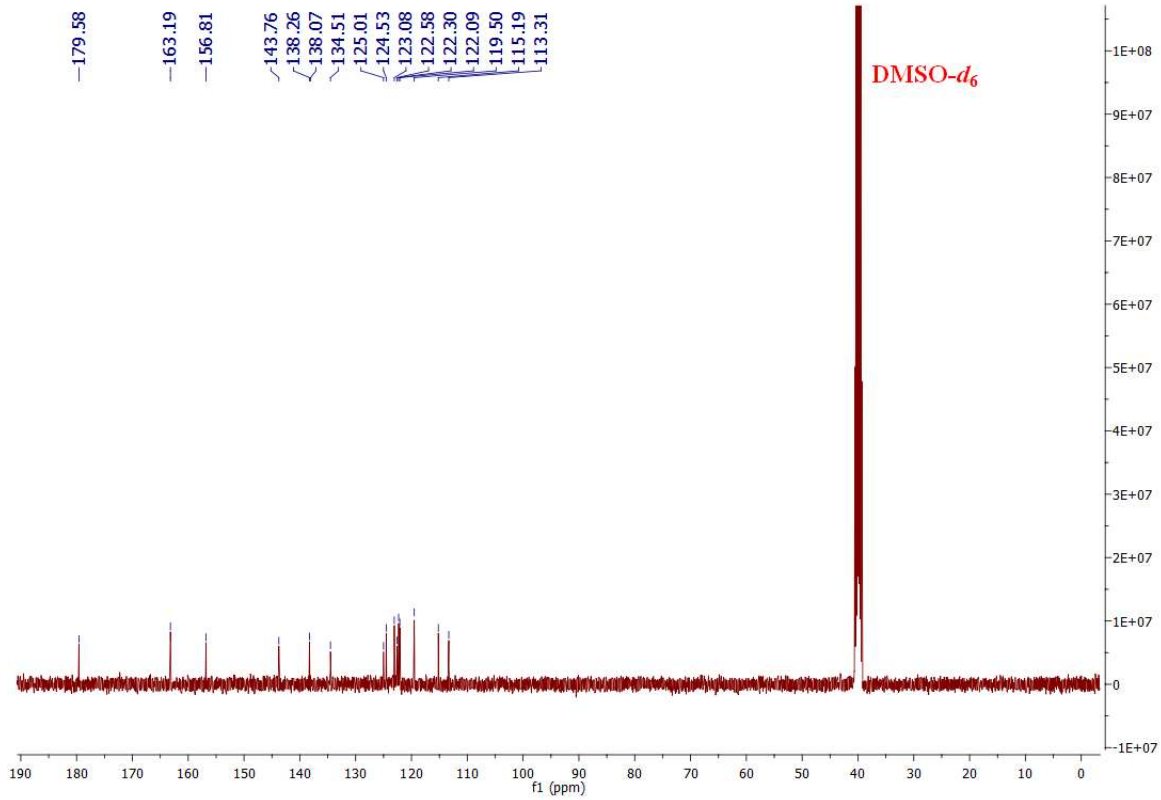

^{1}H and ^{13}C-NMR Spectra of Compound 3c:

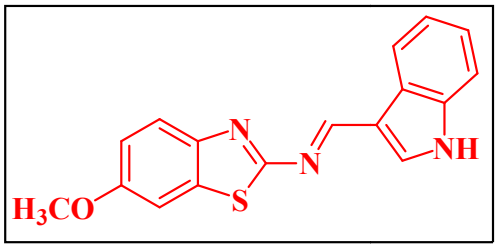

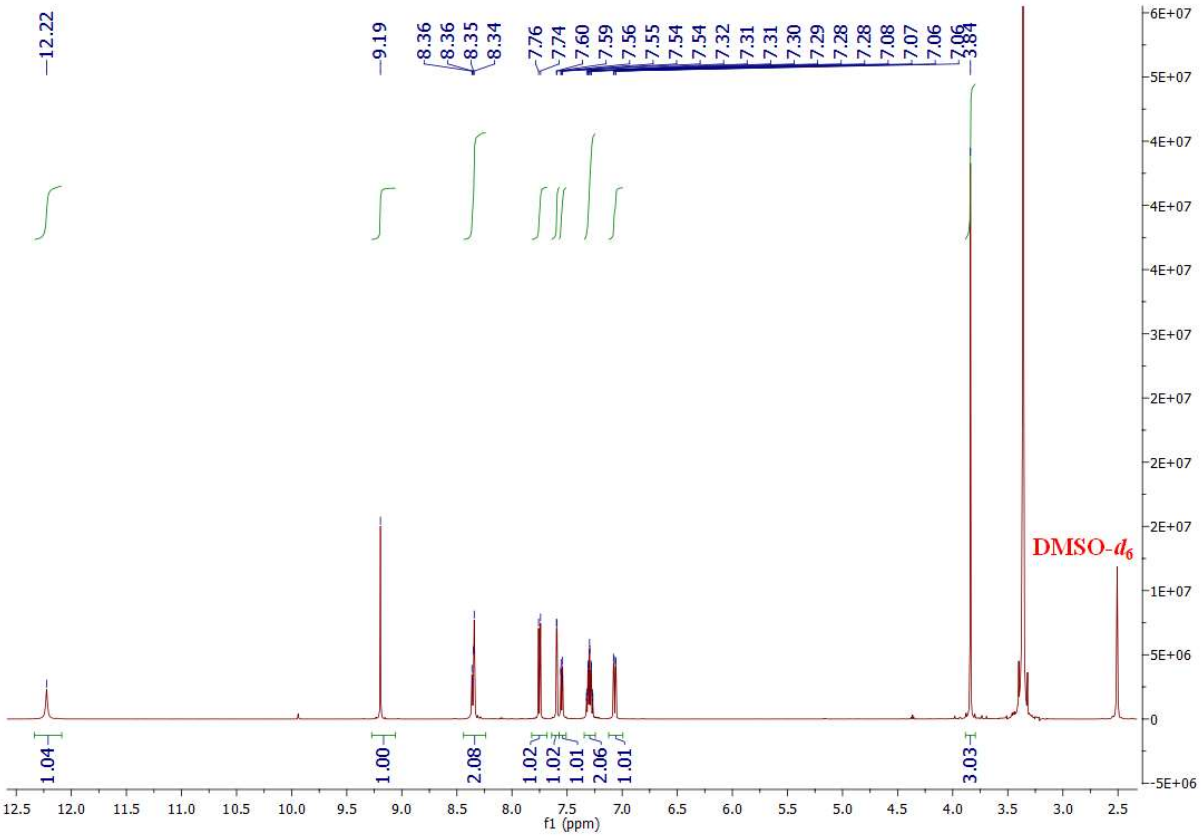
12.22
9.19
8.36
8.36
8.35
8.34
7.76
7.74
7.60
7.59
7.56
7.55
7.54
7.54
7.32
7.31
7.31
7.30
7.29
7.28
7.28
7.08
7.07
7.06
7.06
3.84
DMSO-d_6
1.04
1.00
2.08
1.02
1.02
1.01
2.06
1.01
3.03
f1 (ppm)

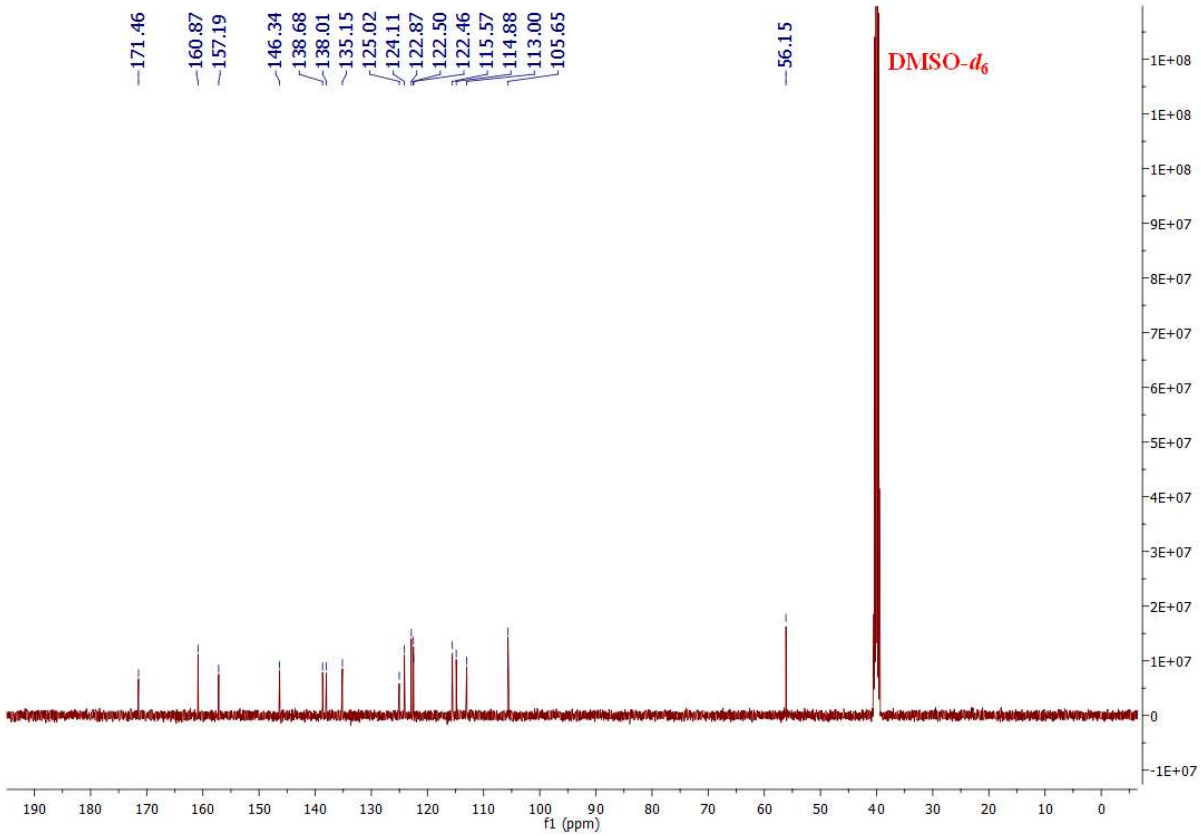

^{1}H and ^{13}C-NMR Spectra of Compound 3d:

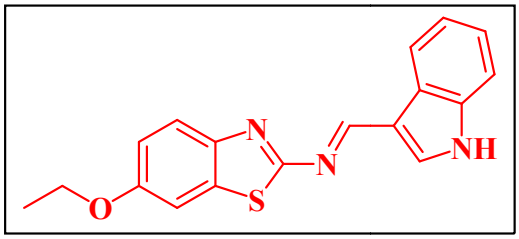

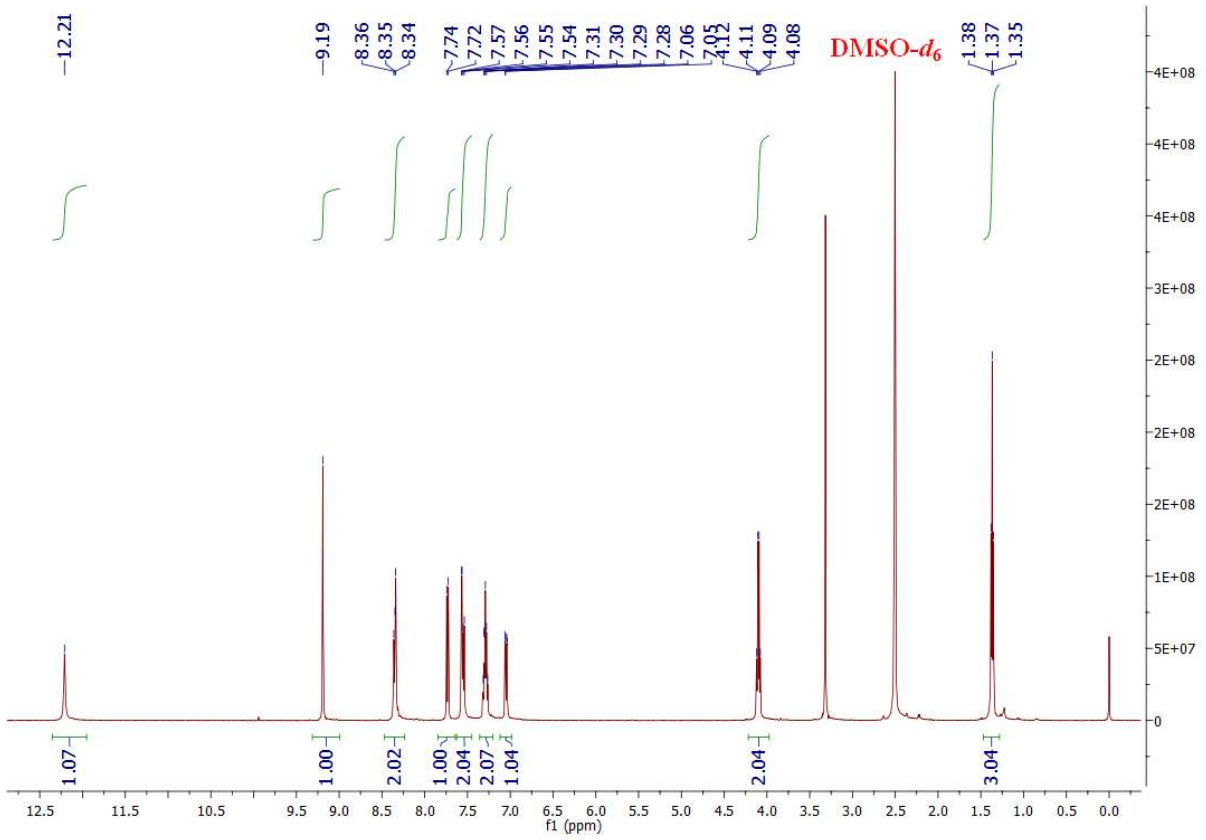
12.21
9.19
8.36
8.35
8.34
7.74
7.72
7.57
7.56
7.55
7.54
7.31
7.30
7.29
7.28
7.06
7.05
4.12
4.11
4.09
4.08
DMSO-d_6
1.38
1.37
1.35
1.07
1.00
2.02
1.00
2.04
2.07
1.04
2.04
3.04
f1 (ppm)

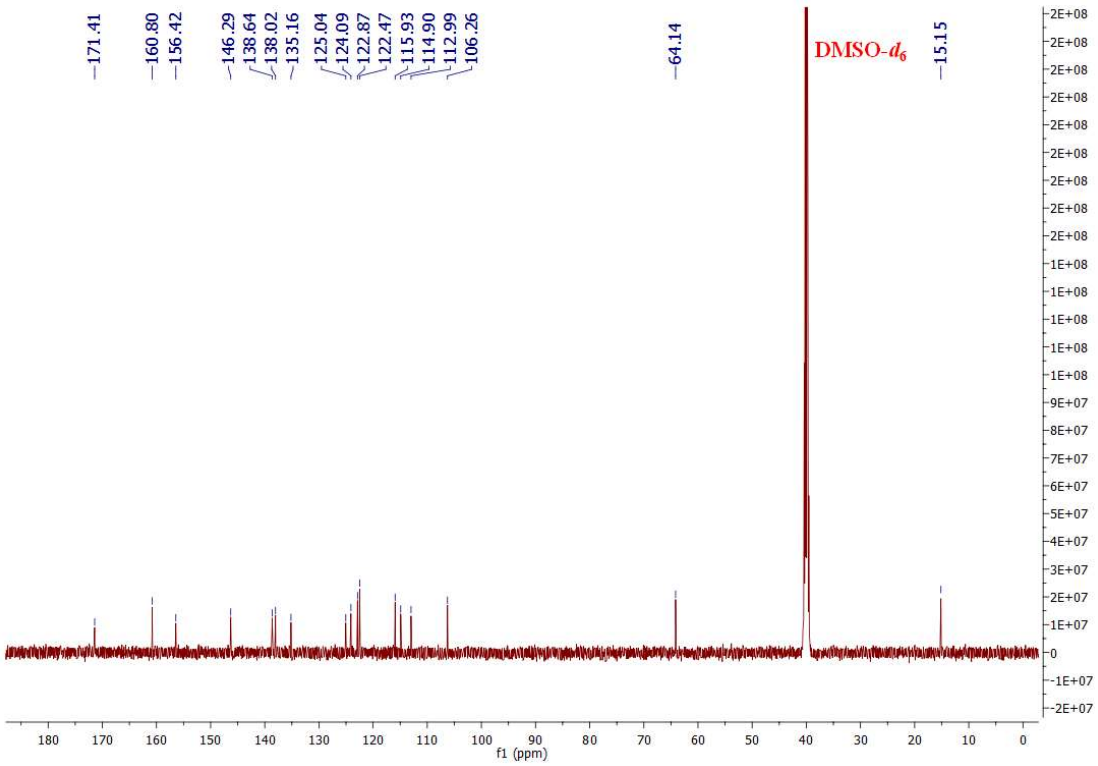

^{1}H and ^{13}C-NMR Spectra of Compound 3f:

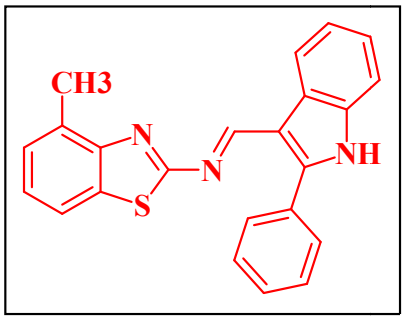

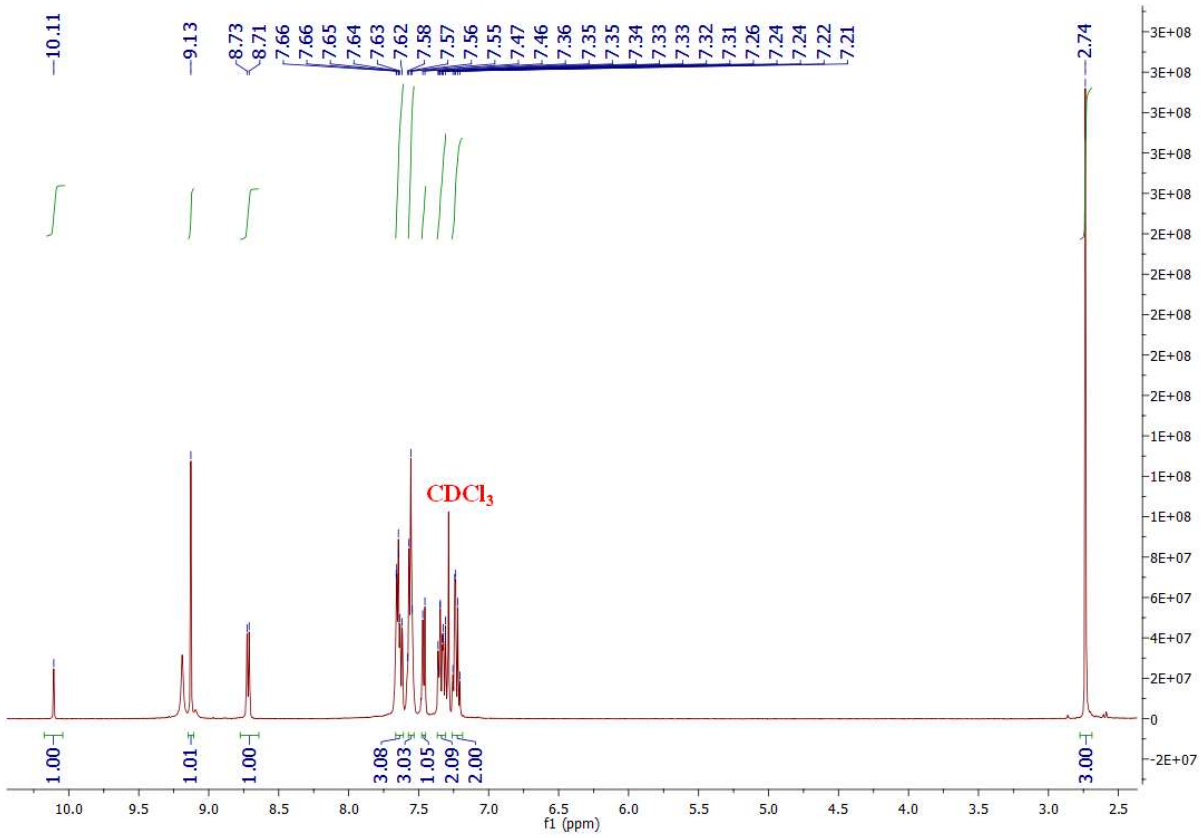
10.11
9.13
8.73
8.71
7.66
7.66
7.65
7.64
7.63
7.62
7.58
7.57
7.56
7.55
7.47
7.46
7.36
7.35
7.35
7.34
7.33
7.33
7.32
7.31
7.26
7.24
7.24
7.22
7.21
2.74
CDCl3
1.00
1.01
1.00
3.08
3.03
1.05
2.09
2.00
3.00
f1 (ppm)

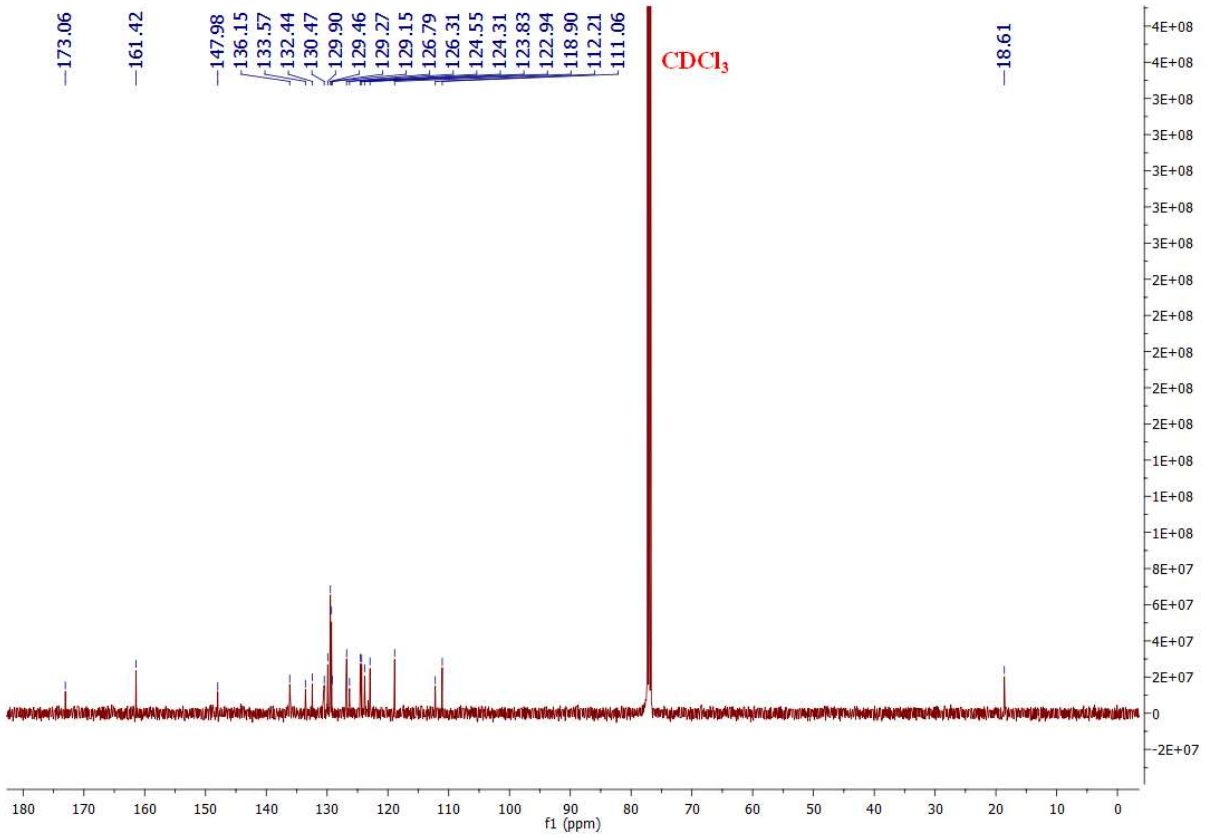

IR Spectrum of Compound 3b:

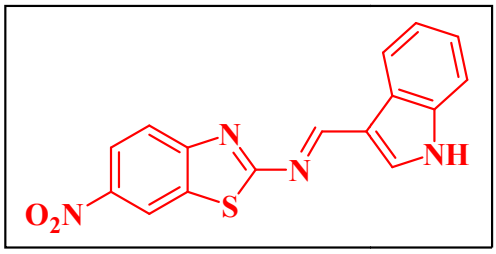

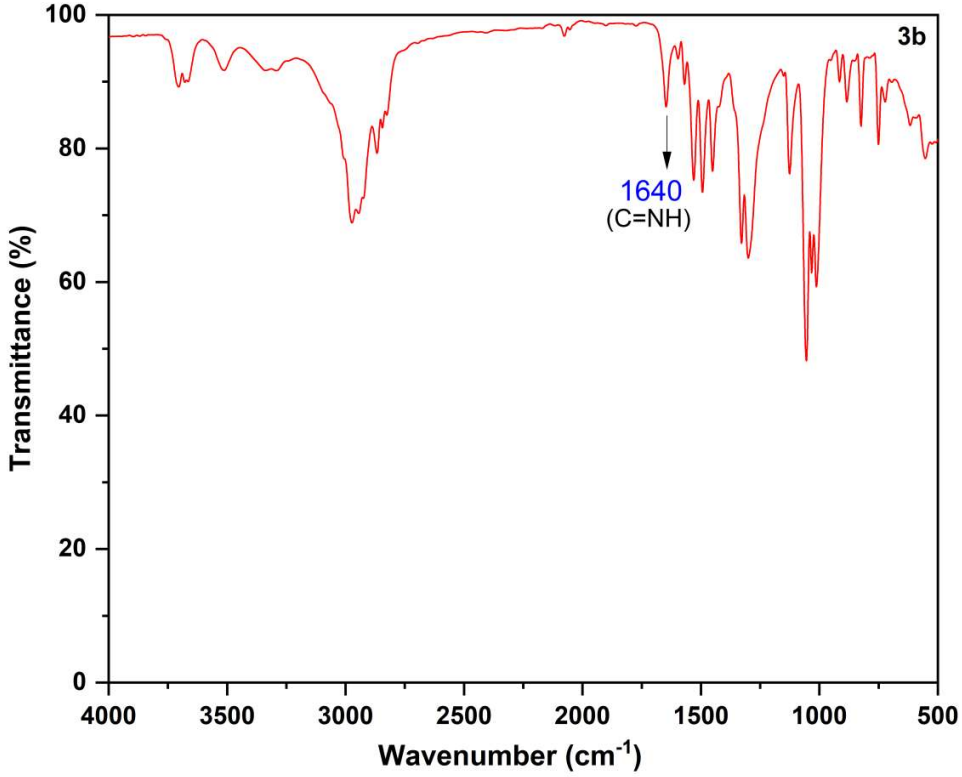

IR Spectrum of Compound 3c:

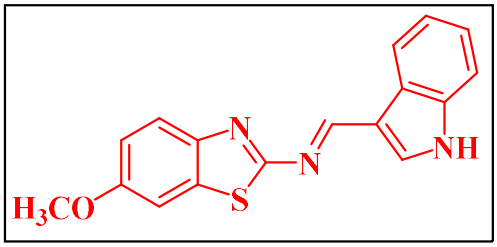

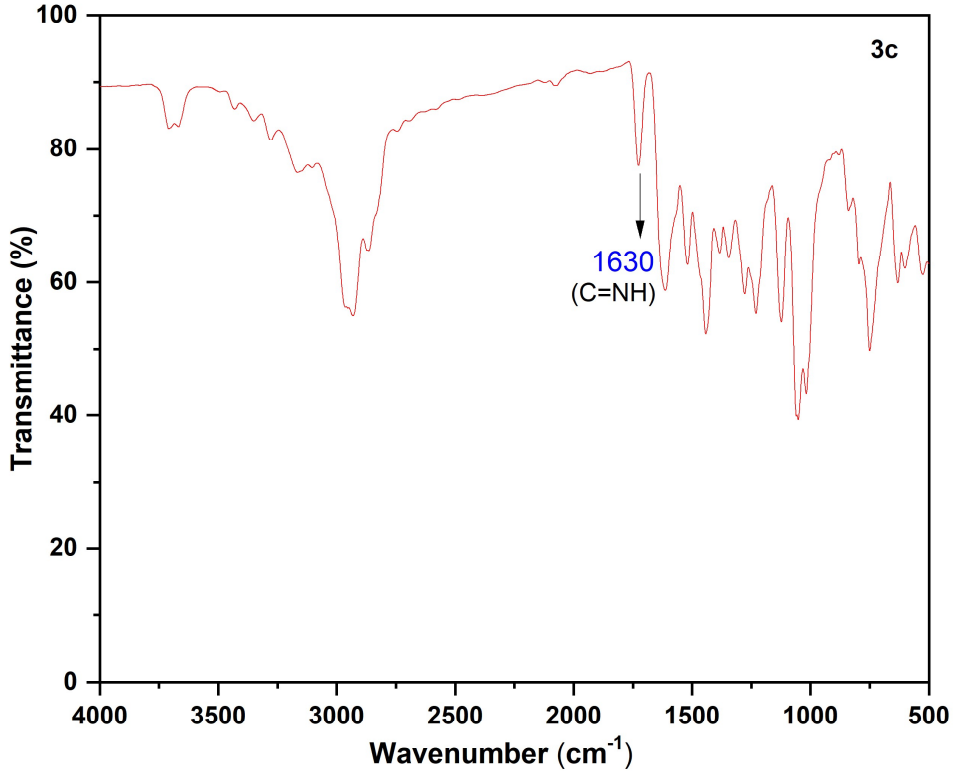

IR Spectrum of Compound 3d:

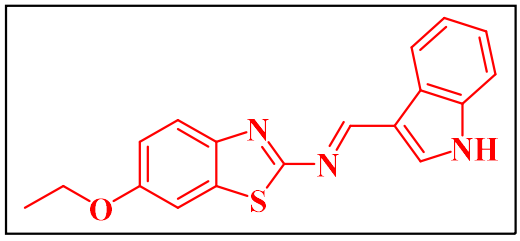

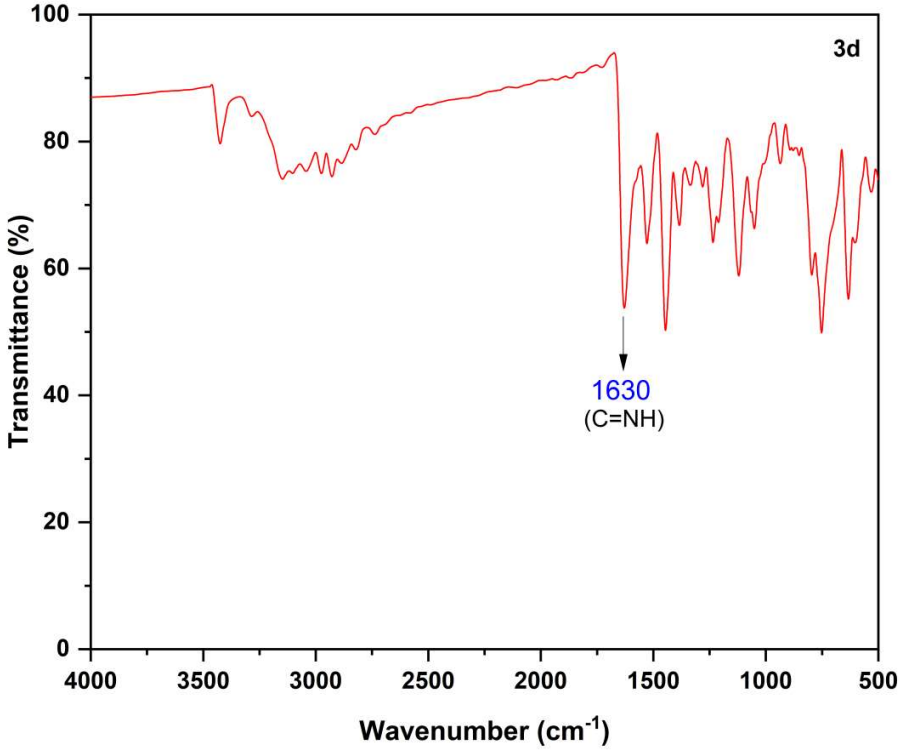

IR Spectrum of Compound 3f:

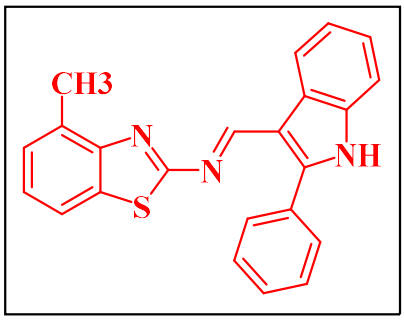

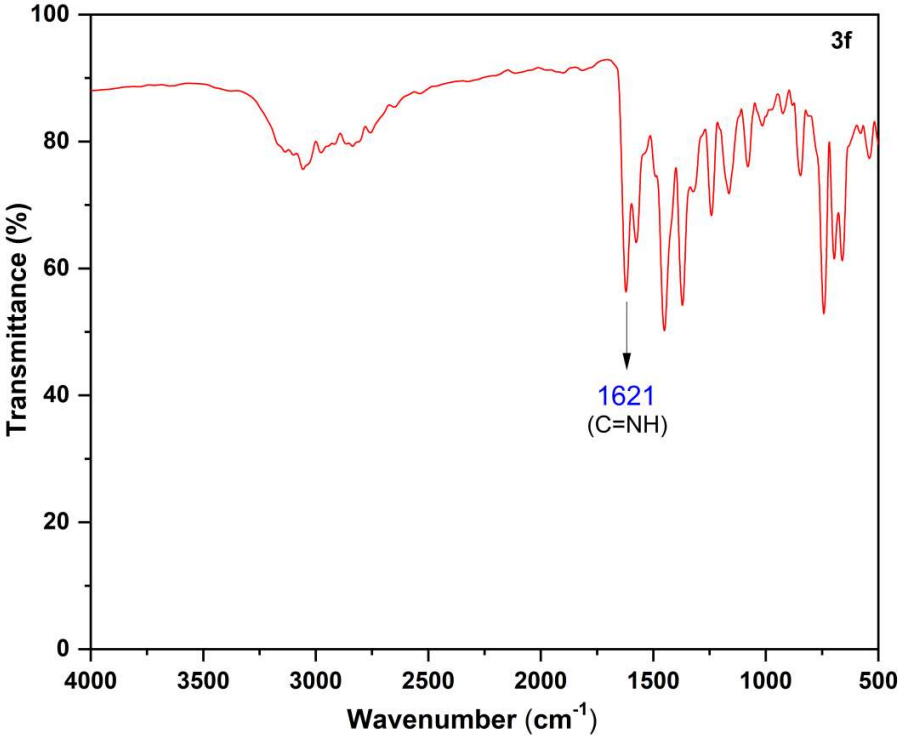
3f
1621
(C=NH)
Transmittance (%)
Wavenumber (cm-1)
100
80
60
40
20
0
4000
3500
3000
2500
2000
1500
1000
500

CHAPTER-8

FUTURE SCOPE

8.1. 2-Azidobenzothiazoles: Important scaffolds for click chemistry

In click chemistry, organic azides play a key role. Applications for the cycloaddition of organic azides and terminal alkynes are numerous, including combinatorial drug development, and bioconjugation. The synthesis of triazoles begins with organic azides, one type of 1, 3-dipole that is particularly significant. These heterocyclic derivatives have important uses in chemical biology, pharmaceuticals, and material science, among others. Additionally, several benzothiazole analogs bearing triazole moiety **(Fig.-8.1)** have been investigated as potential anticancer, anti-inflammatory, anti-nociceptive, FGFR1 inhibitors, analgesic and antimicrobial agents. Fluconazole, other antifungal medications, voriconazole, and albaconazole all include 1, 2, 4-triazole. However, no commercially available medications include the 1, 2, 3-triazole ring. Diligent attempts have been undertaken to integrate 1, 2, 3-triazole into currently available medications, further study is required to identify the lead molecule. Moreover, benzothiazole analogs play a crucial role as a foundational structure for future molecular investigations to produce novel compounds. Hence, we were intrigued by the opportunity to design new compounds that would be very useful in click chemistry (**Scheme-8.1**), for which ***Carolyn R. Bertozzi***, ***Morten Meldal***, and ***K. Barry Sharpless*** got the ***Noble Prize in 2022***, and would be utilized for the formation of biologically significant scaffolds. Recently, Singh *et al*. synthesized triazoles derived from benzothiazole as promising antimicrobial agents, and various substituted aryl azides were reacted with dialkyne substituted 2-aminobenzothiazole to generate desired compounds by click chemistry. Compound (**1**) demonstrated its highest efficacy against both Gram (+) and Gram (-) bacterial strains, boasting a MIC value of 3.12 µg/mL. This potency is twice as effective as the standard drug ciprofloxacin, which has a MIC of 6.25 µg/mL (**Fig.-8.2**). Similarly, Jakopec *et al*. synthesized and assessed the cytotoxicity activity of 1, 2, 3-triazoles of benzothiazole derivatives (**Fig.-8.3**). Both methodologies utilized dialkyne substituted 2-aminobenzothiazoles. Here, we synthesized 2-azidobenzothiazole derivatives which can react with different mono-propargylated and bis-propargylated compounds. The immense importance of 2-azidobenzothiazoles will further proceed when we apply them to the synthesis of pharmacologically significant heterocyclic scaffolds. This may provide an extra credential for the development of innovative protocols that might be worthy of curing diseases of new origin.

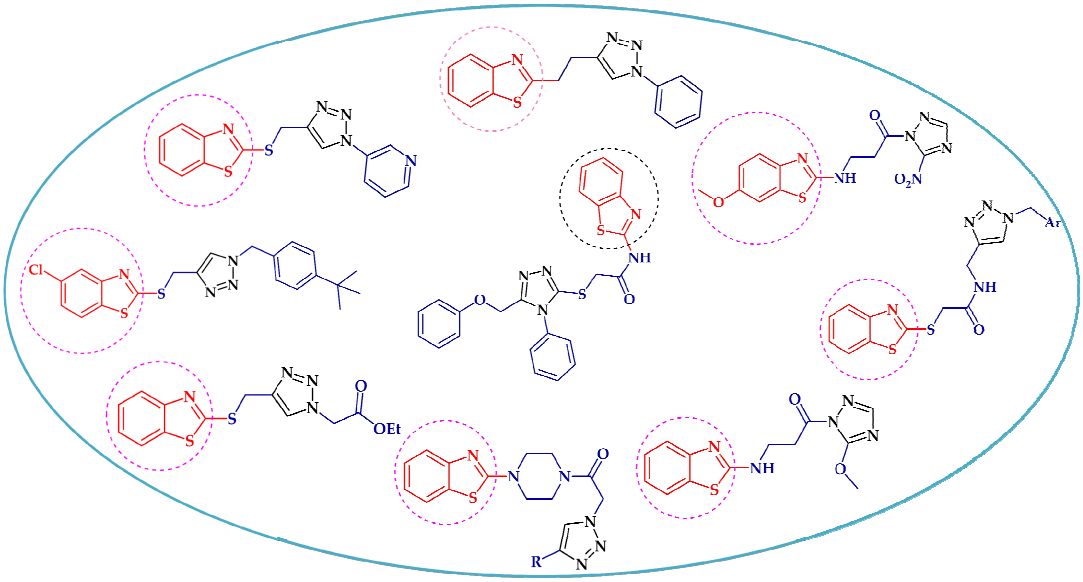

Fig.-8.1: Chemical structure of pharmacologically important triazole-based benzothiazole derivatives.

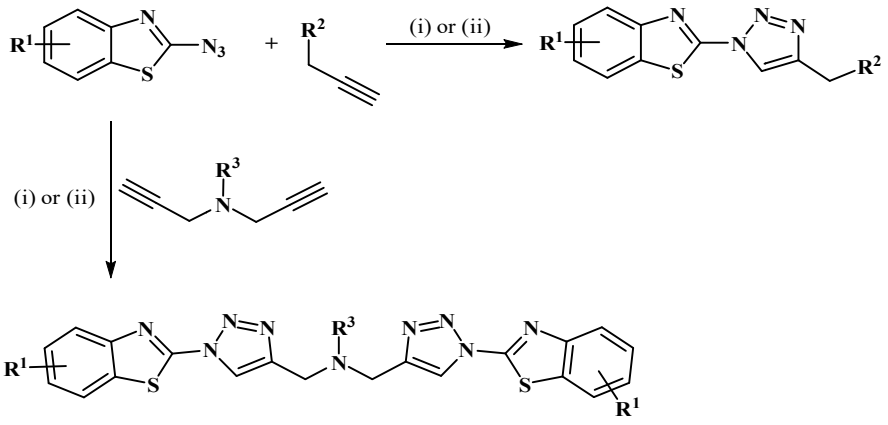

R^1 = H; 6-NO_2; 6-Cl; 6-OCH_3; 6-OC_2H_5; 5-Br; 4,6-F

R^2 = O, N; R^3 = Aryl, Alkyl

Reaction Conditions: (i) $CuSO_4$, Sodium Ascorbate, Tert-butanol:Water(1:1) Ultrasonication, 35° C (ii) $CuSO_4$, Sodium Ascorbate, Tert-butanol:Water(1:1) r.t.

Scheme-8.1: Substrate Scope of 2-azidobenzothiazoles.

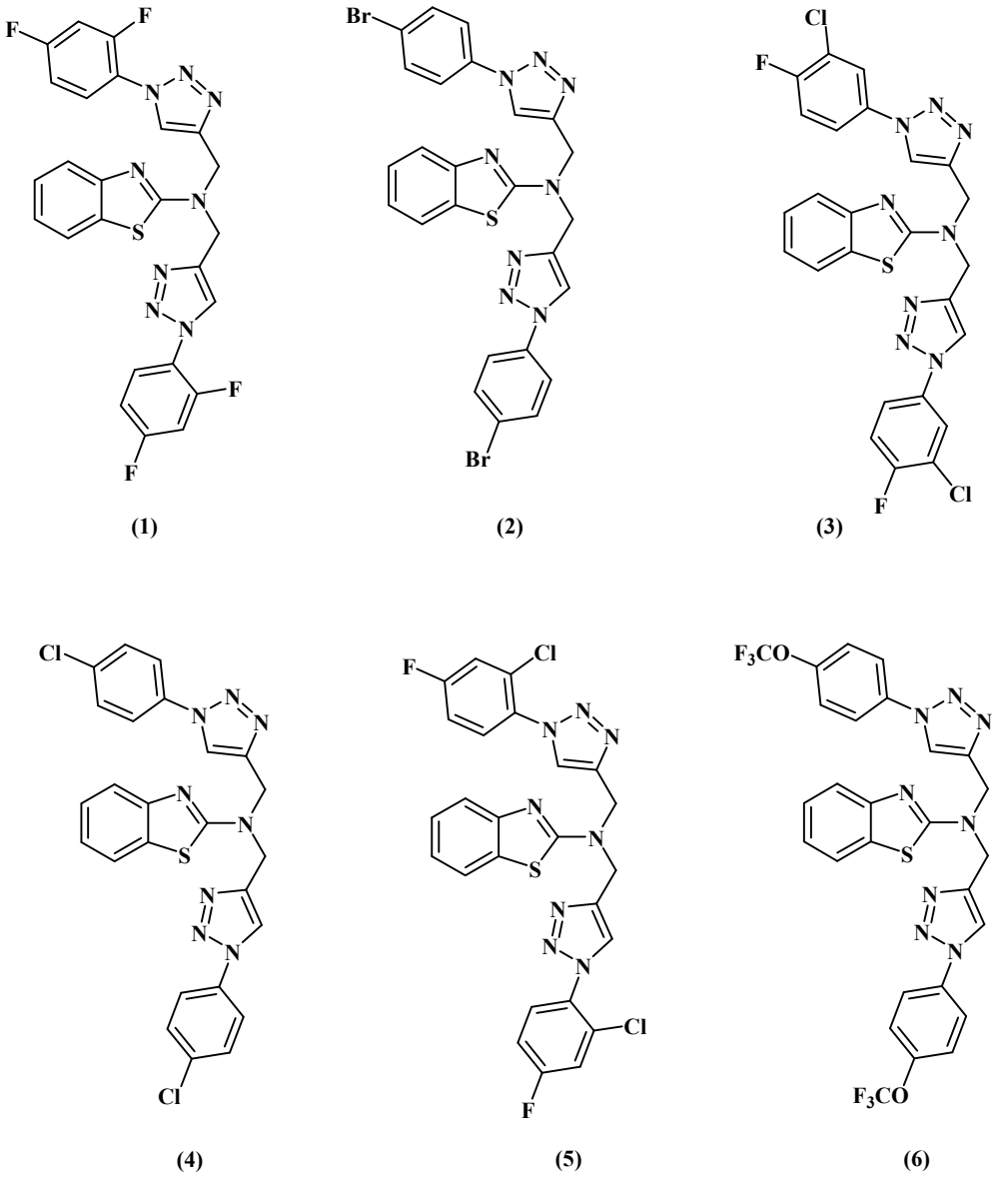

Fig.-8.2: Some compounds containing triazoles of benzothiazole scaffold that are reported as potent antimicrobial agents.

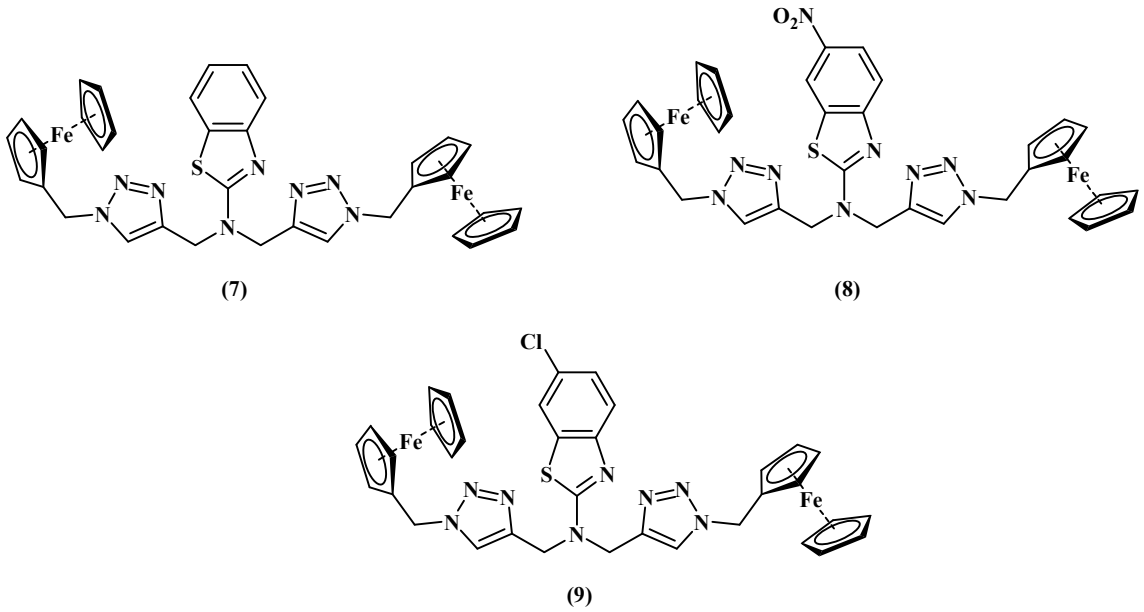

Fig.-8.3: Ferrocene derivatives of benzothiazole as important pharmacophores.

8.2. Benzothiazole amide derivatives as new antimycobacterial chemotypes

The evaluation of benzothiazole-2-carboxamides for their anti-tuberculosis (TB) activity, as described in the study, holds promising implications for the future. The findings, summarized in Chapter 5, reveal that certain compounds within this class, notably ligands **5a, 5e, 5f, 5g,** and **5l**, exhibited significant anti-TB activity at low concentrations, particularly 1.6 μg/mL for **5a**. Importantly, their efficacy is comparable to that of second-line standard drugs like Isoniazid, Ethambutol, and Pyrazinamide, which have long been at the forefront of TB treatment. This suggests that these benzothiazole-2-carboxamides could serve as potential candidates for developing new anti-TB drugs, potentially offering alternatives or adjuncts to the existing treatments. Additionally, the study delves into the structural aspects of these compounds, highlighting the importance of the presence of nitrogen hetero-atoms in the fused ring for enhanced anti-TB activity while revealing that the presence of oxygen and sulphur heteroatoms may hinder their efficacy. Furthermore, the role of specific modifications, such as the methylene group at the *N*-atom of the heterocyclic ring (as observed in **5h**), is also explored, providing valuable insights into the structure-activity relationship. Future research in this area could focus on optimizing the chemical structures of these compounds and conducting further preclinical and clinical studies to potentially develop novel and more effective anti-TB drugs, addressing the urgent global need for improved TB treatment options.

CHAPTER-9

SUMMARY AND CONCLUSION

The present work focused on three significant research areas in the field of organic chemistry. Firstly, a straightforward and high-yielding method for the synthesis of 2-azidobenzothiazoles was developed, exhibiting promising antibacterial activity against various bacterial strains. Secondly, a novel approach for the synthesis of benzothiazole amide derivatives using molecular hybridization was presented. This method combined ethyl benzothiazole-2-carboxylate and alicyclic piperazines without the need for catalysts or solvents, achieving high selectivity in a remarkably short time. This research contributes to sustainable and efficient synthetic methodologies in chemistry. In a separate investigation, the synthesis of Schiff bases with indole aldehydes was explored. Piperidine was utilized as an organic base catalyst to facilitate the synthesis process. This study aimed to provide a comprehensive understanding of the synthesis of these novel Schiff bases and the unique advantages associated with the use of piperidine as a catalyst. This research has contributed significantly to the field of chemistry. The development of a high-yielding method for 2-azidobenzothiazole synthesis with promising antibacterial properties underscores the importance of 2-azidobenzothiazoles in the pharmaceutical industry. Additionally, an innovative approach to benzothiazole amide derivative synthesis, which is catalyst-free and highly selective, opens up new possibilities for sustainable and efficient synthetic methodologies. Furthermore, the exploration of the synthesis of Schiff bases with indole aldehyde and the use of piperidine as a catalyst provides valuable insights into organic chemistry. This research sheds light on the unique advantages of piperidine in this chemical transformation, potentially leading to its wider application in various organic synthesis processes. Overall, this work contributes to the advancement of chemistry and offers promising implications for the development of more sustainable and efficient synthetic methods.

The emergence of antibiotic-resistant bacteria and the increasing prevalence of biofilm-associated infections pose significant challenges to modern healthcare. Therefore, exploring novel therapeutic agents that can effectively combat bacterial growth and biofilm formation is of utmost importance. Moreover, the decline in the development of new antibiotics in recent years has fuelled the urgent need for drug discovery efforts to combat antibiotic resistance and address the challenges posed by biofilm-associated infections.

In this research, we explored the antibacterial and antibiofilm potential of 2-azidobenzothiazoles along with the antimycobacterial activity of benzothiazole amide derivatives through a comprehensive *in vitro* analysis. Our findings shed light on the efficacy and underlying mode of

action of these compounds, offering valuable insights to aid in the creation of novel antimicrobial approaches. In this study, we investigated the antibacterial potential of a series of 2-azidobenzothiazole compounds through a comprehensive *in vitro* analysis, including MIC, MBC and subsequently performed the kill-kinetics, PAE, cell cytotoxicity, biofilm inhibition, biofilm eradication assay of lead compound **2d** that exhibited lowest MIC of 8 µg/mL against *S. aureus* and *E. faecalis*. Our results showed that the series of compounds had antibacterial activity against both Gram (+) and Gram (-) bacteria but the MICs were higher. Among the series of compounds tested, one specific 2-azido-6-nitrobenzothiazole (referred to as compound **2d**) exhibited remarkable potency against Gram (+), *E. faecalis* and *S. aureus*, and remarkably all the compounds were active with a MIC of 128 µg/mL against clinically resistant bacterial strains, Methicillin-Resistant *Staphylococcus aureus* and Multidrug-Resistant *Escherichia coli* surpassing the efficacy of other tested compounds. However, for *P. aeruginosa* and *B. cereus* the MIC values were relatively higher at 64 µg/mL. Additionally, for Gram (-) bacteria *E. coli* and *K. pneumoniae*, the MIC values were 128 µg/mL. The compounds were further assessed for their bactericidal potential against the most susceptible bacteria *S. aureus* and *E. faecalis* and it was found all the compounds in the series demonstrated potent bactericidal effects against both. To elucidate the mechanism of killing, we investigated the kill kinetics and PAE of compound **2d** against *S. aureus* and *E. faecalis*. The kill kinetics analysis revealed a rapid decline in bacterial viability over time, indicating the efficient bactericidal activity of compound **2d**. The PAE assessment demonstrated a prolonged suppression of bacterial growth for approximately 5 hours even after the removal of compound **2d**, which was comparable to that of Ampicillin suggesting its potential for intermittent dosing regimens and reduced frequency of administration. Cytotoxicity studies revealed that compound **2d** exhibited significantly lower toxicity towards human cells at even higher concentrations for a prolonged time compared to bacterial cells, indicating a favorable safety profile for potential therapeutic applications. This selective cytotoxicity suggests that compound **2d** may selectively target bacterial cells while sparing human cells, reducing the risk of adverse effects. Furthermore, we evaluated the ability of compound **2d** to inhibit and eradicate biofilms formed by different bacterial strains. The biofilm inhibition assays showed significant inhibition, up to 50%, at the MIC concentration and higher for *S. aureus* and *E. faecalis*. Moreover, biofilm eradication assays conducted post-biofilm formation (24, 48, and 72 hours) revealed a remarkable eradication percentage of up to 70%,

demonstrating the efficacy of compound **2d** in disrupting and eradicating mature biofilms. These findings suggest that compound **2d** may exert its antibacterial and antibiofilm effects by interfering with these essential bacterial processes. In addition to this benzothiazole amide derivatives has been identified as new antimycobacterial chemotypes having MIC in the low micromolar range or similar to reference drugs. In conclusion, our comprehensive *in vitro* study provides compelling evidence for the potent antibacterial and antibiofilm potential of compound **2d** along with the promising antimycobacterial activity of benzothiazole amide derivatives.

Although our study provides valuable insights into the antibacterial, antimycobacterial, and antibiofilm potential, it is essential to acknowledge some limitations. Firstly, our experiments were conducted *in vitro,* and further investigations should include *in vivo* models to assess the compound's efficacy and safety in more complex biological systems. Our experiments were conducted solely *in vitro*, using laboratory-based assays. While these provide a controlled environment for evaluating the compound's efficacy, they may not fully represent the complexity of bacterial infections in vivo. Further investigations using animal models or clinical studies are necessary to validate the potential therapeutic applications of these compounds. Although we performed a comprehensive analysis, focusing on multiple aspects such as MIC, MBC, kill kinetics, post-antibiotic effect, cytotoxicity, biofilm inhibition, biofilm eradication, and molecular docking, numerous other factors could influence the efficacy and safety of these compounds. Factors such as pharmacokinetics, tissue penetration, drug metabolism, and potential drug-drug interactions were not specifically addressed in our study. Molecular docking investigations offer valuable perspectives into the possible binding interactions between compounds and their target proteins. However, it is important to note that docking simulations have inherent limitations and may not precisely predict the actual binding affinities or biological effects. Further experimental validation and structural elucidation techniques are necessary to confirm the specific binding modes and interactions. While our study identified one potent lead compound **2d** with significant antibacterial and antibiofilm activity and five benzothiazole amide derivatives with potential antimycobacterial activity, it is crucial to explore a broader range of compounds and structural modifications. The development of multiple lead compounds with diverse chemical scaffolds can increase the chances of finding more effective and selective antimicrobial agents. Our study focused primarily on *in vitro* assessments, and clinical data regarding the safety and efficacy of these compounds in human subjects are lacking. Clinical

trials are needed to evaluate the compounds' performance in real-world scenarios and assess factors such as dosage, treatment duration, and potential side effects. While we have provided insights into the potential molecular targets and mechanisms of action through molecular docking studies, further investigations, such as proteomics or transcriptomics, are required to validate and elucidate the precise mechanisms underlying the antibacterial and antibiofilm effects of the compounds. Addressing these limitations and conducting further research will enhance our understanding of the potential of 2-azidobenzothiazoles as antimicrobial agents and pave the way for their future development and clinical application.

Our comprehensive *in vitro* study holds significant implications and contributions to the scientific community. It addresses the issue of antibiotic resistance which is fuelled by the decline in the development of new antibiotics that necessitates the exploration of novel therapeutic agents. Our study provides valuable insights into the antibacterial activity of 2-azidobenzothiazoles, demonstrating their potency against both Gram (+) and Gram (-) bacteria, including drug-resistant strains. Furthermore, infections linked to biofilm formation present a substantial challenge in clinical environments, primarily because they exhibit inherent resistance to traditional antibiotics. Our study reveals the remarkable ability of the lead compound **2d**, to inhibit and eradicate biofilms formed by various bacterial strains. This finding has important implications for developing effective strategies to manage chronic and persistent infections associated with biofilms. The identification of a potent lead compound **2d** with selective cytotoxicity towards bacterial cells while sparing human cells highlights its potential for therapeutic applications. This finding offers promising prospects for the development of safe and effective antimicrobial treatments. Further optimization and exploration of the lead compound, along with other compounds in the series, may lead to the development of novel antibiotics or antimicrobial agents. Our study further exemplifies the importance of drug discovery efforts in combating antibiotic resistance and biofilm-associated infections.

LIST OF PUBLICATIONS

1. **Qadir**, **T**., Altaf, S., Aasif, M., Fadul, A.N., Yatoo, G.N., Jangid, K., Mir, M.A., Shah, W.A. and Sharma, P.K., **2023**. Design, synthesis, and unraveling the antibacterial and antibiofilm potential of 2-azidobenzothiazoles: Insights from a comprehensive in vitro study. ***Frontiers in Chemistry***, *11*, p.1264747.
2. **Qadir, T**., Amin, A., Salhotra, A., Sharma, P.K., Jeelani, I. and Abe, H., **2022**. Recent advances in the synthesis of benzothiazole and its derivatives. ***Current Organic Chemistry***, *26*(2), pp.189-214.
3. **Qadir, T**., Amin, A., Sharma, P.K., Jeelani, I. and Abe, H., **2022**. A review on medicinally important heterocyclic compounds. ***The Open Medicinal Chemistry Journal***, *16*(1).
4. **Qadir, T**., Amin, A., Sarkar, D. and Sharma, P.K., **2021**. A review on recent advances in the synthesis of aziridines and their applications in organic synthesis. ***Current Organic Chemistry***, *25*(16), pp.1868-1893.
5. **Qadir, T**., Aasif, M., Singh, J., Sharma, P.K., **2024**. Exploring Synthesis and Medicinal Applications of Andrographolide Derivatives: A Review. ***Current Organic Chemistry***, pp. 1-14. (*doi: http://dx.doi.org/10.2174/0113852728296785240308054135*)
6. Amin, A., **Qadir, T**., Sharma, P.K., Jeelani, I. and Abe, H., **2022**. A Review on the Medicinal and Industrial Applications of N-Containing Heterocycles. ***The Open Medicinal Chemistry Journal***, *16*(1).
7. Amin, A., **Qadir, T**., Salhotra, A., Sharma, P.K., Jeelani, I. and Abe, H., **2022**. Pharmacological Significance of Synthetic Bioactive Thiazole Derivatives. ***Current Bioactive Compounds***, *18*(9), pp.77-89.
8. Jeelani, I., **Qadir, T**., Bhosale, M., Sharma, P.K., & Amin, A., **2023**. Pongamia Pinnata: An Heirloom Herbal Medicine. ***The Open Medicinal Chemistry Journal***, *17*, pp. 1-14.
9. **Qadir, T**., Jangid, K., Safir, W., Ahmed, K., Sheikh, K., Kanth, S.A., Shah, W.A., Sharma, P.K., **2024**. Catalyst and Solvent-free, Ultrasound Promoted Rapid Protocol for the One-pot Synthesis of Benzothiazol-2-yl(piperazin-1-yl)methanones: Design, Synthesis, Crystallography, *In Vitro*, and *In Silico* Studies. *New Journal of Chemistry* (Under Review).

LIST OF CONFERENCES

1. T. Qadir, P.K. Sharma. Total Synthesis of Biologically Active Natural Products with 6H-Dibenzo [*b, d*] pyran-6-one using Palladium Catalyzed Biaryl Coupling Reactions. **8th World Conference on Pharmaceutical Science and Drug Manufacturing** (17th & 18th April 2021| Thailand).

2. T. Qadir, P.K. Sharma. Study of Medicinally Important Heterocyclic Compounds. **3rd International Conference on Recent Advances in Fundamental and Applied Sciences** (25th & 26th June 2021 | Lovely Professional University, Punjab).

3. T. Qadir, P.K. Sharma. Pharmacological Significance of Synthetic Benzothiazole Derivatives. **International Conference on "Nanotechnology for Better Living" NBL-2021**(7th to 11th September 2021| NIT Srinagar).

4. T. Qadir, P.K. Sharma. Synthesis, Characterization and Biological Evaluation of Novel Schiff Bases of 2-Aminobenzothiazole Derivatives. **International Conference on Innovation and Advances in Pharmaceutical Sciences-Pharmaceutical Science and Drug Manufacturing** (10th & 11th February 2023| Karnataka India).